Master Thesis

Comparison of Numerically Predicted Response and Measured Response for Jacket Structures

Sammenligning av Målt og Beregnet Respons i en Fagverksplattform

Dilly S. Soemantri

Supervisors:

Prof. II. Sverre Haver (Statoil)

Dr. Ing. Ole David Økland (Marintek)

Dr. Thomas B-Johannessen (AkerSolutions)

June 2010

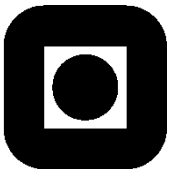

NTNU, Trondheim
Norwegian University of Science and Technology
Faculty of Engineering Science and Technology
Department of Marine Technology
Norway

Abstract

Previous studies on Kvitebjørn jacket have shown that there are discrepancies between the response obtained from numerical simulations and field measurement record. For some cases, numerical simulations under predict the response of the structure when measured wave elevation is used as input. The reason for these discrepancies is so far still in question.

In this study, the following efforts were done to asses other possibilities of discrepancy of the the response:

1. Modification of wave height.
2. Impact assessment due to breaking waves.
3. Observation on NORSOK N-003 recommended hydrodynamic coefficients.

The analyses include the following combinations of kinematics and surface properties:

- Airy kinematics combined with second order surface
- Wheeler stretching kinematics combined with second order surface
- Second order kinematics combined with linear surface

The simulation is done by using the latest updated model developed by MARINTEK (Økland O. D., 2009). The simulation results have shown that the wave crest at platform location is under predicted approximately for 3m. One possible cause for this is the occurrence of pyramid-shaped wave.

The impact assessments in this study are using the wave impact model proposed by Wienke & Oumeraci and by Campbell & Weynberg. Simulations then show that impact profile as proposed by Wienke and Oumeraci may not be suitable for assessing the response. By using this impact profile, the response of the structure is still under predicted. The quasi-static response resulted from this impact profile seems to have under predicted the real response at the estimated impact time. The dynamic response is under predicted too even though the behavior can be modeled pretty well. Impact model as proposed by Campbell and Weynberg was able to approximate the measured response better than the previous impact profile in this case. Total response and dynamic response can be represented pretty well and if the presence of caissons/riser between the legs of the platform is considered, the quasi-static response may be able to be approximated well too.

For the case of slender drag dominated structure like Kvitebjørn, simulations show that a bigger drag coefficient than the one proposed by NORSOK N-003 should be used to approximate the impact load on the structure.

Acknowledgement

This study has been done under the supervision of Prof. Sverre Haver (NTNU/STATOIL). I highly appreciate all discussions, guidance, advice, and reviews that I had with him since the thesis pre-work on autumn 2009 until the completion of this master thesis on June 2010. It has been a pleasure to work together with him and I am looking forward to have more cooperation in the future.

I would like to thank Dr. Ing. Ole David Økland (MARINTEK) for all his assistance. The discussions have been very helpful for me in starting my work and the knowledge that he shared has been very useful for the completion of this study. The analysis input and some computational tools that he gave me were very useful and his experience on Kvitebjørn analysis has helped me a lot in completing this study.

I am also grateful for the reviews by Dr. Thomas B-Johannessen (AkerSolutions) which have been very useful for me in presenting the result of my study better.

I am thankful to Per Erlend Voie for all discussions and guidance in using Matlab. His previous work has been useful as a reference for me in this study. The simdyn version that he had developed was useful in executing the analyses with second order kinematics.

I would also like to acknowledge the assistance from Dr. Gro S. Baarholm (MARINTEK) for her assistance in analyzing impact with simdyn and some other discussions which have also been pleasant and helpful. I would like to thank Mr. Naiquan Ye (MARINTEK) for his help on setting up NIRWANA and solving some installation problems with this software in my computer.

Statoil and Marintek are acknowleged for the permission and access to the data used in this study.

Last but not least, I would like to thank all of my office mates in Marinteknisk Senter: Arild, Line, Børge, Kjersti, Marianne and Jinping for the nice atmosphere and a very wonderful year in the office.

Trondheim, June 2010

Dilly S. Soemantri

Table of Content

List of Figure

List of Table

Nomenclature

The following are the list of symbols which are used in this report. Some symbols may be used for different purpose but explanation on that will be given on the report. The symbols below are the most common ones:

a	Amplitude of wave component
d	Water depth
dz	Segment length of cylinder strip
$f(x)$	General notation for function of x
f	(Wave) frequency
g	Gravity acceleration, normally 9.81 m/s^2
h	Length of time step Δt
k	Wave number
s	Cylinder submergence
t	(Discrete point of) time
u	Wave particle velocity
$\dot{u}$	Wave particle acceleration
x	Displacement or position in horizontal direction
$\dot{x}$	Velocity
$\ddot{x}$	Acceleration
z	Vertical position of the system
C	- Damping - Wave celerity in impact calculation
C_D	Drag coefficient
C_M	Inertia/mass coefficient
C_S	Slamming coefficient
D	Cylinder diameter
F	External force
F_1	Complex Fourier transform of linear wave component
F_1^*	Complex conjugate of F_1
F_D	Drag force
F_I	Impact force
F_M	Inertia force
H	Wave height
$H(f_1, f_2)$	Quadratic transfer function of positive and negative frequency (f_1, f_2) of Fourier component
K	Stiffness
M	Mass
R	Radius of cylinder
T	Wave period
T_0	Natural frequency of the system
T_{impact}	Duration of impact estimated from wave record
T_{wave}	Zero crossing period of wave record

V	Wave velocity
$\alpha_1 \& \alpha_2$	Rayleigh damping coefficients
β	Stability factor on Newmark – β integration
γ	- Numerical damping factor on Newmark – β integration - Member inclination angle in impact load calculation
θ	Averaging parameter in Wilson – θ integration
Δt	Time step or increment of time
Δx	(Horizontal) distance in x direction
Δy	(Horizontal) distance in y direction
μ	Horizontal asymmetry factor for breaking waves
η	Surface elevation
$\eta_1 \, or \, \eta^{(1)}$	Linear (component of) surface elevation
η_2	Second order component of surface elevation
$\eta^{(2)}$	Second order correction to surface elevation
$\eta^{(3)}$	Third order correction to surface elevation
η_b	Crest height of breaking wave
η_c	Crest height
τ	Time increment in Wilson – θ integration
λ	- Wave length - Curling factor in impact calculation due to breaking wave
ρ	Sea water density
ϵ	Crest front steepness
ξ	Damping ratio

Chapter 1
Introduction

1.1 Background

Kvitebjørn, a four-legged jacket structure which was installed in 190 m of water depth, has a natural period which is considered large enough to induce considerable dynamic amplification. Being considered as a slender structure which is influenced by non-linear drag loading, a way to do the structural response analysis is by doing time domain simulation. In this study, the results from the time domain simulation will then be compared with measurement data.

Response measurement data for this platform is available in form of acceleration data at various locations as well as axial force on several structural members. The measurements began since the first winter season after the installation (2003) and lasted until summer 2007. In addition, the wave elevation time history is measured by a looking-down radar located at coordinate (-57.0, -22.0, 26) m relative to the platform origin (Fugro, 2006).

1.2 Motivation of Study

Some previous studies which were done for example by Karunakaran (2004) and by Marintek (Økland, 2009), show that there are discrepancies between the response obtained from numerical simulations and field measurement records. Most of the time, simulations show a reasonable agreement with the measurements. For some cases,

numerical simulations under predict the response of the structure when measured wave elevation is used as input. The very large discrepancies are exceptional to the rest of the simulations. The reason for these discrepancies is so far still in question. This master thesis is aimed to investigate possible reasons for the discrepancies found on this structure.

1.3 Scope of Work

This master thesis is preceded by a project thesis (Soemantri, 2009) as an introductory part to the problems which will be discussed herein. Literature study is essential to have better understanding on the problems and to give wider horizon when suggesting possible solutions. The outline of the study will include:

1. Description of previous studies related to the modeling of Kvitebjørn platform which leads to the discrepancies in terms of under and over predictions of the measured response compared to the simulation results.
2. Introduction to various formulations of time domain simulation.
3. Discussion on the method to shift the measured wave elevation from measuring point to the center of the jacket shall be presented.
4. Time domain comparison between numerical simulation and measured response for certain episodes of events shall be conducted. Total response, quasi-static response, and dynamic response shall be identified by using filtering method. As a first approach, the sea surface elevation will be assumed to be Gaussian and the kinematics can be modeled by Wheeler stretching. The next approach is to assume that the sea surface elevation can be modeled as a second order process.
5. An observation on NORSOK Standard N-003 coefficients shall be done with regards to the presence of dynamics on the structure. The design recipe in the standard is primarily provided for structures which behave quasi-statically, thus an investigation to see if the same value of coefficients can be used for dynamically behaving structures needs to be done.
6. Discussion on the possibility of breaking wave occurrence by the time discrepancies between measured and simulated response occur.

The time domain simulations are to be done by using computer program NIRWANA which was developed by Marintek (Karunakaran, Brathaug, Passano, Økland, & Baarholm, 2008). Simulations with specific kinematic models will be done by using the following version of NIRWANA:

- Airy kinematics and Wheeler stretching: Original NIRWANA Version
- Second order kinematics: Voie NIRWANA Version
- Impact simulation: Impact NIRWANA Version

Chapter 2
Problem Definition

2.1 Previous Studies and Model Development

On May 16th, 2003, Kvitebjørn platform was installed in Northern North Sea. The platform itself is equipped with several sensors to measure the environmental condition as well as structural responses. Sampling of data is done by collecting 20-minute time history continuously with sampling rate of 7.6805 Hz. The wave sensor is located at a distance of 61 m from the center of jacket while the accelerometer and the strain sensor are located at -108m elevation. Figure 2.1 illustrates the position of the sensors on Kvitebjørn.

As a design basis for this platform, topside weight of 23000 tons was used. This together with the soil condition which is originally assumed, resulted in an estimated largest natural period of the structure of around 5 sec. Based on measurement in winter 2003/2004, it is observed that the natural period of the structure is much less than the estimated value in the design phase. A study which was done by 2005 (Karunakaran & Haver, 2005) utilizes topside weight of 18000 tons. In that study, the stiffness of the bottom nodes which simulate the pile-soil interaction was also increased 100 times. This gives an almost fixed support condition between soil and the structure. Other than this study, there are some investigations conducted on this platform as well. One of the findings is that there are some discrepancies between measured response values with numerical simulation result (Økland O. D., 2006).

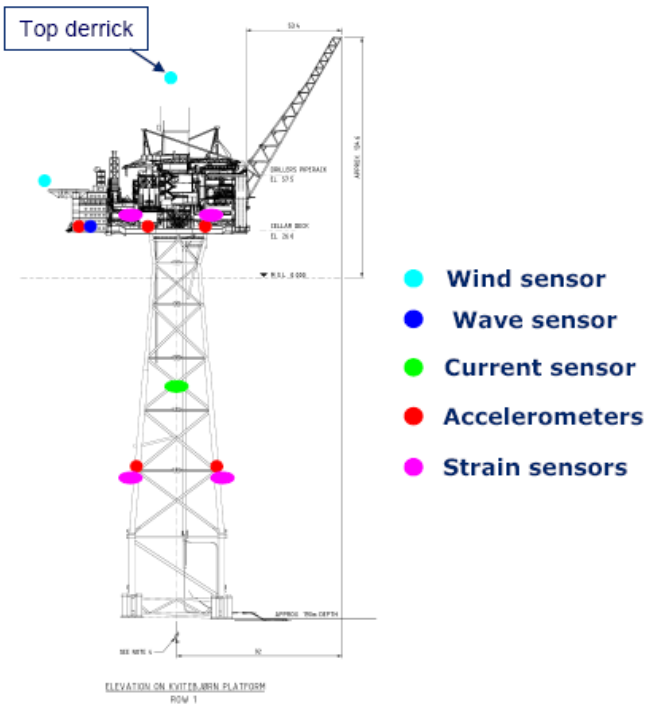

Figure 2. 1 Elevation view of Kvitebjørn including locations of sensors. (Courtesy of Statoil)

These findings lead to more investigation studies which resulted in the update of the model to be able to represent the actual condition. The latest investigation study which produces a more updated model of the platform was done by 2009 by Marintek (Økland O. D., 2009). This study also mentions some previous investigations which give impact to the structural model:

1. Global finite element model review (Stavanger 2006 and Trondheim 2007)
2. Assessment on topside mass distribution (Statoil)
3. Foundation stiffness re-evaluation by AkerSolutions (Akersolutions, 2006)
4. Natural period of Kvitebjørn (Wigaard, 2008) where it was mentioned that stiff joints modelling could be important for the jacket's global stiffness.

The latest model by Marintek (Økland O. D., 2009) incorporates all relevant information on the platform. The updates on the latest model include:

1. Soil stiffness, in terms of spring constants used in NIRWANA
2. Jacket structure stiffness, by changing the wall thickness and/or structural diameter of platform legs and vertical bracings so that the stiffness used in NIRWANA is the same with the SESAM model. The SESAM model was obtained from AkerSolutions from another study. Other modification is done by changing the configuration of some horizontal bracings to match the SESAM configuration.
3. Topside weight of 20000 tons can be used based on Aibel (Aibel, 2008). Despite this, to obtain the corresponding measured natural period, Økland (Økland O. D., 2009), used topside weight of 19000 tons and increase the soil stiffness by 20%. This model will be used further on in our analyses.

4. Steel density of 7800 kg/m3 is used for the vertical bracings and main legs. Density of horizontal bracings is modified to account for the existence of other detailing elements such as riser, conductor, joint stiffeners, etc.
5. Weight of pile-clusters and cans are accounted for by assigning point masses on the main legs.
6. Marine growth on main legs and vertical bracings is accounted for according to the recommendations in NORSOK Standard N-003. For horizontal bracings, equivalent hydrodynamic diameters for drag and mass force are assigned. The values represent the existence of appurtenances such as members supporting the conductors, risers, J-tube, and caissons.
7. Improvement on modeling detail by doing some model corrections which include better caisson, J-tube, conductor, and riser representation.

The topside configuration is not modeled in form of elements in the computer model. The topside is represented by adding the weight on a certain point on top of the jacket structure. This point corresponds to the center of gravity of the topside which is located at coordinate (-3.0, 0.5, 44.5). The weight is introduced as forces and moments to represent the real weight distribution of the topside. For this master thesis, the computer model which will be used is based on the latest modification mentioned above.

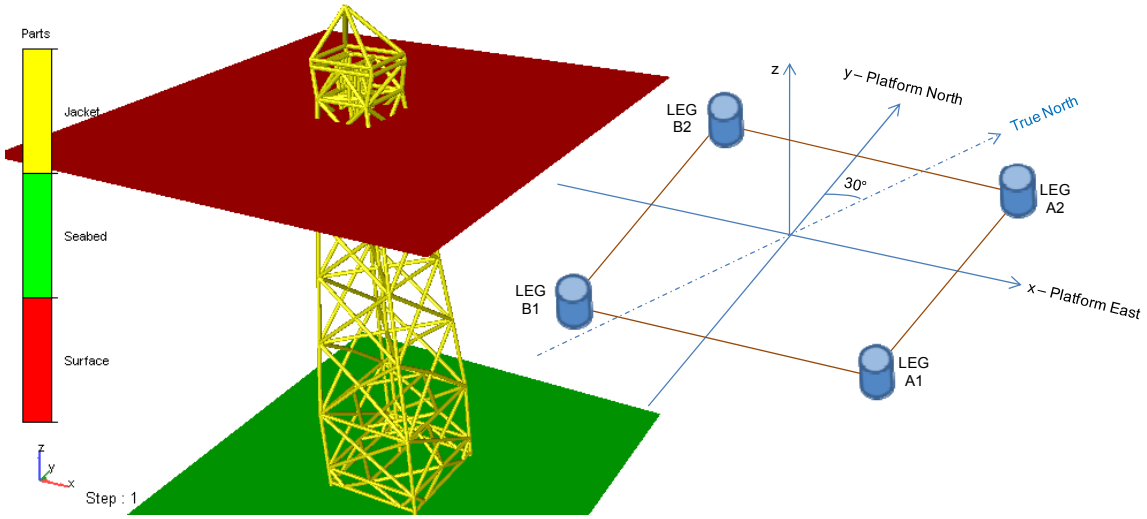

Figure 2. 2 Model representation with corresponding coordinate system

2.2 Introduction to Measured and Predicted Response Discrepancies

In doing a comparison between field measurement data with results obtained from numerical simulations, assumptions on several aspects are sometimes required. For full scale experiments, the input conditions which are related to the prediction of loads are

roughly known. Uncertainties occur in areas such as the prediction of wave direction, degree of short-crestedness, determination of current speed, and wave behavior such as the steepness and breaking possibility. Due to this, an exactly same result between measured and simulated response is impossible to obtain. However, a general impression can show whether numerical simulation is good enough in giving results. The results are said to be reasonably good when they are approximately at the same trend with the full scale measurement. This will be a good indication of the adequacy of the numerical calculation done in the design phase.

Previous studies have shown that there are some episodes of the response where numerical simulations under predict the real response of the platform (Karunakaran & Økland, 2004) and (Økland O. D., 2006). These events are known as the “odd events”. The discrepancy between measured and simulated response is obtained after running 20-minute simulation and comparing the result with the corresponding 20-minute field measurement. Focus has been concentrated on two odd events which are (Økland O. D., 2009):

- Odd event 1:
  Tag: 200401011200 (Measurement on 1 January 2004 at starting at 12:00 for 20 minute)
  Detail: large measured response around t = 700 sec without any corresponding very large wave. Response from simulation is 50%-60% smaller that the real measured response (Voie, 2009).
- Odd event 2:
  Tag: 200401011400 (Measurement on 1 January 2004 at starting at 14:00 for 20 minute)
  Detail: ringing like response occur at around t = 170 sec where Wheeler kinematics under predict the response by 70% (Voie, 2009).

In this master thesis, these two odd events will be the main focus too. As an addition, there is another discrepancy where the simulation shows a high over prediction of the response. This odd event is found at time window 950-1000 sec of the 200401011200 event. This event will also be discussed in this report.

Chapter 3
Data Handling and Processing

3.1 Measurement Data

For this study, the response of the structure in terms of displacement which was deduced from acceleration data, and axial force (at el. -108m) which was deduced from strain measurement (ref. Fig. 2.1) will be observed. The measured data is recorded as continuous 20-minute time history record with sampling time interval 0.1302 sec (7.68 Hz). The data collection calculates axial load from strain measurement. Axial load on the structure can then be directly obtained from the measurement record data, but for the displacement, numerical integration has to be done because the available data is in form of acceleration.

Recording response in form of acceleration is a common practice especially in earthquake engineering. The displacement can be obtained by doing double integration of the acceleration data. As the records are in the form of discrete points in time, the integration may be approached by taking the area under the curve of acceleration-time graph to obtain the velocity. The same procedure is done to obtain the displacement from velocity data. This technique is commonly known as the trapezoidal rule. This method is advantageous to be used for integrating discrete sample with constant time step. A simple explanation on this method is that for a function, $f(x)$, one can calculate the area under the function by approximating the shape of the area with a trapezium.

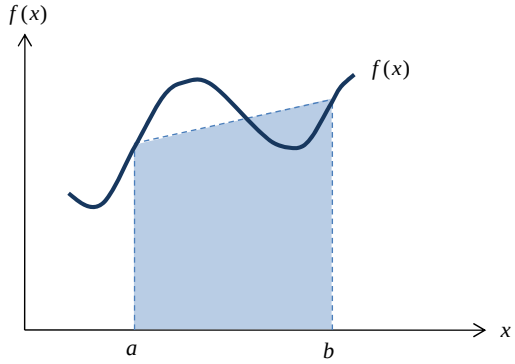

Figure 3. 1 Illustration for the trapezoidal integration method

As mentioned previously, the sampling interval for the acceleration data is 0.1302 sec, thus the distance of a-b represents the time interval of 0.1302 sec. In the above figure, $f(x)$ is the acceleration as recorded by the measuring device. The area under the curve is approximated as the area of trapezium according to the following equation:

$$\int_a^b f(x)dx \approx (b-a)\frac{f(a)+f(b)}{2} \tag{3.1}$$

Introducing numbers into the above equation and having $f(x)$ as the acceleration, the velocity can be obtained. Further on, by replacing $f(x)$ with the velocity, the displacement will be obtained. If we denote the time interval, acceleration, velocity, and displacement respectively as Δt, $\ddot{x}$, $\dot{x}$, and x; the following formulas are the basic formulas to calculate displacement from acceleration:

$$\dot{x}_t = \dot{x}_{t-1} + \ddot{x}_t.\Delta t \tag{3.2}$$

$$x_t = x_{t-1} + \dot{x}_t.\Delta t \tag{3.3}$$

After doing the integration, low frequency result may pollute the displacement values. By applying a high pass filter, the low frequency component can be removed thus the reasonable displacement data can be obtained (Ref. Fig . 4.5 and 4.12 in Chapter 4 to see an illustration of frequency domain plot).

Data for wave elevation is also available in 20-minute record of same sampling frequency (7.68 Hz). As mentioned previously, the wave radar is installed at a coordinate of (-57.0, -22.0, 26) m relative to the center of platform. This denotes that there is a distance of approximately 61 meter between the sampling point and the center of platform. To obtain the corresponding wave elevation at the platform origin, prediction of the elevation by doing some elevation shift from the measurement location to the center of platform should be done. Voie (Voie P. E., 2008) discusses a method of shifting wave elevation in space. The prediction of spatial variations of wave heights is using the assumption that the wave is of linear order and that the wave components are dispersive and can be propagated. The sequence of procedure in shifting the wave in space is as follows:

1. First, the record in time domain is transformed into frequency domain by Fourier transformation.
2. In the frequency domain, the Fourier amplitudes are phase shifted by multiplying each of the amplitude with $e^{ik_n \Delta x}$, where k_n denotes the wave number of the n-th Fourier component, and Δx is the distance from observation point to new location. The wave number is obtained from the dispersion relation.
3. At this point, the wave is already propagated to a new position in frequency domain. Inverse Fourier transform is done to reconstruct the data into time domain.

For further details on this, interested readers may refer to the works done by Voie (Voie, 2008), (Voie, 2009). This feature has also been adopted in NIRWANA version modified by the same author. In using NIRWANA for this purpose, one has to input the linearized wave record together with the propagation distance of the wave. The program will do the routine as mentioned on the above procedure automatically. Note that the latest NIRWANA program cannot proceed with too many discrete points of time history to be analyzed. The limit is 2^{12} or 4096 discrete points. Adding more points will result in inaccurate result in the time domain integration. This “bug” shall be fixed in the future to give a more robust simulation tool.

In the measured data for wave elevation, non linear components are actually included. In order to use the above procedure in a consistent way, the non-linear contributions should be removed first. This is a complicated matter. An approximation can be done which is by assuming the surface to be a realization of a second order process. It is then possible separate the linear and second order components of the wave.

3.2 Second Order Random Wave Formulations

The measured data recorded by the wave radar contains the second order process of wave trace. Several studies by Stansberg have discussed the properties and basic formulations of the second order random waves. As an excerpt to that, the following formulation (Stansberg, 1998) can be used as a basis to our further step in modeling second order random wave. Let the measured wave record is composed as follows:

$$\eta = \eta_1(t) + \eta_2(t) \tag{3.4}$$

On the above equation, the linear component, η_1, can be regarded as:

$$\eta_1(t) = \int_{-\infty}^{\infty} F_1 \, e^{i2\pi f t} df \tag{3.5}$$

F_1 is the complex Fourier transform of the linear wave elevation, and f is the wave frequency. The Fourier transform F_x shall at a given frequency f_x be statistically independent of F_y at frequency f_y and thus the resulting linear elevation will be normally distributed.

The second order component of the wave (η_2) can be expressed as:

$$\eta_2(t) = \int_{-\infty}^{\infty}\int_{-\infty}^{\infty} F_1^*(f_1).F_1(f_2).H(f_1,f_2)e^{i2\pi(f_2-f_1)t}df_1df_2 \tag{3.6}$$

In the above equation, f_1 and f_2 are positive and negative frequencies of the Fourier component. F_1^* is the complex conjugate of F_1 and vice versa. $H(f_1,f_2)$ is known as the quadratic transfer function. When long crested wave and deep water are taken as assumptions, the quadratic transfer function can be expressed as:

$$H(f_1,f_2) = \frac{B}{2}|k_2 + B\,k_1| = \frac{B}{2g}(2\pi)^2\left|f_2^2 + B\,f_1^2\right| \tag{3.7}$$

$$B = \begin{cases} +1\ for\ f_1.f_2 < 0\ (sum-frequency) \\ -1\ for\ f_1.f_2 > 0\ (difference-frequency) \end{cases} \tag{3.8}$$

Here, k is the wave number and g is the gravity acceleration. As deep water assumption is used, the parameters also fulfilled the deep water equations as can be found on Faltinsen's book page 16 (Faltinsen, 1990).

3.3 Identification of Linear Wave Content

The procedure to identify linear wave content has been presented by Stansberg (Stansberg, 2003), (Stansberg, 2008) and cited by Voie(2009). Briefly, the procedure is as follows:

1. Raw estimation of the second order component is established by firstly using the measured data record as the "linear" input. Ref. to equation (3.6)
2. Ref. to equation (3.4), find the linear component by substracting the second order component from previous step to the measured wave record.
3. Define an upper frequency limit (f_{max}) so that it fulfils $k_{max}.A_{max,R} > 2$ by using linear dispersion equation. k_{max} is the highest angular wave number and $A_{max,R}$ is the expected highest amplitude from Rayleigh theory.
4. Do a low pass filter for the result from 2. at the frequency f_{max} and high pass filter at an appropriate low frequency (typically 1/25 Hz full scale).

Note that the data available is a digitized data not a continuous one. The integral terms on the equations can be replaced by the summation function. For the detail of implementation of these theories mentioned so far in NIRWANA including the basics for second order kinematics, interested reader may refer to Voie's master thesis (Voie, 2009).

There are actually some other approaches in determining the linear wave content from a measured wave record for example as proposed in Johannessen (2009a and 2009b) and Winterstein et.al. (1999). Johannessen's method will be mentioned here briefly.

In his paper, Johannessen (2009b) proposes a linearization procedure which can be expressed by the following equation:

$$\eta - \eta'^{(2)} = \left(\eta^{(1)} + \eta^{(2)} + \cdots\right) - \left(\eta^{(2)} + O^{(3)}\right) = \eta^{(1)} + O^{(3)} \tag{3.9}$$

The above equation expresses the linear surface elevation correct to third order. $\eta'^{(2)}$ in the above equation denotes the measured wave elevation history. The third order error contains:

- Real third order wave components which have not been removed from the measured wave history
- Third order error introduced in $\eta'^{(2)}$.

The other symbols on the equation can be expressed as:

Surface elevation:

$$\eta = \eta^{(1)} + \eta^{(2)} + \eta^{(3)} + \cdots \tag{3.10}$$

Linear surface elevation:

$$\eta^{(1)} = \sum_{n=1}^{N} a_n cos(\phi_n) \tag{3.11}$$

Second order correction to surface elevation:

$$\eta^{(2)} = \sum_{n=1}^{N} \left(\frac{1}{2} a_n^2 k_n cos(2\phi_n) + \sum_{m=n+1}^{N} \frac{1}{2} a_n a_m \left((k_n + k_m) cos(\phi_n \phi_m) - (k_m - k_n) cos(\phi_m - \phi_n) \right) \right) \tag{3.12}$$

Third order wavenumber sum correction to the free surface:

$$\eta^{+(3)} = \sum_{n=1}^{N} \frac{3}{8} a_n (a_n k_n)^2 cos(3\phi_n) + \sum_{m=1}^{n-1} \frac{1}{8} a_n a_m \left(a_n (2k_n + k_m)^2 cos(2\phi_n + \phi_m) + a_m (k_n + 2k_m)^2 cos(\phi_n + 2\phi_m) \right) + \sum_{l=1}^{m-1} \frac{1}{4} a_m a_m a_l \left((k_n + k_m + k_l)^2 cos(\phi_n + \phi_m + \phi_l) \right) \tag{3.13}$$

Where:

$$\omega_n^2 = g k_n \tag{3.14}$$

$$\phi_n = k_n x - \omega_n t + \varepsilon_n$$

The expression for the second order surface elevation (Eq. (3.12)) becomes inaccurate for interaction between long and short waves (Johannessen, 2009a). A maximum allowable bandwidth, $d\omega$, is introduced thus the interaction between wave components

with frequencies outside $d\omega$ is ignored. A bandwidth of $0.7\omega_1$ is then chosen, where ω_1 is the central frequency based on the zeroth and first spectral moments.

3.4 Time Domain Simulation

3.4.1 General

The dynamic response of a system due to time historical loading is obtained by doing the so called time domain simulation. Time domain simulation method can be divided into two major groups (Langen & Sigbjörnsson, 1979), which are:

1. Methods based on differential formulation.
2. Methods based on numerical integration.

The method based on differential formulation consists of the second central difference and the Houboult's method. These methods are based on Newton's equidistant interpolation formula based on backward differentiation. The second central difference method is conditionally stable which means that the result may deviate from the exact value or becomes unstable when time step is larger than certain critical value of time step. Houbolt's method is unconditionally stable (Johnson, 1966) but will give an artificial damping. This group of method will not be further discussed here, but interested readers are referred to (Langen & Sigbjörnsson, 1979) for further details.

The method based on numerical integration consists of several integration methods such as:

1. Euler's method
2. Euler-Gauss method
3. Newmark-β family
4. Runge-Kutta method
5. Bossak method
6. Hilber-Hughes-Taylor method
7. Park-Housner method
8. Wilson-θ method

Discussion in this report will be limited to the methods which are commonly used and will be considered for the simulations. Several text books are available for interested readers, but for a summary on several methods mentioned earlier, readers may refer to (Bajer, 2002). For the analysis by using NIRWANA, only the Newmark-β family and the Wilson-θ method which are the unconditionally stable methods will be considered. These two methods will be briefly discussed in this chapter.

For finite element analysis by using NIRWANA, direct numerical integration is done to the dynamic equation of motion. The integration demands a discretization of the load history so that the total duration of observed event is divided into time steps. By introducing the initial value of acceleration, velocity and displacement, one can predict the solution at the end of first step. Solution from the first time step will become the initial value for the next step, and this process is continued until the end of the load history.

This way, the final solution for the equation of motion for the given load history can be obtained.

3.4.2 The nature of time integration

As a result of load discretization, the responses obtained by time integration will also be discrete. This means that the result will be correct at the discreted time position, but not necessarily correct at the position between those time points. Result will depend on the length of the time step and the assumption made on the distribution of acceleration, velocity, and displacement between the discrete points of time. Smaller time steps will give a more accurate result, but on the other hand cause a longer computation time especially for multi degree of freedom systems.

Another important aspect of time integration is the stability criteria. A stable calculation will give a similar result with the correct solution, but an unstable one will give solution with considerable deviation from the correct solution. An integration method is called *implicitly stable* when time step has no significant effect on the result (changing time step will not cause large deviation to the exact value). If an integration method requires certain length of time step to yield a correct solution, then the method is said to be *conditionally stable*.

3.4.3 Method of integration

Newmark-β Family

For the equation of motion denoted by

$$M\ddot{x}_{t+1} + C\dot{x}_{t+1} + Kx_{t+1} = F_{t+1} \tag{3.15}$$

Newmark (Newmark, 1959) derived the general equation for velocity and displacement based on the utilization of Taylor series as:

$$\dot{x}_{t+1} = \dot{x}_t + h(1-\gamma)\ddot{x}_t + \gamma h\ddot{x}_{t+1} \tag{3.16}$$

$$x_{t+1} = x_t + h\dot{x}_t + h^2\left(\frac{1}{2} - \beta\right)\ddot{x}_t + \beta h^2\ddot{x}_{t+1} \tag{3.17}$$

The aforementioned three equations will enable us to find the solutions for displacement, velocity, and acceleration at the end of a time step. The parameter h denotes the length of each time step Δt. The parameters β and γ are related to stability and accuracy of the method. γ is a parameter which appears in combination with damping term, C. This parameter controls the numerical damping in the solution algorithm by the following manner (Larsen, 2007):

γ = ½ no numerical damping

γ > ½ positive numerical damping will occur and amplitude decay will happen

γ < ½ negative numerical damping will occur and lead to instability

Based on the above condition, γ = ½ is usually chosen and will be used in our analyses too. The Newmark method is said to be unconditionally stable if the following conditions are fulfilled:

$$\gamma \geq {}^{1}/_{2}\ and\ \beta \geq \frac{1}{4}\left(\gamma + \frac{1}{2}\right)^{2} \tag{3.18}$$

The method becomes conditionally stable for β values which are smaller than stated on the above formula. The stability limit of this method is given by (Larsen, 2007):

$$h_{limit} = \frac{T_0}{2\pi} \cdot \frac{1}{\sqrt{\frac{1}{4}\left(\gamma + \frac{1}{2}\right)^{2} - \beta}} \tag{3.19}$$

T_0 denotes the natural frequency of the system (or the shortest eigenperiod in multi-degree of freedom system). The above description of this method denotes that for unconditionally stable integration, the parameters should be γ = ½ and β = ¼. There are other values of these parameters that can be used with a corresponding stability limit. This will be presented on Table 3.1, but it is a good practice to choose the unconditionally stable parameters to be used in NIRWANA. Thus, $\gamma = ½$ and $\beta = ¼$ will be used in the simulations.

Wilson-θ Method

The Wilson-θ method (Bathe & Wilson, 1976) is a modification of Newmark's method with linear acceleration. This method is unconditionally stable with γ = ½ and β = 1/6. If we use τ as the time increase where the acceleration is linear within 0 < τ < θh; θ>1, then we will have the acceleration vector expressed as:

$$\ddot{x}_\tau = \ddot{x}_t + (\ddot{x}_{t+1} - \ddot{x}_t)\frac{\tau}{h} \tag{3.20}$$

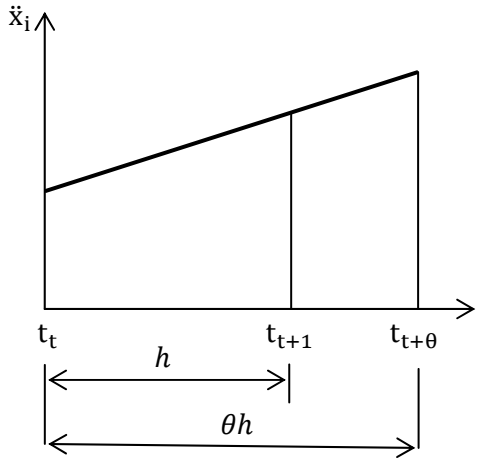

Figure 3. 2 Illustration for the Wilson-θ method – distribution of acceleration, as adapted from (Karunakaran, Brathaug, & Passano, 1990)

Using the integration relationship between acceleration, velocity, and displacement, one will have the expressions for velocity and displacement as:

$$\dot{x}_\tau = \dot{x}_t + \ddot{x}_t\tau + (\ddot{x}_{t+1} - \ddot{x}_t)\frac{\tau^2}{2h} \tag{3.21}$$

$$x_\tau = x_t + \dot{x}_t\tau + \ddot{x}_t\frac{\tau^2}{2} + (\ddot{x}_{t+1} - \ddot{x}_t)\frac{\tau^3}{6h} \tag{3.22}$$

Taking $\tau = \theta h$, for time $t_t + \theta h$, we will have:

$$\dot{x}_{t+\theta} = \dot{x}_t + \frac{\theta h}{2}(\ddot{x}_t + \ddot{x}_{t+\theta}) \tag{3.23}$$

$$x_{t+\theta} = x_t + \theta h\dot{x}_t + (\theta h)^2\left(\frac{1}{3}\ddot{x}_t + \frac{1}{6}\ddot{x}_{t+\theta}\right) \tag{3.24}$$

In this case, the equation of motion will be expressed in time $t_{t+\theta}$:

$$M\ddot{x}_{t+\theta} + C\dot{x}_{t+\theta} + Kx_{t+\theta} = F_{t+\theta} \tag{3.25}$$

Inserting $\ddot{x}_{t+\theta}, \dot{x}_{t+\theta}$, and $x_{t+\theta}$ expressions into the last equation, we will be able to express $\ddot{x}_{t+1}$. We can then solve for the acceleration $\ddot{x}_{t+1}$ and by utilizing $\tau = h$ we will have:

$$\dot{x}_{t+1} = \dot{x}_t + \frac{h}{2}(\ddot{x}_t + \ddot{x}_{t+1}) \tag{3.26}$$

$$x_{t+1} = x_t + h\dot{x}_t + \frac{h}{3}\ddot{x}_t + \frac{h^2}{6}\ddot{x}_{t+1} \tag{3.27}$$

The Wilson-θ method is unconditionally stable for $\theta > 1.37$ but we must note that the accuracy is decreasing with increasing θ. It is favorable to use $\theta = 1.4$ (Karunakaran, Brathaug, & Passano, 1990).

The following table presents the values of integration parameters with corresponding stability limit (Langen & Sigbjörnsson, 1979).

Table 3. 1 Newmark-β and Wilson-θ Parameters

Method	γ	β	θ	Stability
Second central difference	½	0	1	$h < 0.318\,T$
Fox-Goodwin	½	1/12	1	$h < 0.389\,T$
No Name	½	1/8	1	$h < 0.450\,T$
Linear Acceleration	½	1/6	1	$h < 0.551\,T$
No Name	½	1/5	1	$h < 0.712\,T$
Constant average acceleration	½	¼	1	Unconditional
Wilson-θ	½	1/6	1.4	Unconditional

3.4.4 Selection of time integration method

There are two kinds of error mainly known about time integration, i.e. the amplitude decay and period elongation error. The comparison of these errors can be seen on the following figures:

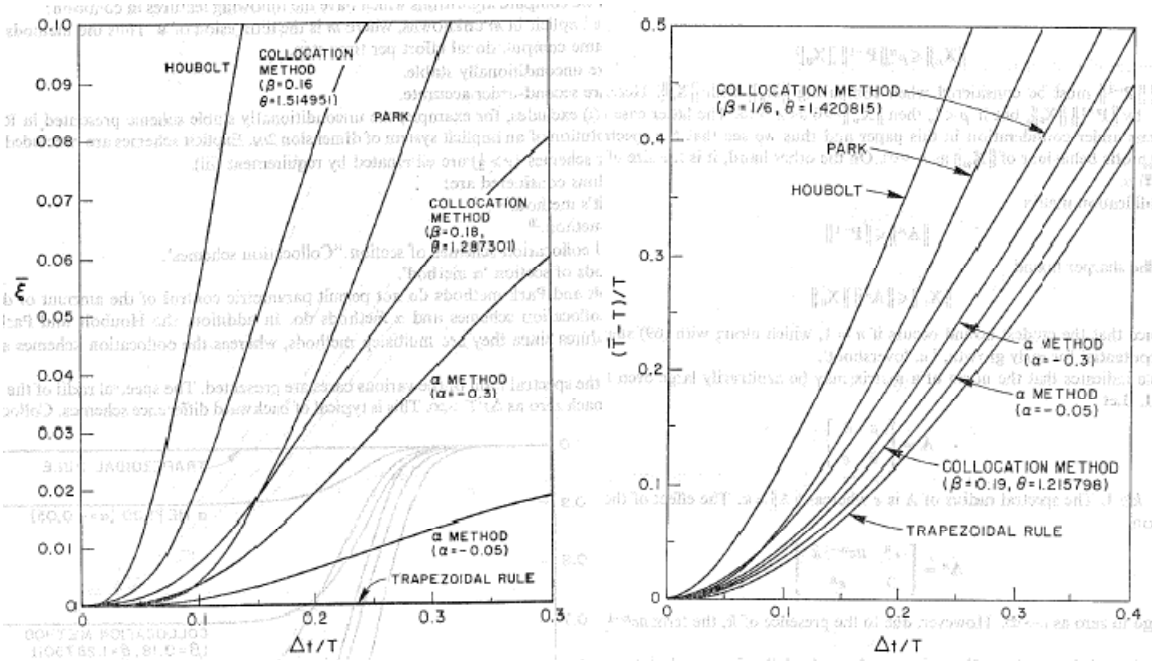

Figure 3. 3 Damping ratios and relative period errors for several integration methods (Hilber & Hughes, 1978)

The amplitude decay error is related to the generation of artificial damping in the integration method. This type of error is however can be managed by selecting γ value which brings no artificial damping as mentioned previously. From the above figure, it can be seen that for Wilson-θ method, both period elongation and amplitude decay will occur. For a given h/T, Wilson-θ method will give more error if compared to the Newmark-β method with β = ¼.

On a study by (Hilber & Hughes, 1978), it is mentioned that based on the finding of (Goudreau & Taylor, 1972) the Wilson-θ method tends to overshoot exact solutions significantly in the early steps. They also mention that the Newmark-β method (trapezoidal) displays no overshoot in displacements. Other literature also mentions that by utilizing the Wilson-θ method, for a given time step, the lower modes will be damped less than the higher ones (Langen & Sigbjörnsson, 1979).

Based on these properties of the two unconditionally stable methods mentioned here, the Newmark-β method will be used further on in the analyses due to simplicity, stability, and its property against error.

Chapter 4
Discussion on Odd Events

4.1 Identification of Odd Events

As mentioned in Chapter 2, three odd events will be discussed in this study. The term odd event here refers to the wave measurement tag 200401011200 and 200401011400 where at certain time windows there is discrepancy between measured and simulated response. The simulation is either under predict or over predict the measured response.

In the result by utilizing the wave measurement tag 200401011200, there are two discrepancies found. The first one is at the time window between t = 650 and t = 700 sec. In this time window, the measured axial response is under predicted by the simulations. The second odd event during the 20-minute period is located at the time window between 950 sec and 1000 sec. In this time window, the simulation over predicts the measured response.

For the 200401011400 event, discrepancy is found at time window t = 150 sec and t = 200 sec. In this time window, the simulation under predicts the real response on the platform.

The illustration of the odd events can be seen on the following figures:

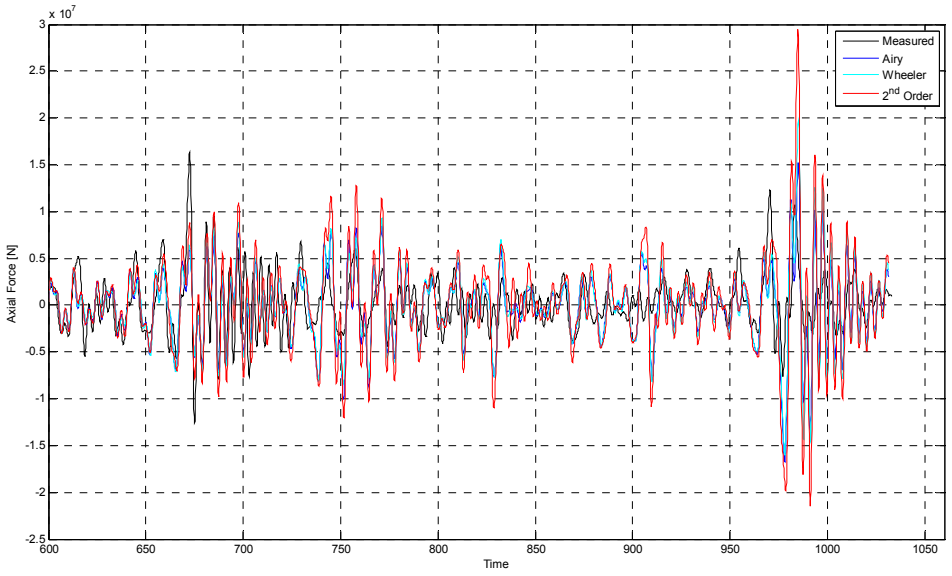

Figure 4. 1 Measured versus simulated responses on wave tag 200401011200 – Axial leg A2 (-108m)

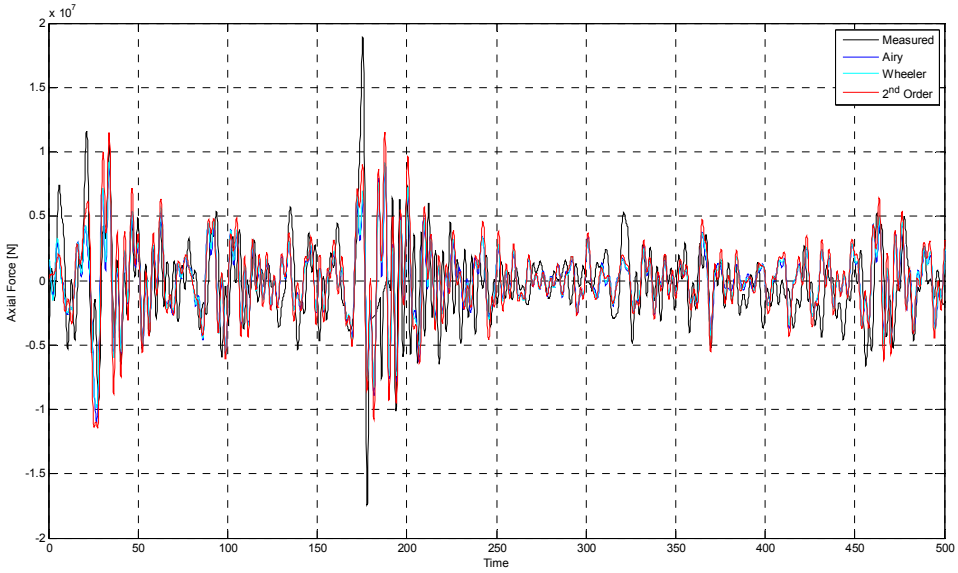

Figure 4. 2 Measured versus simulated responses on wave tag 200401011400– Axial leg A2 (-108m)

In this report, when reading the figures related to measured response VS simulated response, the following meanings of the graph's legends are used:

Table 4. 1 Simulation scheme explanation

Legend	Wave Component	Kinematics
Airy	Second order	Airy
Wheeler	Second order	Wheeler Stretching
2nd Order	Linear	Second order

4.2 Possible Reasons for Discrepancies

Regarding the discrepancies between the measured and simulated responses, several suggestions on the causes of discrepancies are proposed on some previous studies (Haver, 2004), (Karunakaran & Haver, 2005), (Økland O. D., 2009), (Voie, 2009):

1. Radar measurement error.
2. Modeling error.
3. Storm surge or tidal wave elevation effect may not be captured.
4. Spatial transformation error from the wave radar position to the position of the jacket legs.
5. Simplifications for example in the wave kinematics may give lower result.
6. Existence of short crested wave which brings large wave amplitude at platform location.

Some of these possibilities will be capture herein.

4.2.1. Radar measurement error

Based on verification work about the performance of wave radar on winter 2008/2009, it is confirmed that the radar which was used to measure wave elevation at the time of odd events was actually working properly (Voie, 2009).

4.2.2. Modeling error

Regarding the modeling error, an updated model is now available based on work done by Marintek (Økland O. D., 2009). Brief description about the updated model was also presented in Chapter 2 of this report.

4.2.3. Storm surge and tide effect

The effect of storm surge or tide may be observed by first looking at the behavior of water level variation from the available measurement data. Some error records were found thus these records are excluded from consideration. The error records are identified by the following tag numbers:

Winter 2003:

- 200401010700
- 200401011420

Winter 2004 – 2005:

- 200411081900
- 200411082040
- 200501110000

By saying error, it means that the data shows large discrepancies in measurement, for example large mean value difference and data incompleteness. The existence of these "errors" is deemed to be insignificant to the assessment of tidal effect.

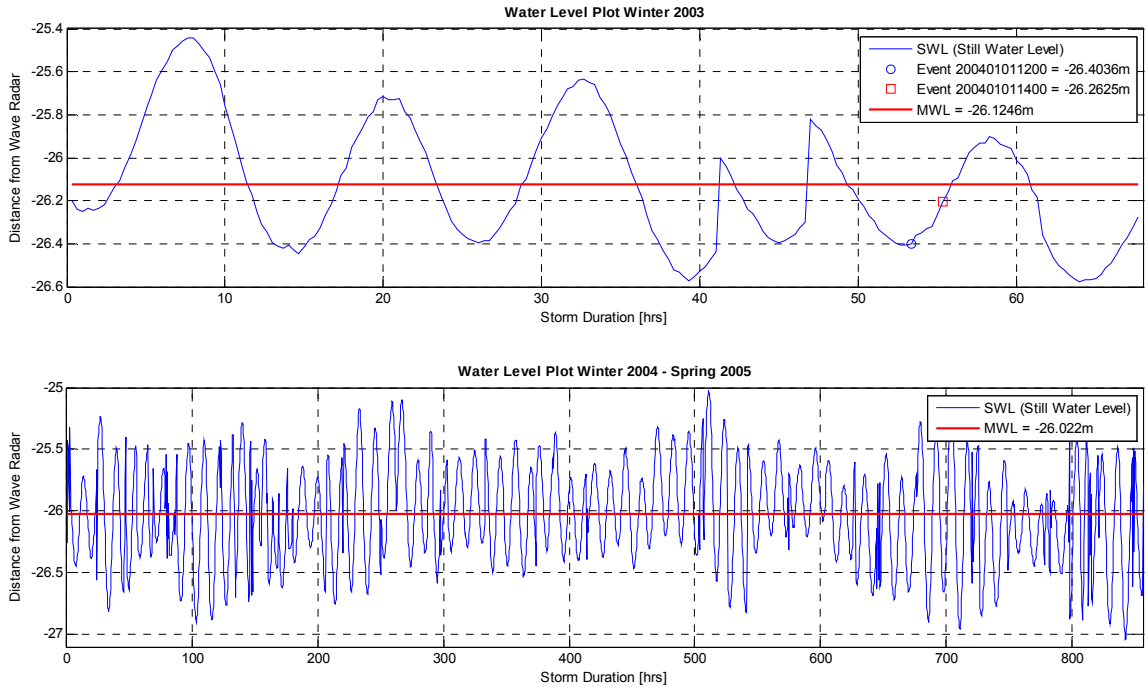

Figure 4. 3 Water level plots from winter 2003 to spring 2005

Both odd events which are being analyzed happened on winter 2003 and indicated in Figure 4.3. It can be seen that for winter 2003, the variation of SWL ranges from approximately -25.4 m to -26.6 m from the elevation of the radar. To see the effect of these changes comparison of simulation results in terms of axial force is done. Note that for this purpose, kinematics with Wheeler stretching combined with the second order surface is deemed sufficient to show the comparison. Tidal elevation of ±0.6 m is used for the analysis. Identifying the values of global maxima between zero upcrossings (Ref. Fig. 4.16), the result can be seen on the following figure:

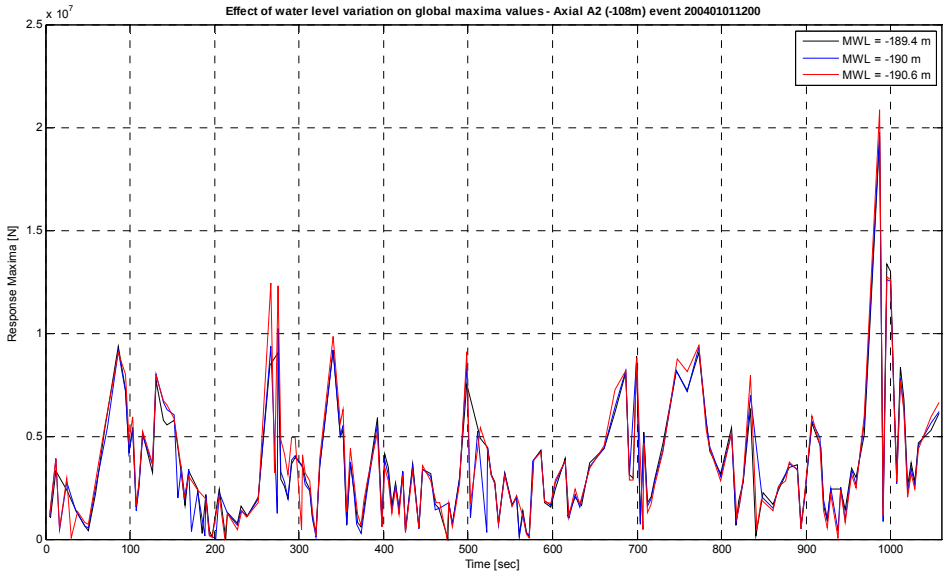

Figure 4. 4 Effect of mean water level variation on global maxima distribution

Figure 4.4 indicates that the effect of changes in mean water level to the structural response is within the range of 5.5% (see Table 4.2 also) which is not a significant value.

Table 4. 2 Maximum response change due to MWL change

Event	**200401011200**		
MWL (m)	**189.4**	**190**	**190.6**
Max Response (N)	19523580	19763106	20842784
% Max Response Change		1.211986	5.463099

This concludes that for the sea states being observed, even though the tidal variation is not included in our analysis, no significant difference should appear if compared to those analyses which incorporate tidal change. Increasing (or decreasing) the mean water level for approximately 0.6m will not give significant effect to the analysis. Thus, it can be concluded that storm or tide does not give a significant difference to the analyses.

4.2.4. Other possibilities of discrepancies

The other possible reasons are related to the wave treatment and modeling. The method of shifting wave elevation (Voie, 2008) as also mentioned in Chapter 3, has been verified with some lab measurement data. Based on that study, the method is said to give satisfactory result. Here, the same method is also applied in the modified version of NIRWANA.

The study by Voie in 2009 (Voie, 2009) incorporates second order modeling of wave kinematics. In general, the second order kinematic model gives higher predictions if compared to those using Wheeler stretching, but in some episodes still under predicts the measured responses. Despite that fact, statistically speaking, the second order

kinematic model represents the real events quite satisfactorily if compared to Wheeler stretching model.

The last possible reason is that the under prediction may be caused by some "additional loads" which cannot be captured by our model. This includes impact forces such as the one resulted by breaking waves. More on this matter will be discussed later on in this report.

4.3 Observation on Odd Events

4.3.1. Event 200401011200

This event is simulated with the estimated wave direction of 65 degrees (Økland O. D., 2009) relative to the positive x-axis (ref. Figure 2.2). For comparison purpose, the quasi-static and resonance response will be separated. To decide the separation point, one needs to observe the data in frequency domain. This involves Fourier transformation of the data. For further details on Fourier transform, interested readers may refer to e.g. Newland (Newland, 1974). For this event, the cut-off point between quasi-static and resonance response is taken to be 0.18 Hz. The cut-off point is taken based on visual observation on the spectrum, thus for different event, the cut-off point may differ. Band pass filter is utilized and the windows are:

- Quasi-static : 0.03 Hz – 0.18 Hz
- Resonance : 0.18 Hz – 0.5 Hz

Note that by choosing 0.03 Hz as a starting point for filtering, the noise from low frequency component of the response will be removed.

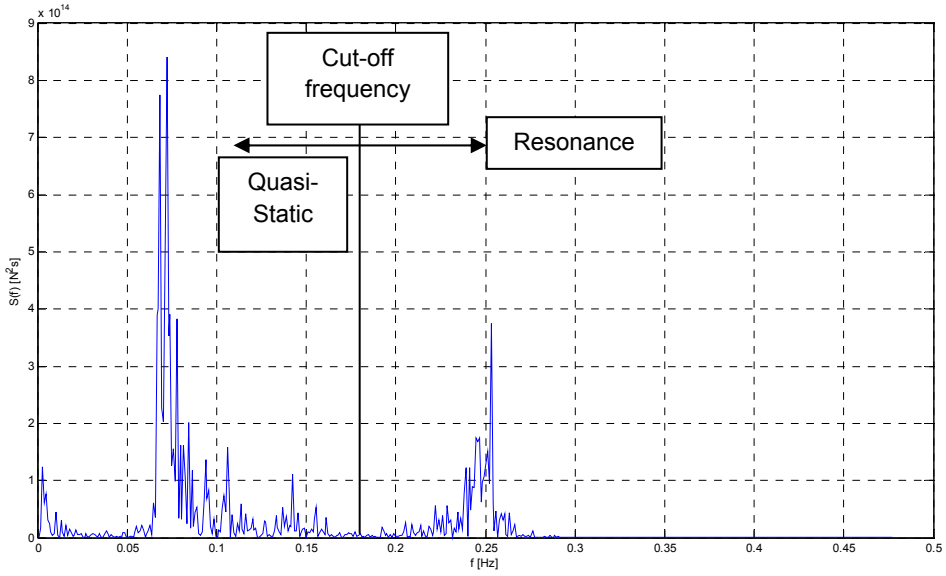

Figure 4. 5 Spectral plot for axial force at A2 (-108 m) event 200401011200

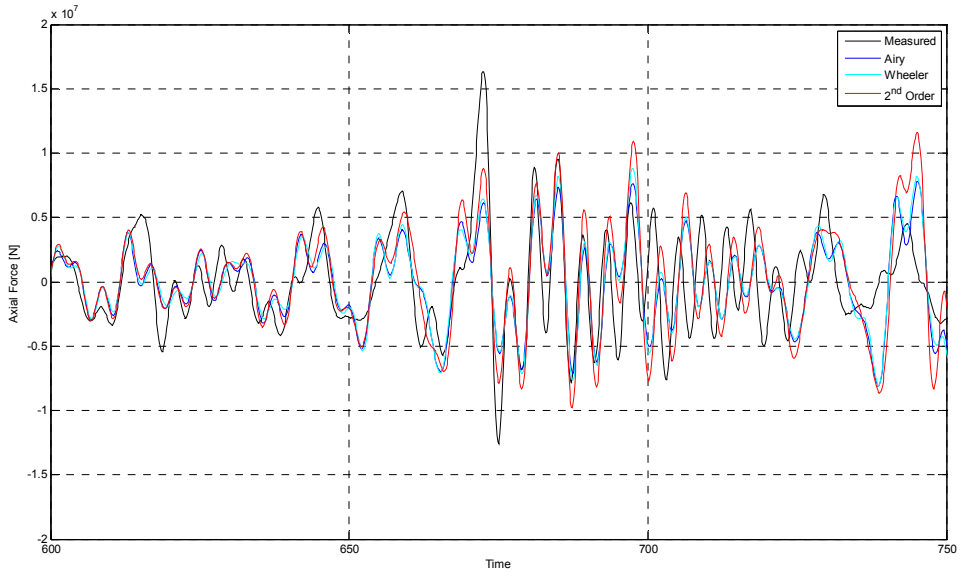

Figure 4. 6 Total axial response Leg A2 (-108 m) event 200401011200 (t = 600 – 750 sec)

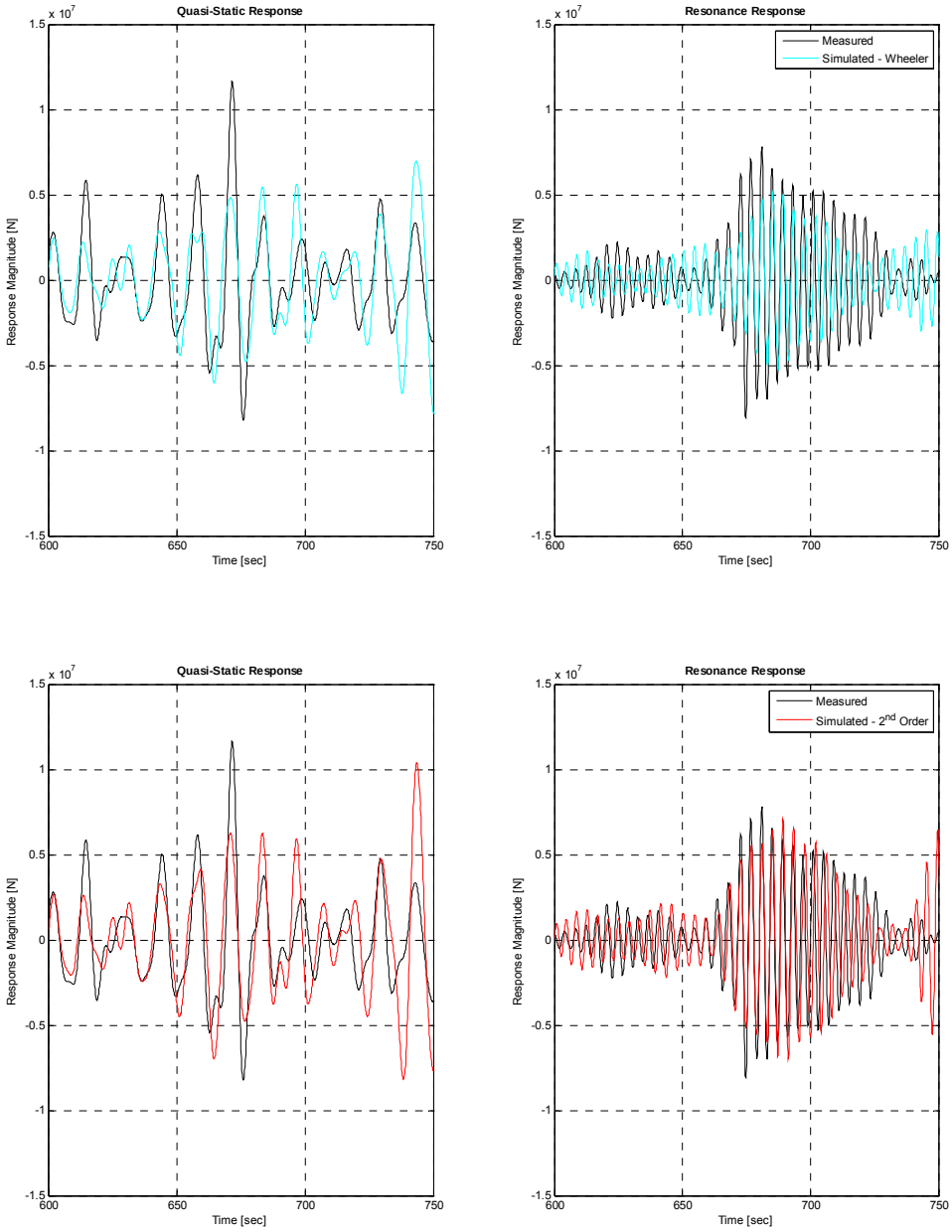

Figure 4. 7 Quasi-static and resonance response A2 (-108 m) event 200401011200 (t = 600 – 750 sec)

From the above figures, it can be seen that the total axial response is under predicted by all simulation models at t = 672.5 sec. After separating the quasi-static and resonance part of the response, it can be seen that the same phenomenon happens on the quasi-static part where the simulations under predict the response that occur. The dynamic response is represented considerably well by the second order model, while simulation using Wheeler kinematics still shows under prediction.

Another odd event on this 20-minute series appears at time window 950 – 1000 sec. In contrast with the previous odd event, this time the simulation yields a higher value of response than the one measured on field.

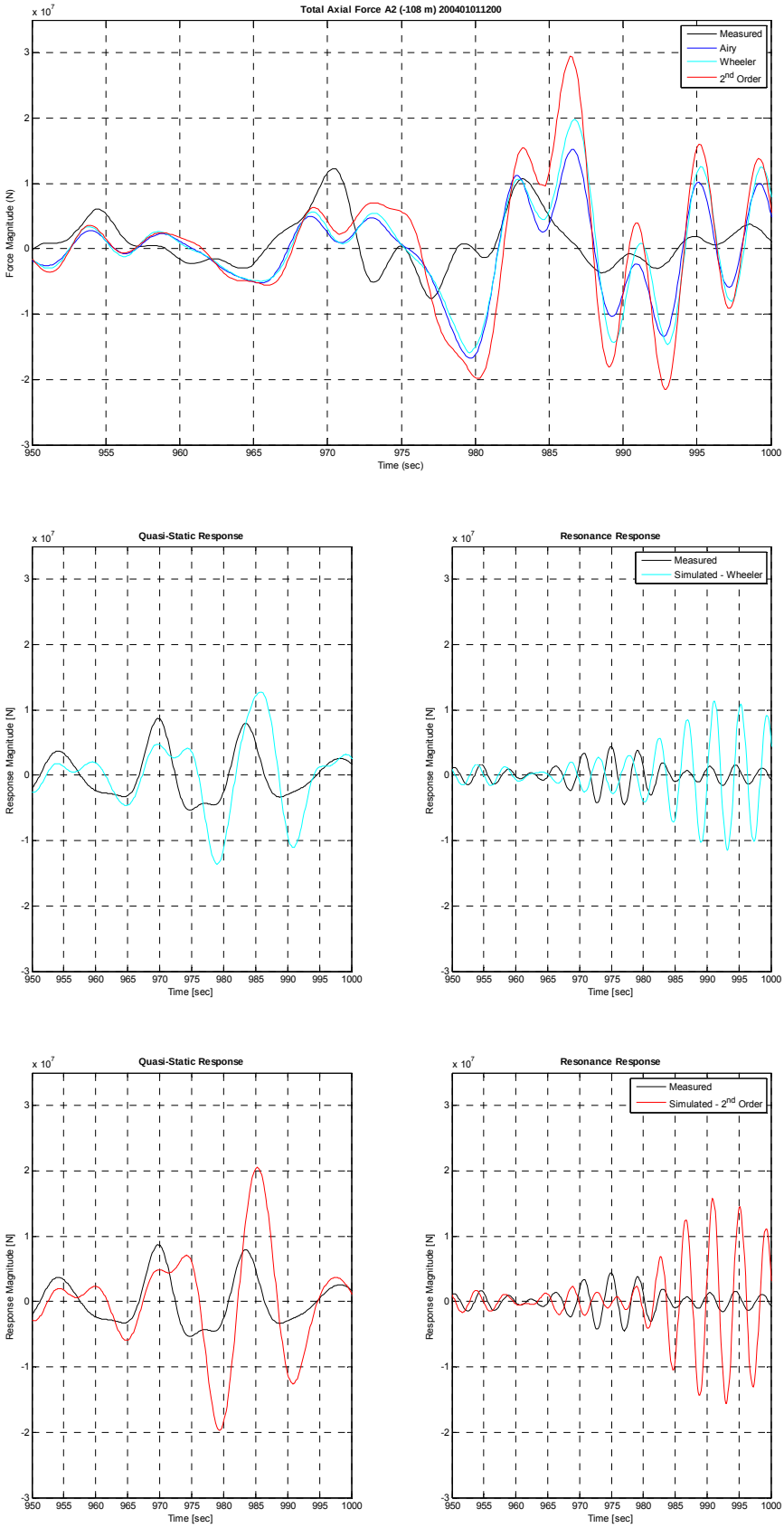

Figure 4. 8 Axial response Leg A2 (-108 m) event 200401011200 (t = 950 – 1000 sec)

From the above figure, it can be seen that the simulation highly under predicts the measured response. The most interesting part can be found on the dynamic response. Simulation shows a significant dynamic response of the structure, while the measurement not.

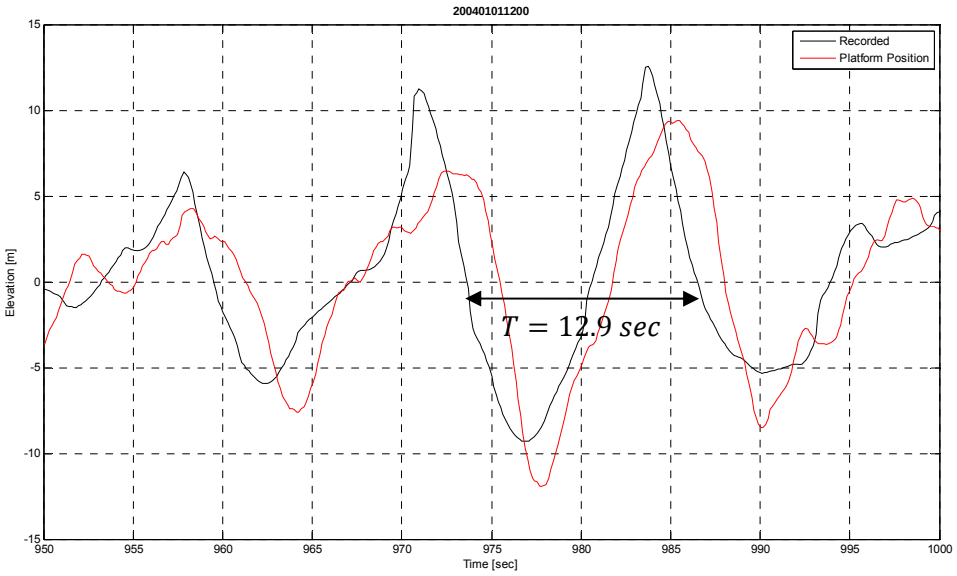

Figure 4. 9 Recorded (second order) wave elevation at sampling point (radar position) and predicted at platform location

The maximum over prediction happens at t = 986.4 sec. Predicting the wave elevation at platform location by using the aforementioned method, one can see that at time window 980-990 sec, the wave crest in the platform location should be lower than the measuring point. However, the predicted crest height is still more than 8m. The maximum measured wave crest at this time window is 12.53m while the predicted crest at platform location is 9.418m. In this condition, some horizontal bracings will be exposed to wave. It is then understandable if the result of simulation is high. This can also answer the highly dynamic behavior on the simulation. On the other hand, the real response is not that high. This may mean that the wave crest at the platform position is actually lower than predicted as a result of the irregular shape of wave.

There is randomness in the behavior of waves. This includes the shape and direction of the propagating wave which may depend on the wind, water depth, and obstructions (such as platform legs). For the over prediction case, wave in the shape of pyramid may have been occurred. In addition, at this point of time, the displacement of the top of the jacket is Δx = -37.081 m and Δy = 36.31 m which suggests that the wave that hits the platform is in the direction of 135.6° relative to the positive x-axis of the platform coordinate system (ref. Figure 2.2) not 65° as the analysis model assumes.

This may bring to a possible reason of over prediction which is that even though the elevation measured at the sampling point is high (high crest), the opposite happens at the platform location. Assuming long crested waves, the following illustration can be used to ease the comprehension. Note that the wave length predicted from the zero

crossing period (12.9 sec, Ref. Fig. 4.9) by using the formula $\lambda = gT^2/(2\pi)$ is predicted to be 260m.

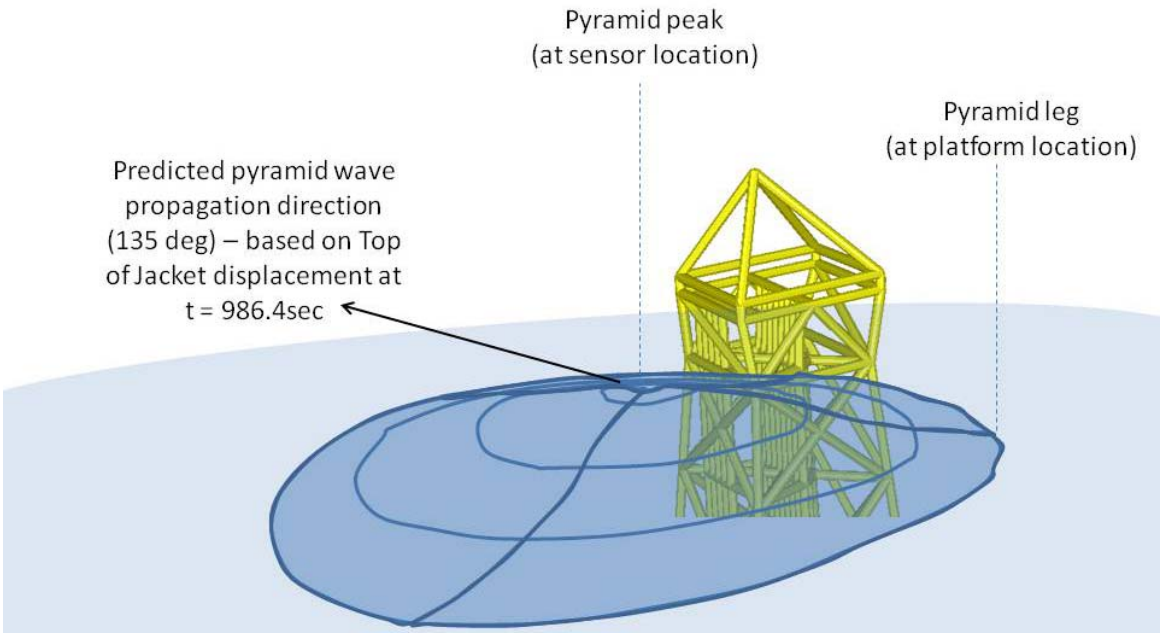

Figure 4. 10 3D Illustration of pyramid wave that is causing over prediction

Despite this over prediction, focus will be emphasized on the under prediction of the real response of the platform. The following part of this chapter will discuss the statistical distribution of global maxima during the events where the response is under predicted.

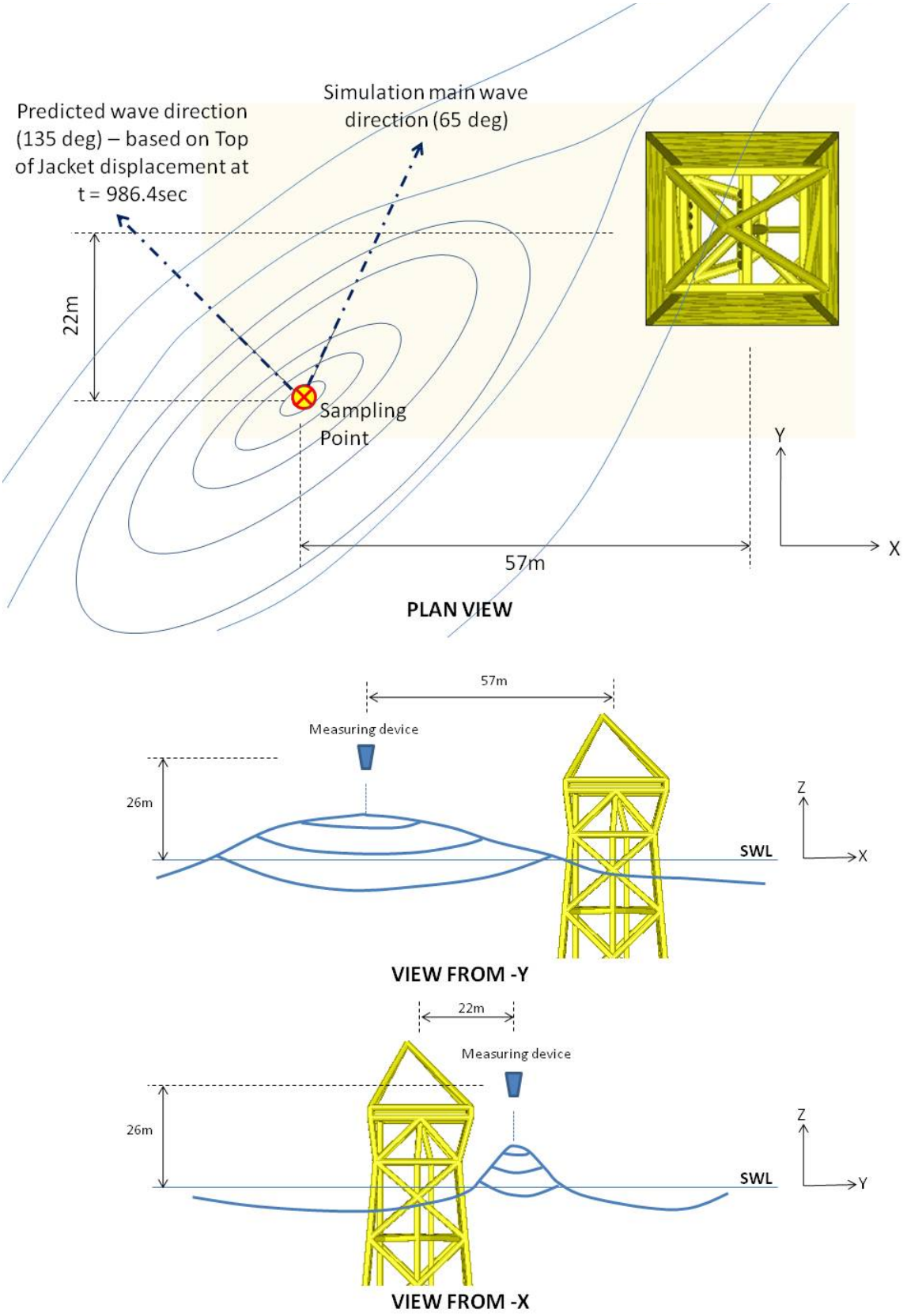

Figure 4. 11 Possible wave condition that causes over prediction at 200401011200

4.3.2. Event 200401011400

This event is simulated with the estimated wave direction of 75 degrees (Økland O. D., 2009) relative to the positive x-axis (ref. Figure 2.2).The cut-off frequency between quasi-static and dynamic force is 0.2 Hz. Band pass filter is utilized and the windows are:

- Quasi-static : 0.03 Hz – 0.2 Hz
- Resonance : 0.2 Hz – 0.5 Hz

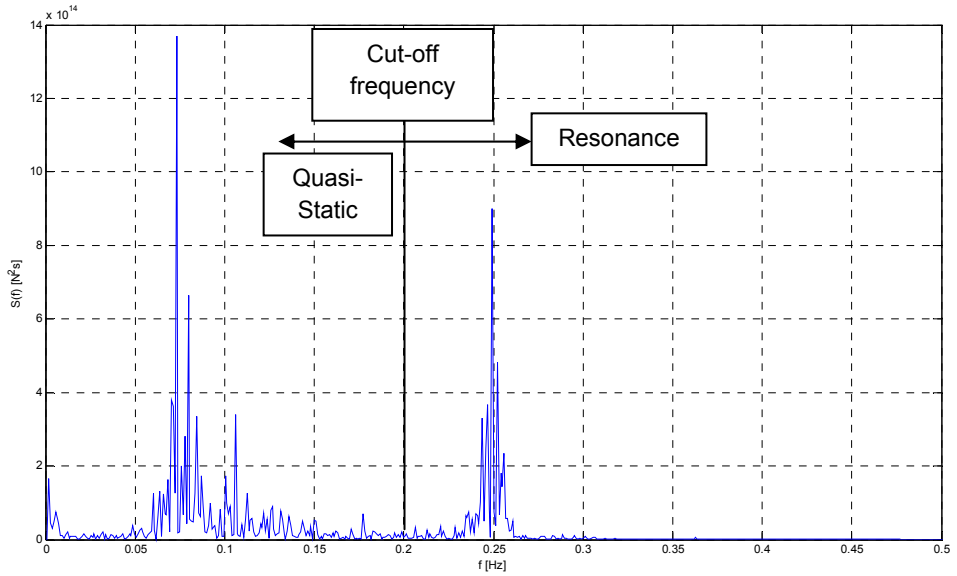

Figure 4. 12 Spectral plot for axial force at A2 (-108 m) event 200401011400

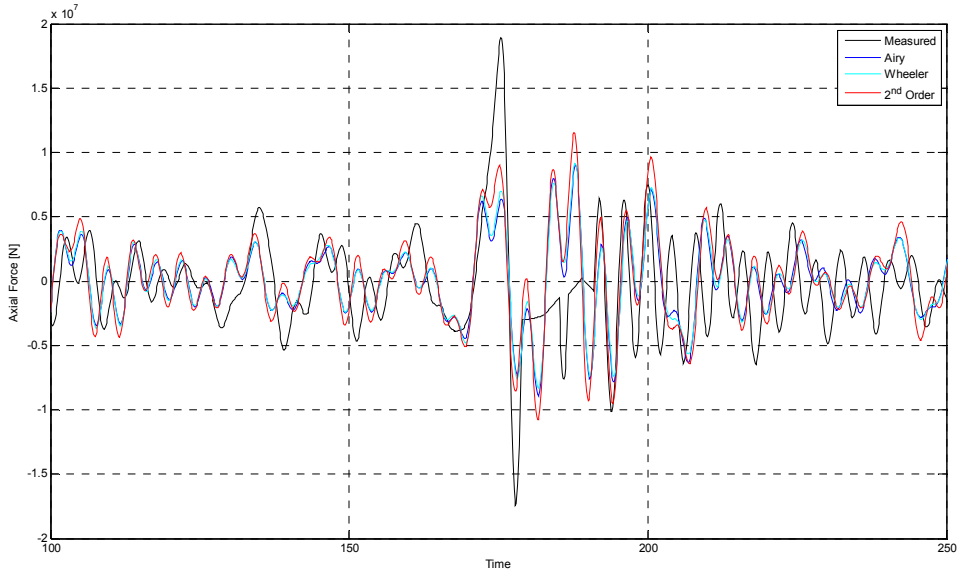

Figure 4. 13 Total axial response Leg A2 (-108 m) event 200401011400

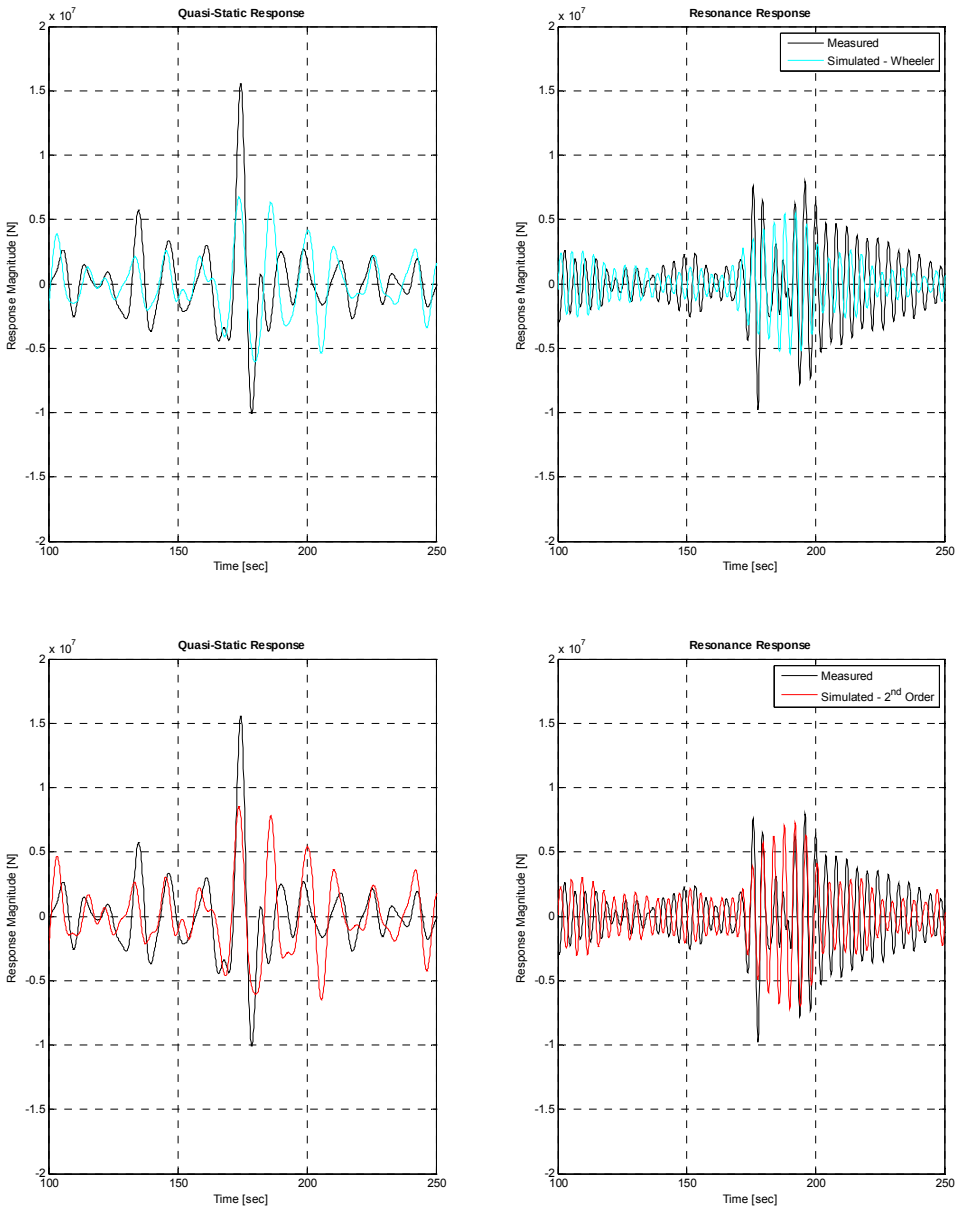

Figure 4. 14 Quasi-static and resonance response A2 (-108 m) event 200401011400

All simulation models under predict the total response. For this event, both Wheeler+second order surface and 2nd order kinematics+linear surface do not represent the dynamic resonance response well enough. The measured dynamic response shows an impact-like response at t = 175.9 sec and t = 196 sec. For the quasi-static response, simulations under predict the measured response.

Observing the measured total axial response, it can be seen that the measurement record shows some odd values when the response is plotted against time. This is deemed as a local measurement error. The rest of the measured response in the time series is considered to be valid and not affected by this error which might be caused by equipment error. To verify this, the following figure as a comparison of measured axial force on leg A2 and B1 shows that the measured responses on both legs have similar

behavior apart from the local error at leg A2. Leg A2 and leg B1 is located in the opposite location so it is reasonable to see that the response on these legs mirrors each other. Response in the main wave direction should behave like this: if leg B1 is in tension, then leg A2 will be in compression, and vice versa. Refer to Fig. 2.2 to see the position of these legs.

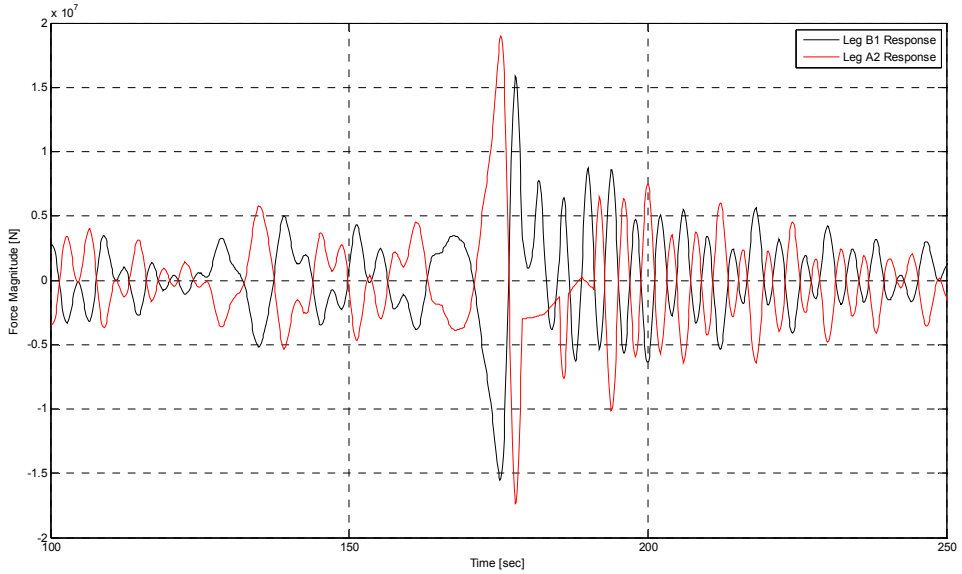

Figure 4. 15 Measured axial force on leg B1 VS leg A2 - 200401011400

4.4 Global Maxima Distribution of Response History

In order to determine whether simulations are statistically conservative or not, distribution of global maxima will be observed. Here, for the response time series, global maxima will be determined and the result from measured and simulated response will be compared. The term “global maxima” refers to the maximum response between zero upcrossing response values.

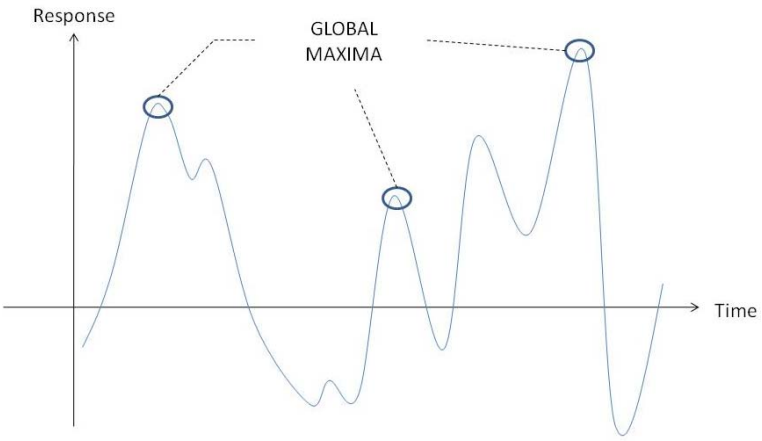

Figure 4. 16 Definition of global maxima

4.4.1. Global maxima distribution on 200401011200

The following figures show the distribution of maxima for event 200401011200. The data is fitted into Weibul paper which is deemed a good statistical model for the responses.

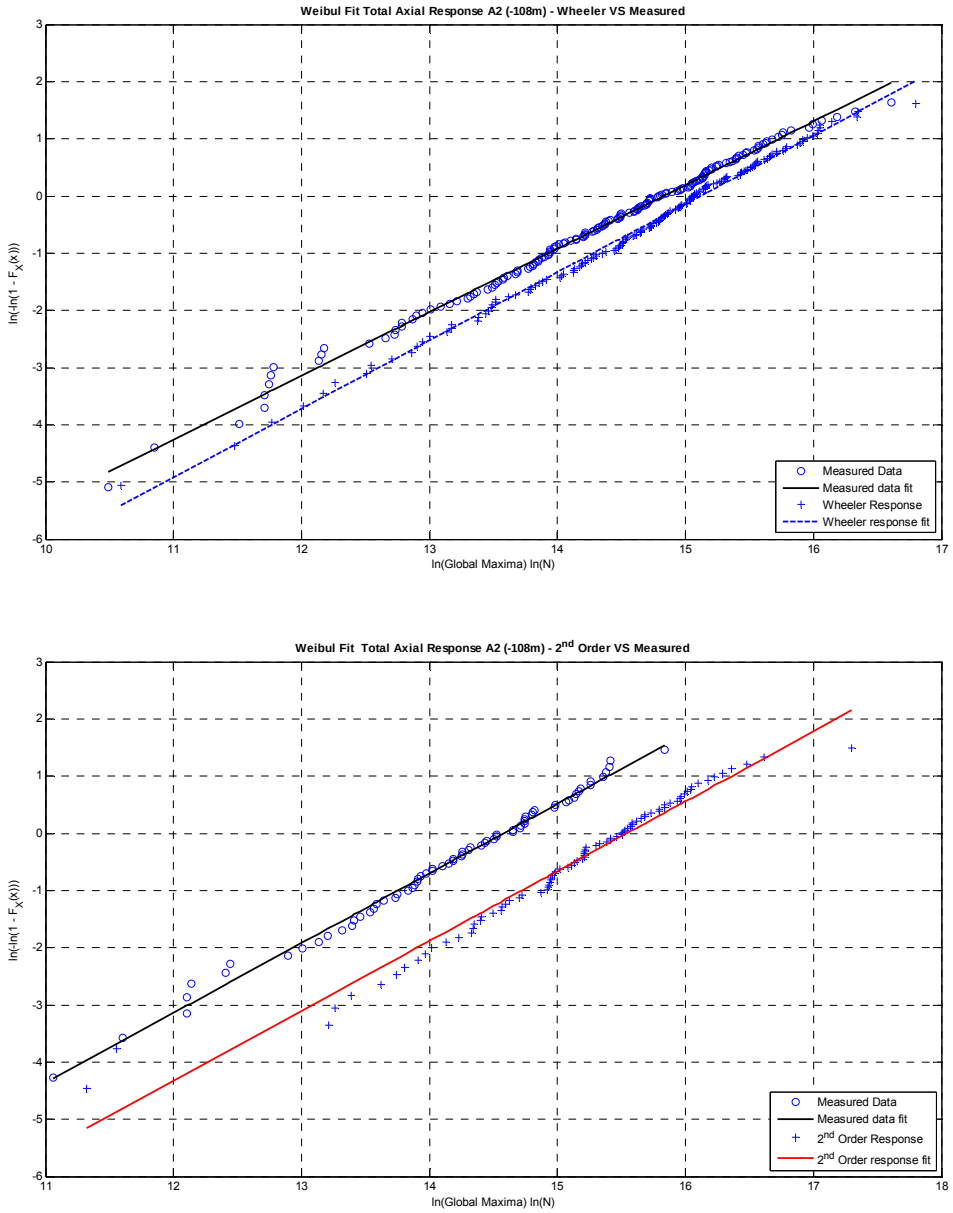

Figure 4. 17 Global maxima distribution (total axial response) leg A2 (-108m) 200401011200

From the above figure, it can be inferred that statistically speaking, simulation by using Wheeler kinematics and second order surface is conservative to be adapted. For a given percentile, the response obtained from simulation is higher than the measured one. Second order kinematics combined with linear surface condition even gives a more conservative result.

When the quasi-static and dynamic response of the structure is separated, the simulation result shows a conservative prediction of the dynamic response. Quasi-static response is under predicted on the upper tail of the Weibul plot. This constitutes that one should be careful in assessing the quasi-static response. This constitutes that there may be a loading mechanism that is causing quasi-static response which is not being captured in the simulation of this event. Quasi-static response can be caused by a steady load. For

offshore jacket, wave load without breaking may be considered as a steady load. Since the response is proportional to the wave crest height, there might be an under estimation of wave crest height on the platform location. Thus, under prediction of the response happens. In the next chapter, a modification of wave crest and/or trough is done to investigate the possibility of under estimated wave height on platform location.

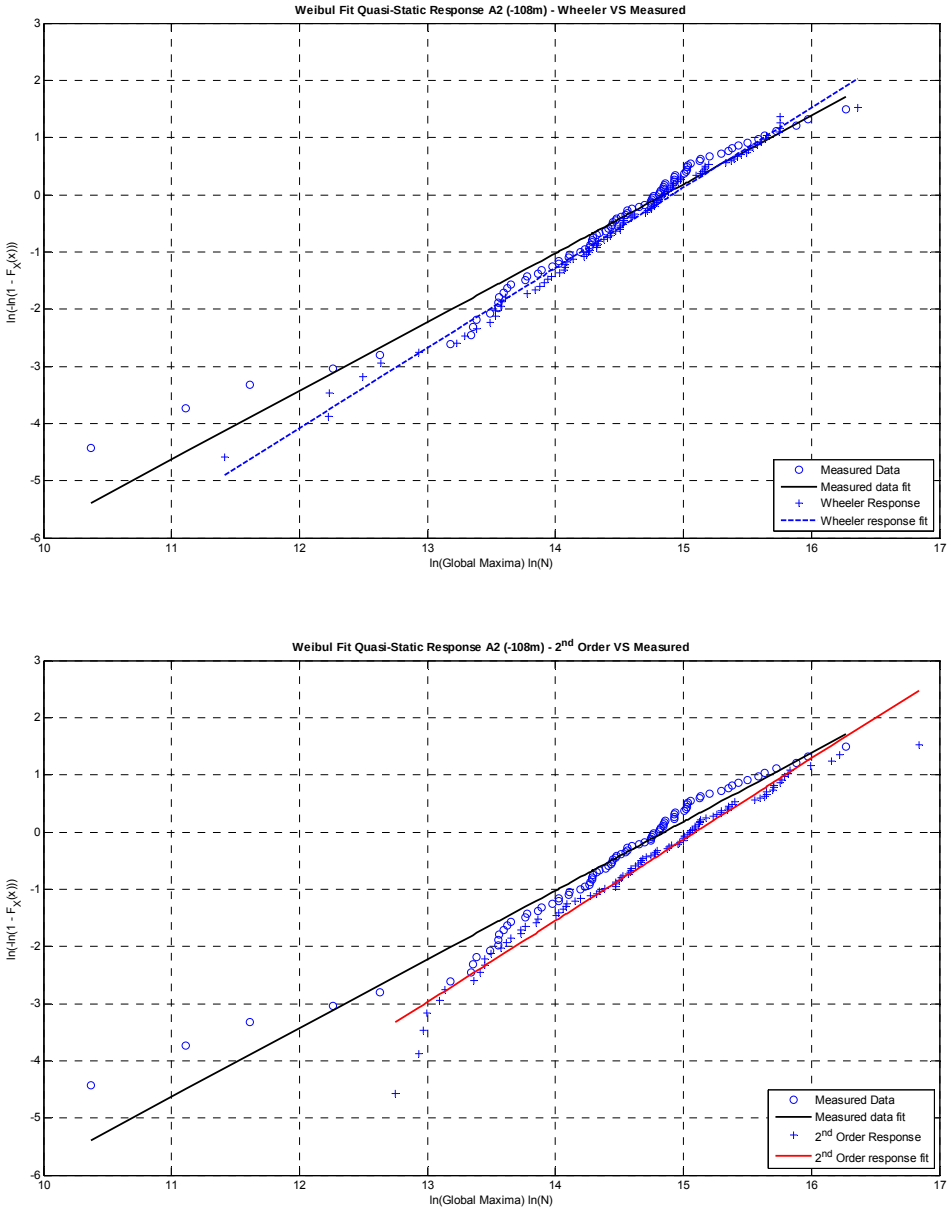

Figure 4. 18 Global maxima distribution – Quasi-static plot – 200401011200 leg A2 (-108m)

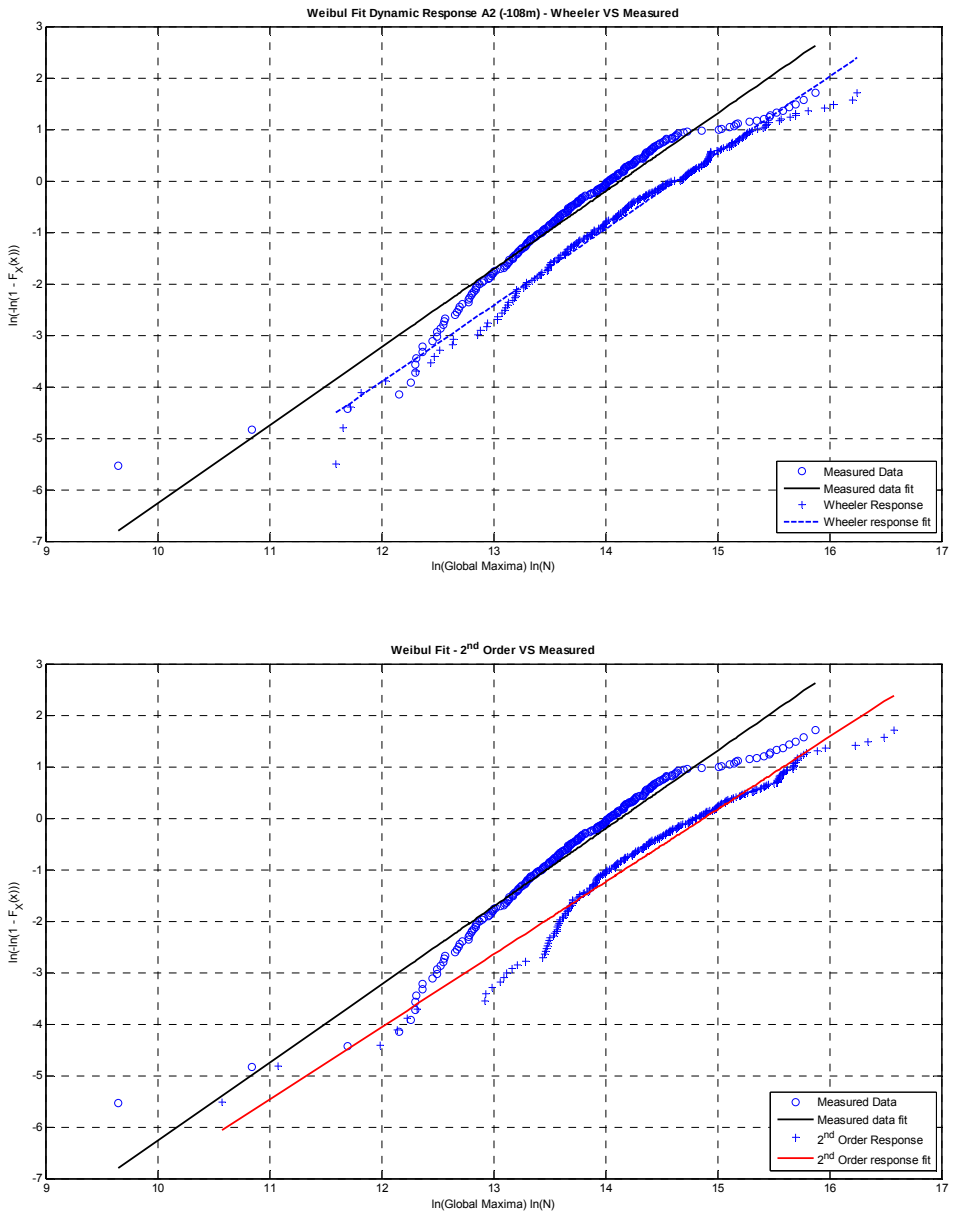

Figure 4. 19 Global maxima distribution – Dynamic plot – 200401011200 leg A2 (-108m)

4.4.2. Global maxima distribution on 200401011400

The following figures show the distribution of maxima for event 200401011400. The data is fitted into Weibul paper which is deemed a good statistical model for the responses. Wheeler stretching combined with second order surface will not be conservative in this case, but second order kinematics together with linear surface condition will give a conservative prediction in terms of the total response.

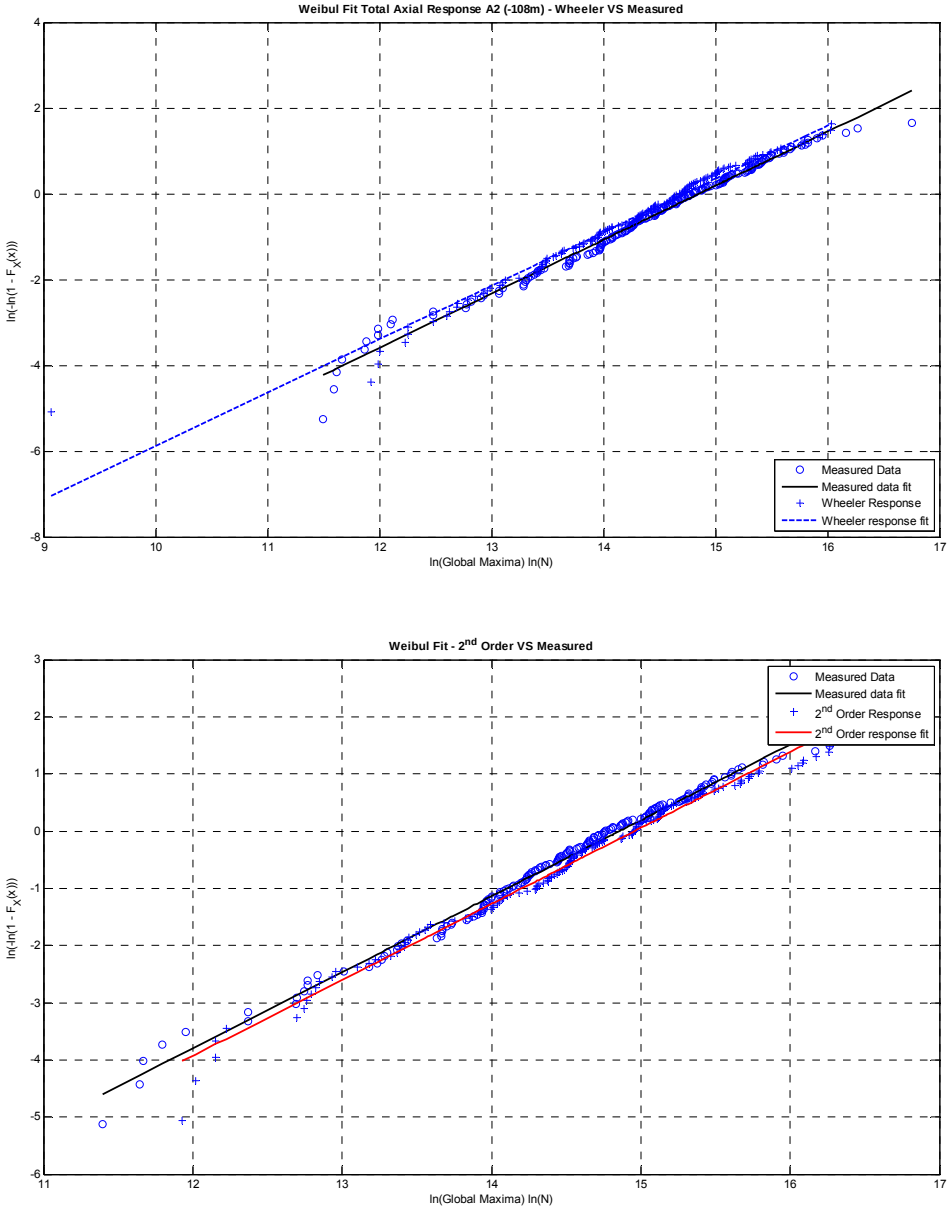

Figure 4. 20 Global maxima distribution (total axial response) leg A2 (-108m) 200401011400

When the quasi-static and dynamic response is separated, it can be seen that for the quasi-static force, both simulations are conservative. In this case, the second order kinematics combined with linear surface gives a more conservative result.

For the dynamic response, Wheeler stretching with second order surface gives a non conservative result. The simulation under predicts the response. The second order kinematics combined with linear surface condition gives a conservative result on the upper tail of the Weilbul distribution. Since the high fractile is the main interest in the analyses, using 2nd order kinematics is favorable in this case. The under prediction might be caused by the presence of dynamic loads which are not captured by the simulations. These loads may exist in form of impact from breaking waves. In the next chapter, a

discussion on response of the structure due to impact from breaking waves will be presented.

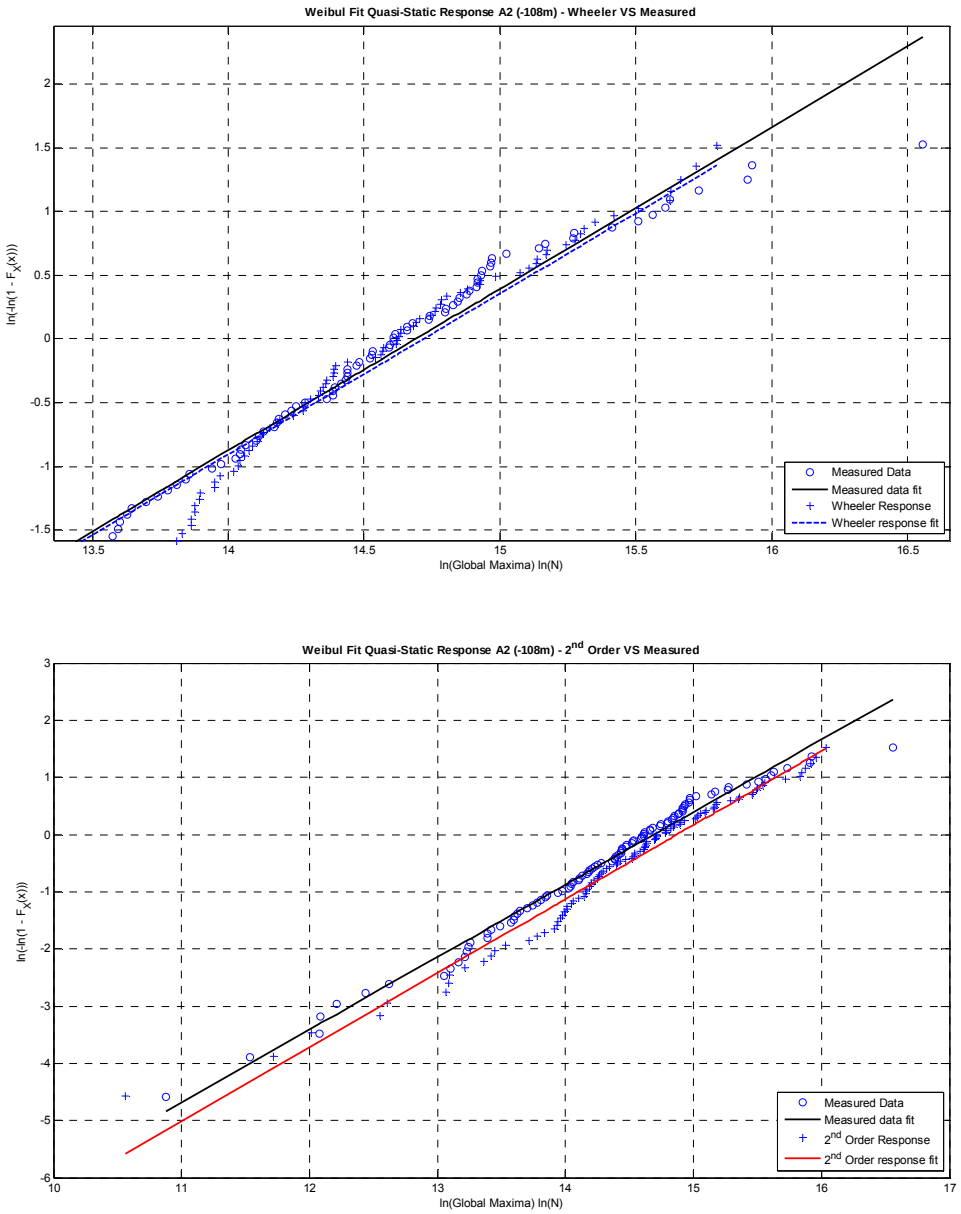

Figure 4. 21 Global maxima distribution – Quasi-static plot – 200401011400 leg A2 (-108m)

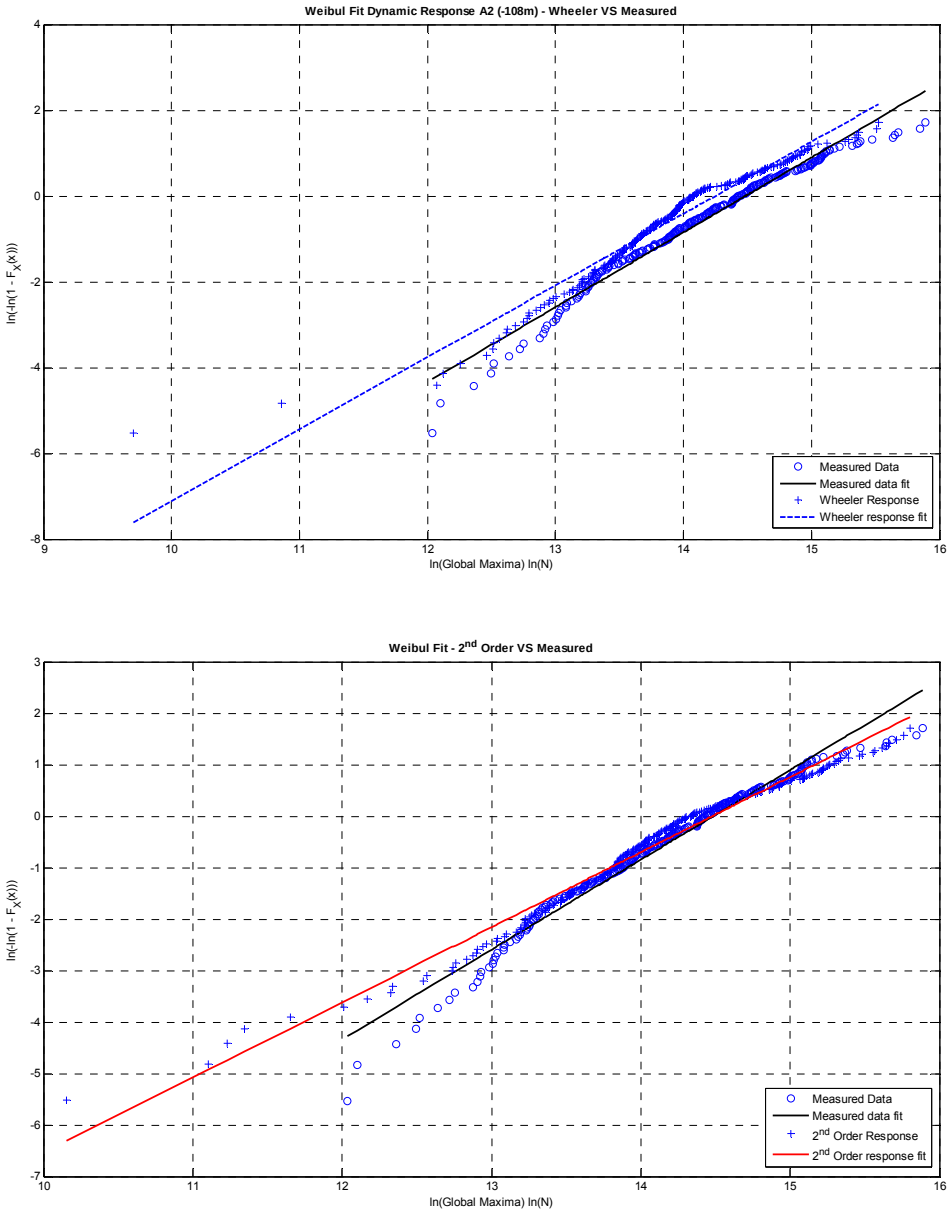

Figure 4. 22 Global maxima distribution – Dynamic plot – 200401011400 leg A2 (-108m)

Chapter 5
An Insight to other Possible Causes of Odd Events

5.2 Wave Height Modification

5.1.1. Crest and Trough Modification

The intent of this effort is to see the corresponding wave heights that give or approximate the measured response values. Modification is done by adding some meters of wave elevation to the measured wave elevation at a time frame when odd events occur. After some trials, the following wave modifications are obtained:

- Wave 200401011200
  Increase wave crest and decrease trough at time frame 668.6 sec to 680.7 sec as much as:
  a. 3m (case 1)
  b. 4m (case 2)

- Wave 200401011400
  Increase wave crest and decrease trough at time frame 172 sec to 184.2 sec as much as:
  a. 2m (case 1)
  b. 3m (case 2)

The modified wave profile can be seen on the following figure:

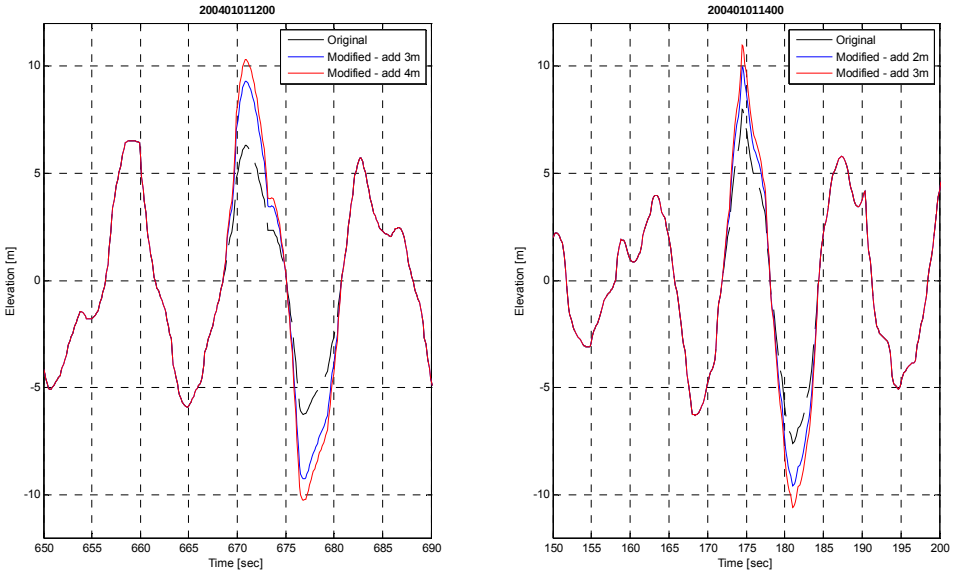

Figure 5. 1 Wave crest and trough modification

Such modification gives steeper waves if compared to the original data. The analysis result for the corresponding time instance has shown that higher response values are obtained. The results can be seen on the following figures:

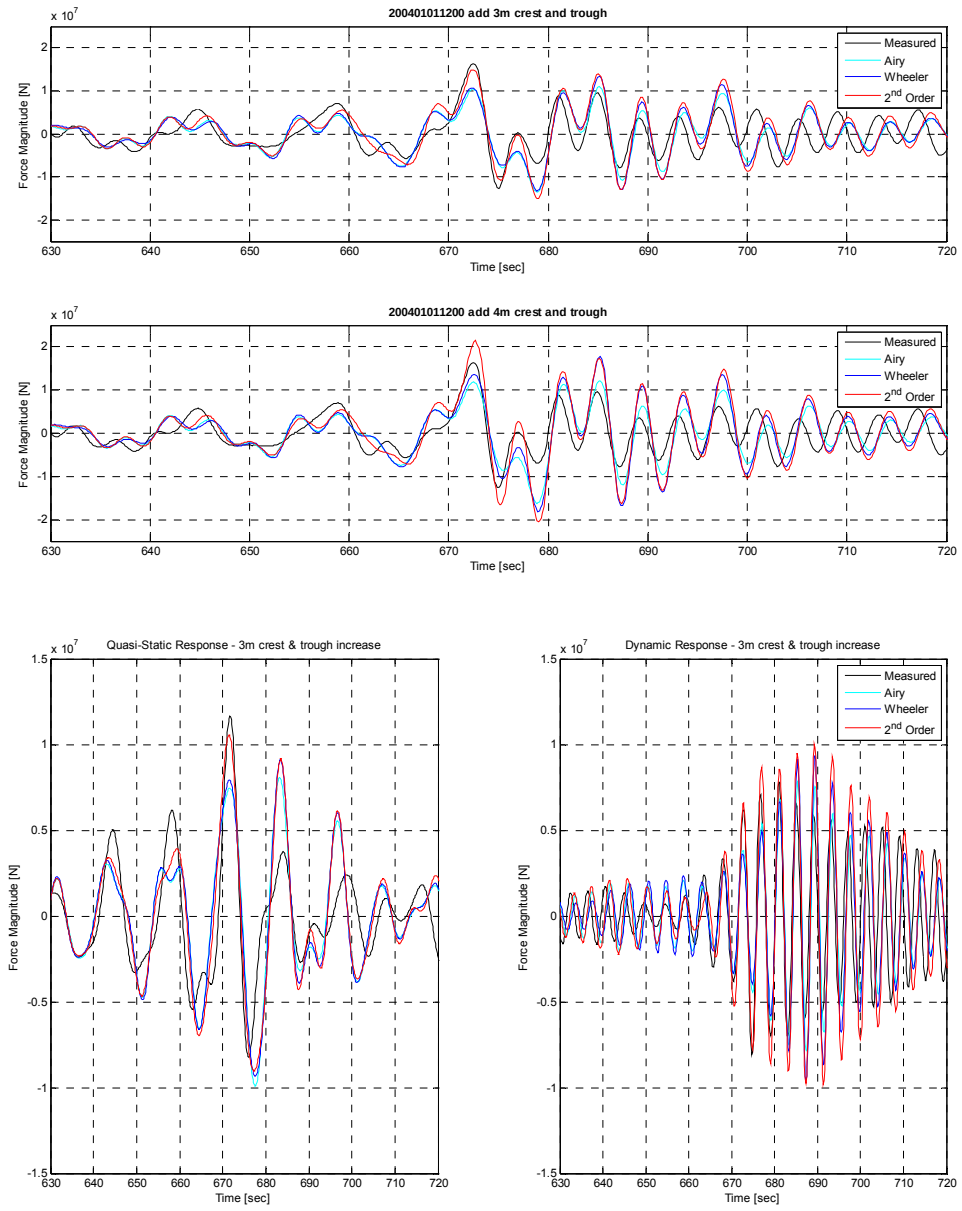

Figure 5. 2 Response due to wave modification on record 200401011200 – Leg A2 (-108m)

For the 200401011200 event, from the above figures, it is observed that to be able to reach the value of measured total axial response, there has to be an increase in the measured wave height in the range of 3 to 4 meter. With 4m increase, second order model will give higher result than the measured response, while Wheeler and Airy still under predict the response but approach the value of measured response quite well. The quasi-static response can be simulated by second order kinematics very well. The dynamic response is over predicted by both Wheeler and second order kinematics analysis, but the measured response behavior is resembled well enough by both Wheeler and second order analysis.

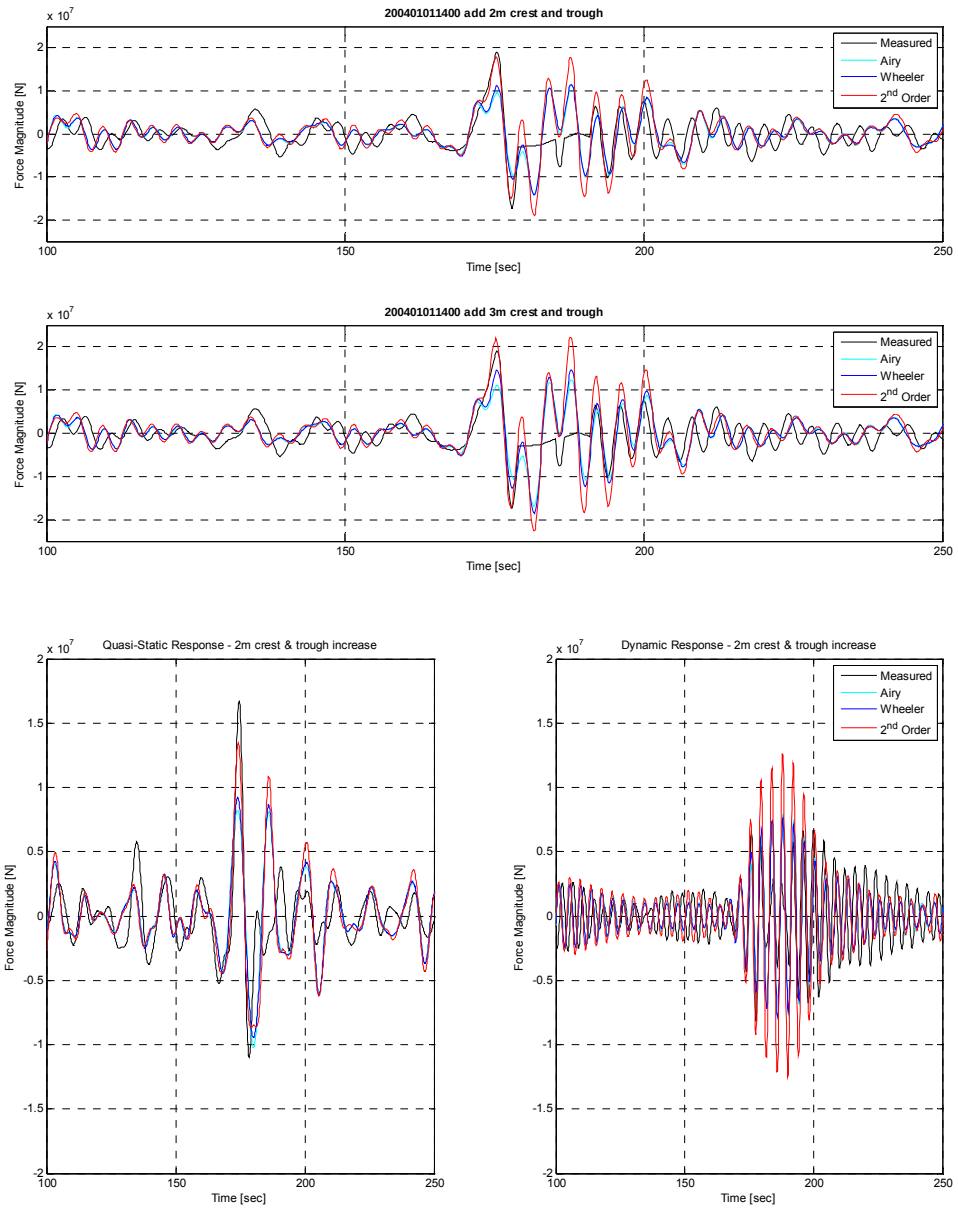

Figure 5. 3 Response due to wave modification on record 200401011400 – Leg A2 (-108m)

For the 200401011400 event, from the above figures, it can be seen that by modifying the measured wave crest and trough by 2 to 3m, the simulated total axial responses can represent the measured total axial response very well especially for the second order model which is just slightly different than the measured response. Similar with the previous event, quasi-static behavior is represented well by the second order kinematics simulation, while the dynamic behavior is over predicted by all kinematics models.

In general, it is observed that by modifying the wave crest and trough, the total and quasi-static response can be represented by the simulation very well. The dynamic response is over predicted but the behavior is represented reasonably well. There are uncertainties in the wave behavior thus dynamic accuracy is rather difficult to obtain when doing a comparison between measured and simulated response.

Increasing crest height and trough by 3-4 m on 200401011200 and by 2-3 m on 200401011400 results in wave crest of more 10 m height at the sampling point. For this situation, water hits the horizontal bracings which are located at el. +8m. This condition will add more resistance against the wave thus resulting higher response values. The following table presents the wave modification data that best simulates the measured response.

Table 5. 1 Wave crest and trough modification data

Wave Record	Original Elevation (m)		Increment (m)			Time Window (sec)	New Elevation (m)	
	Crest	Trough	Crest	Trough	Wave Height		Crest	Trough
200401011200	6.28	-6.23	3	3	6	668.6-680.7	9.28	-9.23
200401011400	7.97	-7.59	2	2	4	172.0-184.2	9.97	-9.59

The effect of modifying the measured wave record on the predicted wave elevation on the platform position can be seen by observing the wave elevation at leg B1. Here, leg B1 is chosen due to estimated wave direction. By using the wave direction which is 65 deg for event 200401011200 and 75 deg for event 200401011400, the first leg which will be hit by the wave is leg B1. These wave directions are relative to the x-axis of the platform system as can be seen on Figure 2.2. The following figures show the wave elevation measured at sampling point in comparison with the wave elevation at platform location after adding 3m of crest and trough on the originally measured record.

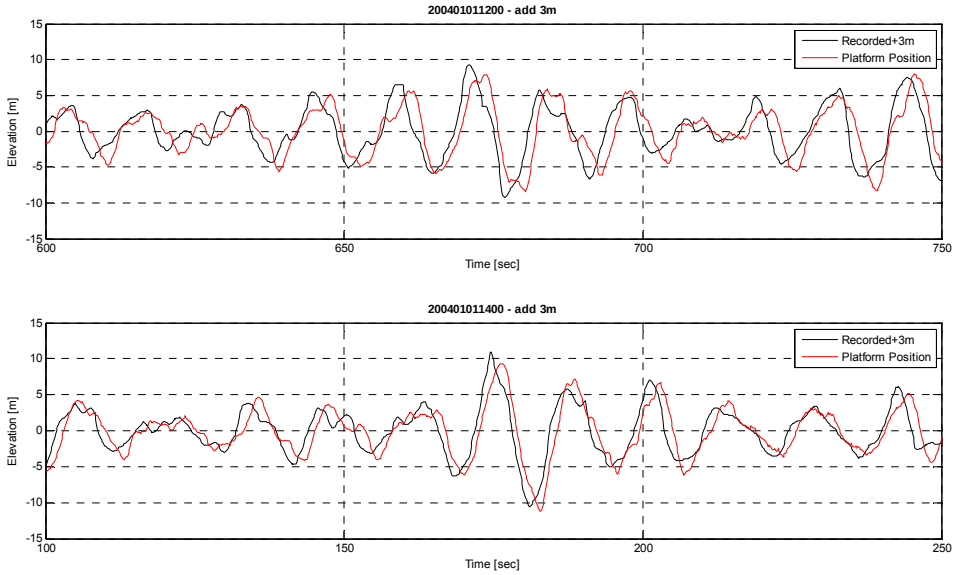

Figure 5. 4 Modified wave record at sampling point VS elevation at platform location (Leg B1) – Second order wave

The figure shows that the predicted wave elevations at platform location are (by the time odd events occur) lower than the wave elevation at sampling point. Even so, the wave crest at platform location is still around 8m which means that horizontal bracings will potentially be exposed to wave.

The wave pattern which is not captured by the measuring device in this case may be the reason why the odd events occur. Based on the discussion above, one can say that the wave crest measured at sampling point is approximately 3m lower than the elevation at platform location by the time odd events occur. The prediction of wave elevation by shifting the wave elevation from sampling point to platform location suggests that the wave elevation at platform location should be less than the one measured at sampling point. On the other hand, to obtain the value of measured response, higher wave crest should be imposed to the structure. This means that there is a highly irregular wave shape on this sea state where the wave crest at platform location is approximately 3m higher than the wave crest measured at sampling point.

A possible realization of wave profile is in form of a pyramid-shaped wave same as mentioned in the previous chapter. In this case, different scenario happens. The peak of the wave occurs on the platform location and not captured by the wave sensor. In propagating direction, wave height from sampling point decreases as predicted by shifting procedure, but on the platform position, there is a peak of wave happens. This is in the opposite scenario compared to the discussion on chapter 4. To ease the visualization of this kind of wave, the following figure gives an illustration.

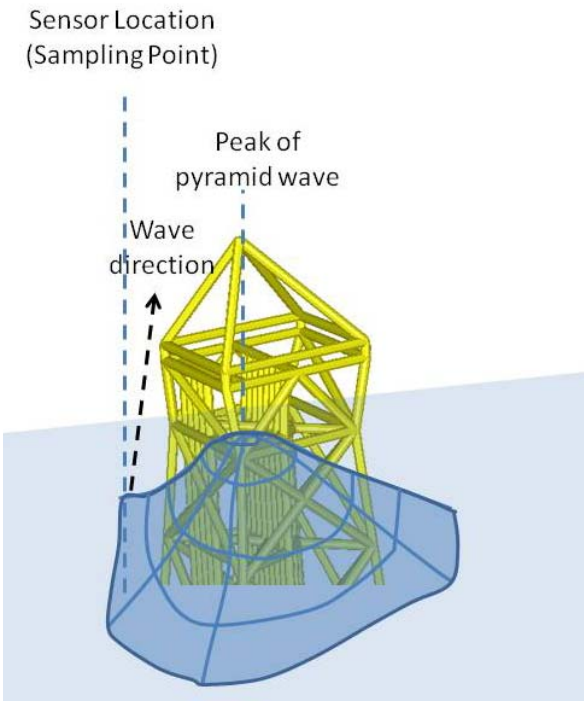

Figure 5. 5 3D Illustration of pyramid wave that is causing under prediction

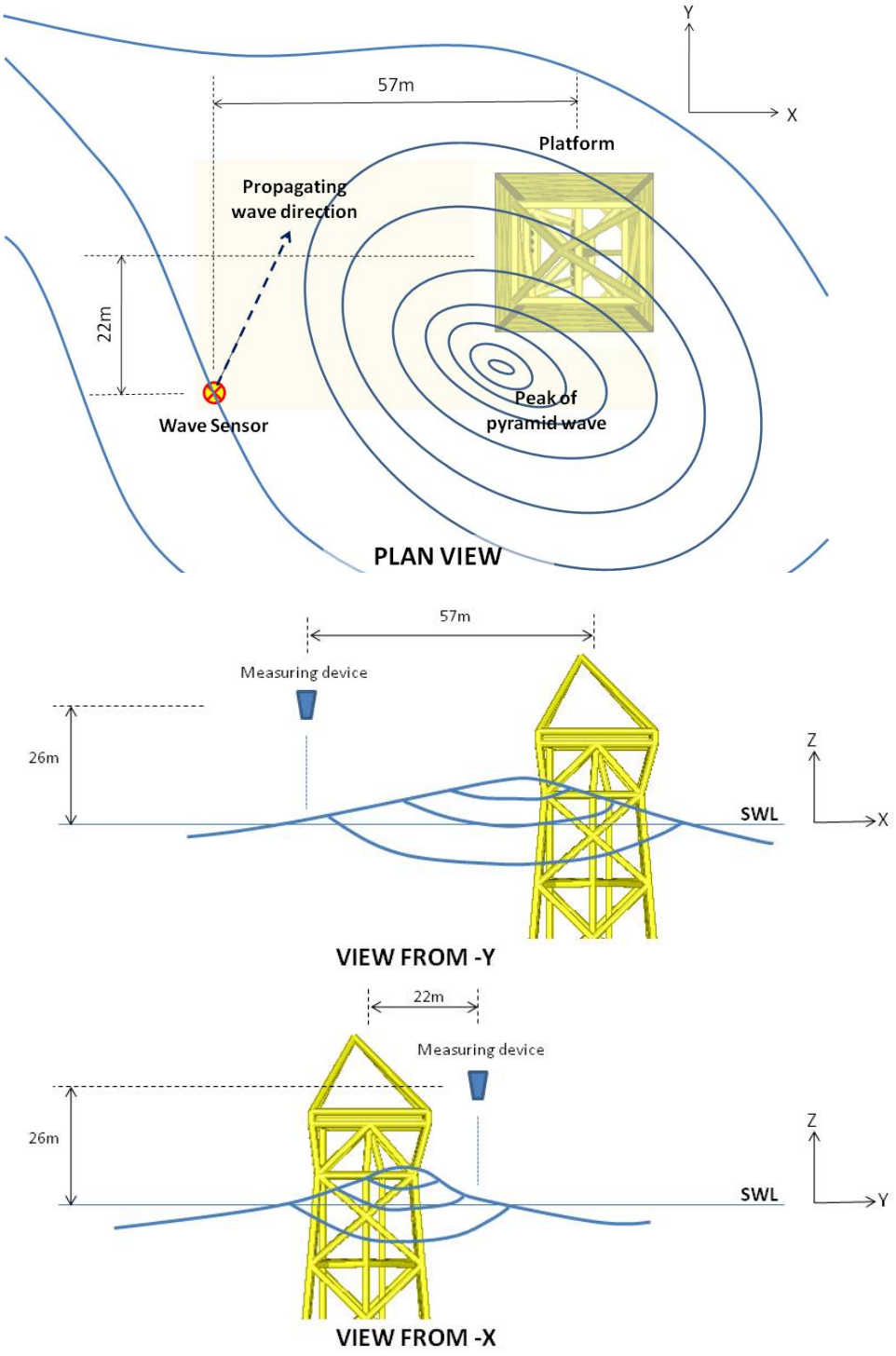

Figure 5. 6 Possible wave condition that causes under prediction

The wave behavior as illustrated on the above figure is so far hypothetical. By the time this thesis is written, the author did not find any literature related to the mentioned phenomenon. Future assessment and verification can be done on the existence of the mentioned wave phenomenon if deemed needed.

5.1.2. Modification of Crest Height only

On the above discussion, analyses are done based on adding some meters of wave height. Modifications were done to the crest height and trough elevation. In this part of the report, the effect of increasing the wave crest only will be discussed. Crest height of 3m will be added to wave record 200401011200 and crest height of 2m will be added to wave record 200401011400.

Table 5. 2 Wave crest modification data

Wave Record	Original Elevation (m)		Increment (m)			Time Window (sec)	New Elevation (m)	
	Crest	Trough	Crest	Trough	Wave Height		Crest	Trough
200401011200	6.28	-6.23	3	0	3	668.6-675.0	9.28	-6.23
200401011400	7.97	-7.59	2	0	2	172.0-178.1	9.97	-7.59

The modified wave record can be seen on the following figure:

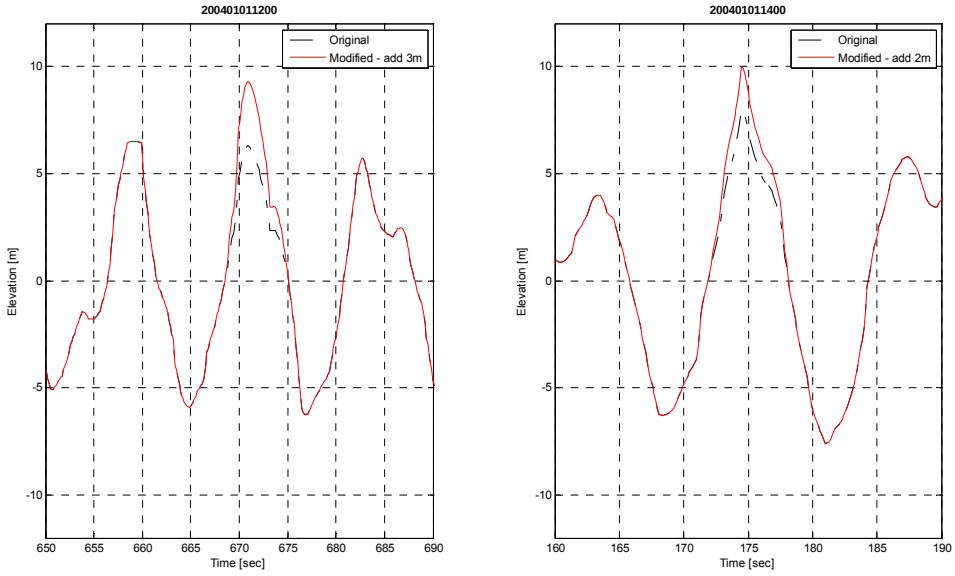

Figure 5. 7 Wave crest modification

The simulation results show that the second order kinematics can represent the total measured response very well. Even though the dynamic response is over predicted by the simulation, but the quasi-static responses are approximated very well by the simulations, even better than the previous effort of modifying both wave crest and trough. This means that the wave crest height is significant in predicting the structural response. The simulation results can be seen on the following figures:

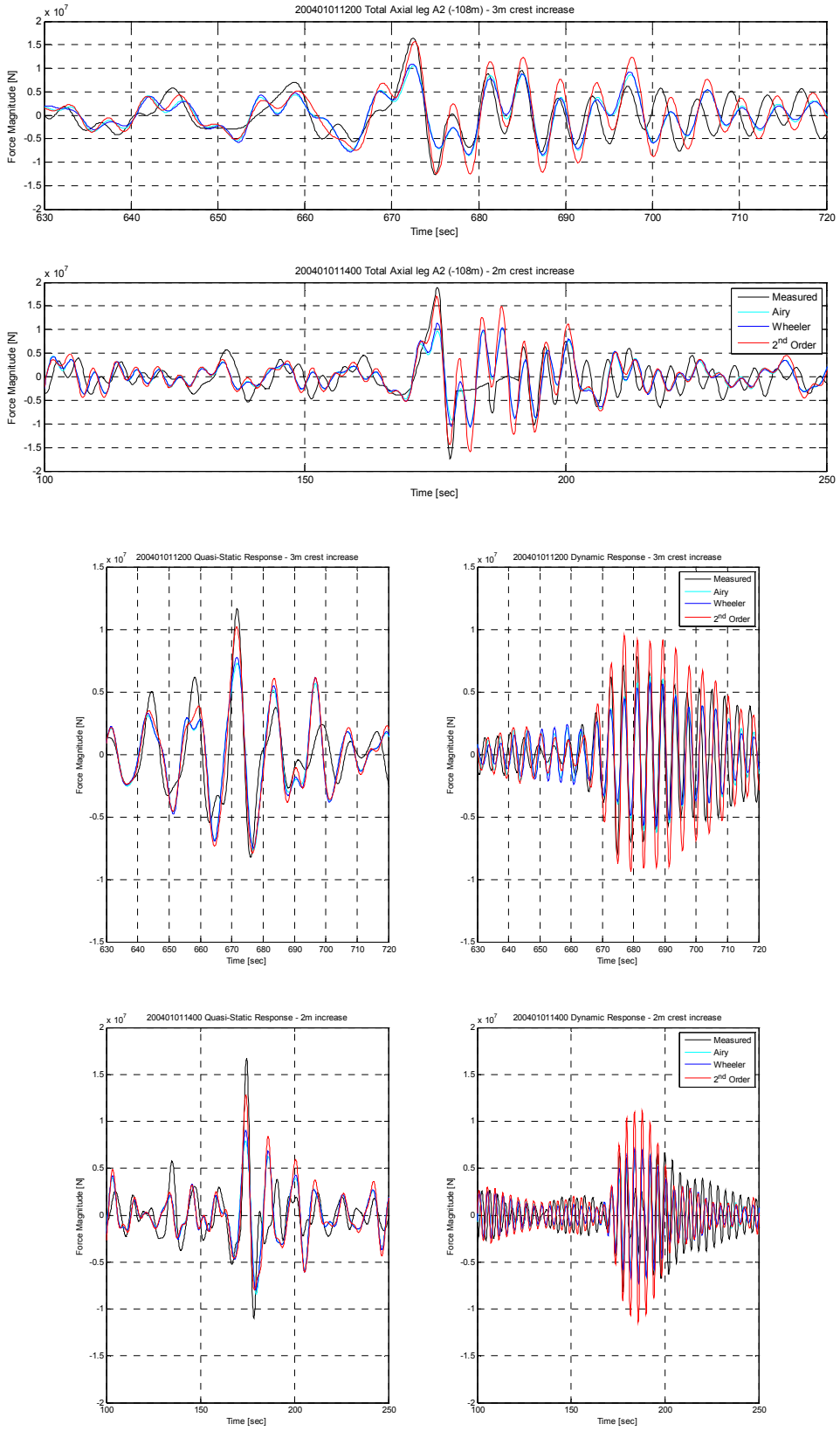

Figure 5. 8 Axial response leg A2 (-108m) due to wave crest modification

It is interesting to compare the result from the modification of crest and trough against the modification of crest only. Since the second order kinematics simulations are deemed to be representative in modeling the measured response, here the comparison of second order results is presented. Note that the following terms are used to address the wave modification scheme:

- Case A: Modification on wave crest only
- Case B: Modification on both wave crest and trough

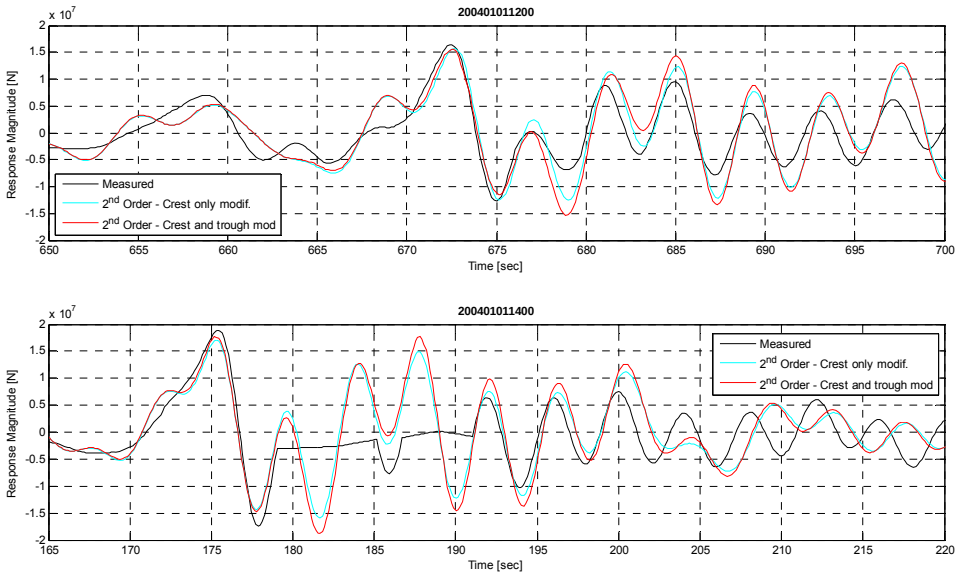

Figure 5. 9 Leg A2 (-108m) response: Case A VS Case B

It can be seen that the results from case A and B have no significant difference. However, modification of wave crest only gives a better estimation on the structural response. Increasing the crest height only may make the wave property similar to breaking waves where the horizontal asymmetry factor is high. Increasing both crest and trough keeps the horizontal asymmetry factor proportional with the original wave condition. More discussion about the horizontal asymmetry factor and other properties of breaking waves can be read in e.g. Bonmarin (1989) and Lader (1998). Just for illustration, the following figure explains what horizontal asymmetry (μ) factor is.

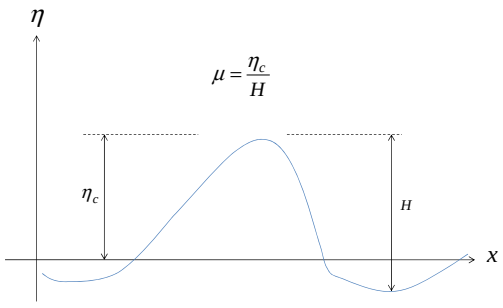

Figure 5. 10 Horizontal asymmetry factor (Lader, Grytøyr, Myrhaug, & Pettersen, 1998)

For the wave modification done in this study, the following wave horizontal asymmetry factor is obtained:

Table 5. 3 Horizontal asymmetry factor (μ) for modified wave

Case		η_c	H	$\mu = \eta_c / H$
200401011200	A	9.28	15.51	0.59
	B	9.28	18.51	0.50
200401011400	A	9.97	17.55	0.57
	B	9.97	19.55	0.51

For linear wave, the horizontal asymmetry factor, $\mu = 0.5$. It can be seen that case B in the analyses represents wave condition which is in similar form with linear wave. Case A shows an increase in wave horizontal asymmetry. However, the value of μ is still far from the breaking criteria for plunging breakers as indicated in the study done by Lader et.al. (1998). Lader's study indicates that the range of μ which is typical for breaking waves is around 0.85 to 0.95 (Ref. Fig. 5.11).

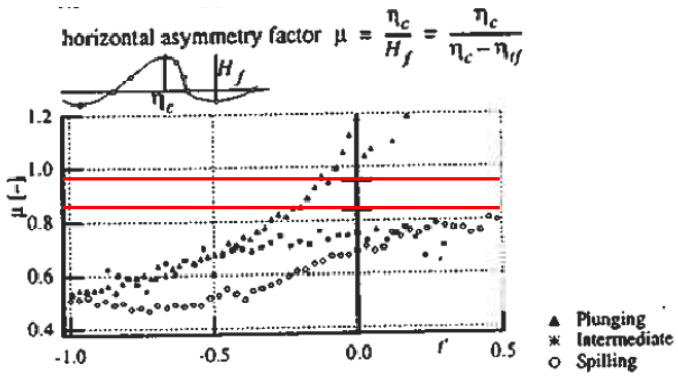

Figure 5. 11 Range of horizontal asymmetry factor (Lader, Grytøyr, Myrhaug, & Pettersen, 1998)

The red lines on the above figure indicate the interval that is typical for breaking waves (Lader, Grytøyr, Myrhaug, & Pettersen, 1998). Referring to Table 5.3. the horizontal asymmetry factors for the modified wave are not inside the range, thus breaking wave may not be the case here. However, impact assessment will be done for verification.

5.3 Impact Assessment due to Breaking Waves

When wave amplitude reaches certain critical level and steepness, there will be large amount of energy to dissipate. In this condition, the wave becomes unstable thus the so called breaking wave phenomenon happens. Since the wave particle on a wave crest is proportional to the height of the crest itself, increasing wave crest can make the particle velocity equals or even higher that the wave celerity. At the condition where the velocity of water particle is higher than the velocity of the wave profile, the wave starts to break.

There are four main types of breaking waves, which are (adapted from Wikipedia):

- Plunging breaker
- Spilling breaker
- Collapsing breaker
- Surging breaker

Plunging breaker is characterized by the existence of wave jet running from the wave crest. As the crest curls over and jet propagates on the wave direction, at some distance, the jet will hit the base of the wave and generate a considerable splashing effect. A lot of studies were done related to the behavior of plunging breaker due to the severity of its impact to offshore structures. This type of breaking wave is characterized by the steep and non symmetrical wave shape. For plunging breakers, the free surface velocity is expected to be higher than the phase velocity at the breaking point (Lader, Myrhaug, & Pettersen, 2000).

Spilling breaker or also known as whitecaps is characterized by the formation of foams on the front face of a wave crest. The process is gradual and the foam will last for considerable distance after the wave breaks. This type of breaker is the most common type happens in deep water. For this type of breaking wave, there is no significant change in wave symmetry. Surface velocity when approaching breaking point is increasing. The development of surface velocity for spilling breakers is pretty much the same with plunging breakers (Lader, Myrhaug, & Pettersen, 2000).

Collapsing breaker is the type of breaking wave which has a transitional characteristic between the spilling and plunging breaker. The wave front becomes steep but curls and jet are not created. As vertical wave front created, the wave breaks generating foams on the wave profile like spilling breaker does.

Surging breaker occurs on steep seabed profile, mostly on beaches. The waves do not break until they reach the shoreline. The form up process is pretty much like the plunging breaker but before the crest curls and jet falls, the wave toe surges to the beach forming foams.

For spilling and plunging breakers, as the wave propagates toward its breaking point, experiment (Lader, Myrhaug, & Pettersen, 2000) has shown the following properties of the particle velocity of breaking waves:

- Particle velocity increases at the surface
- Particle velocity at still water level is relatively constant

The following figure shows the development of wave kinematics for breaking waves:

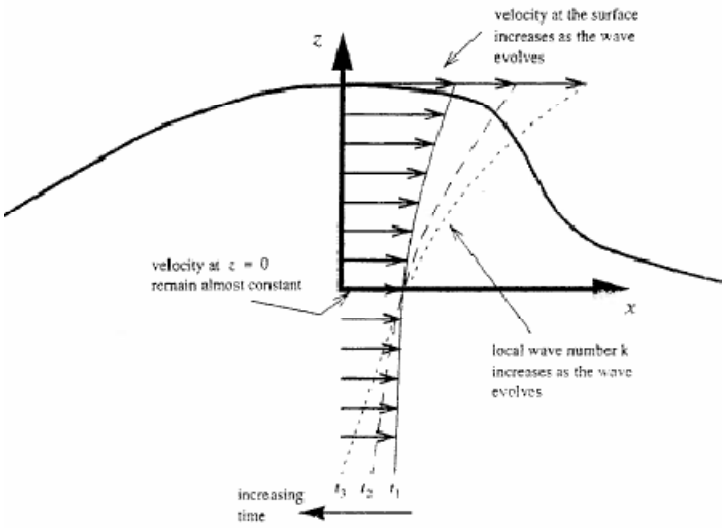

Figure 5. 12 Development of kinematics in the crest of breaking waves (Lader, Myrhaug, & Pettersen, 2000)

Illustrations for the aforementioned types of breaking waves can be seen on the following figure – adapted from Capital Regional District of British Columbia, Canada website (http://www.crd.bc.ca/watersheds/protection/geology-processes/Waves.htm):

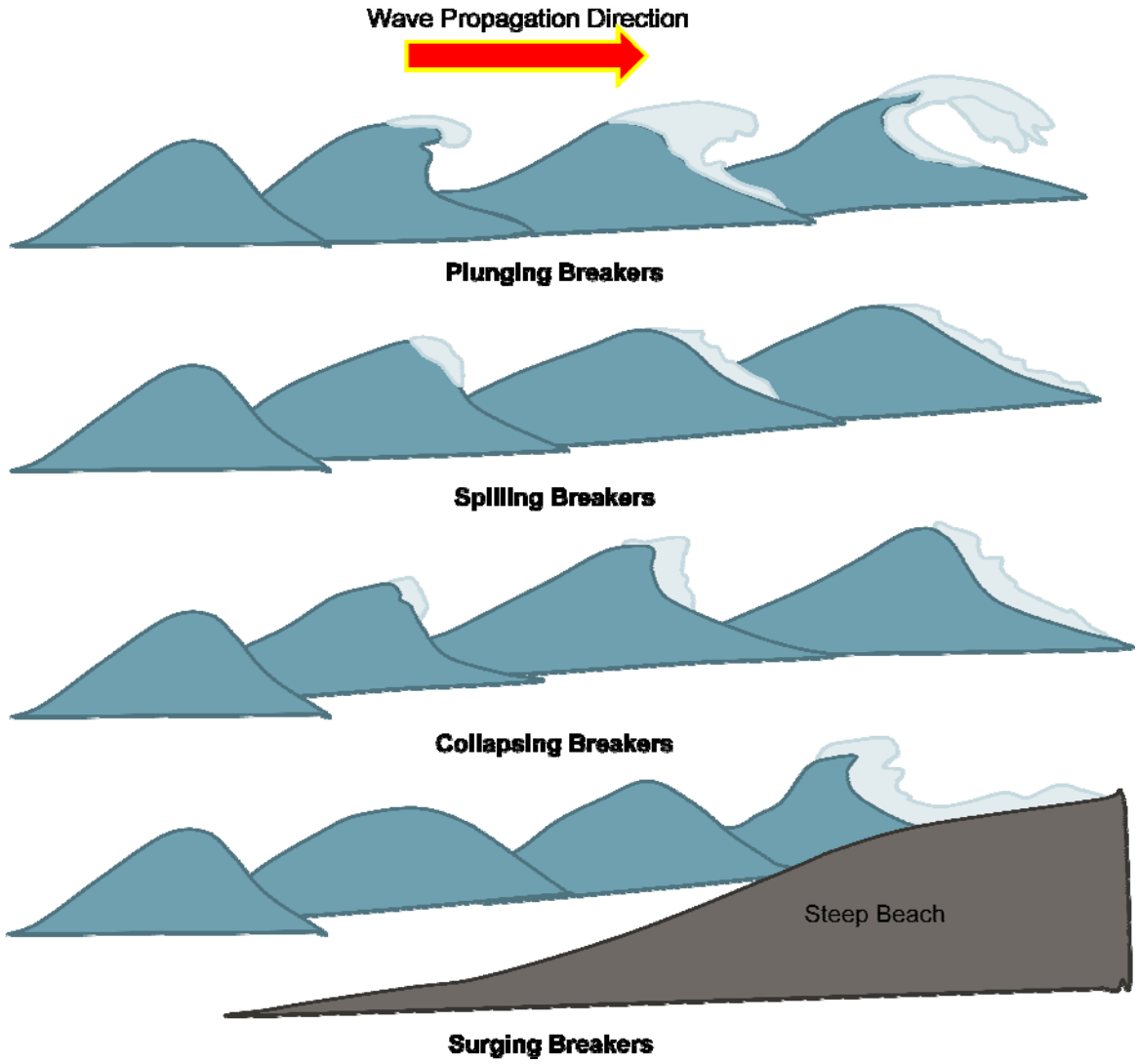

Figure 5. 13 Illustration of breaking waves

While near shore breaking waves may cause damage to coastal structure and enhance beach abrasion, offshore breaking wave may also cause damage to offshore structures due to the impact force. The impact is a rather localized phenomenon. Most of impact studies are related to the plunging breakers because this type of breaking wave is deemed to be more severe than the other types.

There are several criteria of breaking wave for example the global limiting wave steepness criteria (Massel, 2007). In this study, the selection of breaking wave on the wave record is merely based on location of wave record where response discrepancies happen. No other specific criteria were used.

5.2.1. Impact Assessment according to Wienke and Oumeraci Impact Model

The assessment of force on a cylinder mostly involved the utilization of Morison equation. This equation involves the contribution of forces from inertia and drag force. The inertia term of this equation related to the acceleration of the water particle while the

drag term is related to the quadratic value of the velocity of the particle. While it has been long used as an appropriate tool to predict load on a cylinder, the equation cannot represent the impact or slamming term which has been suspected to appear on the Kvitebjørn jacket structure. For this, Wienke and Oumeraci (Wienke & Oumeraci, 2004) mentioned that the impact term should be added to the original Morison equation as an additional term representing the short term load. Impact description in this subchapter will then be based on the proposed theory by Wienke and Oumeraci. The total wave force equation thus becomes:

$$F_{TOT} = F_M + F_D + F_I \tag{5.1}$$

The first two terms on the right hand side of the above equation are the terms taken from Morison equation while the last term represents the impact/slamming force. For a strip of the cylinder, dz, each term on the right hand side of the above equation is expressed by:

$$F_M(z) = \int_{-d}^{\eta} C_M . \rho . \frac{\pi D^2}{4} \dot{u}(z) dz \tag{5.2}$$

$$F_D(z) = \int_{-d}^{\eta} C_D . \rho . \frac{D}{2} u(z)|u(z)| dz \tag{5.3}$$

$$F_I(t) = \lambda . \eta_b . \rho . C_S . R . C^2 \left(1 - \frac{C}{R} t\right) \tag{5.4}$$

Here, C_M and C_D are the mass and drag coefficients. In the analysis of this study, these coefficients are taken based on NORSOK (NORSOK, 1999) recommendation. R is the radius of the cylinder and D is the diameter. C is wave celerity, $u(z)$ is the water particle velocity, and $\dot{u}(z)$ is the water particle acceleration. dz denotes the length of cylinder strip being considered. C_S is the slamming coefficient and ρ is the density of sea water. The term $\lambda . \eta_b$ represents the portion of wave height that is the breaker front or the impact area.

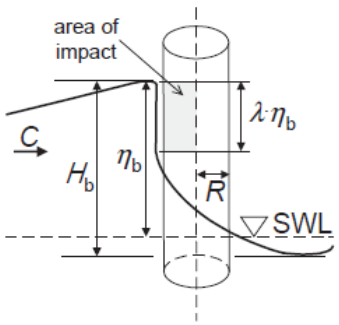

Figure 5. 14 Illustration of breaking wave parameters (Wienke & Oumeraci, 2004)

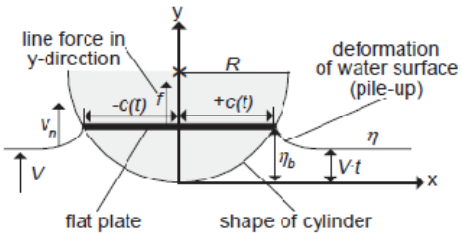

Figure 5. 15 Impact pressure plane idealization by a flat plate (Wienke & Oumeraci, 2004)

Equation (5.2) and (5.3) depend on the elevation while equation (5.4) is time dependent. The impact term (Eq. (5.4)) is developed from the theory proposed by Goda (Goda, Haranaka, & Kitahata, 1966) as cited by Wienke and Oumeraci (Wienke & Oumeraci, 2004). Goda's theory corresponds to the Von Karman theory by utilizing slamming coefficient, $C_S = \pi$. Wienke and Oumeraci propose a modification to Goda's theory by replacing Von Karman with Wagner slamming theory $(C_S = 2\pi)$. Both theories assume that pressure plane can be represented by a flat plate (Ref. Fig. 5.15, $V = C$). It is assumed that for breaking waves, the water particle velocity at the crest is close to the phase velocity, thus $V = C$ (Nestegård, Kalleklev, Hagatun, Wu, Haver, & Lehn, 2004). The modification is made because the original theory is formally not consistent with the flat plate approximation (Wienke & Oumeraci, 2004). Wagner theory considers the wave pile-up effect and as a final result, the force calculated by using this theory is twice of the one calculated using based on Von Karman theory. In their study, Wienke and Oumeraci assume that the fluid is frictionless and incompressible, and the flow is irrotational. The surface tension of water, damping effect and forces due to gravity were neglected. The theory proposed by Wienke and Oumeraci was verified by an experiment and shows a considerably good agreement with the experiment result.

In our structure, impact is considered to happen on the main legs. As can be seen on the structural plot (ref Fig. 2.2), the legs are not vertical, but has certain angle against vertical axis. Due to this, the impact area will be larger than impact which happens on vertical cylinder. The impact duration will also be larger because on the water plane, the leg section is no longer circular but ellipsoid, thus the travel time of the wave will be higher since ellipse has longer major axis than circle (see Fig. 5.16 where it can be seen that at Z=0, the section of the leg is ellipsoid for inclined members). In the calculation, this condition is considered by introducing a variable γ which is the inclination angle of the cylinder.

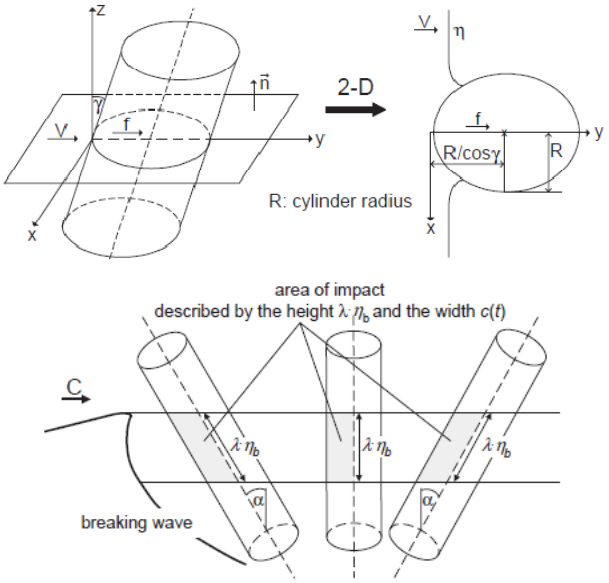

Figure 5. 16 Impact on inclined cylinder (Wienke & Oumeraci, 2004)

Taking $C_s = 2\pi$ and by incorporating the inclination angle γ to the equation, the expression of impact force on an inclined cylinder can be written as (Wienke & Oumeraci, 2004):

For $0 \leq t \leq \frac{1}{8}\frac{1}{cos\gamma}\frac{R}{V}$

$$F_I(t) = \lambda.\eta_b.\rho.R.V^2.cos\gamma\left(2\pi.cos\gamma - 2.\sqrt{cos\gamma\frac{V}{R}t}.atanh\sqrt{1-\frac{1}{4}.\frac{1}{cos\gamma}.\frac{V}{R}.t}\right) \quad (5.5)$$

For $\frac{3}{32}\frac{1}{cos\gamma}\frac{R}{V} \leq t' \leq \frac{12}{32}\frac{1}{cos\gamma}\frac{R}{V}$ where $t' = t - \frac{1}{32}\frac{1}{cos\gamma}\frac{R}{V}$

$$F_I(t) = \lambda.\eta_b.\rho.R.V^2.cos\gamma\left(\pi.\sqrt{\frac{1}{6}cos\gamma\frac{1}{\frac{V}{R}t'}} - \sqrt[4]{\frac{8}{3}cos\gamma.\frac{V}{R}t'}.atanh\sqrt{1-\frac{V}{R}t'\sqrt{\frac{6}{cos\gamma}.\frac{V}{R}t}}\right) \quad (5.6)$$

The total impact duration can be estimated by using the following expression:

$$T = \frac{13}{32}\frac{1}{cos\gamma}\frac{R}{V} \quad (5.7)$$

The total impact duration used in this method is the duration starting from the immersion of front line of the cylinder until complete immersion of half cylinder (or ellipse in case of inclined members).

For our structure, the inclination angle to be $\gamma = 6.18°$ for 200401011200 and $\gamma = 5.69°$ for 200401011400. The difference occurs due to the different wave directions on both events.

The wave velocity is estimated from the wave record by observing the zero down crossing period (T_{wave}) where $V = gT/(2\pi)$. The particle velocity at the crest of the breaking wave will be close to the wave (phase) velocity/celerity (Nestegård, Kalleklev, Hagatun, Wu, Haver, & Lehn, 2004). For event 200401011200 and 200401011400 the wave velocity is consecutively 21.078 m/s and 19.2041 m/s. DNV's recommended practice mentions that the impact velocity should be taken as 1.2 times the phase velocity of the most probable highest breaking wave in n years (DNV-RP-C205, April 2007). Here, for our analysis, the wave velocity is also increased 20% accordingly to DNV recommendation.

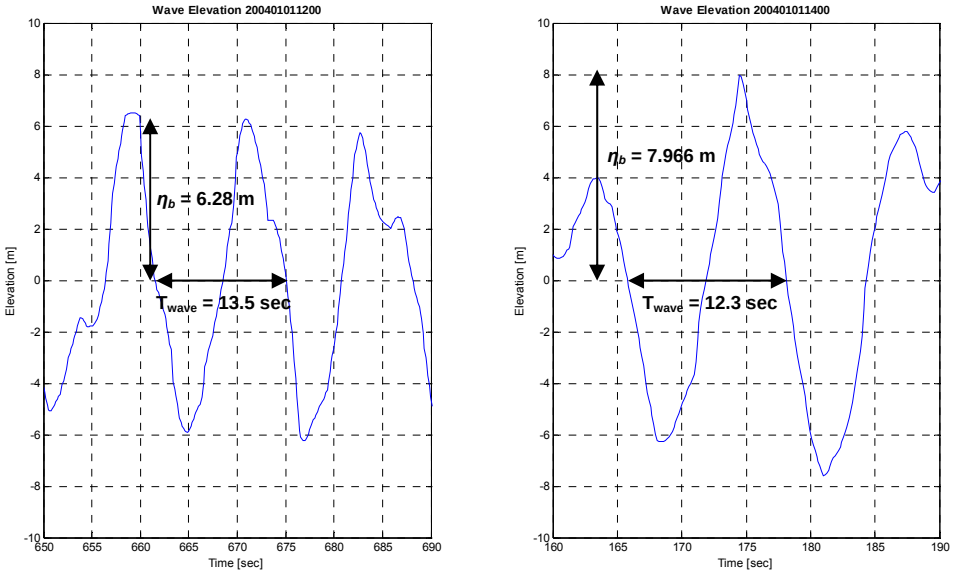

Figure 5. 17 Wave height and period estimation from wave record

The $\lambda.\eta_b$ term on the impact formula is related to the type of breaking wave and wave horizontal asymmetry factor (μ). In this study, it is assumed that the breakers are in form of plunging break. This type of breaking wave is the severe type and will cause high impact value. For this, the curling factor, $\lambda = 0.5$ is taken (Wienke, Sparboom, & Oumeraci, 2004). The breaking wave crest (η_b) and wave height (H) is related to each other by the horizontal asymmetry factor (μ) such that $\mu = \frac{\eta_b}{H}$. Since the complete wave record is available, η_b will simply be determined by observing the wave record profile. In this case, the parameter μ will not be used. For the cases where only the wave height is known, μ should be used to determine the breaking wave crest height.

Based on a study by Myrhaug and Kjeldsen (Myrhaug & Kjeldsen, 1986), one can see the values of μ. The following figure shows the plot of crest front steepness (ϵ) versus the horizontal asymmetry factor (μ). Here $\epsilon = \frac{\eta'}{\left(\frac{g}{2\pi}\right)T.T'}$. Reference can be made to the following figures for clarity of the parameters used, note that $\eta_b = \eta'$ in Fig. 5.18. From Fig. 5.19, it is deemed conservative to take $\mu = 0.9$.

Introducing numbers, the impact load profile can be created. This can be seen on Fig. 5.20. Note that the duration of impact is very short, thus a small time step of integration is required to capture the impact load profile.

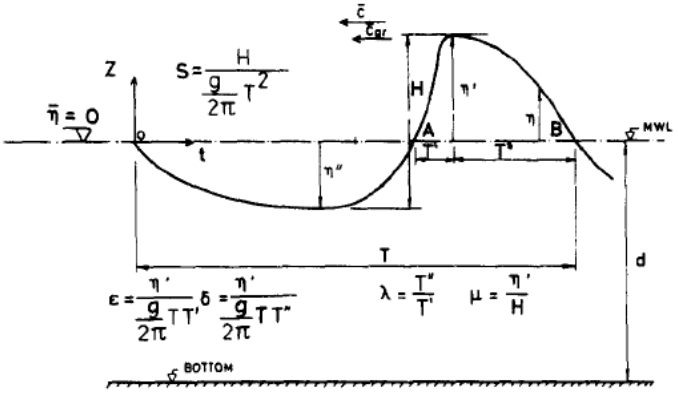

Figure 5. 18 Asymmetric wave properties (Myrhaug & Kjeldsen, 1978)

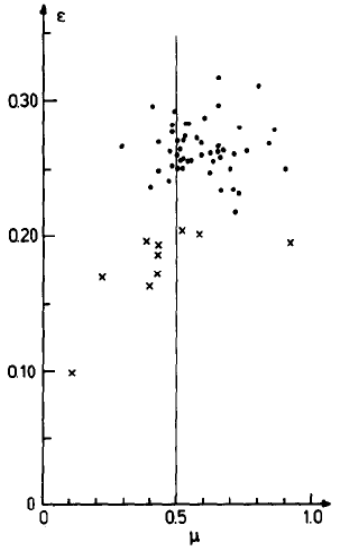

Figure 5. 19 Crest front steepness versus horizontal asymmetry factor (Myrhaug & Kjeldsen, 1986)

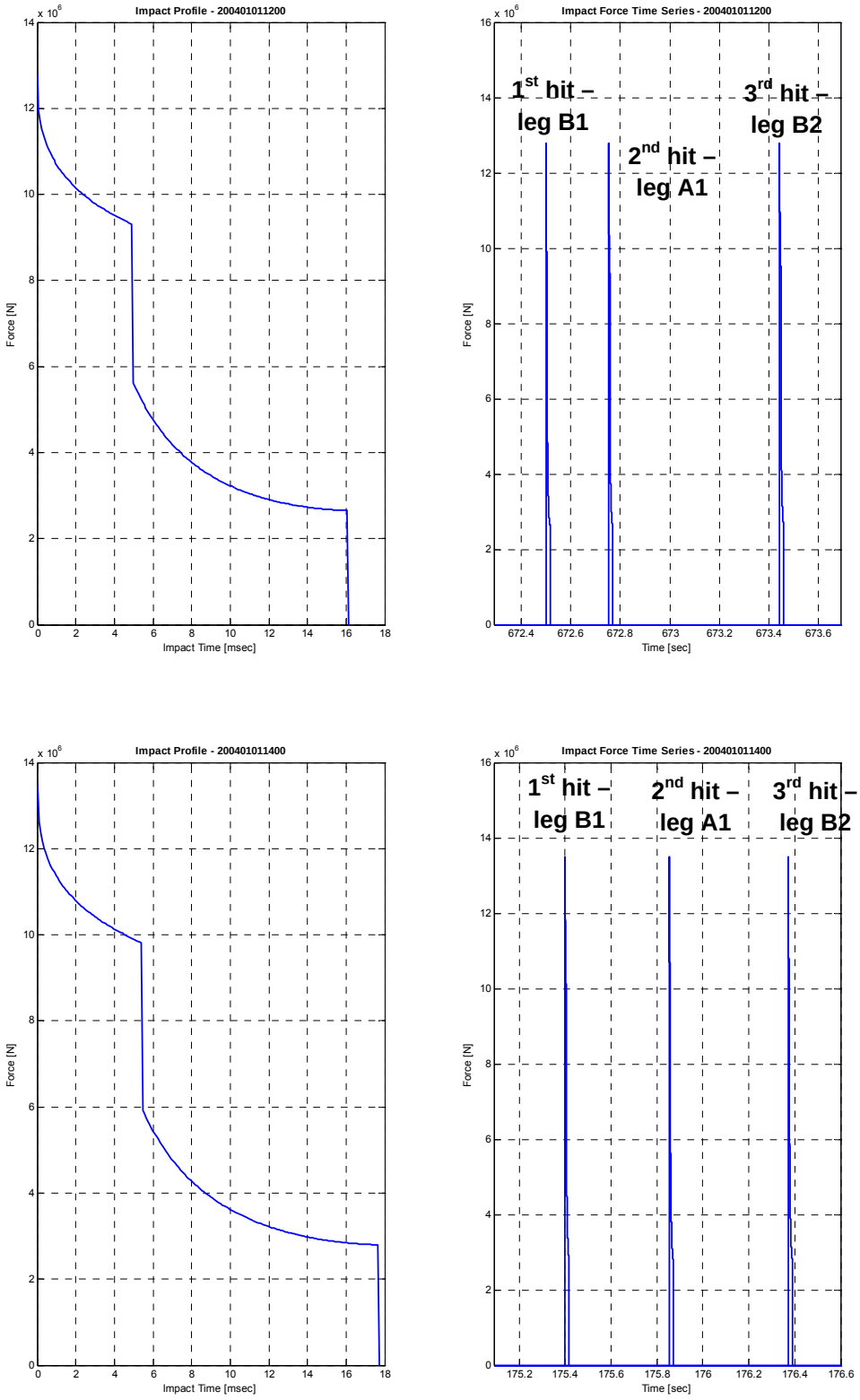

Figure 5. 20 Impact force profile (in wave direction) – Wienke & Oumeraci model

The impact force as can be seen on the left hand side of the above figure is applied to three legs of the structure. Not all legs are loaded with impact, only leg B1, A1, and B2. Due to the wave direction and structural configuration, it is assumed that leg A2 will not be imposed to the breaking wave. The force will decay as it hits conductors/risers before it reaches leg A2 (Ref. Fig. 5.21). It is also assumed that the same impact profile is applicable for the three loaded legs, only with different timing (Ref. Fig. 5.20). The working point of load is taken to be 0.75 times the breaking wave crest height. This is due to the assumption that $\lambda = 0.5$. The wave kinematics is simulated by using Wheeler stretching and second order surface is used.

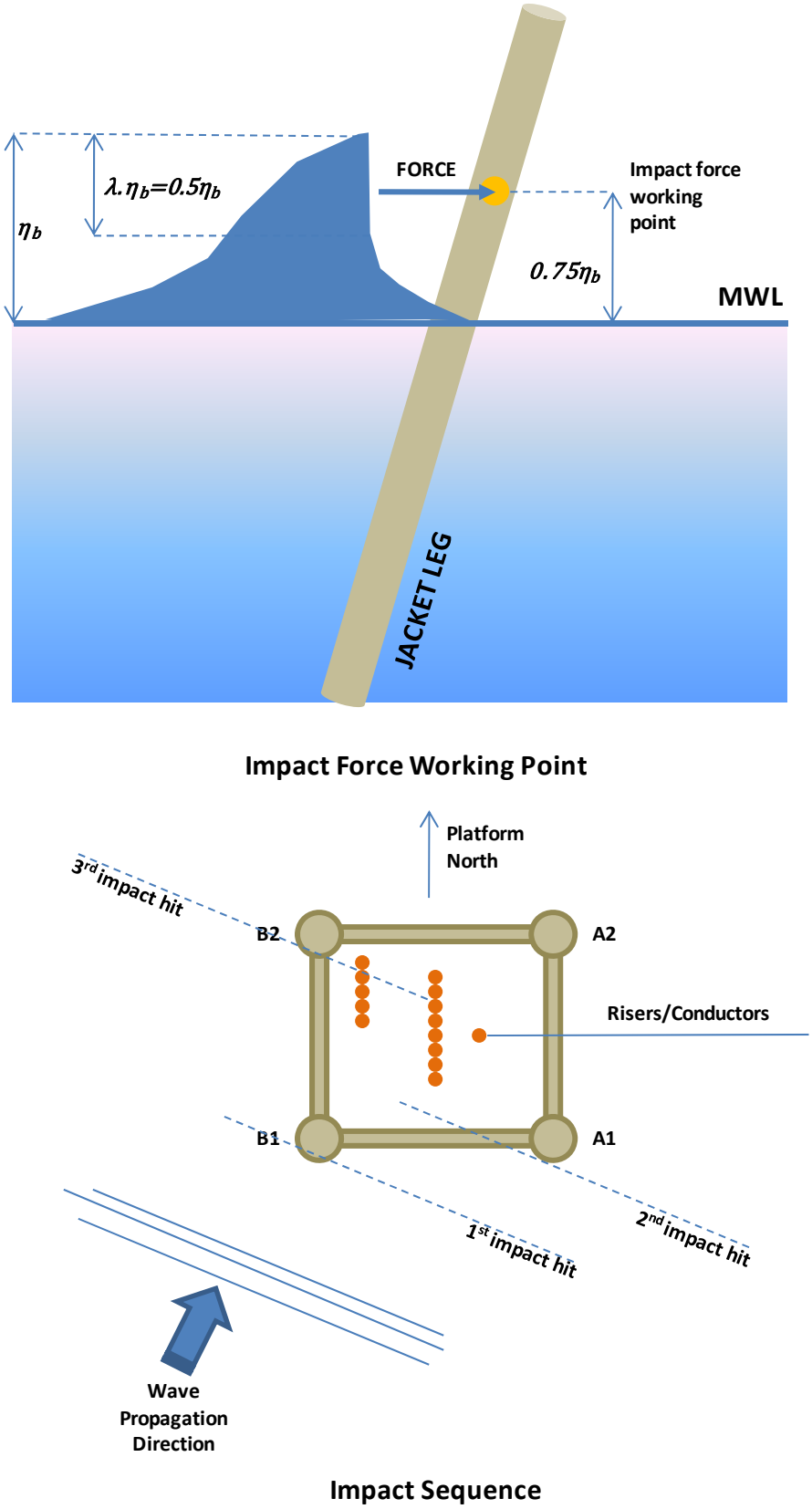

Figure 5. 21 Impact force working point location and impact sequence

Load from wave and impact will mostly be transferred to leg B1 and A2. The analysis result from combination of Morison force and impact force can be seen as the following:

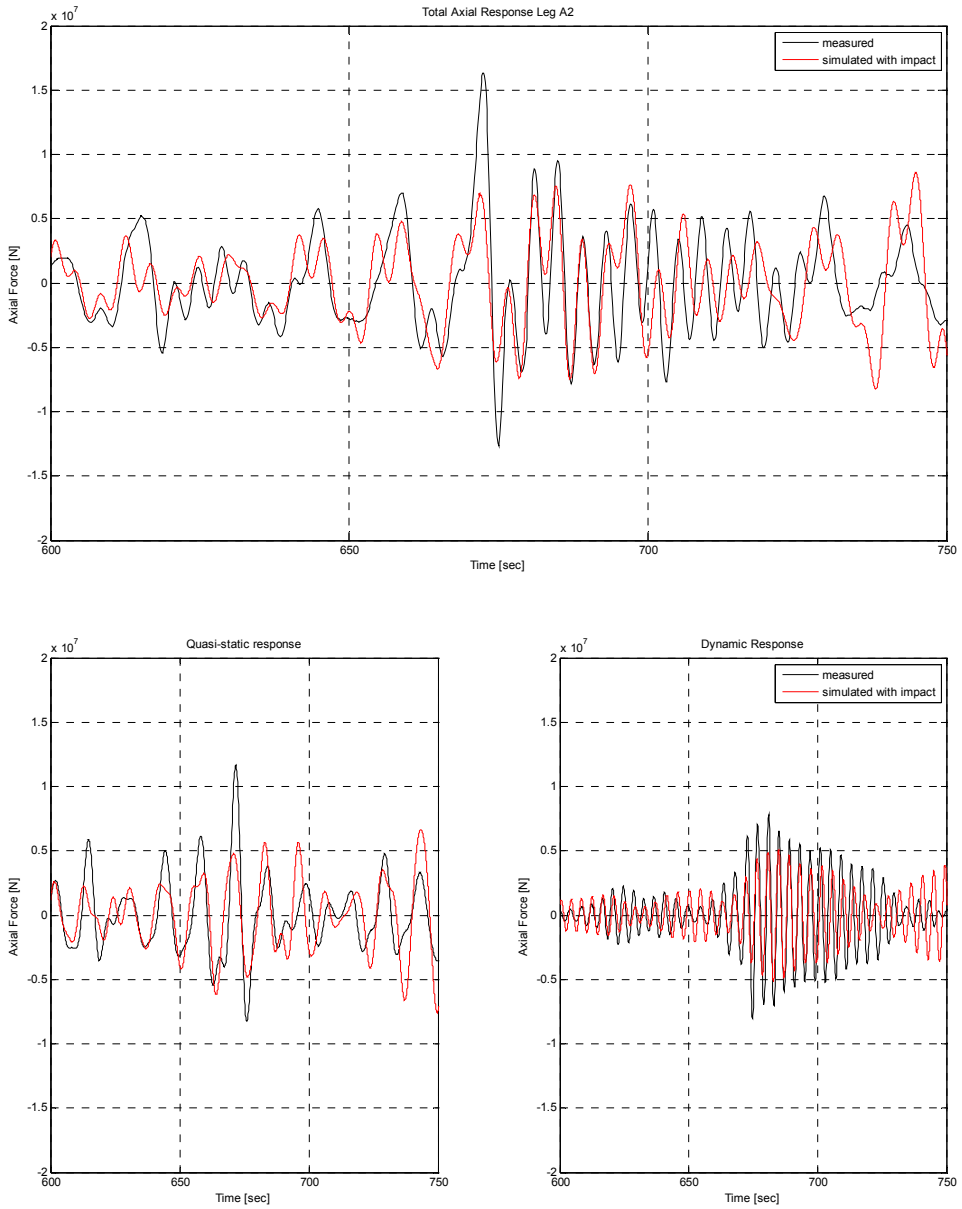

Figure 5. 22 Response of leg A2 (-108m) 200401011200 – Morison + Impact Force (Wienke & Oumeraci impact profile)

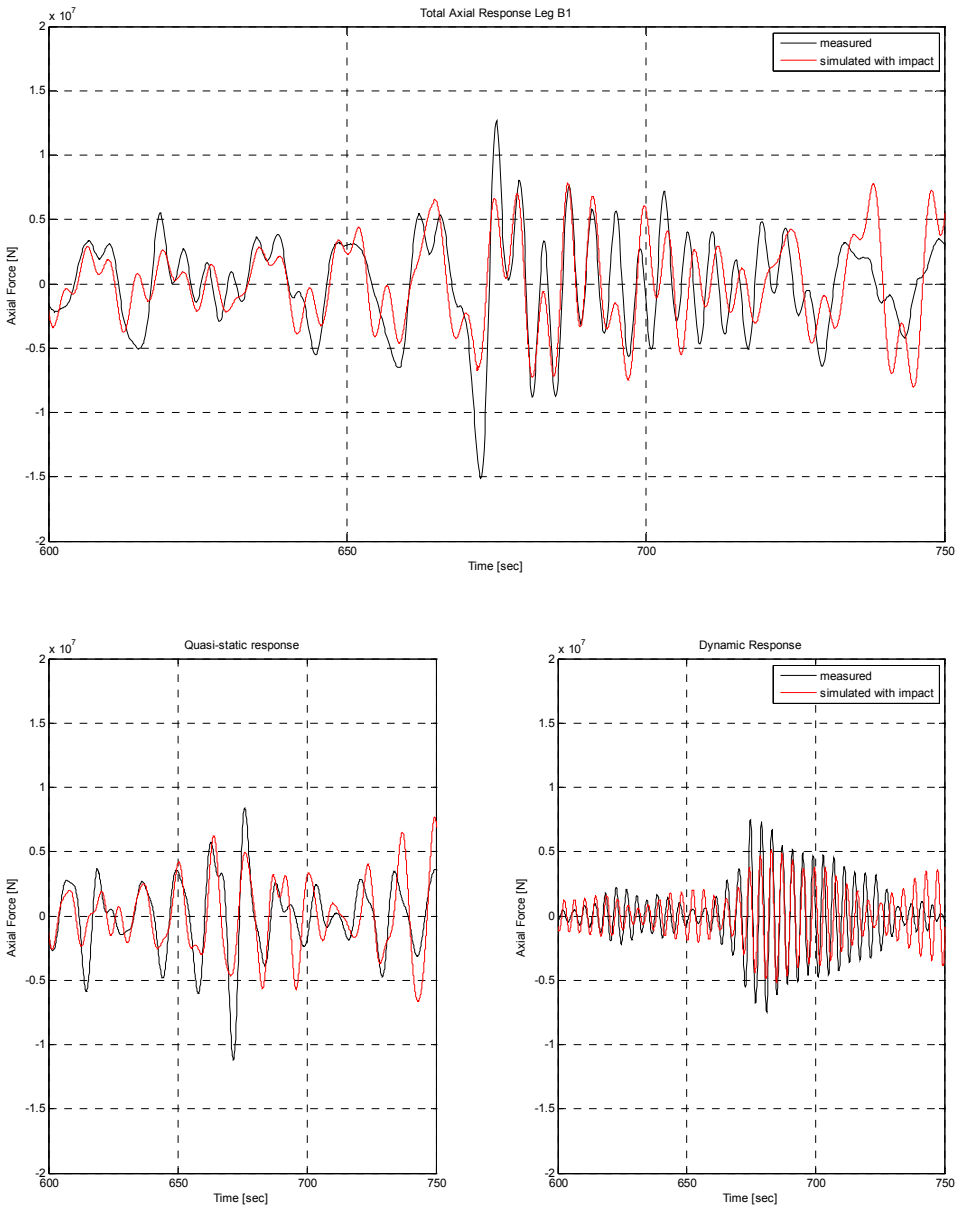

Figure 5. 23 Response of leg B1 (-108m) 200401011200 – Morison + Impact Force (Wienke & Oumeraci impact profile)

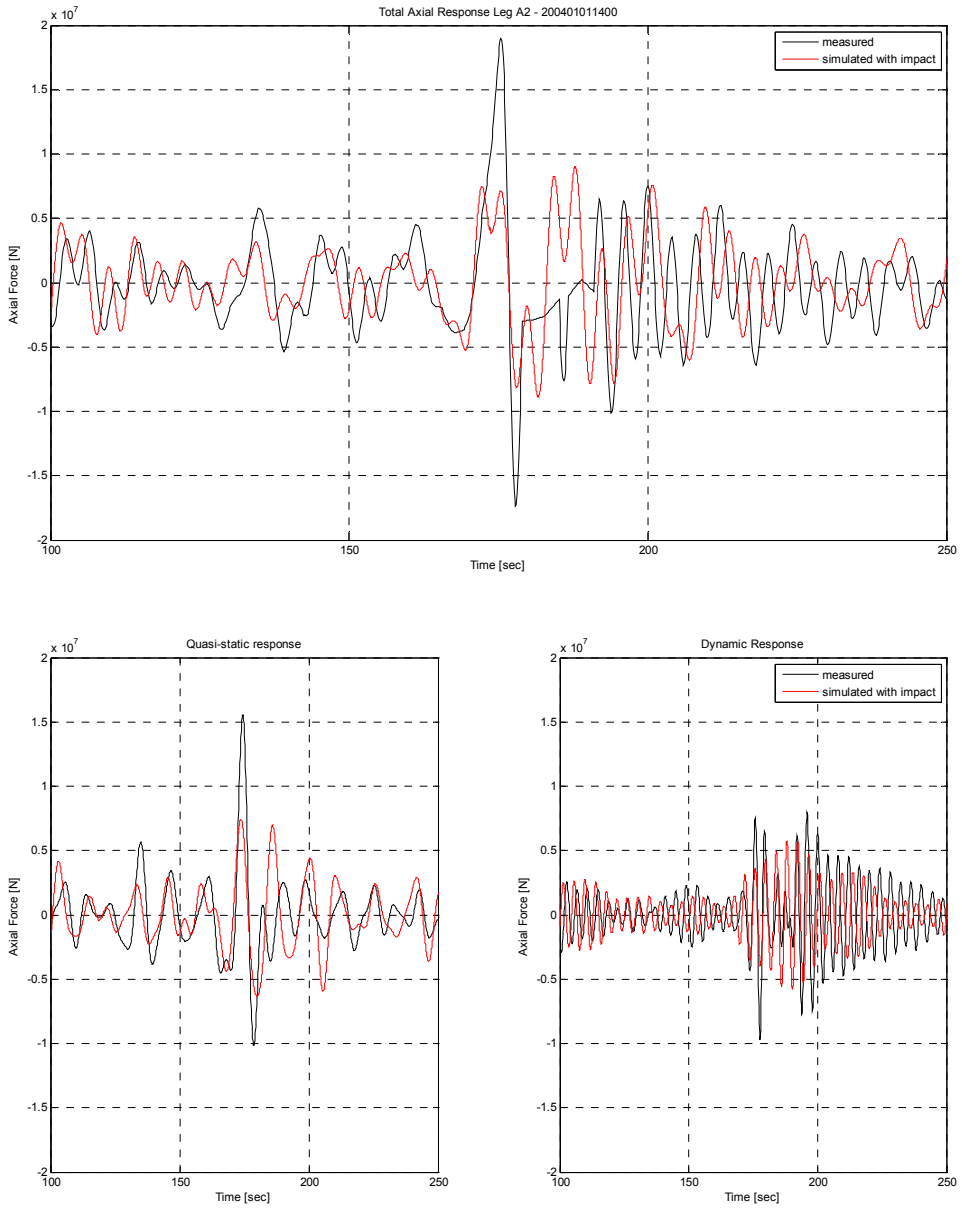

Figure 5. 24 Response of leg A2 (-108m) 200401011400 – Morison + Impact Force (Wienke & Oumeraci impact profile)

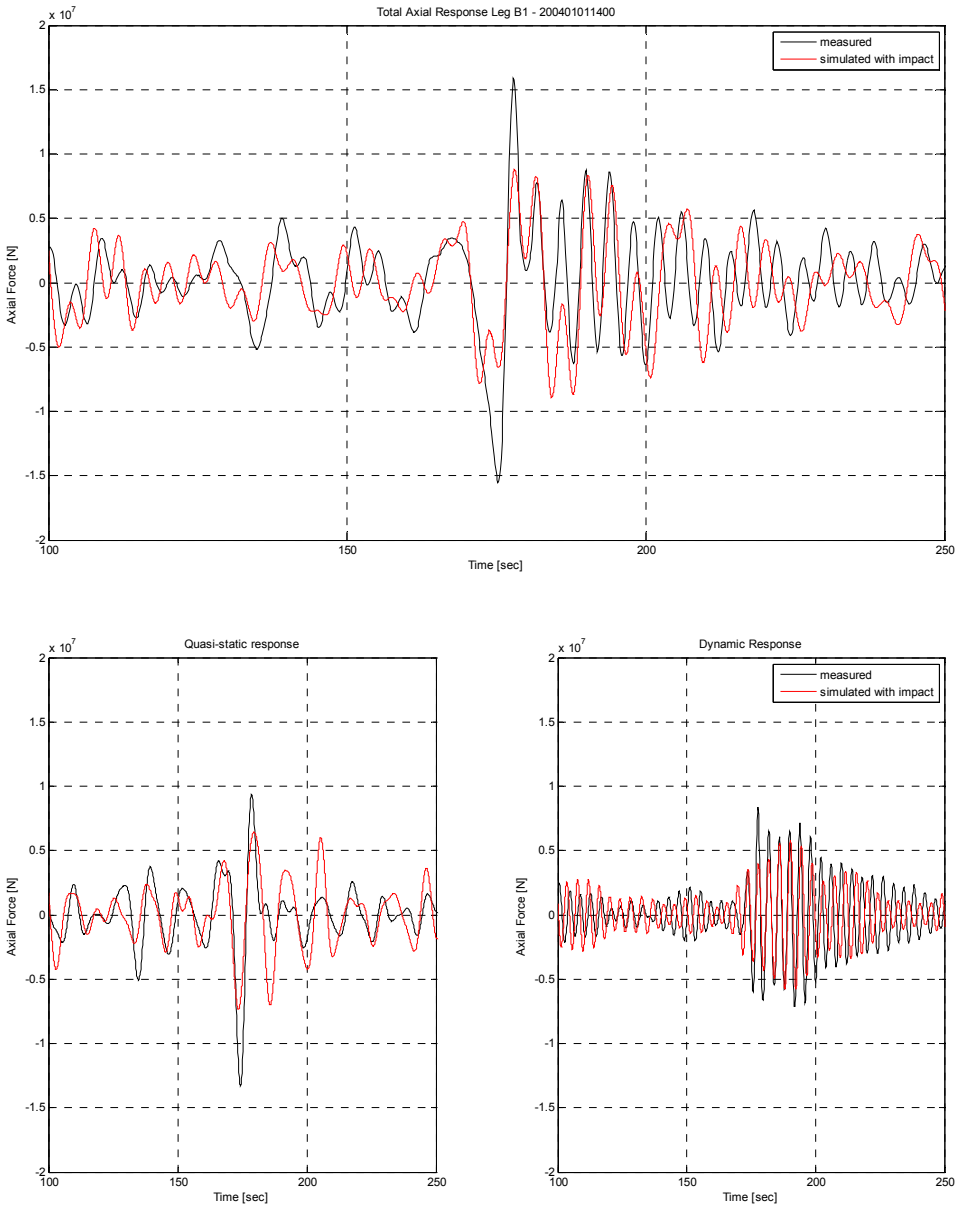

Figure 5. 25 Response of leg B1 (-108m) 200401011400 – Morison + Impact Force (Wienke & Oumeraci impact profile)

From Figure 5.22 to Figure 5.25, it can be seen that the impact does not contribute significantly to the total structural response. The simulated total axial response still shows an under prediction compared to the measured response. This is because of the response magnitude that is caused by impact is small if compared to the force from Morison. The impact magnitude is in the order of 10^5 while the response magnitude from Morison equation reaches the order of 10^7. For the quasi-static response, by the time discrepancy happens, the response is still under predicted by the simulation, but for approximately 25 sec after that, simulation shows an over prediction. The dynamic response in general is under predicted. Simulated dynamic response shows different behavior compared to the measured response. The most distinct difference can be seen

on Fig. 5.24 where measurement data shows that there are two “shocks” happening on leg A2 where this is not represented by the simulated dynamic response. In reality, there might be two consecutive impacts happening on this time instant, locally on leg A2 only. The presence of only one shock on leg B1 and two shocks on leg A2, constitutes that there are dynamic phenomena happen as the wave passes trough the caissons/risers which are located among the legs of the jacket. This is difficult to simulate, but it can be said that caissons may work as wave obstructions which cause the wave to break more thus causing more frequent impact on leg A2.

These simulations show that it may be possible that the impact profile is not suitable for Kvitebjørn case where more dynamic events may occur between the legs of the jacket due to the presence of caissons. This impact profile as proposed by Wienke and Oumeraci is based on an experiment for single cylinder. The example of application of this impact profile (Wienke, Sparboom, & Oumeraci, 2004) also uses the offshore windmill structure which is basically a single cylinder structure in 25 m of water depth. The impact duration only considers the duration starting from the immersion of front line of the cylinder until complete immersion of half cylinder thus very short duration is predicted.

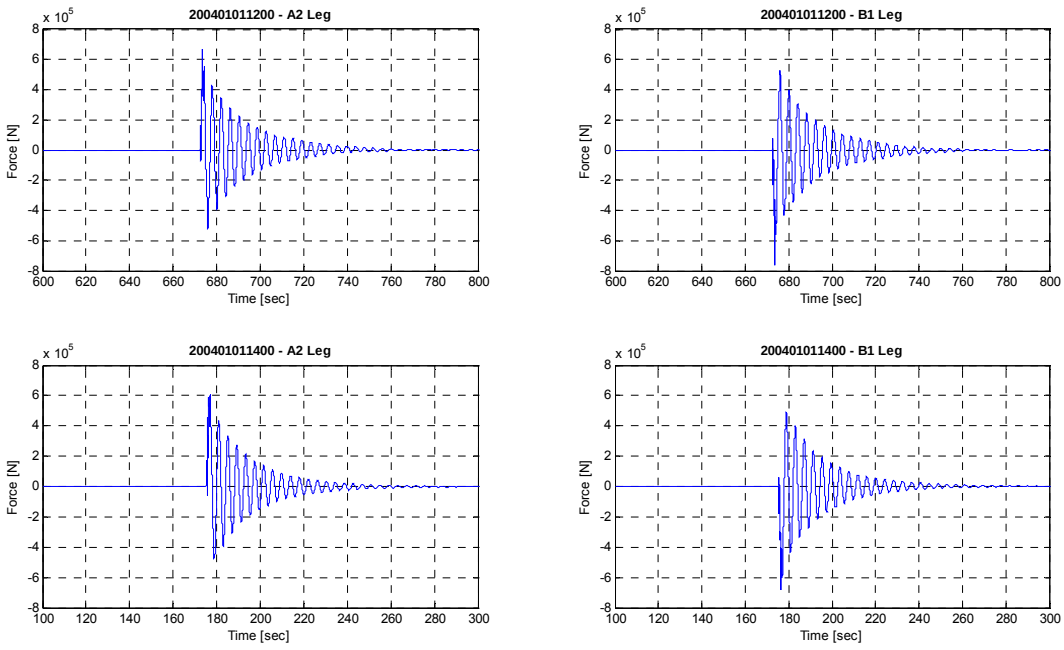

Figure 5. 26 Response due to impact only – Wienke & Oumeraci model

In an effort to distinguish how big the impact force should be so that the simulated response can approximate the measured response, it is found that if one multiplies the original impact force with a factor of 10, the simulated responses represent the measured response better than before. This constitutes that the total impact force will be 30 times higher that the original one and that the response due to impact only will be in the order of 10^6. The results can be seen on the following figures:

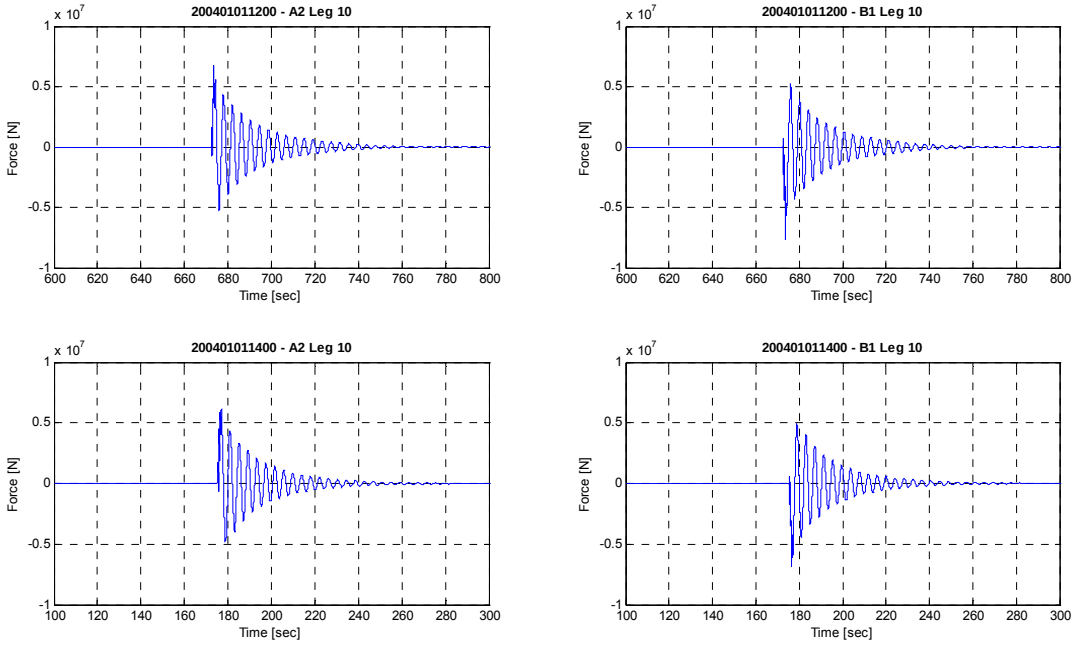

Figure 5. 27 Response due to impact only (impact force x 10) – Wienke & Oumeraci model

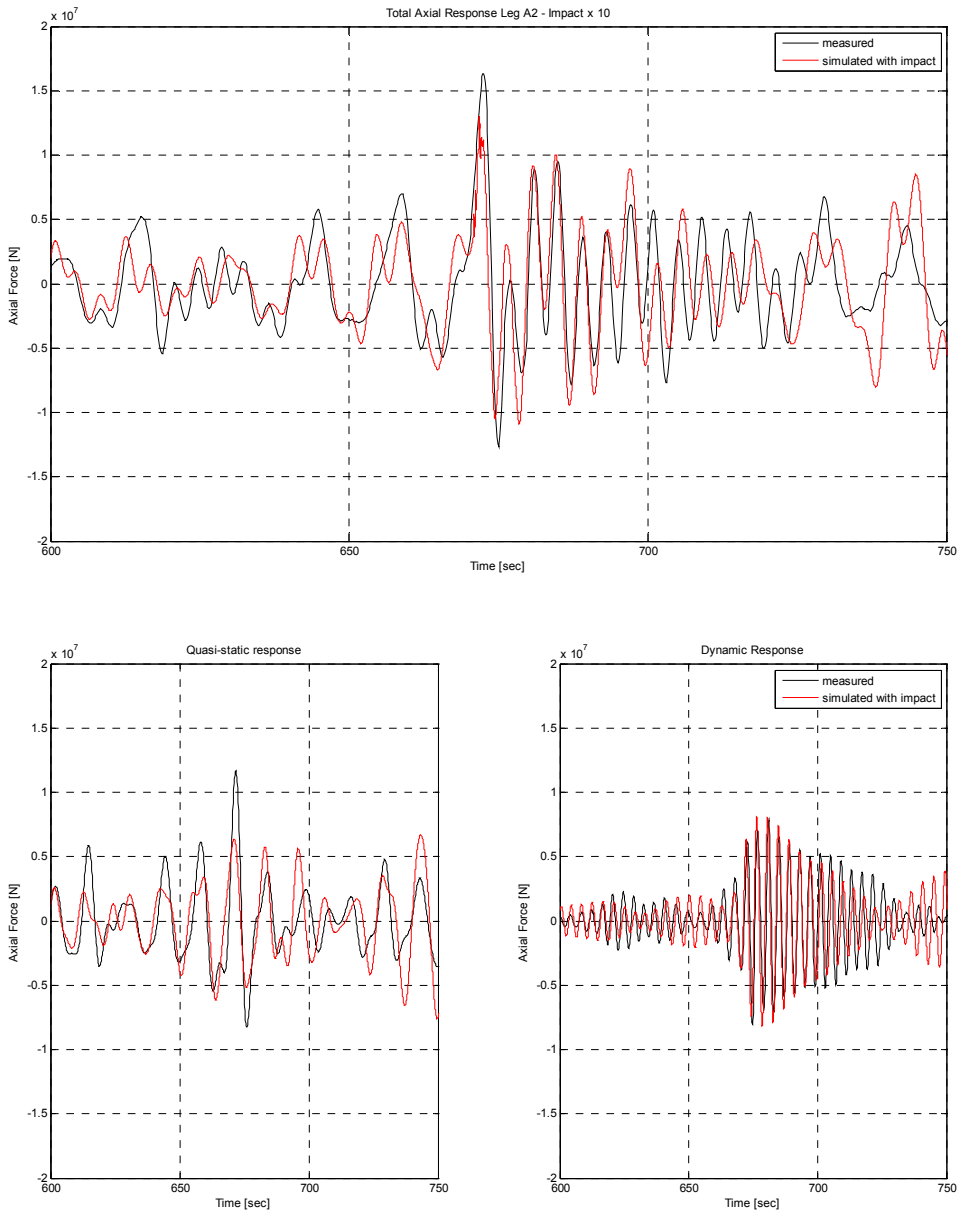

Figure 5. 28 Response of leg A2 (-108m) 200401011200 – Morison + (Impact Force x 10)

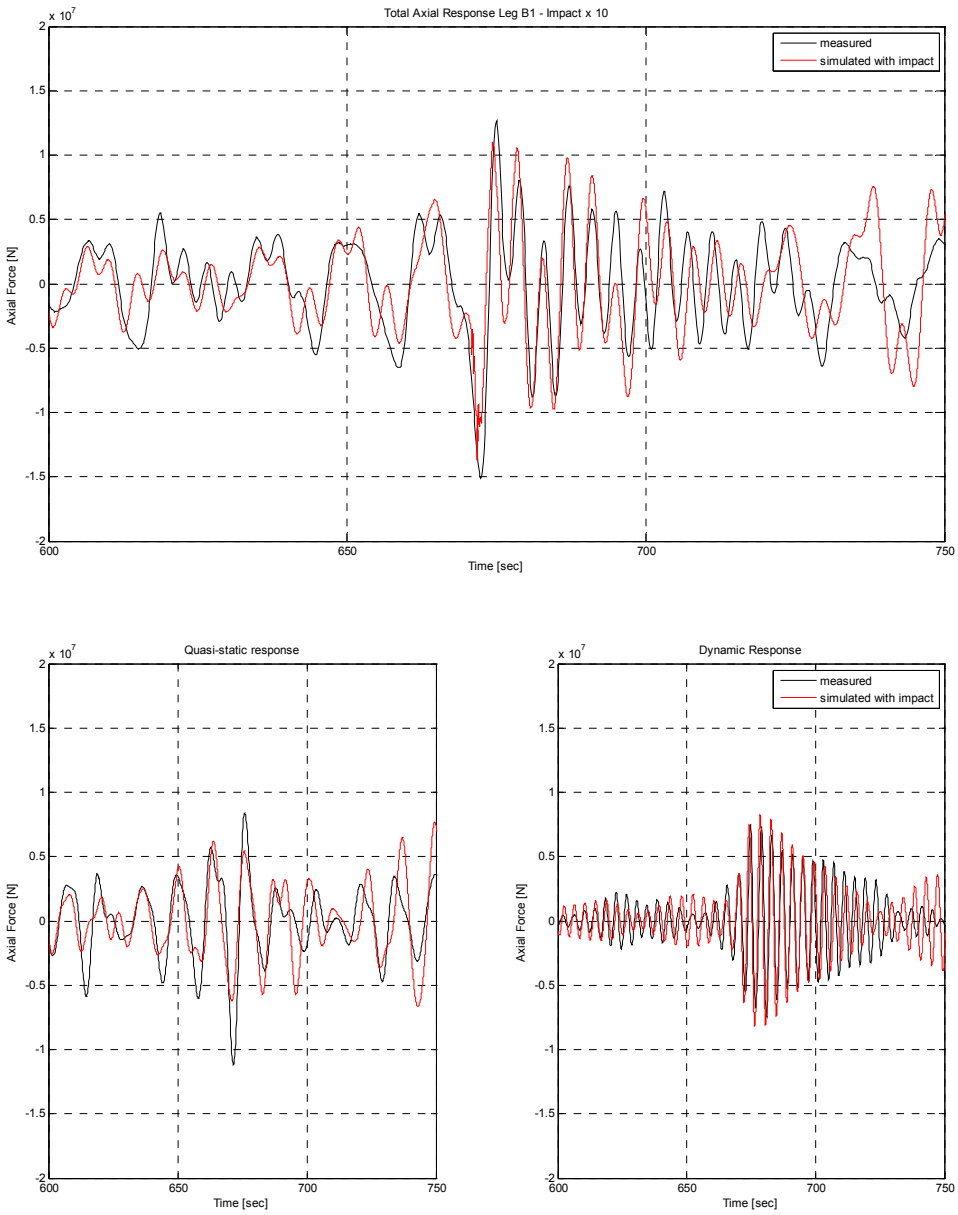

Figure 5. 29 Response of leg B1 (-108m) 200401011200 – Morison + (Impact Force x 10)

From Figure 5.28 and 5.29, after multiplying the impact force on the three legs with a factor of 10, it is observed that the dynamic response is represented by the simulation reasonably well. The magnitude of quasi-static response at the time of high measured response is represented better than when impact is not multiplied by 10 for each leg, especially for leg B1. The total axial response is predicted nicely by the simulation. However, multiplication factor of 10 for each leg seems unreasonable in our case. Even if the impact on risers and conductors are considered, the magnitude will not increase with a factor of 3 x 10 = 30.

5.2.2. Impact Assessment according to Campbell and Weynberg Impact Model

This impact model has been used in a study about impact load assessment on risers in a semisub (Nestegård, Kalleklev, Hagatun, Wu, Haver, & Lehn, 2004). It is assumed that for slender structural elements where the diameter is much smaller than the wave length, wave diffraction can be neglected and undisturbed wave velocity can be used as an input to the load model. The leg diameter of Kvitebjørn is 2 m and the wave length is predicted as 284.6m (200401011200) and 236.2m (200401011400). The existence of risers and bracings will be neglected thus it is deemed that the assumption of neglecting the diffraction of wave is valid in this case.

In Campbell and Weynberg model, impact is accounted for by modifying the drag term in Morison equation (Eq. (5.8)). Thus only the first two terms of Eq. (5.1) is used to calculate the force on the structure. The modification is done by introducing a slamming coefficient, C_s, whose values can be calculated by the following equation (Eq. (5.9)):

$$F_D(z,t) = \frac{1}{2}\rho . C_s . D . V^2 \tag{5.8}$$

$$C_s(s) = 5.15\left[\frac{D}{D+19s} + \frac{0.107s}{D}\right] \tag{5.9}$$

The slamming coefficient is equal to $C_D = 0.8085$ by the time the cylinder is fully submerged, $C_s(D) = C_D$, and $s = s(t)$ is the function of cylinder submergence over time. Having the leg diameter of 2m, the following changes in C_s is observed as a function of submergence of cylinder:

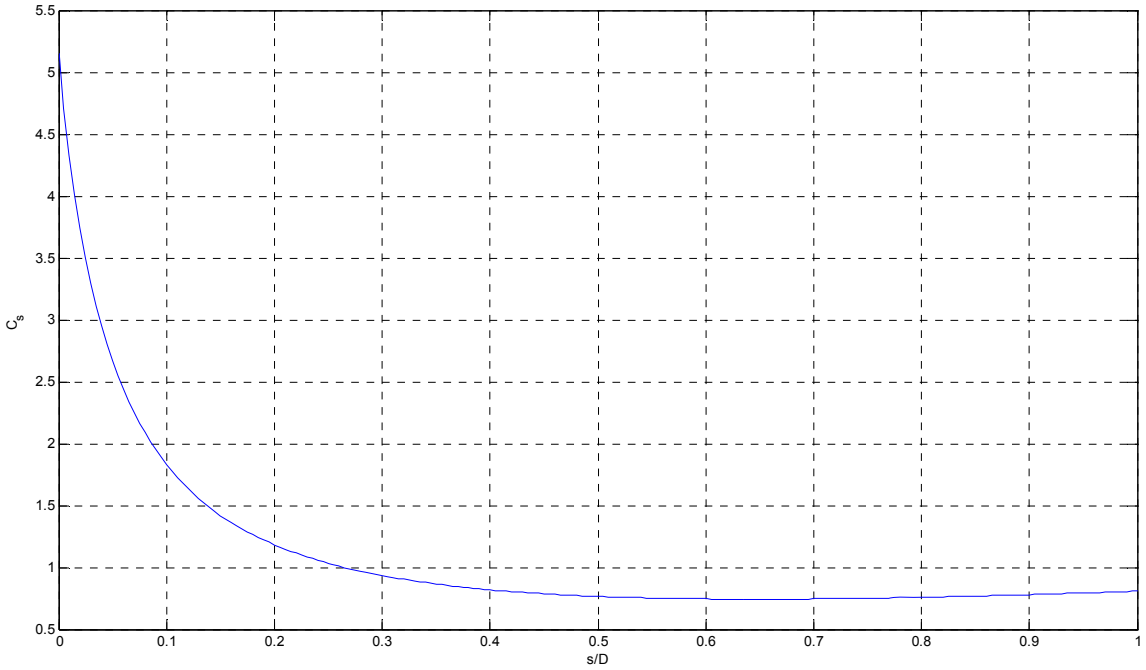

Figure 5. 30 Change in C_s as a function of cylinder submergence

The same assumption as the previous impact observation will be used. It is assumed that the breaker is of plunging type where $\lambda = 0.5$. The impact duration in this case is determined by observing the wave profile. As the working point of the force is at 0.75 times the crest height, then the duration of impact is the duration of wave passage through the cylinder at 0.75 times crest height elevation as can be seen on the following figure:

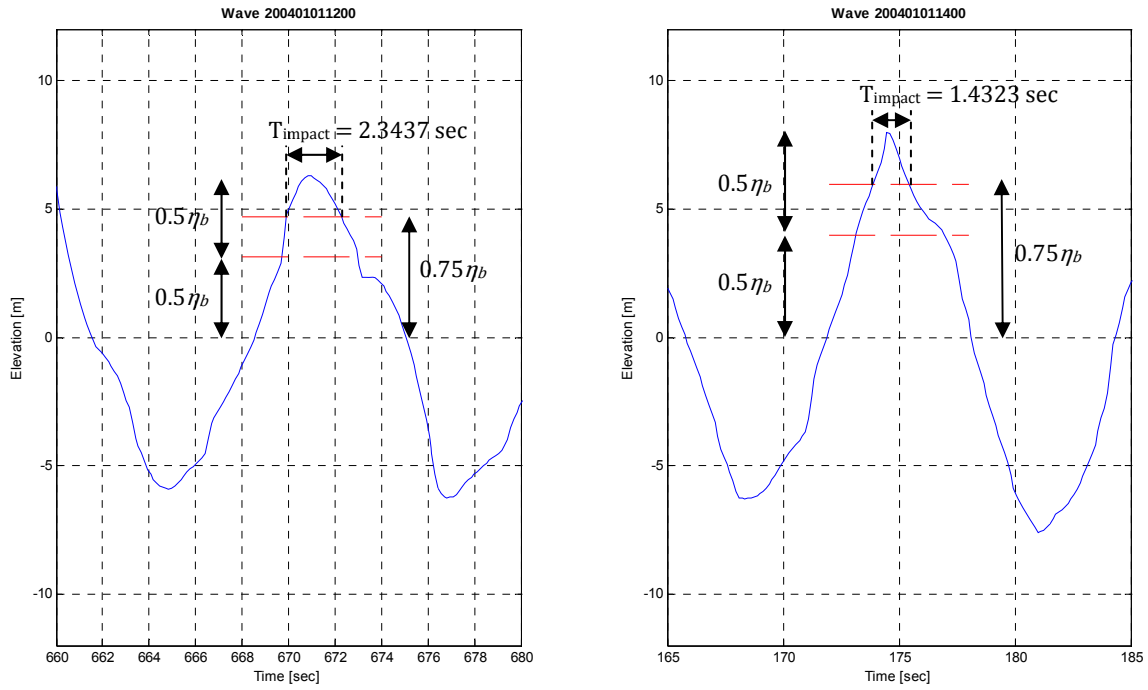

Figure 5. 31 Prediction of impact duration

Introducing numbers to Eq. (5.8) and (5.9), the impact force profile for leg B1, A1 and B2 can be obtained. Here, it is assumed that introducing the impact load to the three main legs will give representative result for the analysis. The existence of risers and bracings among the legs will in reality give additional impact area and thus larger impact force, but for this study, only the three main legs are loaded with impact. In this part of analysis, Wheeler stretching method is used to predict the particle velocity beneath the crest and second order surface is used.

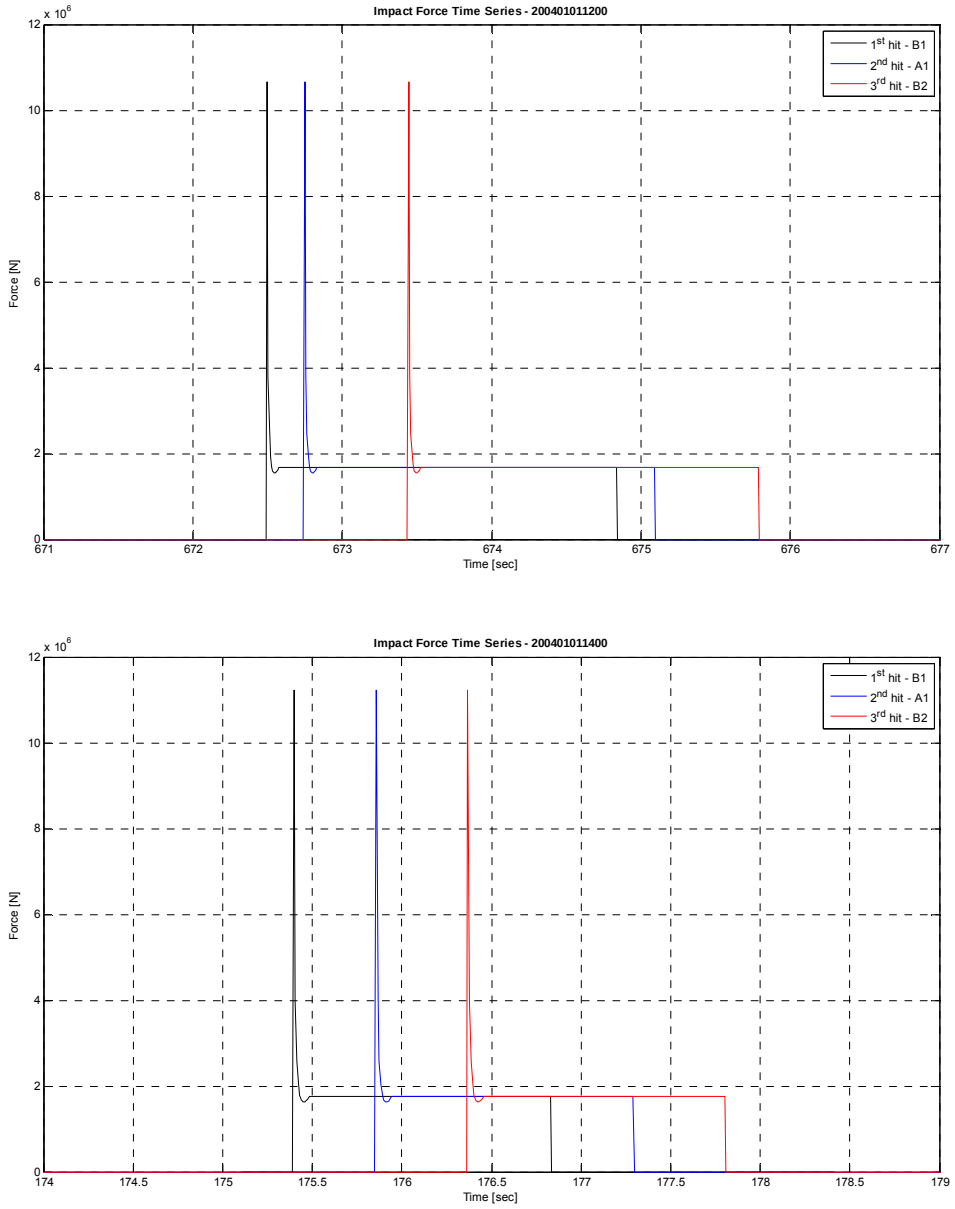

Figure 5. 32 Impact force profile (in wave direction) – Campbell and Weynberg model

Compared to the impact profile by using Wienke and Oumeraci calculation, Campbell and Weynberg impact profile lasts longer. The simulation results by using Campbell and Weynberg impact profile can be seen on the following figures:

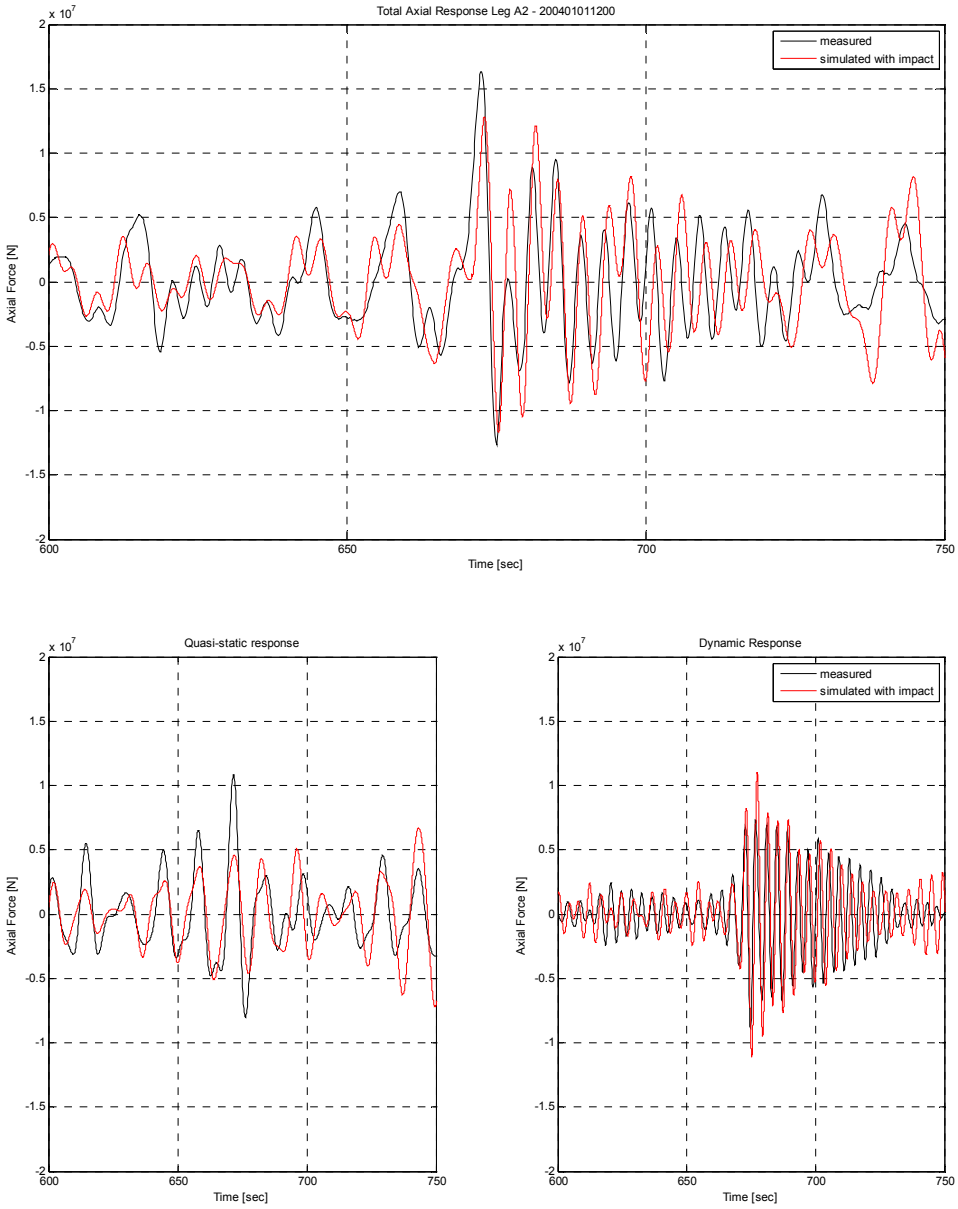

Figure 5. 33 Response of leg A2 (-108m) 200401011200 – Morison + Impact Force (Campbell & Weynberg impact profile)

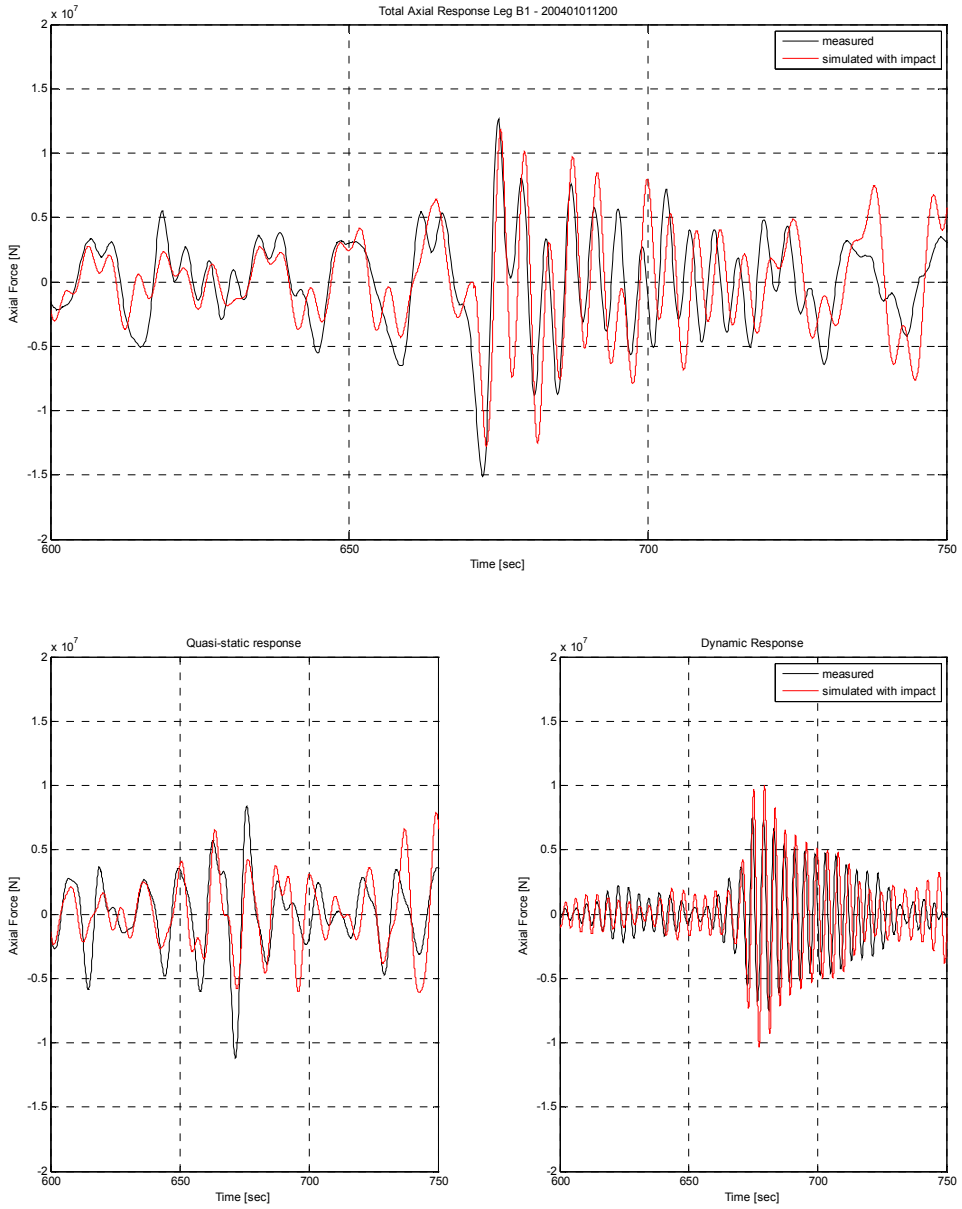

Figure 5. 34 Response of leg B1 (-108m) 200401011200 – Morison + Impact Force (Campbell & Weynberg impact profile)

For the 200401011200 event, the total axial response is to some extent approximated pretty well by the simulation. The quasi-static force is still under predicted and the dynamic response is over predicted at the beginning of the impact, but becomes a little under predicted after a while. However, the dynamic response is represented well enough by the simulation.

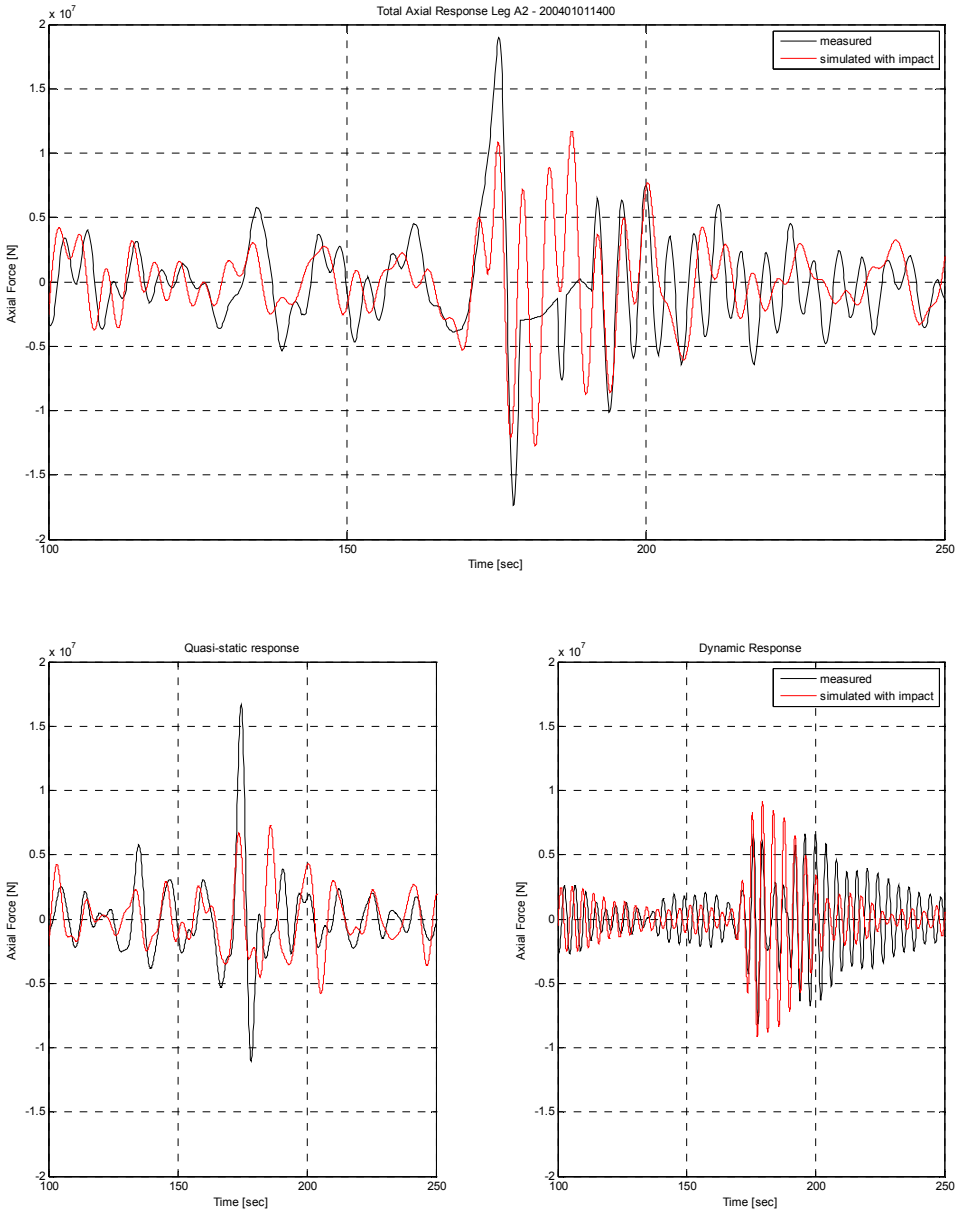

Figure 5. 35 Response of leg A2 (-108m) 200401011400 – Morison + Impact Force (Campbell & Weynberg impact profile)

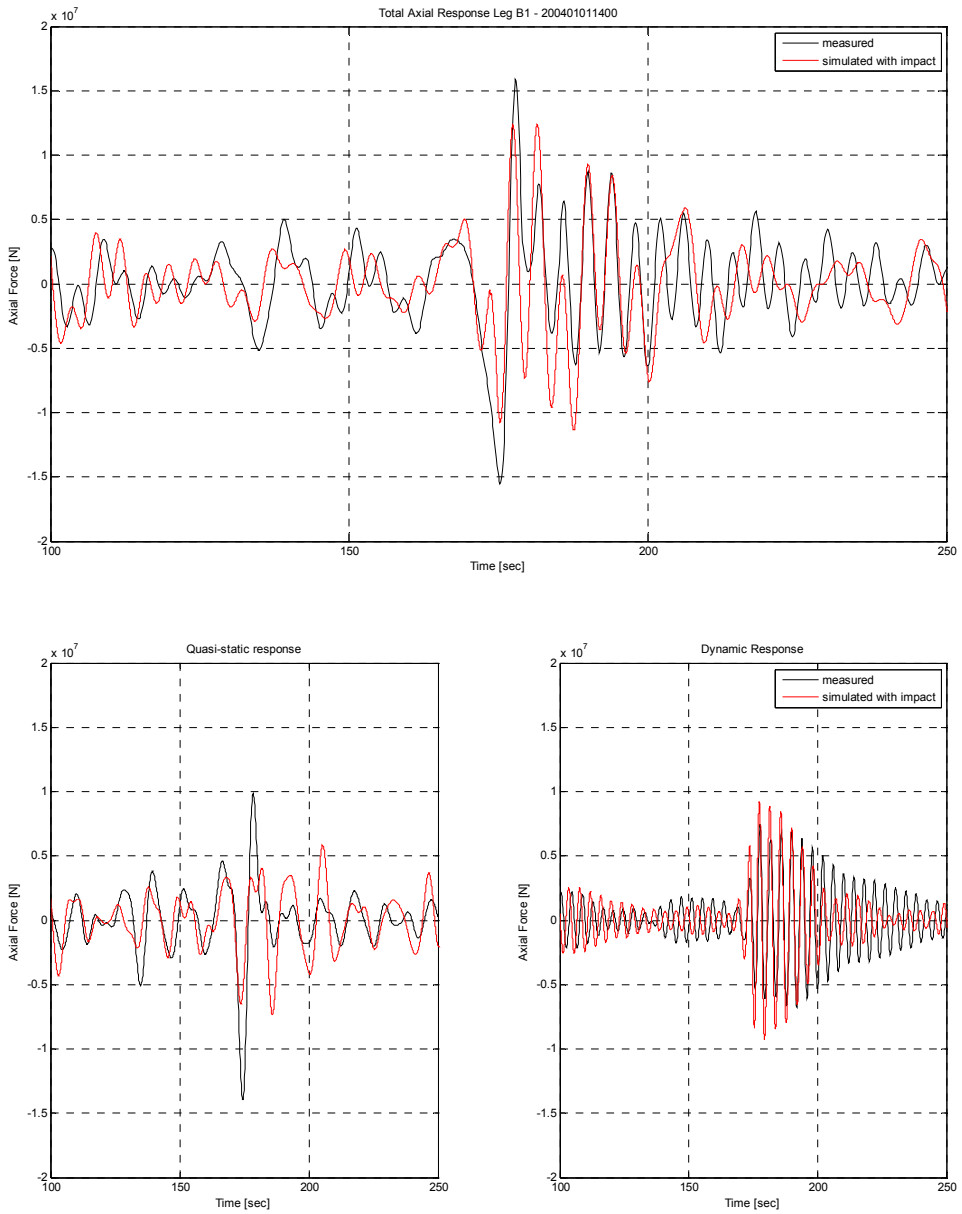

Figure 5. 36 Response of leg B1 (-108m) 200401011400 – Morison + Impact Force (Campbell & Weynberg impact profile)

For the 200401011400 event, the total axial response is still under predicted by the simulation. The quasi-static response is under predicted predicted too and the dynamic response is over predicted at the beginning of the impact, but becomes under predicted after a while.

By using the impact model by Campbell and Weynberg, simulations can approximate the measurement record directly without having to multiply the impact value with certain multiplication factor. This is due to the condition where the duration of the impact is longer. When the second impact happens, the first impact is still ongoing (ref. Fig. 5.32), and so as for the third impact, thus larger impact value in total is implied to the structure

during the estimated total impact duration. This results in total impact response in the order of 10^7 which is comparable to the response caused by Morison forces.

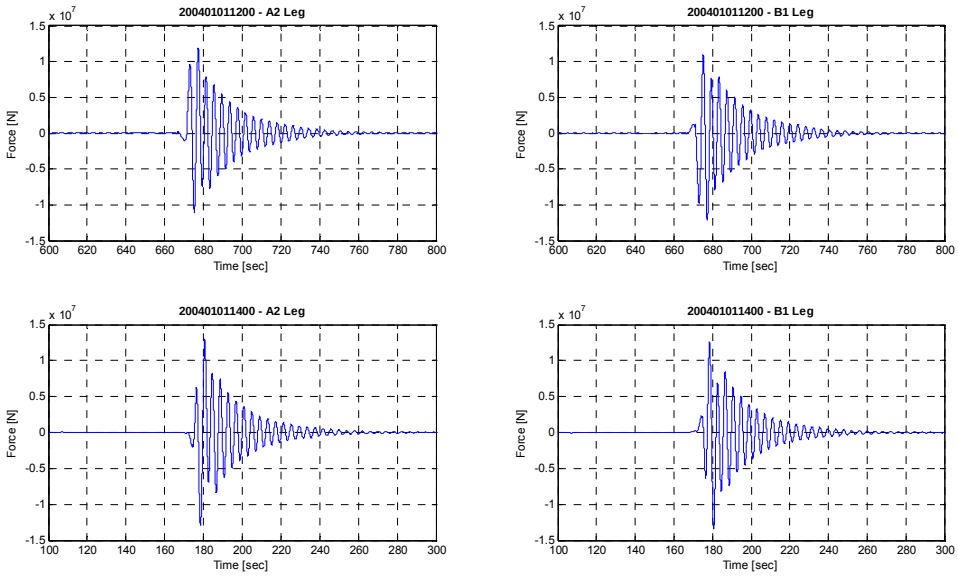

Figure 5. 37 Response due to impact only – Campbell & Weynberg model

The following figure shows the comparison between simulations with and without impact model. It can be seen that impact model increases the response so that the value approximates the measured response.

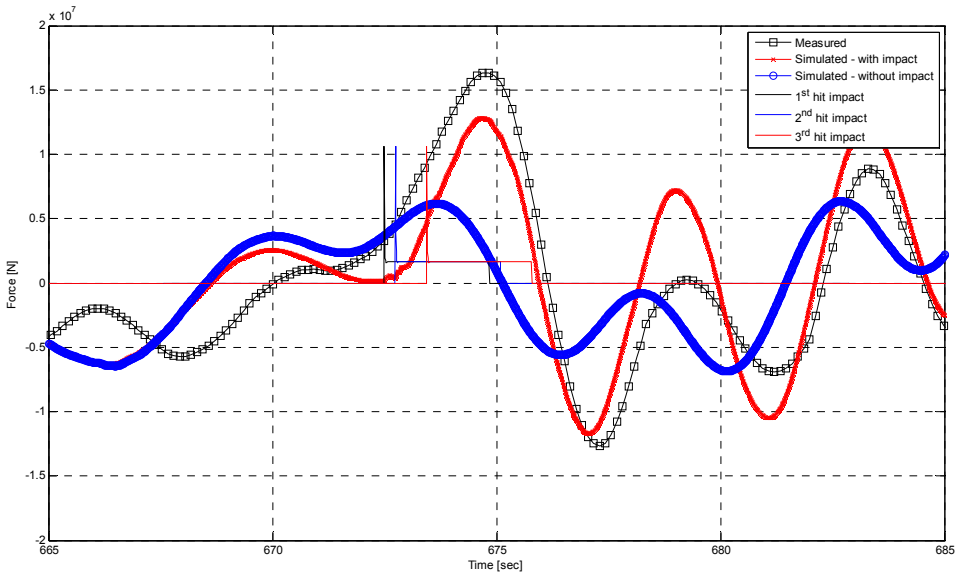

Figure 5. 38 Response behavior with and without impact – Leg A2 (-108m) 200401011200

Generally speaking about impact, after doing impact assessments based on the two impact profiles, it can be seen chosing the appropriate impact profile can be beneficial for the simulation. Under prediction in the impact analysis quasi-static result may be overcome by considering the impact force on risers/caissons on the jacket too. In this study, the impact profile proposed by Campbell and Weynberg is deemed to be most appropriate to be used in the simulations.

To simulate the contribution of caissons/risers between the legs of the jacket, an increase in impact load is introduced. Here, the impact load is multiplied by two and the load is applied to leg B2 and A1 (Ref. Fig. 2.2). This is of course just an approach to see the effect of higher impact load. The following impact profile is then applied to each case:

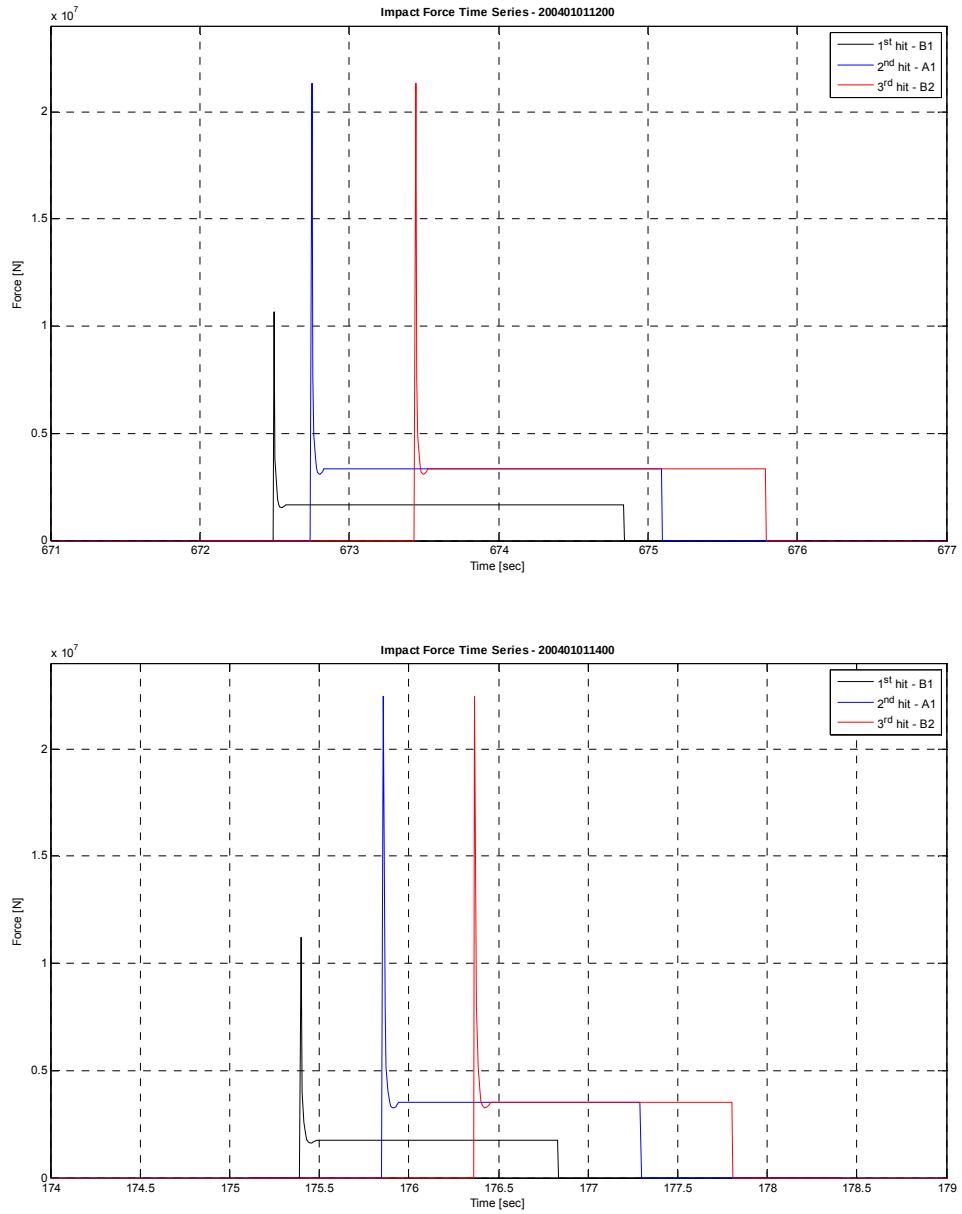

Figure 5. 39 Impact force profile (in wave direction) – Campbell and Weynberg model – 2nd and 3rd hit impact modification to account for load on caissons

For the 200401011200 event, the simulation results show that the total axial response is over predicted. A high increase in dynamic response is also observed that is causing over prediction in the response of the structure. The quasi-static response can be represented well by the simulations. However, this has shown that to reach the value of measured quasi-static axial response, simulations have to incorporate large impact loads which on the other hand is unlikely because by increasing the impact load, the total response and the dynamic response will be over predicted. The over prediction in the dynamic response even can be approximately 100% which is a large deviation from the measured dynamic response.

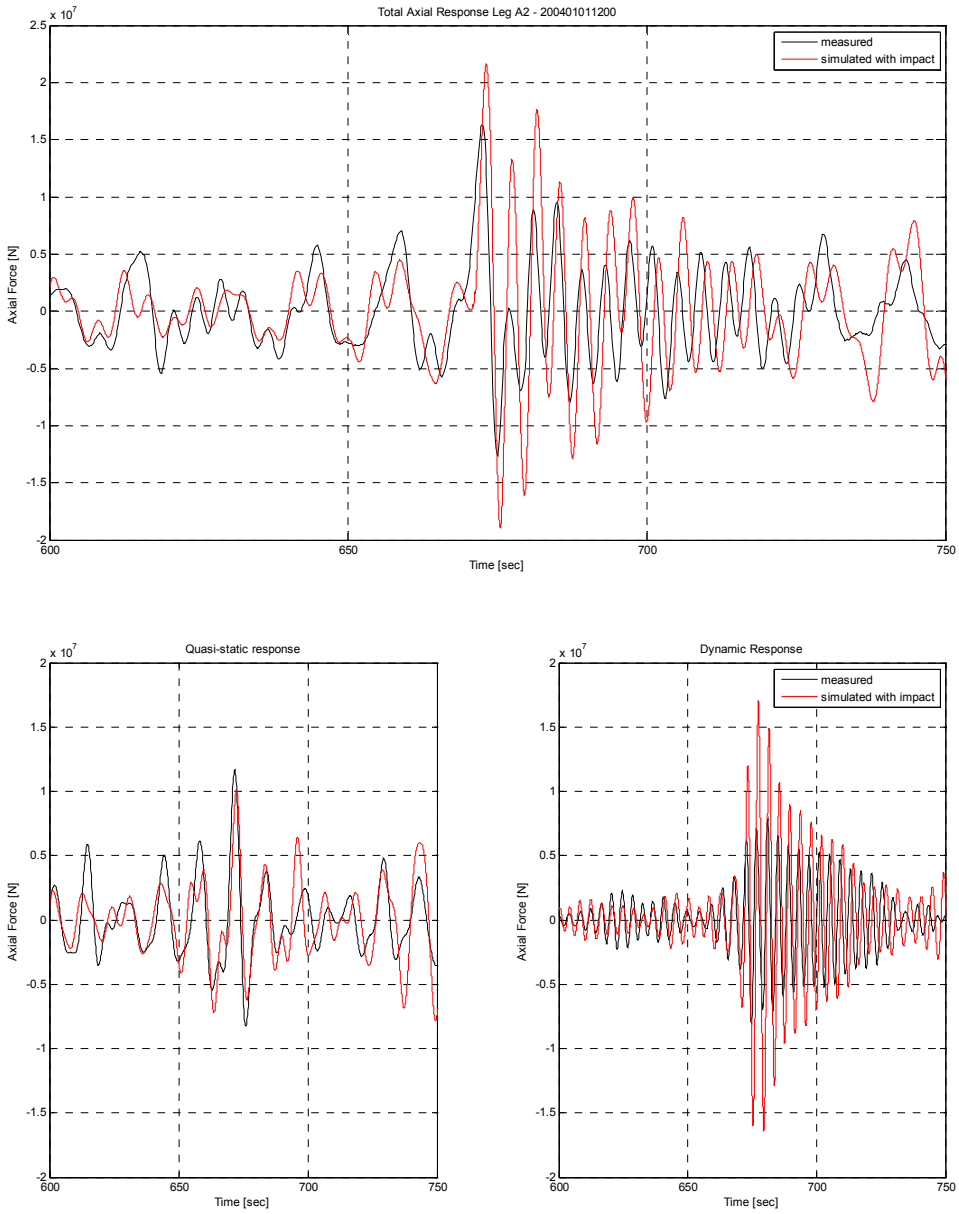

Figure 5. 40 Response of leg A2 (-108m) 200401011200 – Morison + Impact Force (Campbell & Weynberg impact profile) – with modified impact profile for leg A1 and B2

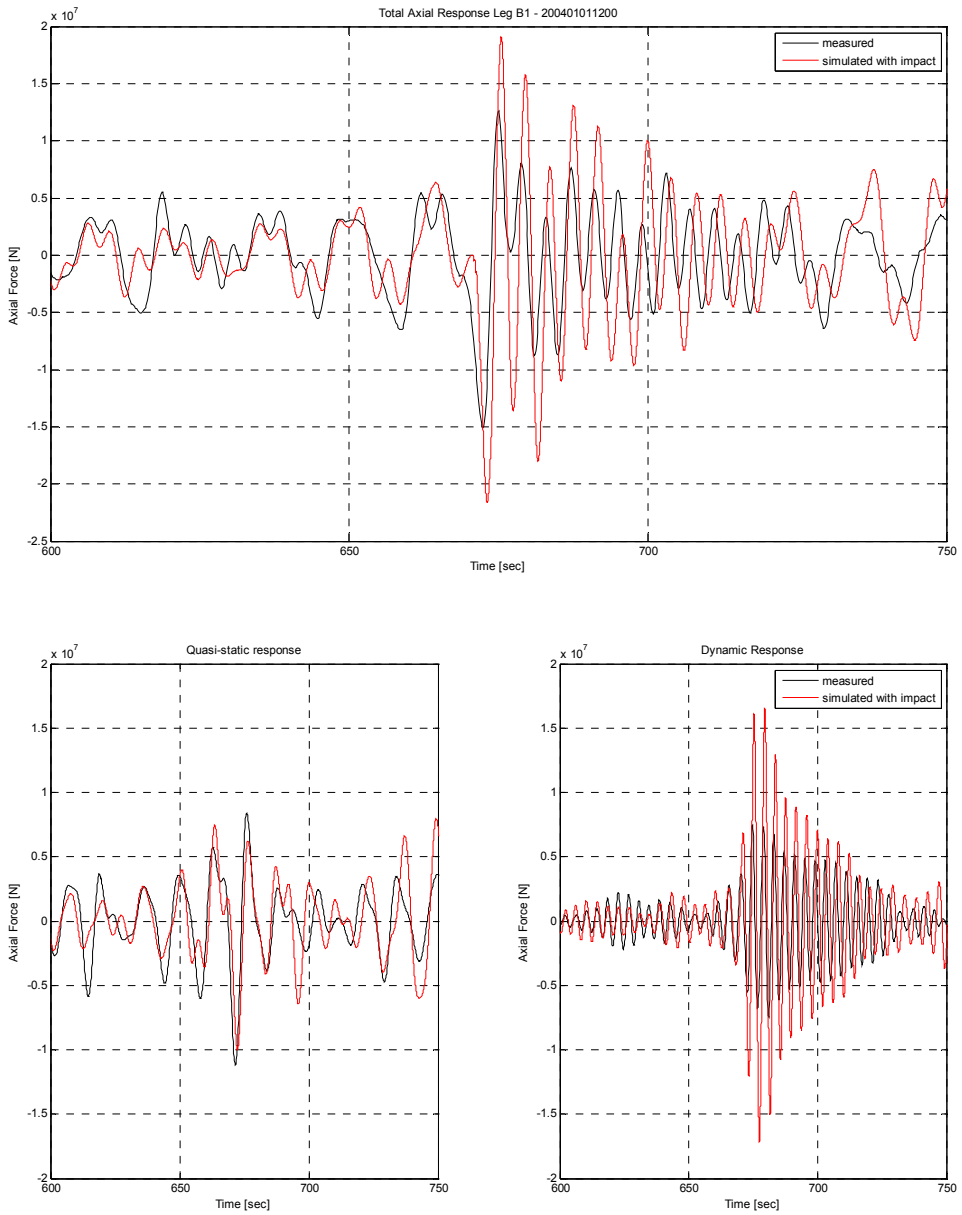

Figure 5. 41 Response of leg B1 (-108m) 200401011200 – Morison + Impact Force (Campbell & Weynberg impact profile) – with modified impact profile for leg A1 and B2

For the 200401011400 event, the simulation results show that the total response can be represented very well. The quasi-static response is still under predicted, and the dynamic response is highly over predicted. This also shows that the discrepancies might not be caused by impact force. Similar as before, to reach the value of measured quasi-static axial response, simulations have to incorporate larger impact loads which on the other hand is unlikely because by increasing the impact load, the total response and the dynamic response will be over predicted. The over prediction in the dynamic response even can be approximately 100% which is a large deviation from the measured dynamic response.

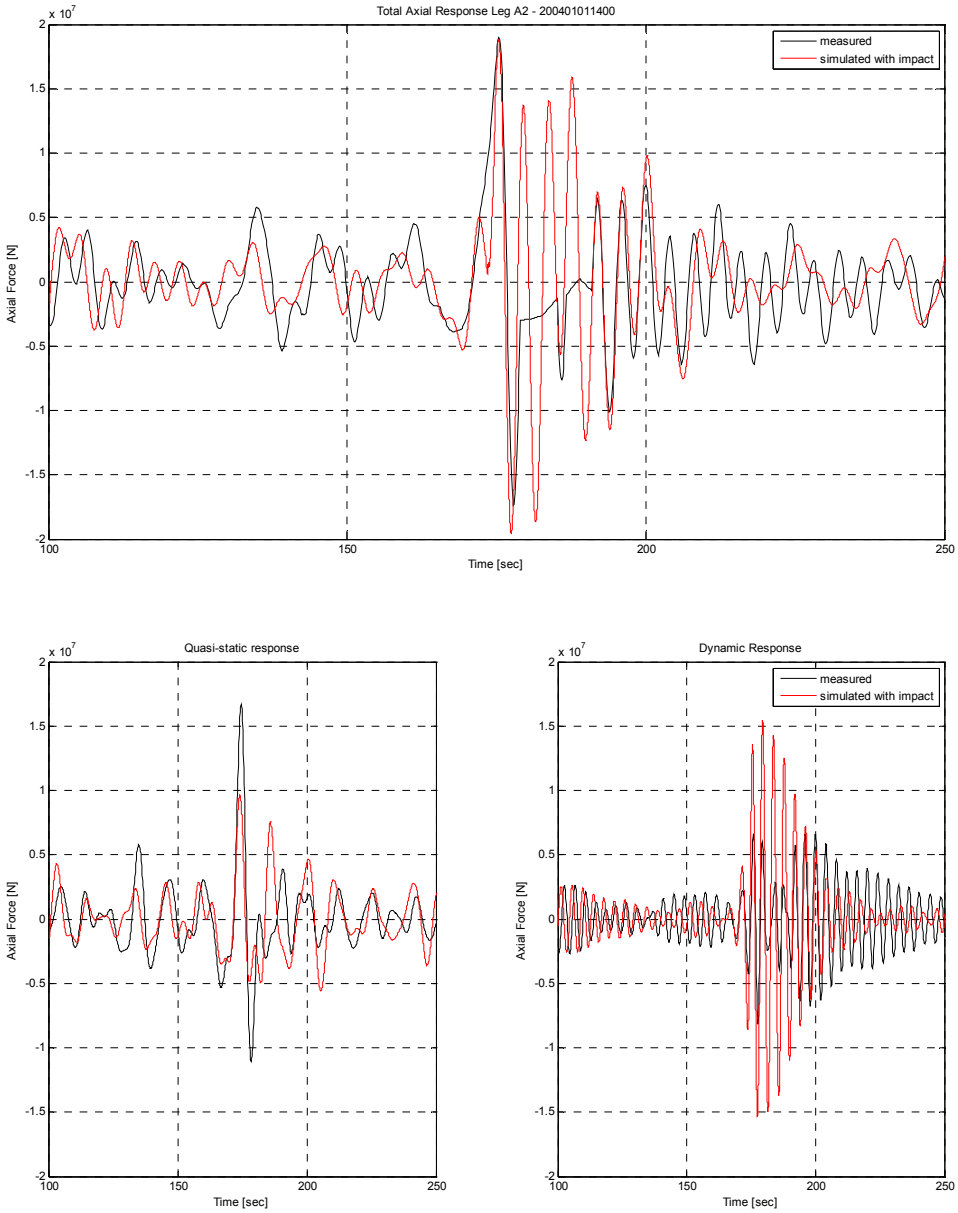

Figure 5. 42 Response of leg A2 (-108m) 200401011400 – Morison + Impact Force (Campbell & Weynberg impact profile) – with modified impact profile for leg A1 and B2

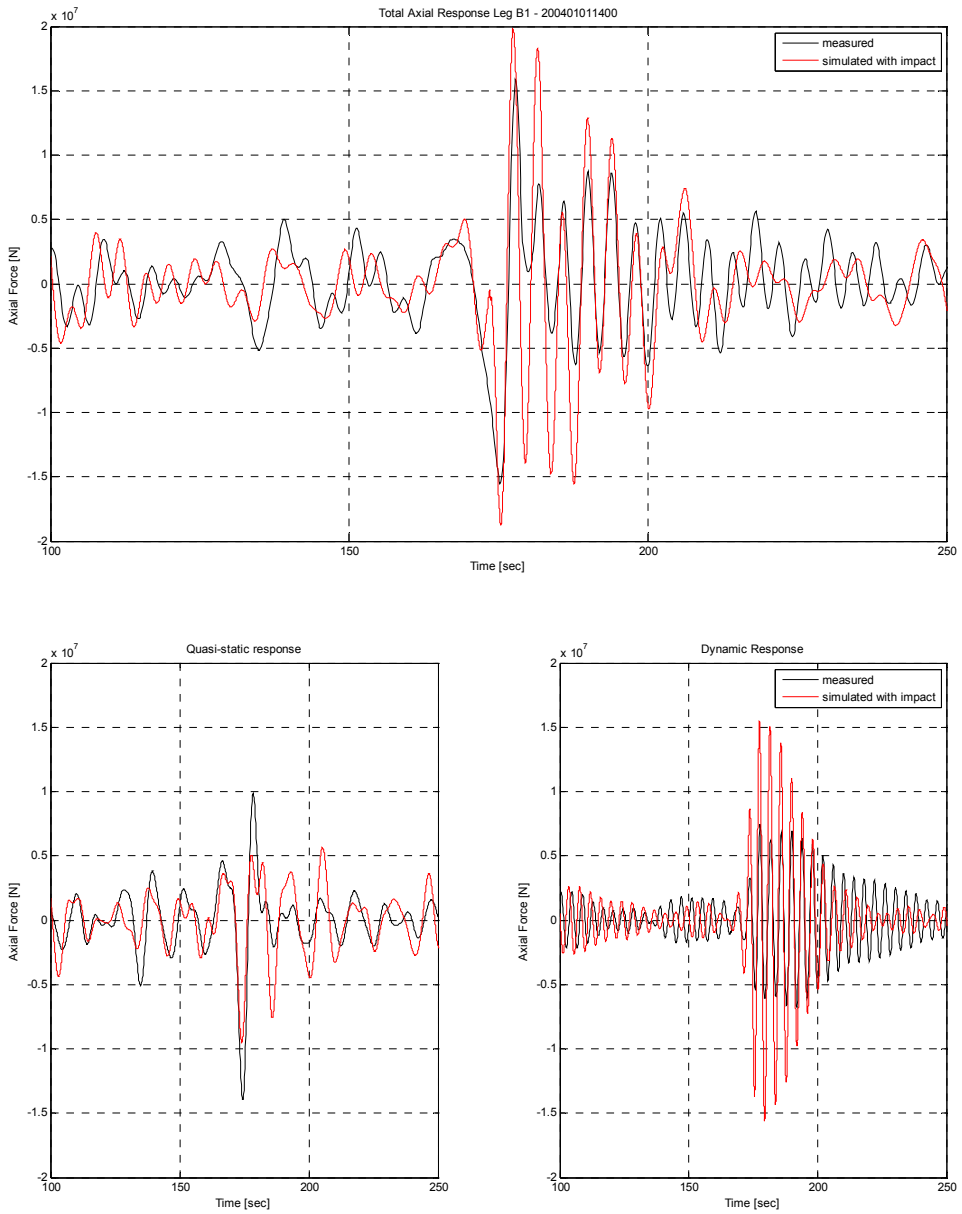

Figure 5. 43 Response of leg B1 (-108m) 200401011400 – Morison + Impact Force (Campbell & Weynberg impact profile) – with modified impact profile for leg A1 and B2

5.4 Effect of Damping Increase on the Structural Response

From the latest discussion above, it is identified that the dynamic response is in general over predicted. An increase in damping ratio of the structure will be introduced to see the effect of damping increase to the structural response. The simulation models so far have been using damping ratio of 2%. The damping ratio is influenced by the damping coefficient, mass, and eigen frequency of the structure. Exact damping value is actually difficult to obtain, thus the value of damping ratio used in the analysis is just an approximation and best practice. The damping ratio (ξ) is expressed as:

$$\xi = \frac{c}{2m\omega} \tag{5.10}$$

Where c, m, ω are respectively damping, mass and eigen frequency of the structure. In the analysis model being used in this study, proportional or Rayleigh damping has been used. Details about Rayleigh damping can be seen, among others, on NIRWANA user manual (Karunakaran D. , Brathaug, Passano, Økland, & Baarholm, 2008). In Rayleigh damping, the damping matrix is proportional to either the mass matrix and/or the stiffness matrix.

$$C = \alpha_1 M + \alpha_2 K \tag{5.11}$$

To introduce the damping to the simulation model, the parameter α_1 and α_2 in the damping matrix equation should be determined first. These parameters are a function of the eigen frequency and the damping ratio for the first and second mode of displacement. They can be expressed as:

$$\alpha_1 = 2\frac{\omega_1\omega_2}{\omega_2^2 - \omega_1^2}(\xi_1\omega_2 - \xi_2\omega_1) \tag{5.12}$$

$$\alpha_2 = 2\frac{\omega_1\omega_2}{\omega_2^2 - \omega_1^2}\left(\frac{\xi_2}{\omega_1} - \frac{\xi_1}{\omega_2}\right) \tag{5.13}$$

In this part of this study, the following modifications to the structural damping is introduced to see the effect of damping increase on structural response:

Table 5. 4 Structural damping modification parameters

Mode	$T_{structure}$	$\omega_{structure}$	ξ original	α original	ξ modified	α modified
1	4.09 sec	1.536 Hz	2%	0.0419	5%	0.076906
2	4.08 sec	1.539 Hz	2%	0.0008	5%	0.032507

Here, Wheeler stretching is used for the kinematic model, second order surface is used, and impact profile as proposed by Campbell and Weynberg is utilized. The simulation results show that the total axial response has less dynamic behavior. But by changing the damping ratio to 5%, the simulation not only under predicts total axial response at the beginning of the impact but also under predicts the response after that (time window 700-725 sec for 200401011200 and time window 180-250 sec for 200401011400). The simulation with 2% damping can simulate the total axial response better than the 5% damping model (Ref. Fig. 5.33, 5.34, 5.44, and 5.45). There is no difference in the quasi-static response. This proves that damping is essential to reduce dynamic response of the structure. The 5% damping model can simulate the dynamic/resonance response at the beginning of the impact very well. But then the response is under predicted. The 2% damping model (Ref. Fig. 5.33-5.36) over estimates the response at the beginning of the impact but then approximates the response after the impact starts pretty well. Thus, it can be said that having damping ratio of 2% is suitable for our simulations. 5% damping will give lower estimation of the response after the impact so that the result is less conservative. The simulation result can be seen on the following figures:

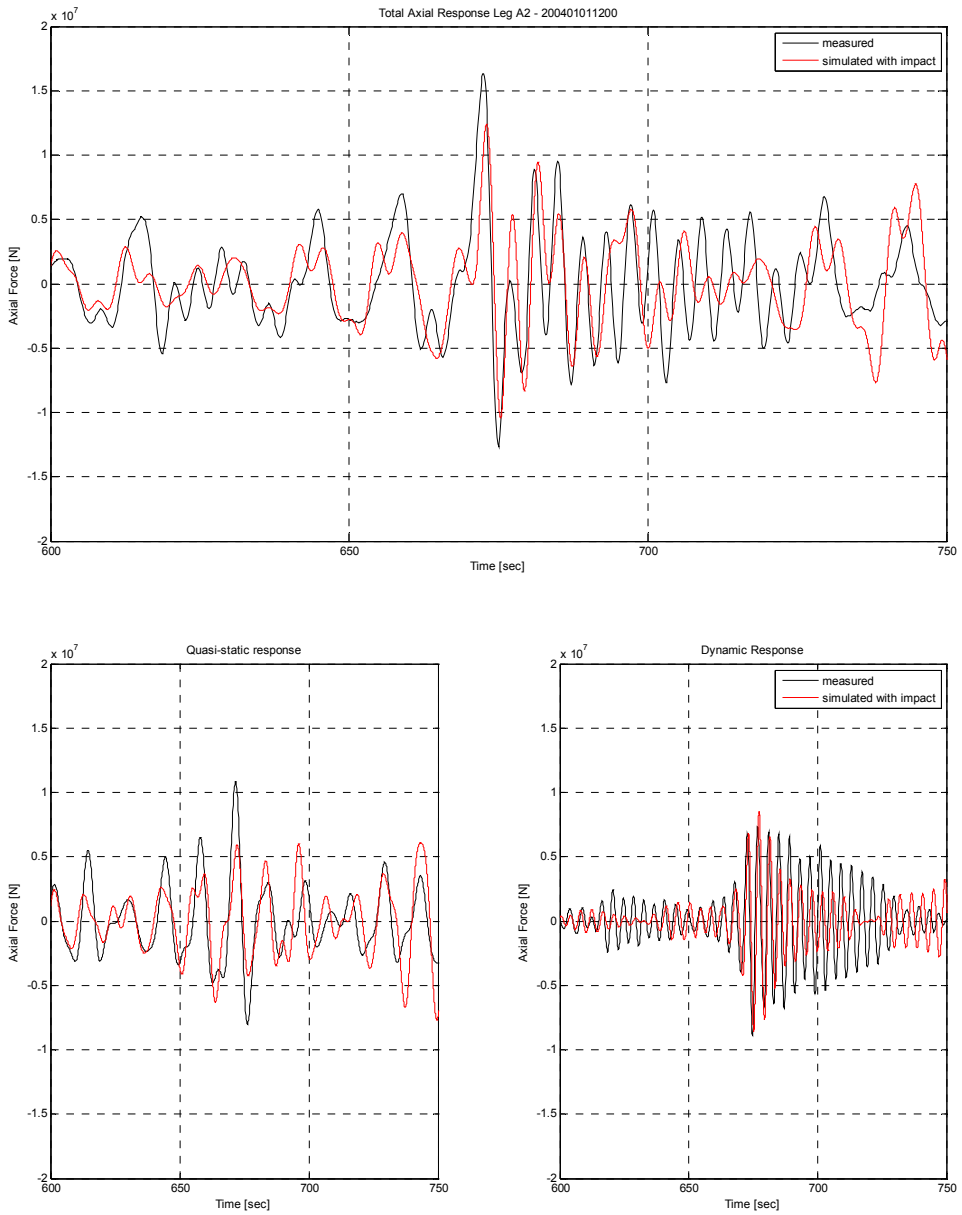

Figure 5. 44 Response of leg A2 (-108m) 200401011200 – Morison + Impact Force (Campbell & Weynberg impact profile) – damping ratio 5%

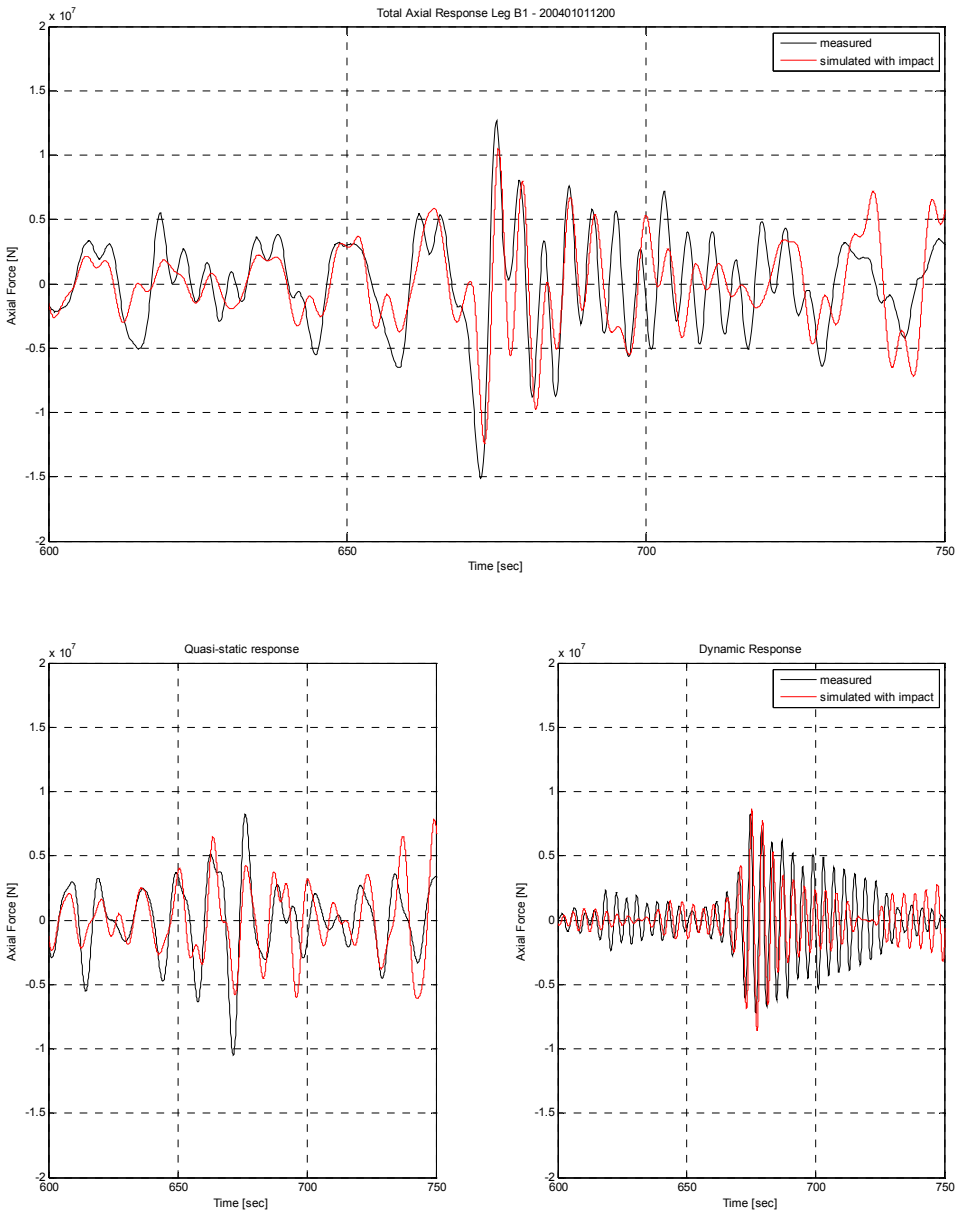

Figure 5. 45 Response of leg B1 (-108m) 200401011200 – Morison + Impact Force (Campbell & Weynberg impact profile) – damping ratio 5%

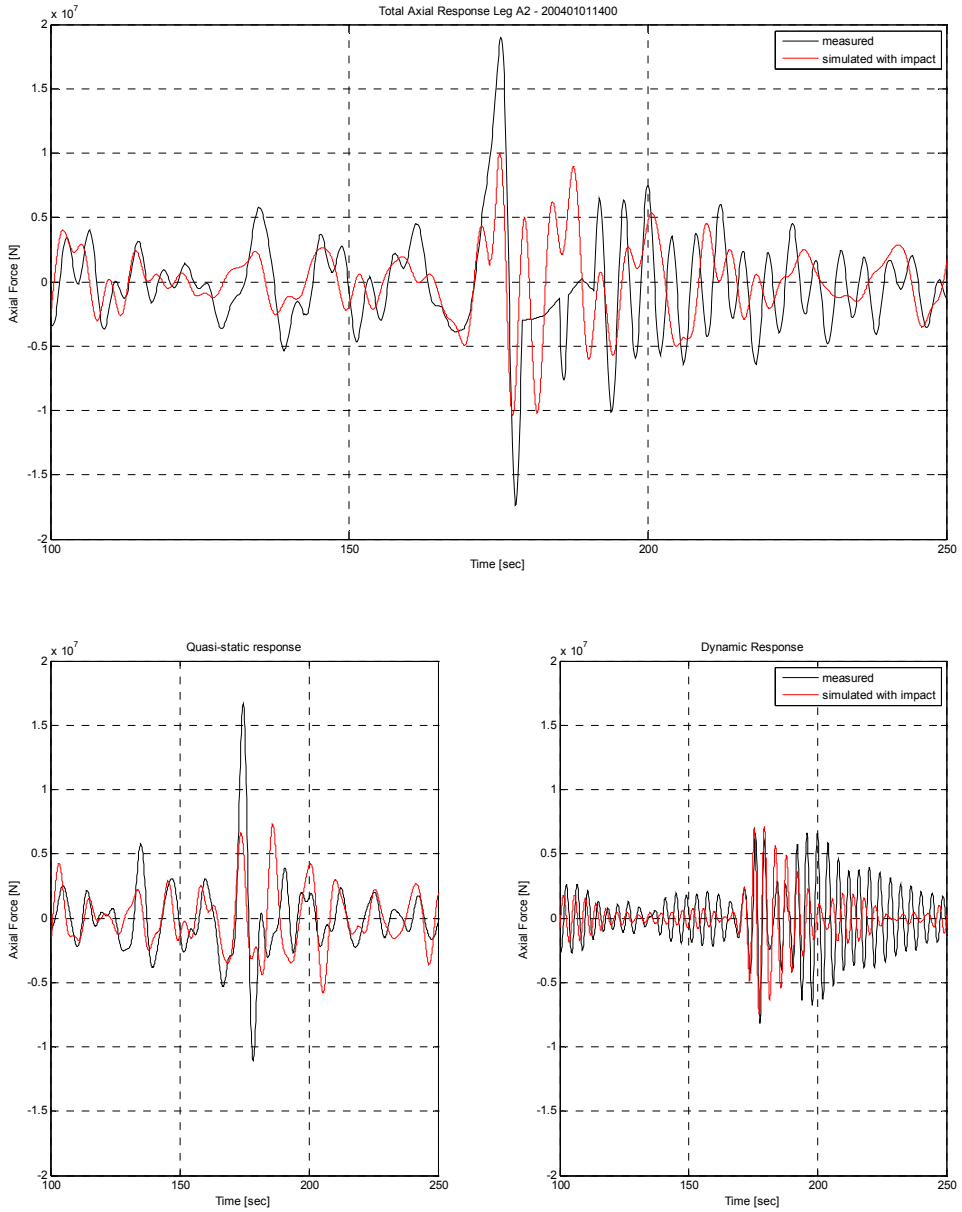

Figure 5. 46 Response of leg A2 (-108m) 200401011400 – Morison + Impact Force (Campbell & Weynberg impact profile) – damping ratio 5%

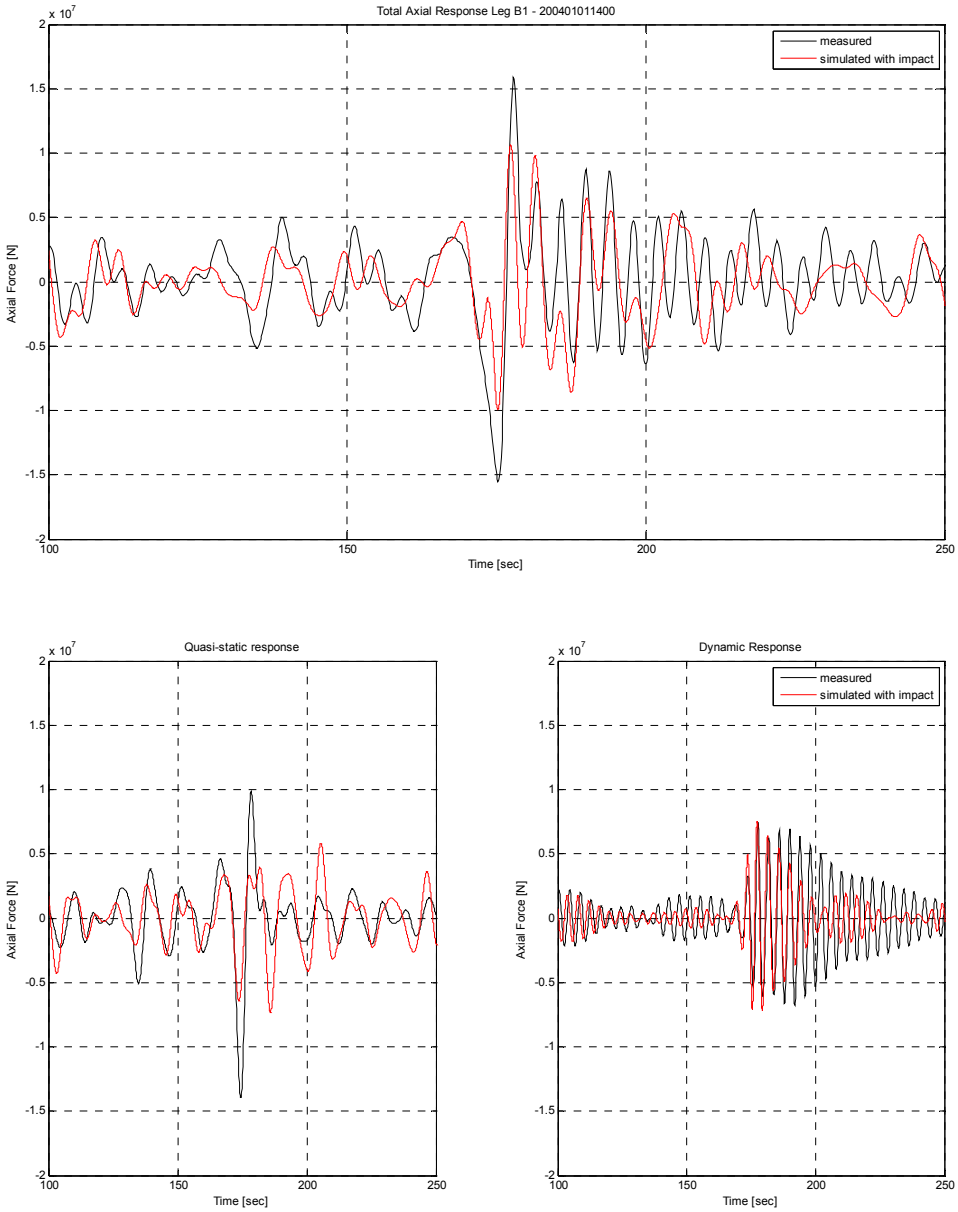

Figure 5. 47 Response of leg B1 (-108m) 200401011400 – Morison + Impact Force (Campbell & Weynberg impact profile) – damping ratio 5%

5.5 Comment on the Utilization of NORSOK Coefficient in Simulations

To some extent, it may not be practical to assess impact or slamming phenomenon in detail for design engineering. One common practice is to approximate slamming by modifying the original Morison equation. One way to do it is by modifying the hydrodynamic coefficients involved in the equation.

NORSOK N-003 recommends the following hydrodynamic values for tubular slender members whose acting forces calculated by Morison equation:

- $C_D = 0.65$ and $C_M = 1.60$ (smooth members)
- $C_D = 1.05$ and $C_M = 1.20$ (rough members)

The standard also mentions that during operations, members which are located 2m above MWL are considered smooth.

A sensitivity analysis on the hydrodynamic coefficients was done by Voie (Voie, 2009). In his study, several scenarios of mass and drag coefficients were looked through, which are:

- $C_D = 1.05$ and $C_M = 1.80$ (case 1)
- $C_D = 1.05$ and $C_M = 1.20$ (case 2)
- $C_D = 0.70$ and $C_M = 2.00$ (case 3)
- $C_D = 1.20$ and $C_M = 1.20$ (case 4)

The result mentions that based on those four cases, it can be concluded that the large under prediction is not caused by the application of inappropriate coefficients in the simulations. However, it can be seen that the four cases of simulation which were done by Voie did not represent major changes in drag coefficient but more on the mass coefficient. If wave impact is suspected to cause the discrepancies, more attention should be put on the drag coefficient.

In a study by Økland (Økland O. D., 2009), an increase of MWL of 2m was introduced and drag coefficient of 5.0 for horizontal bracings, legs, and risers/conductors starting from el. +8m up, was used. This is done to approximate the impact load which is caused by the wave crest higher than 8m. The result shows that by doing such modification, the dynamic response contribution becomes more similar to the measured response.

In the paper by Wienke and Oumeraci, it is cited that impact force may be approximated by multiplying the drag term on Morison equation by 2.5 (Wienke & Oumeraci, 2004). In order to do this, one can multiply the drag coefficient by the mentioned multiplication factor.

In the latest model developed by Marintek (Økland O. D., 2009), hydrodynamic coefficients $C_D = 0.85$ and $C_M = 1.40$ were used for members which are in the transition zone from rough to smooth. Members which are located between MWL and EL. +8m are assigned these hydrodynamic coefficients. These values are the average values for smooth and rough member coefficients suggested by NORSOK N-003. These coefficients are chosen as an approximation to the suggested NORSOK coefficients for simplicity of the model. By doing so, no additional nodes should be created at elevation +2m to be able to separate the smooth and rough members.

The measured wave profile (ref. Figure 5.1), during the occurrence of odd events, has a wave crest that can reach approximately +8m. Modification to analysis model is done by multiplying the drag coefficients to members (including risers, conductors and horizontal bracings) in the transition zone by 2.5 to see the applicability of the citation mentioned

above to our case. Thus, the following hydrodynamic coefficients are used for members in the transition zone:

- $C_D = 2.125$ and $C_M = 1.40$

Note that the same coefficients were used during the whole 20-minute simulation. Focus should be put on the time window where the impact is suspected to happen (t = 650-700s for 200401011200 event and t = 150-200s for 200401011400 event). In the analyses, the original damping ratio is used i.e. 2% of damping ratio. The following figures show the result of the simulations.

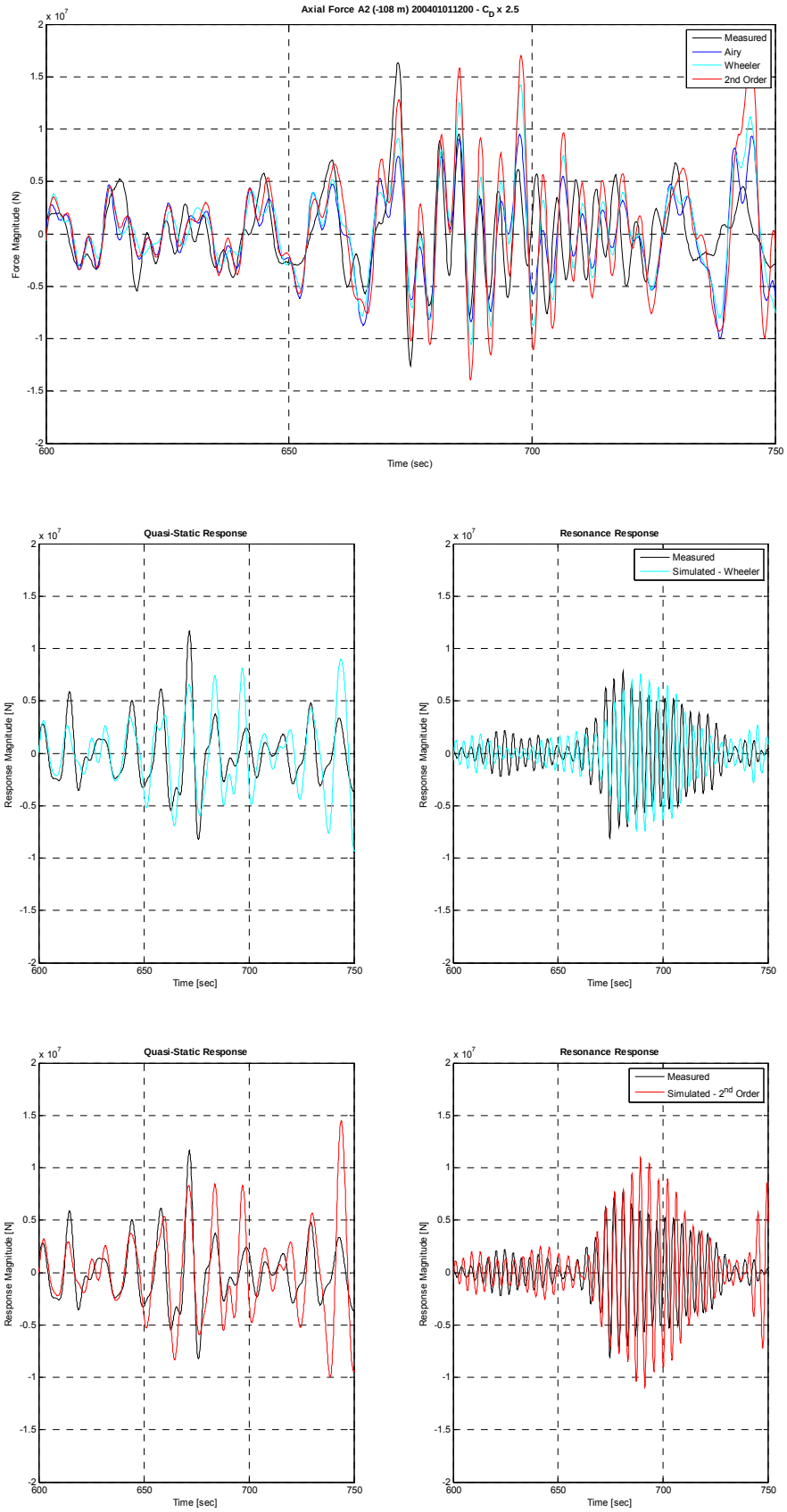

Figure 5. 48 Quasi-static and dynamic response 200401011200 after C_D Modification

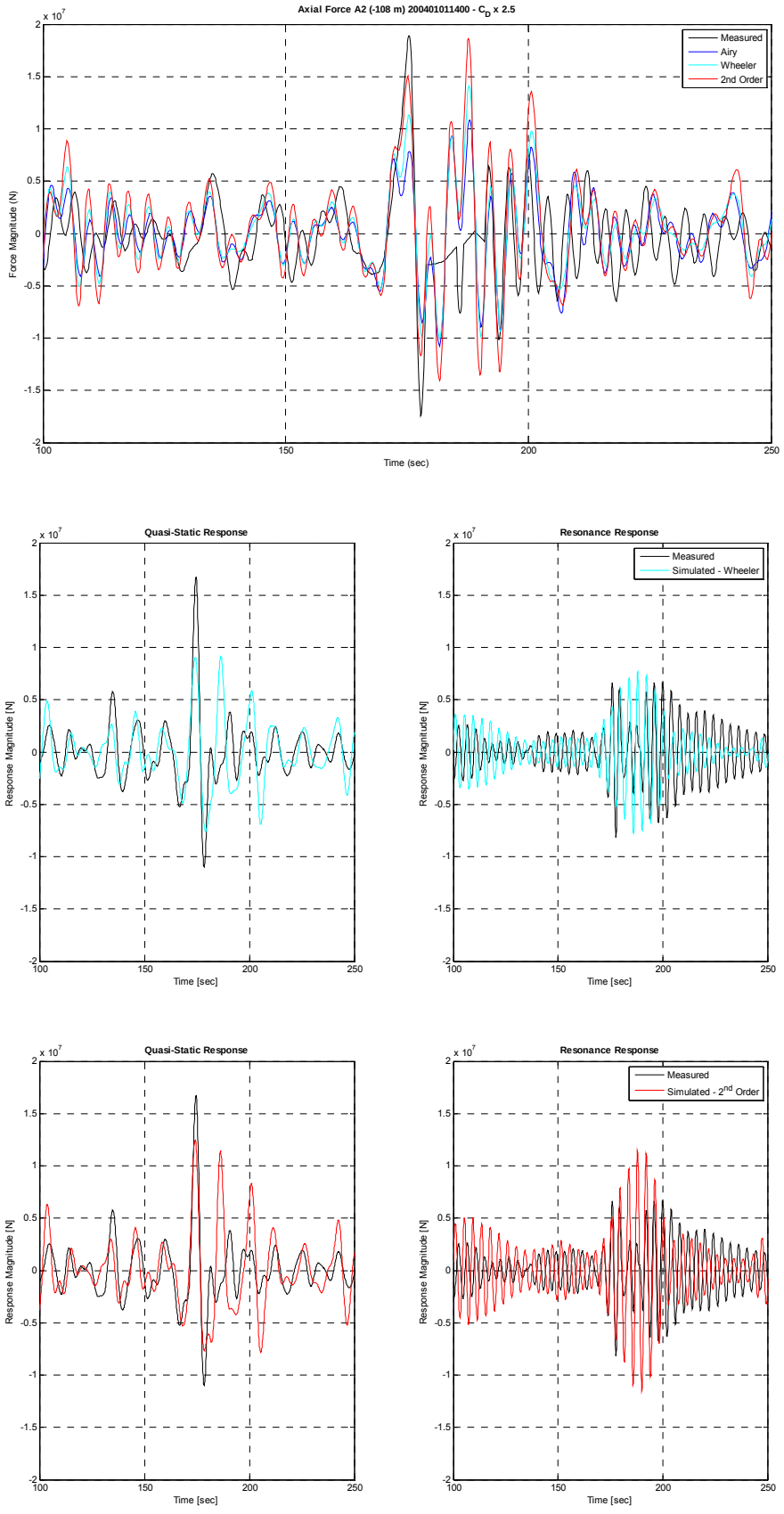

Figure 5. 49 Quasi-static and dynamic response 200401011400 after C_D Modification

From the above figures, it can be seen that increasing the drag coefficient to some extent reduce the gap between the measured response and the simulated ones. Increasing the drag coefficient 2.5 times the original value reduces the under prediction down to 14% from the original under prediction of up to 48%. The quasi-static response can be represented reasonably well by the second order simulation even though the measured response is still higher than the simulated values. Dynamic response can be simulated well enough by using Wheeler kinematics while second order model shows over prediction on the dynamic response. Despite the result on dynamic response, this constitutes that a higher multiplication factor of drag coefficient should be applied to a slender drag dominated structure like the one being observed in this study. To simulate impact phenomenon, an increase in the drag coefficient is needed.

Chapter 6
Conclusions and Recommendations

6.1 General

The present study has been done to explore the other possible causes of discrepancies between measured and simulated response on Kvitebjørn jacket. There are two main events which contain discrepancies between measurement and simulations, i.e. event 200401011200 and 200401011400. In event 200401011200, simulation shows an under prediction at time window 650 – 700 sec and an over prediction at time window 950-1000 sec. in event 200401011400, simulation shows an under prediction at time window 150-200 sec. The under predictions happen without the occurrence of very large wave. Some kinematics models are used in the simulations, which are:

- Airy kinematics combined with second order surface
- Wheeler stretching kinematics combined with second order surface
- Second order kinematics combined with linear surface

At the beginning of the study, statistical distributions of global maxima from the original simulations are being observed to see if the simulations are on conservative side. The structural model which is being used in this study was taken from the latest model update done by MARINTEK (Økland O. D., 2009).

Some efforts have been done in this study to determine the most possible cause of discrepancy of response in this jacket, including:

1. Modification of wave height.

   This part of this study is related to modification of measured wave crest and/or trough. The measured crest height and/or trough is enlarged for some meters and then used as wave input for the simulations.

2. Impact assessment due to breaking waves.

   Previous studies on this subject (Økland O. D., 2009), (Karunakaran & Økland, 2004) suggest that the odd events in terms of under prediction of responses may be caused of the impact force from breaking waves. Since original Morison equation cannot represent the impact, an additional impact force should be imposed on the structure. There are two impact profiles which are used in this study, i.e. impact profile proposed by Wienke and Oumeraci, and impact profile proposed by Campbell and Weynberg.

3. Observation on the influence of damping ratio of the structure to the response.

   The original simulation model utilizes 2% of damping ratio for the analysis. An increase of damping ratio to 5% in introduced in the simulation to see the effect of damping to structural response. The background of this effort is that the dynamic response from impact profile as proposed by Campbell & Weynber is to some extent over predicted at the beginning of the impact.

4. Observation on NORSOK N-003 recommended hydrodynamic coefficients.

   As an adaptation of NORSOK hydrodynamic coefficients, the latest model by MARINTEK utilizes the coefficients $C_D = 0.85$ and $C_M = 1.40$ for members which are in the transition zone from rough to smooth. Members which are located between MWL and EL. +8m are assigned these hydrodynamic coefficients. These values are the average values between the coefficients suggested by NORSOK N-003. These coefficients are chosen as an approximation to the suggested NORSOK coefficients for simplicity of the model. By doing so, no additional nodes should be created at elevation +2m to be able to separate the smooth and rough members.

6.2 Conclusions

Based on the above mentioned efforts, the following conclusions can be drawn:

1. Even though for some episodes the simulations show under predictions, in general, simulations are still statistically conservative. The distribution of global maxima in the 20-minute series shows that simulations are conservative enough to be used to estimate the real structural response.
2. Separating the total response of the structure into quasi-static and dynamic response, it can be seen that the dynamic response in general is represented better than the quasi-static response. This may become an indication that impact-like additional forces may not be the reason of under prediction.

3. It seems that the wave crest at platform location is under predicted approximately for 3m. To be able to produce the simulated response which approximates the measured response, the wave crest at the platform location should be around 10 meter while the measured wave crest is only around 7m. One possible phenomenon for this is the occurrence of pyramid-shaped wave. Pyramid wave may cause under prediction if the wave is measured as the pyramid leg on the sensor location, but in platform location the peak of the pyramid occurs. On the other hand, the pyramid wave may cause over prediction if the wave is measured as peak on the sensor location, while in the platform location the leg of pyramid wave actually occurs. So far, this is the most possible cause of discrepancies on the response of this platform based on the simulation results.
4. Impact profile as proposed by Wienke and Oumeraci may not be the reason of under prediction. By using this impact profile, the response of the structure is still under predicted. The quasi-static response resulted from this impact profile seems to have under predicted the real response. The dynamic response is under predicted too even though the behavior can be modeled pretty well. One will have to multiply the impact force with a factor of 10 to be able to obtain the total axial measured response value. This condition is deemed to be unreal because even though the impact on risers and conductors are considered in the model, the magnitude of total impact force should not be that big.
5. Impact model as proposed by Campbell and Weynberg was able to approximate the measured response better than the previous impact profile in this case. Total response and dynamic response can be represented pretty well. The quasi-static response still under predicts the response but if the presence of risers/caissons between the legs of the platform, the quasi-static response may be able to be approximated better.

   Since the exact impact calculation on the caissons is rather complicated, the impact on those members is approximated by increasing the original impact load with a multiplication factor (here = 2) and the loads are applied to leg A1 and B2 of the jacket. For the 200401011200 event, the results show a very good agreement in quasi-static load, but over predictions happen on the total and dynamic response. For the 200401011400 event, the total response can be represented very well. The quasi-static response is still under predicted, and the dynamic response is highly over predicted. This has shown that to reach the value of measured quasi-static axial response, simulations have to incorporate large impact loads which on the other hand is unlikely because by increasing the impact load, the total response and the dynamic response will be over predicted. For both events, the over prediction in the dynamic response even can be approximately 100% which is a large deviation from the measured dynamic response.

6. The presence of only one shock on leg B1 and two shocks on leg A2 on the measurement record at event 200401011400 at time window 150-200sec (Ref. Fig. 5.24 and 5.25), constitutes that there are dynamic phenomena happen as the wave passes trough the caissons/risers which are located among the legs of the jacket. This is difficult to simulate, but it can be said that caissons may work as wave obstructions which cause the wave to break more thus causing more frequent impact on leg A2.

7. Increasing the damping ratio of the structure (original = 2%, new = 5%) will reduce the dynamic response of the structure. The total response is represented better by the 2% damping model. The 5% damping simulation not only under predicts total axial response at the beginning of the impact but also under predicts the response after that (time window 700-725 sec for 200401011200 and time window 180-250 sec for 200401011400). The dynamic response at the beginning of the impact is represented very well by the 5% damping model, but shortly after the impact begins, the dynamic response is under predicted, unlike the 2% damping model which represents the dynamic behavior after the beginning of the impact better. This phenomenon may suggest that during the whole response of the structure, the damping value is not constant. Since simulating a structure with updated damping value over time is not a simple task, it is advisable to use damping ratio of 2% in this case.
8. For the case of slender drag dominated structure like Kvitebjørn, simulations show that a bigger drag coefficient than the one proposed by NORSOK N-003 should be used to represent impact.
9. In general, simulations by using second order kinematics have shown results that approach the values of measured response better than other kinematic models by the time under prediction happens. Innacuracies may be caused by spreading (directional) effect of the wave. For most simulations, the quasi-static response is under predicted. This may mean that there are quasi-static loads which are not captured by the simulations. Under prediction of wave crest may be one of the reason because simulations have shown that by increasing the wave crest, the response of the structure can be simulated well.

6.3 Recommendations

1. So far, the impact analysis in this study has been based on plunging breakers behavior of breaking waves. This is because more literatures were found on this type of breaking wave compared to the other types. Considering the effect from spilling breakers or the other types may be useful for comparison.
2. Using another method of identifying the linear wave content and shifting wave elevation in space may be beneficial for validation. Other methods are proposed by for example Johannessen (2009a and 2009b) and Winterstein et.al. (1999).
3. The term pyramid-shaped wave is so far hypothetical. More evidence of the existence of such wave should be made available.
4. The NIRWANA program to simulate the second order kinematics can only simulate 2^{12} discrete points of integration. If more points to be simulated, the result will be wrong. An upgrade to the program may be useful for future use. Also, integration of several available versions of the program into one final version is favorable.

Bibliography

Aibel. (2008). *Global Dynamic Re-Analysis.* Aibel Report No. 004544-0012, Rev 01.

Akersolutions. (2006). *Kvitebjørn Jacket Re-evaluation of Foundation Stiffness.* Akersolutions.

Bajer, C. (2002). *Time integration methods - still questions.* Warsaw: Theoretical Foundations of Civil Engineering. W. Szcześniak, ed., v. 1. pp 45-54.

Bathe, K. J., & Wilson, E. (1976). *Numerical Methods in Finite Element Analysis.* New Jersey: Prentice Hall.

Bonmarin, P. (1989). Geometric properties of deep-water breaking waves. *Journal of fluid mechanics* , 405-433.

Campbell, I. M., & Weynberg, P. A. (1980). *Measurement of parameters affecting slamming.* Southampton University: Wolfson Unit for Marine Technology.

Capital Regional District - Waves. (n.d.). Retrieved from CRD: http://www.crd.bc.ca/watersheds/protection/geology-processes/Waves.htm

DNV-RP-C205. (April 2007). *Environmental Conditions and Environmental Loads.* Høvik, Norway: Det Norske Veritas.

Ergin, A. *CE 491 COASTAL ENGINEERING I Lecture Notes - Chapter 9.* Ankara, Turkey: Middle East Technical University.

Faltinsen, O. M. (1990). *Sea Loads on Ships and Offshore Structures.* Cambridge, United Kingdom: Cambridge University Press.

Fugro. (2006). *Ambient Vibration System Identification Analysis Kvitebjorn Platform.* Fugro Structural Monitoring. Report no C30173\R001\Issue.

Goda, Y., Haranaka, S., & Kitahata, M. (1966). *Study on impulsive breaking wave forces on piles.* Japan: Report Port and Harbour Technical Research Institute 6 (5), 1– 30 (in Japanese).

Goudreau, G. L., & Taylor, R. L. (1972). *Evaluation of Numerical Integration Methods in Elasto-dynamics.* Computer Methods in Applied Mechanics and Engineering, Vol.2, No.1, pp. 69-97.

Haver, S. (2004). *Kvitebjørn Jacket, Oppsummering av hva som er målt når det gjelder plattformoppførsel.* Tech. Report Statoil.

Hilber, H. M., & Hughes, T. J. (1978). Collocation, Dissipation, and 'Overshoot' for Time Integration Schemes in Structural Dynamics. *Earthquake Engineering and Structural Dynamics, Vol. 6* , 99-117.

Johannessen, T. B. (2009a). Calculations of kinematics underneath measured time histories of steep water waves. *Applied Ocean Research.*

Johannessen, T. B. (2009b). Nonlinear superposition methods applied to continuous ocean wave spectra. *JOMAE.*

Johnson, D. E. (1966). *A Proof of the Stability of the Houbolt Method, AIAA Journal, Vol. 4. pp. 1450-1451.*

Karunakaran, D. (2004). *Kvitebjørn Jacket - Analysis of Measured Platform Data and Comparison to Calculated Response.* Trondheim: Tech. Rep. Marintek.

Karunakaran, D., & Haver, S. (2005). *Dynamic Behaviour of Kvitebjørn Jacket Structure - Numerical Predictions versus Full-Scale Measurements.* Paris: Eurodyn Conference.

Karunakaran, D., & Haver, S. (2005). *Dynamic Behaviour of Kvitebjørn Jacket Structure - Numerical Predictions versus Full-Scale Measurements.* Tech. Report Statoil.

Karunakaran, D., & Økland, O. D. (2004). *Kvitebjørn Jacket - Analysis of Measured Platform Data and Comparison to Calculated Response.* Trondheim: Marintek Report MT70 F04-232.

Karunakaran, D., Brathaug, H. P., & Passano, E. (1990). *NIRWANA - User's Manual including Theoretical Basis.* Trondheim: SINTEF Report.

Karunakaran, D., Brathaug, H. P., Passano, E., Økland, O. D., & Baarholm, G. S. (2008). *NIRWANA Version 1.2 User Manual.* Trondheim: Marintek.

Lader, P. F., Grytøyr, G., Myrhaug, D., & Pettersen, B. (1998). Breaking wave geometry with emphasis on Steepness and Curvature. *Proceedings of the 1998 international OTRC symposium* (pp. 281-289). Houston, Texas: ASCE.

Lader, P. F., Myrhaug, D., & Pettersen, B. (2000). Wave crest kinematics of deep water breaking waves. *Coastal engineering 2000* (pp. 355-369). Sydney, Australia: ASCE.

Langen, I., & Sigbjörnsson, R. (1979). *Dynamisk Analyse av Konstruksjoner.* Trondheim: Tapir.

Larsen, C. M. (2007). *TMR 4180 Marine Dynamics Compendium.* Trondheim.

Massel, S. R. (2007). *Ocean Waves Breaking and Marine Aerosol Fluxes.* New York: Springer.

Myrhaug, D., & Kjeldsen, S. P. (1978). *Kinematics and Dynamics of Breaking Waves.* Trondheim, Norway: Report No. STF60 A78100, Ships in Rough Seas, Part 4. Norwegian Hydrodynamic Laboratories.

Myrhaug, D., & Kjeldsen, S. P. (1986). Steepness and Asymmetry of Extreme Waves and the Highest Waves in Deep Water. *Ocean Engineering* (pp. 549-568). Pergamon Journals Ltd.

Nestegård, A., Kalleklev, A. J., Hagatun, K., Wu, Y. L., Haver, S., & Lehn, E. (2004). Resonant vibrations of riser guide tubes due to wave impact. *23rd International Conference on Offshore Mechanics and Arctic Engineering* .

Newland, D. E. (1974). *Random Vibrations, Spectral and Wavelet Analysis.* New York: John Wiley & Sons Inc.

Newmark, N. M. (1959). *A Method of Computation sor Structural Dynamics.* ASCE Journal of the Engineering Mechanics Division, Vol. 85 No. EM3.

NORSOK. (1999). *Action and action effects.* NORSOK N-003 Rev. 1.

Økland, O. D. (2009). *Kvitebjørn Jacket - Analysis of Extreme Responses.* Trondheim: Marintek Report.

Økland, O. D. (2006). *Kvitebjørn Jacket Analysis - Analysis of Full Scale Measurements and Comparison with Calculated Response for Storms in December 2003 and January 2004.* Trondheim: MARINTEK Report MT70 F06-042.

Soemantri, D. (2009). *Response of Slender Jacket Structure in Deep Water.* Trondheim, Norway: Project Thesis, NTNU.

Stansberg, C. T. (2008). A Wave Impact Parameter. *Proceedings of the ASME 27th International Conference on Offshore Mechanics and Arctic Engineering.* Estoril, Portugal: OMAE2008.

Stansberg, C. T. (1998). Non-Gaussian Extremes in Numerically Generated Second-Order Random Waves on Deep Water. *Proc. of the 8th International Offshore and Polar Engineering Conference* (pp. 103-110). Montréal, Canada: ISOPE.

Stansberg, C. T. (2003). Second-Order Effects in Random. *Proc., 13th ISOPE Conference* (pp. 137-144). Honolulu, Hawaii, USA: ISOPE.

Voie, P. E. (2009). *An Investigation of the Standard Approach for Calculation of Hydrodynamic Loads on Slender Structures.* Trondheim: NTNU: Master Thesis.

Voie, P. E. (2008). *Investigating the Adequacy of the Standard Procedure for Calculating Loads on Slender Structures.* Trondheim: NTNU: Project Thesis:.

Wienke, J., & Oumeraci, H. (2004). Breaking Wave Impact Force on a Vertical and Inclined Slender Pile - Theoretical and Large-Scale Model Investigations. *Coastal Engineering Journal* , 435-462.

Wienke, J., Sparboom, U., & Oumeraci, H. (2004). Theoretical Formulae for Wave Slamming Loads on Slender Circular Cylinders and Application for Support Structures of Wind Turbines. *ICCE 2004.* Further details not known.

Wigaard, J. (2008). *Dynamic Analysis of Kvitebjørn.* Memo, Oct 2008 (As cited in Økland (2009)).

Wikipedia - Breaking Wave. (n.d.). Retrieved from Wikipedia: http://en.wikipedia.org/wiki/Breaking_wave

Winterstein, S. R., & Sweetman, B. (1999). *Second-order random ocean waves: Prediction of temporal and spatial variation from fixed and moving references.* Department of Civil Engineering, Stanford University.

Appendix

A.1 Thesis Problem Description

M.Sc. thesis 2009

for

Stud.techn.
Dilly S. Soemantri

Comparison of numerically predicted response and measured response for jacket structures

(Sammenligning av målt og beregnet respons i en fagverksplattform)

A jacket structure, Kvitebjørn, installed in 190m of water is to be considered. A figure of the platform is included in Fig. 1. The natural period of the platform is so large that a considerable dynamic amplification is expected. This together with the non-linear drag loading make it necessary to base the design load calculations on time domain simulations. There is limited experience regarding time domain simulations of jackets heavily exposed to dynamics. It is therefore of interest to compare various formulations of the time domain simulations with available measurements.

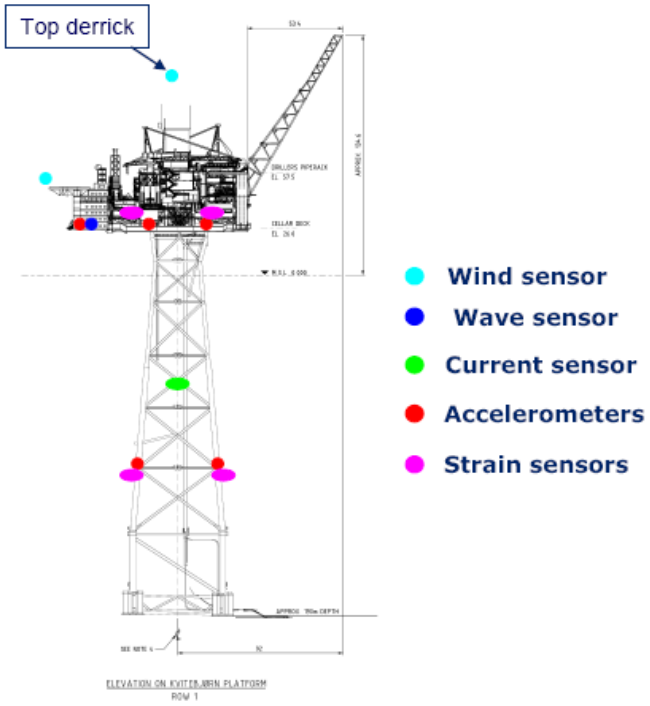

Fig. A.1 Kvitebjørn jacket and the locations of the various types of measurements.

For Kvitebjørn, platform response has been measured from installation in 2003 and until summer 2007. Accelerations at various locations as well as strain of several structural members are recorded. Time histories for the surface elevation are obtained using a down-looking radar device. Thus for a number of short term events, simultaneous measurements of the wave process and corresponding structural response are available.

When designing a platform at the Norwegian Continental Shelf, several limit states have to be considered: Serviceability Limit State (SLS), Fatigue Limit State (FLS), Ultimate Load Limit State (ULS) and Accidental Limit State (ALS). In the thesis one shall focus on a comparison of simulated platform response using measured wave train with simultaneously measured response. However, summarizing the work, consequences of findings in the thesis regarding ULS shall be discussed.

For full scale experiments like this, the input conditions of interest regarding load predictions are merely roughly known, e.g. for the Kvitebjørn case current speed is not known, degree of short crestedness of the waves is not known, etc.. Accordingly, we can not expect simulated and measured time histories exactly, but the general impression based on the results obtained by Marintek during their verification work is that in most cases a reasonable agreement is achieved.

However, for some few cases a significant under prediction is obtained for the simulations when using measured wave as input. These events are also among the most severe response events that have been measured. So far the reason for this discrepancy between measured and simulated response is not resolved. An aim of this work is to identify and review possible reasons for the observed difference.

The time domain simulation of platform behaviour for a given wave history is to be done using the computer program Nirwana. This will partly be done by the standard version of Nirwane, but some of the work is to be carried out the Nirwana version prepared in Voie (2009).

The work should be carried out in steps as follows:

1. As an extended introduction various formulations of time domain simulations shall be discussed. It shall clearly be presented which approaches that will be adopted in the thesis. Effects of different assumptions shall as far as possible be indicated for the platform. For this part of the work, the input wave is simulated from a wave spectrum.

2. As an introduction to the episodes where a considerable underprediction of the measured response is indicated by previous studies, one shall discuss the results of previous investigations. A time domain comparison shall be done as well as a comparison of distribution of maxima. One shall look at total response, quasistatic response and resonant response by introducing adequate filters. One shall in particular investigate the simulated response in view of the simultaneous wave events. Focus is to be given to the storm still water level.

3. The standard Morrison equation shall briefly be discussed. In the Norsok Standard, N-003, a well defined recipe is found regarding the coefficients. This is primarily suggested for structures behaving quasi-statically. Will the same coefficient be adequate when considerable dynamics are present? Will the same coefficients be of adequate if second order wave kinematics is adopted.

4. A fact is that the wave elevation is measured about 60m from the centre of the jacket. It shall be demonstrated how one can calculate the corresponding surface elevation in platform centre. The shift of the time history shall be done both using a Gaussian stochastic process for the measured process as well as assuming the measured process to be a second order process.

5. Identify a number of 20-minute storm episodes for which both the history and the simultaneous response histories are available. These will be the reference response histories that the various time domain simulations will be compared against. The selection can be based on the work done by Marintek.

6. A first approach is to assume sea surface elevation to be Gaussian. Assume that kinematics can be calculated using Wheeler stretching. Comparison is to be made against measured response.

7. Next approach is to assume the sea surface can be modelled as a second order process. One shall then use to kinematics models: i) Wheeler stretching, ii) Second order kinematics. The kinematics shall be compared in connection with interesting wave events. Predicted response shall be compared with measured response.

8. It shall be considered if breaking waves can be of concern regarding response of jacket structures. How this is to be done is to be discussed with supervisors. A possibility is to identify possible breaking wave events and establish an additional

load to be introduced to the computer program.

9. Finally, the work is to be summarized. Findings shall be clearly pointed out. Recommendations for future work should also be included.

The work may show to be more extensive than anticipated. Some topics may therefore be left out after discussion with the supervisor without any negative influence on the grading.

The candidate should in his report give a personal contribution to the solution of the problem formulated in this text. All assumptions and conclusions must be supported by mathematical models and/or references to physical effects in a logical manner. The candidate should apply all available sources to find relevant literature and information on the actual problem.

The report should be well organised and give a clear presentation of the work and all conclusions. It is important that the text is well written and that tables and figures are used to support the verbal presentation. The report should be complete, but still as short as possible.

The final report must contain this text, an acknowledgement, summary, main body, conclusions, suggestions for further work, symbol list, references and appendices. All figures, tables and equations must be identified by numbers. References should be given by author and year in the text, and presented alphabetically in the reference list. The report must be submitted in two copies unless otherwise has been agreed with the supervisor.

The supervisor may require that the candidate should give a written plan that describes the progress of the work after having received this text. The plan may contain a table of content for the report and also assumed use of computer resources.

From the report it should be possible to identify the work carried out by the candidate and what has been found in the available literature. It is important to give references to the original source for theories and experimental results.

The report must be signed by the candidate, include this text, appear as a paperback, and - if needed - have a separate enclosure (binder, diskette or CD-ROM) with additional material.

The work will be carried out in cooperation with Statoil.

Supervisor: Prof. II Sverre Haver, Senior Spesialist, Statoil.

Co-supervisor: Dr. Ing. Ole David Økland, Research Manager, Marintek.

Co-supervisor: Dr. Thomas B-Johannessen, Chief Engineer, Aker Solutions

A.2 Matlab Code – Impact Wienke & Oumeraci Calculation

```
close all;
clear all;

%% Impact Load Calculation (Wienke, Oumeraci (2005))
% References:
% - Wienke, J., Sparboom, U., Oumeraci, H. 2004. Theoretical formulae
%   for wave slamming loads on slender circular cylinders and application
%   for support structures of wind turbines
% - Wienke, J., Oumeraci, H. 2004. Breaking wave impact force on a vertical
%   and inclined slender pile - theoretical and large-scale model
%   investigations
% - Myrhaug, D., Kjeldsen, S. 1986. Steepness and asymmetry of extreme
%   waves and the highest waves in deep water


D = 2.0;         %[m]    diameter of cylinder
R = 0.5*D;       %[m]    radius of cylinder
h = 190;         %[m]    water depth
g = 9.81;        %[ms-2] gravity acceleration
rho = 1025;      %[kg/m3]    sea water density

%% Sea state 200401011200
gamma = 6.18;            %[deg]  cylinder inclination angle relative to vertical axis
Twav = 675-661.5;        %[sec]  wave period 200401011200
H = 6.28+5.903;          %[m]    wave height 200401011200
wave_angle = 65;         %[deg]  wave angle 200401011200
t_top = 672.5;           %[sec]  time of top crest 200401011200
%t_top = 672.5-500;
b1b2 = 23.877;           %[m]    leg B1 - B2 distance
b1a1 = 6.398;            %[m]    leg B1 - A1 distance
crest = 6.28;

%% Sea state 200401011400
%gamma = 5.69;             %[deg]  200401011400
%Twav = 178.1-165.8;       %[sec]  wave period 200401011400
%H = 7.966+6.277;          %[m]    wave height 200401011400
%wave_angle = 75;          %[deg]  wave angle 200401011400
%t_top = 175.4;            %[sec]  time of top crest 200401011400
%b1b2 = 22.4039;           %[m]    leg B1 - B2 distance
%b1a1 = 10.4471;           %[m]    leg B1 - A1 distance
%crest = 7.966;

%% Use Deep Water Theory

C = g*Twav/2/pi*1.2;       %[m/s]  1.2 x wave celerity (DNV)
miu = 0.90;                %       horizontal assymmetry factor (Myrhaug, Kjeldsen,
1986)
%eta_b = H*miu;             %[m]    breaking wave crest
eta_b = crest;
lambda = 0.5;              %       curling factor (plunging breakers)
yy = cos(gamma*pi/180);
sinw = sin(wave_angle*pi/180);
cosw = cos(wave_angle*pi/180);

t_impact = 13/32*(R/C);      %[sec]  impact duration
t_lim = 1/8*R/C;             %[sec]  time limit 1 for impact profile
%t_incr = t_impact/200;       %[sec]  time increment on load
t_incr = 0.0009637;

him = eta_b*lambda;          %[m]    height of impact area
count = 1;

f(count) = rho*R*C*C*yy*(2*pi*yy); %[N]   impact load at t = 0 sec
waktu = 1000*(0:t_incr:t_impact+t_incr);%[ms]   time axis for plot

for t = t_incr:t_incr:t_impact
    count = count+1;
    if t <= t_lim
        f(count) = rho*R*C*C*yy*(2*pi*yy - ...
            2*sqrt(yy*C*t/R)*atanh(sqrt(1-0.25*C*t/R/yy)));
    else
        t_aksen = t-R/32/C;
        f(count) = rho*R*C*C*yy*(pi*sqrt(1/6*yy*1/(C*t_aksen/R))-...
            ((8/3*yy*C*t_aksen/R)^0.25)*...
```

```
                atanh(sqrt(1-C*t_aksen/R*sqrt(6*C*t_aksen/R/yy))));
        end
    end

    f(count+1) = 0;
(80) F = f*him;

    display('F_nol =')
    F(1)

    skala = 0:t_incr:1050;              %for 200401011200
    %skala = 0:t_incr:550;               %for 200401011400


    %% Force on B1
(90) Force_B1 = zeros(length(skala),1);
    lokasi_B1 = round(t_top/t_incr)+1;

    for j = 1:length(waktu)
        Force_B1(lokasi_B1) = F(j);
        lokasi_B1 = lokasi_B1 + 1;
    end

    Fx_B1 = Force_B1*cosw;
    Fy_B1 = Force_B1*sinw;
(100) Fz_B1 = 0*Force_B1;
    Mx_B1 = 0*Force_B1;
    My_B1 = 0*Force_B1;
    Mz_B1 = 0*Force_B1;

    %% Force on B2
    Force_B2 = zeros(length(skala),1);
    lokasi_B2 = round((t_top+b1b2/C)/t_incr)+1;

    for j = 1:length(waktu)
(110)       Force_B2(lokasi_B2) = F(j);
        lokasi_B2 = lokasi_B2 + 1;
    end

    Fx_B2 = Force_B2*cosw;
    Fy_B2 = Force_B2*sinw;
    Fz_B2 = 0*Force_B2;
    Mx_B2 = 0*Force_B2;
    My_B2 = 0*Force_B2;
    Mz_B2 = 0*Force_B2;
(120)
    %% Force on A1
    Force_A1 = zeros(length(skala),1);
    lokasi_A1 = round((t_top+b1a1/C)/t_incr)+1;

    for j = 1:length(waktu)
        Force_A1(lokasi_A1) = F(j);
        lokasi_A1 = lokasi_A1 + 1;
    end

(130) Fx_A1 = Force_A1*cosw;
    Fy_A1 = Force_A1*sinw;
    Fz_A1 = 0*Force_A1;
    Mx_A1 = 0*Force_A1;
    My_A1 = 0*Force_A1;
    Mz_A1 = 0*Force_A1;

    %% Force on Riser 1, 2, 3, 4
    %Force_R1234 = zeros(length(skala),1);
    %lokasi_R1234 = round((t_top+b1a1/C)/t_incr)+1;
(140) %
    %for j = 1:length(waktu)
    %    Force_R1234(lokasi_R1234) = F(j);
    %    lokasi_R1234 = lokasi_R1234 + 1;
    %end
    %
    %Fx_R1234 = 0.75*1.22/2*Force_R1234*cosw;
    %Fy_R1234 = 0.75*1.22/2*Force_R1234*sinw;
    %Fz_R1234 = 0*Force_R1234;
    %Mx_R1234 = 0*Force_R1234;
(150) %My_R1234 = 0*Force_R1234;
    %Mz_R1234 = 0*Force_R1234;
```

```
%
%% Force on Riser 5
%Force_R5 = zeros(length(skala),1);
%lokasi_R5 = round((t_top+b1a1/C)/t_incr)+1;
%
%for j = 1:length(waktu)
%    Force_R5(lokasi_R5) = F(j);
%    lokasi_R5 = lokasi_R5 + 1;
%end
%
%Fx_R5 = 0.8*0.72/2*Force_R5*cosw;
%Fy_R5 = 0.8*0.72/2*Force_R5*sinw;
%Fz_R5 = 0*Force_R5;
%Mx_R5 = 0*Force_R5;
%My_R5 = 0*Force_R5;
%Mz_R5 = 0*Force_R5;
%
%% Force on Riser 6 - 13
%Force_R613 = zeros(length(skala),1);
%lokasi_R613 = round((t_top+b1a1/C)/t_incr)+1;
%
%for j = 1:length(waktu)
%    Force_R613(lokasi_R613) = F(j);
%    lokasi_R613 = lokasi_R613 + 1;
%end
%
%Fx_R613 = 0.75*0.76/2*Force_R613*cosw;
%Fy_R613 = 0.75*0.76/2*Force_R613*sinw;
%Fz_R613 = 0*Force_R613;
%Mx_R613 = 0*Force_R613;
%My_R613 = 0*Force_R613;
%Mz_R613 = 0*Force_R613;
%
%% Force on Conductor
%Force_con = zeros(length(skala),1);
%lokasi_con = round((t_top+b1a1/C)/t_incr)+1;
%
%for j = 1:length(waktu)
%    Force_con(lokasi_con) = F(j);
%    lokasi_con = lokasi_con + 1;
%end
%
%Fx_con = 0.6*1.65/2*Force_con*cosw;
%Fy_con = 0.6*1.65/2*Force_con*sinw;
%Fz_con = 0*Force_con;
%Mx_con = 0*Force_con;
%My_con = 0*Force_con;
%Mz_con = 0*Force_con;
%
%% Graphs

figure(1)
plot(waktu,F,'b','LineWidth',2);
grid on;
title('Impact Profile','fontweight','bold');
xlabel('Impact Time [msec]');
ylabel('Force [N]');

figure(2)
plot(skala,Force_B2,'LineWidth',2);hold on;
plot(skala,Force_B1,'LineWidth',2);hold on;
plot(skala,Force_A1,'LineWidth',2);
axis([672.49 673.49 0 16000000]);    %for 200401011200
%axis([175.39 176.6 0 16000000]);   %for 200401011400
grid on;
title('Impact Force Time Series','fontweight','bold');
xlabel('Time [sec]');
ylabel('Force [N]');

%y = [transpose(skala) Fx_B2 Fy_B2 Fz_B2 Mx_B2 My_B2 Mz_B2...
%    Fx_B1 Fy_B1 Fz_B1 Mx_B1 My_B1 Mz_B1...
%    Fx_A1 Fy_A1 Fz_A1 Mx_A1 My_A1 Mz_A1];
%%    Fx_R1234 Fy_R1234 Fz_R1234 Mx_R1234 My_R1234 Mz_R1234... %R1
%    Fx_R1234 Fy_R1234 Fz_R1234 Mx_R1234 My_R1234 Mz_R1234... %R2
%    Fx_R1234 Fy_R1234 Fz_R1234 Mx_R1234 My_R1234 Mz_R1234... %R3
%    Fx_R1234 Fy_R1234 Fz_R1234 Mx_R1234 My_R1234 Mz_R1234... %R4
%    Fx_R5 Fy_R5 Fz_R5 Mx_R5 My_R5 Mz_R5...                   %R5
```

```
        %    Fx_R613 Fy_R613 Fz_R613 Mx_R613 My_R613 Mz_R613...       %R6
(230)   %    Fx_R613 Fy_R613 Fz_R613 Mx_R613 My_R613 Mz_R613...       %R7
        %    Fx_R613 Fy_R613 Fz_R613 Mx_R613 My_R613 Mz_R613...       %R8
        %    Fx_R613 Fy_R613 Fz_R613 Mx_R613 My_R613 Mz_R613...       %R9
        %    Fx_R613 Fy_R613 Fz_R613 Mx_R613 My_R613 Mz_R613...       %R10
        %    Fx_R613 Fy_R613 Fz_R613 Mx_R613 My_R613 Mz_R613...       %R11
        %    Fx_R613 Fy_R613 Fz_R613 Mx_R613 My_R613 Mz_R613...       %R12
        %    Fx_R613 Fy_R613 Fz_R613 Mx_R613 My_R613 Mz_R613...       %R13
        %    Fx_con Fy_con Fz_con Mx_con My_con Mz_con];             %cond

        %dlmwrite('C:\Users\soemantr\Documents\Trymatlab\ok\imp_200401011400bf525_10.txt',...
(240)   %    y, '-append', 'precision', '%15.8f', 'delimiter',' ',...
        %    'newline','pc','roffset', 1);

        %fid = fopen('C:\Users\soemantr\Documents\Try
        matlab\New\impact_200401011400_500.txt', 'w');
        %fprintf(fid,'%14.8f %15.8f %15.8f %15.8f %15.8f %15.8f %15.8f\n', y);
        %fclose('all');
```

A.3 Matlab Code – Impact Campbell & Weynberg Calculation

```
clear all;
close all;

%% Impact Load Calculation
%  Reference:
%  - Campbell,Weynberg. 1980. Measurement of Parameters Affecting Slamming.
%  - Nestegård, Kalleklev, Hagatun, Wu, Haver, Lehn. 2004. Resonant
%    Vibrations of Riser Guide Tubes due to Wave Impact.

D = 2;          %[m] Leg diameter
s = 0:0.01:D;   %[m] cylinder submergence
rat = s/D;

R = 0.5*D;      %[m]    radius of cylinder
h = 190;        %[m]    water depth
g = 9.81;       %[ms-2] gravity acceleration
rho = 1025;     %[kg/m3]    sea water density

%% Sea state 200401011200
gamma = 6.18;           %[deg]  cylinder inclination angle relative to vertical
axis
Twav = 675-661.5;       %[sec]  wave period 200401011200
Timpact = 2.3437;       %[sec]  impact duration
H = 6.28+5.903;         %[m]    wave height 200401011200
wave_angle = 65;        %[deg]  wave angle 200401011200
t_top = 672.5;          %[sec]  time of top crest 200401011200
%t_top = 672.5-500;
b1b2 = 23.877;          %[m]    leg B1 - B2 distance
b1a1 = 6.398;           %[m]    leg B1 - A1 distance
crest = 6.28;

%% Sea state 200401011400
%gamma = 5.69;              %[deg]  200401011400
%Twav = 178.1-165.8;        %[sec]  wave period 200401011400
%Timpact = 1.4323;          %[sec]  impact duration
%H = 7.966+6.277;           %[m]    wave height 200401011400
%wave_angle = 75;           %[deg]  wave angle 200401011400
%t_top = 175.4;             %[sec]  time of top crest 200401011400
%b1b2 = 22.4039;            %[m]    leg B1 - B2 distance
%b1a1 = 10.4471;            %[m]    leg B1 - A1 distance
%crest = 7.966;

%% Use Deep Water Theory

C = g*Twav/2/pi*1.2;        %[m/s]  1.2 x wave celerity (DNV)
dt = D/10/C;                %[sec]  time increment
skala = 0:dt:dt*2^17;       %[sec]  time scaling on x-axis
eta_b = crest;              %[m]    impact crest height
lambda = 0.5;               %       curling factor (plunging breakers)

yy = cos(gamma*pi/180);
sinw = sin(wave_angle*pi/180);
cosw = cos(wave_angle*pi/180);

for st = 1:length(s)
    cs(st) = 5.15*((D/(D+19*s(st)))+(0.107*s(st)/D));
end

time = 0;

for t = 1:round(Timpact/dt)+1
    if (t<=round(D/dt/C+1))
        Cs (t) = 5.15*((D/(D+19*C*time))+(0.107*C*time/D));
        time = time + dt;
    else
        Cs (t) = 5.15*(1/20+0.107);
    end
end

%% Force at Leg B1
Force_B1 = zeros(length(skala),1);
lokasi_B1 = round(t_top/dt)+1;

for j = 1:length(Cs)
```

```
            Force_B1(lokasi_B1) = eta_b*lambda/yy*Cs(j)*0.5*rho*D*C*C;
            lokasi_B1 = lokasi_B1 + 1;
        end

        Fx_B1 = Force_B1*cosw;
 (80)   Fy_B1 = Force_B1*sinw;
        Fz_B1 = 0*Force_B1;
        Mx_B1 = 0*Force_B1;
        My_B1 = 0*Force_B1;
        Mz_B1 = 0*Force_B1;

        %% Force at Leg B2
        Force_B2 = zeros(length(skala),1);
        lokasi_B2 = round((t_top+b1b2/C)/dt)+1;

 (90)   for j = 1:length(Cs)
            Force_B2(lokasi_B2) = eta_b*lambda/yy*Cs(j)*0.5*rho*D*C*C;
            lokasi_B2 = lokasi_B2 + 1;
        end

        Fx_B2 = Force_B2*cosw;
        Fy_B2 = Force_B2*sinw;
        Fz_B2 = 0*Force_B2;
        Mx_B2 = 0*Force_B2;
        My_B2 = 0*Force_B2;
(100)   Mz_B2 = 0*Force_B2;

        %% Force at Leg B3
        Force_A1 = zeros(length(skala),1);
        lokasi_A1 = round((t_top+b1a1/C)/dt)+1;

        for j = 1:length(Cs)
            Force_A1(lokasi_A1) = eta_b*lambda/yy*Cs(j)*0.5*rho*D*C*C;
            lokasi_A1 = lokasi_A1 + 1;
        end
(110)
        Fx_A1 = Force_A1*cosw;
        Fy_A1 = Force_A1*sinw;
        Fz_A1 = 0*Force_A1;
        Mx_A1 = 0*Force_A1;
        My_A1 = 0*Force_A1;
        Mz_A1 = 0*Force_A1;

        %% Plot figures

(120)   figure(1)
        plot(rat,cs)
        %title('Drag/slamming Coefficient Change');
        xlabel('s/D');
        ylabel('C_s');
        grid on;

        figure(2)
        plot(skala,Force_B1,'k',skala,Force_A1,'b',skala,Force_B2,'r')
        grid on;
(130)   axis([671 677 0 12*10^6]);      % 200401011200
        %axis([174 179 0 12*10^6]);      % 200401011400
        title('Impact Force Time Series - 200401011200','fontweight','bold');
        xlabel('Time [sec]');
        ylabel('Force [N]');
        legend('1^{st} hit - B1','2^{nd} hit - A1','3^{rd} hit - B2');

        %% Write File

        y = [transpose(skala) Fx_B2 Fy_B2 Fz_B2 Mx_B2 My_B2 Mz_B2...
(140)       Fx_B1 Fy_B1 Fz_B1 Mx_B1 My_B1 Mz_B1...
            Fx_A1 Fy_A1 Fz_A1 Mx_A1 My_A1 Mz_A1];

        %dlmwrite('C:\Users\soemantr\Documents\Try
        matlab\ok\imp_200401011200af500_10.txt',...
        %    y, '-append', 'precision', '%15.8f', 'delimiter',' ',...
        %    'newline','pc','roffset', 1);
```

A.4 Nirwana Input Code

```
(1)    HEAD 2.1
       Kvitebjorn analysis - Master Thesis
       Author: DSS, 2010-04-08
       '
       '
       CONTROL
       '   NNOD    NEL     NAS     NMAT    MCOD   NDCOD    NDYN  IPLSTR  NPDEL   LSTORE  IBLFAC
       CFLOA  DTLOA
           218     426       4       15       2       1       2       0       0       3       4
(10)   imp_200401011200_ha 0.00790725677650619
       '  NNSPR  IDAMP    NPURE  NUMSEA  IRUN  CZMUD
            0      1       0       1       2 -190.000
       '
       '
       ACTI
       '  INOD    KN       X       Y       Z      Status codes
             1      0 -25.000 -25.000 -190.000      0 0 0 0 0 0
             2      0  25.000 -25.000 -190.000      0 0 0 0 0 0
             3      0  25.000  25.000 -190.000      0 0 0 0 0 0
(20)         4      0 -25.000  25.000 -190.000      0 0 0 0 0 0
             5      0 -25.000 -25.000 -188.000      0 0 0 0 0 0
             6      0 -17.000 -25.000 -188.000      0 0 0 0 0 0
             7      0  17.000 -25.000 -188.000      0 0 0 0 0 0
             8      0  25.000 -25.000 -188.000      0 0 0 0 0 0
             9      0  25.000 -17.000 -188.000      0 0 0 0 0 0
            10      0  25.000  17.000 -188.000      0 0 0 0 0 0
            11      0  25.000  25.000 -188.000      0 0 0 0 0 0
            12      0  17.000  25.000 -188.000      0 0 0 0 0 0
            13      0 -17.000  25.000 -188.000      0 0 0 0 0 0
(30)        14      0 -25.000  25.000 -188.000      0 0 0 0 0 0
            15      0 -25.000  17.000 -188.000      0 0 0 0 0 0
            16      0 -25.000 -17.000 -188.000      0 0 0 0 0 0
            17      0 -25.000 -25.000 -179.000      0 0 0 0 0 0
            18      0   0.000 -25.000 -179.000      0 0 0 0 0 0
            19      0  25.000 -25.000 -179.000      0 0 0 0 0 0
            20      0  25.000   0.000 -179.000      0 0 0 0 0 0
            21      0  25.000  25.000 -179.000      0 0 0 0 0 0
            22      0   0.000  25.000 -179.000      0 0 0 0 0 0
            23      0 -25.000  25.000 -179.000      0 0 0 0 0 0
(40)        24      0 -25.000   0.000 -179.000      0 0 0 0 0 0
            25      0   0.000 -17.000 -179.000      0 0 0 0 0 0
            26      0   0.000   0.000 -179.000      2 0 2 0 0 0
            27      0   0.000  17.000 -179.000      0 0 0 0 0 0
            28      0   0.000 -25.000 -163.000      0 0 0 0 0 0
            29      0  25.000   0.000 -163.000      0 0 0 0 0 0
            30      0   0.000  25.000 -163.000      0 0 0 0 0 0
            31      0 -25.000   0.000 -163.000      0 0 0 0 0 0
            32      0 -25.000 -25.000 -147.000      0 0 0 0 0 0
            33      0   0.000 -25.000 -147.000      0 0 0 0 0 0
(50)        34      0  25.000 -25.000 -147.000      0 0 0 0 0 0
            35      0  25.000   0.000 -147.000      0 0 0 0 0 0
            36      0  25.000  25.000 -147.000      0 0 0 0 0 0
            37      0   0.000  25.000 -147.000      0 0 0 0 0 0
            38      0 -25.000  25.000 -147.000      0 0 0 0 0 0
            39      0 -25.000   0.000 -147.000      0 0 0 0 0 0
            40      0   0.000 -17.000 -147.000      0 0 0 0 0 0
            41      0   0.000   0.000 -147.000      0 0 0 0 0 0
            42      0   0.000  17.000 -147.000      0 0 0 0 0 0
            43      0   0.000 -23.440 -124.500      0 0 0 0 0 0
(60)        44      0  23.440   0.000 -124.500      0 0 0 0 0 0
            45      0   0.000  23.440 -124.500      0 0 0 0 0 0
            46      0 -23.440   0.000 -124.500      0 0 0 0 0 0
            47      0 -22.070 -22.070 -108.000      0 0 0 0 0 0
            48      0  22.070 -22.070 -108.000      0 0 0 0 0 0
            49      0  22.070  22.070 -108.000      0 0 0 0 0 0
            50      0 -22.070  22.070 -108.000      0 0 0 0 0 0
            51      0   0.000   0.000 -108.000      0 0 0 0 0 0
            52      0   0.000 -20.550  -89.830      0 0 0 0 0 0
            53      0  20.550   0.000  -89.830      0 0 0 0 0 0
(70)        54      0   0.000  20.550  -89.830      0 0 0 0 0 0
            55      0 -20.550   0.000  -89.830      0 0 0 0 0 0
            56      0 -19.220 -19.220  -74.000      0 0 0 0 0 0
            57      0  19.220 -19.220  -74.000      0 0 0 0 0 0
            58      0  19.220  19.220  -74.000      0 0 0 0 0 0
```

```
             59      0 -19.220  19.220  -74.000      0 0 0 0 0 0
             60      0   0.000   0.000  -74.000      0 0 0 0 0 0
             61      0   0.000 -17.930  -58.520      0 0 0 0 0 0
             62      0  17.930   0.000  -58.520      0 0 0 0 0 0
             63      0   0.000  17.930  -58.520      0 0 0 0 0 0
(80)         64      0 -17.930   0.000  -58.520      0 0 0 0 0 0
             65      0 -16.790 -16.790  -45.000      0 0 0 0 0 0
             66      0  16.790 -16.790  -45.000      0 0 0 0 0 0
             67      0  16.790  16.790  -45.000      0 0 0 0 0 0
             68      0 -16.790  16.790  -45.000      0 0 0 0 0 0
             69      0 -10.000 -10.000  -45.000      0 0 0 0 0 0
             70      0 -10.000  10.000  -45.000      0 0 0 0 0 0
             71      0   4.000  -4.000  -45.000      0 0 0 0 0 0
             72      0   4.000   4.000  -45.000      0 0 0 0 0 0
             73      0   0.000   0.000  -45.000      0 0 0 0 0 0
(90)         74      0   0.000 -15.440  -28.790      0 0 0 0 0 0
             75      0  15.440   0.000  -28.790      0 0 0 0 0 0
             76      0   0.000  15.440  -28.790      0 0 0 0 0 0
             77      0 -15.440   0.000  -28.790      0 0 0 0 0 0
             78      0 -14.280 -14.280  -15.000      0 0 0 0 0 0
             79      0  14.280 -14.280  -15.000      0 0 0 0 0 0
             80      0  14.280  14.280  -15.000      0 0 0 0 0 0
             81      0 -14.280  14.280  -15.000      0 0 0 0 0 0
             82      0 -10.000 -10.000  -15.000      0 0 0 0 0 0
             83      0 -10.000  10.000  -15.000      0 0 0 0 0 0
(100)        84      0   4.000  -4.000  -15.000      0 0 0 0 0 0
             85      0   4.000   4.000  -15.000      0 0 0 0 0 0
             86      0   0.000   0.000  -15.000      0 0 0 0 0 0
             87      0 -13.250 -13.250   -2.670      0 0 0 0 0 0
             88      0  13.250 -13.250   -2.670      0 0 0 0 0 0
             89      0  13.250  13.250   -2.670      0 0 0 0 0 0
             90      0 -13.250  13.250   -2.670      0 0 0 0 0 0
             91      0   0.000 -13.250   -2.670      0 0 0 0 0 0
             92      0  13.250   0.000   -2.670      0 0 0 0 0 0
             93      0   0.000  13.250   -2.670      0 0 0 0 0 0
(110)        94      0 -13.250   0.000   -2.670      0 0 0 0 0 0
             95      0 -12.360 -12.360    8.000      0 0 0 0 0 0
             96      0   0.000 -12.360    8.000      0 0 0 0 0 0
             97      0  12.360 -12.360    8.000      0 0 0 0 0 0
             98      0  12.360   0.000    8.000      0 0 0 0 0 0
             99      0  12.360  12.360    8.000      0 0 0 0 0 0
            100      0   0.000  12.360    8.000      0 0 0 0 0 0
            101      0 -12.360  12.360    8.000      0 0 0 0 0 0
            102      0 -12.360   0.000    8.000      0 0 0 0 0 0
            103      0 -10.000 -10.000    8.000      0 0 0 0 0 0
(120)       104      0 -10.000  10.000    8.000      0 0 0 0 0 0
            105      0   4.000  -4.000    8.000      0 0 0 0 0 0
            106      0   4.000   4.000    8.000      0 0 0 0 0 0
            107      0   0.000   0.000    8.000      0 0 0 0 0 0
            108      0 -14.000 -11.250   21.200      0 0 0 0 0 0
            109      0 -10.000 -11.250   21.200      0 0 0 0 0 0
            110      0   1.000 -11.250   21.200      0 0 0 0 0 0
            111      0  16.000 -11.250   21.200      0 0 0 0 0 0
            112      0  16.000  11.250   21.200      0 0 0 0 0 0
            113      0   1.000  11.250   21.200      0 0 0 0 0 0
(130)       114      0 -10.000  11.250   21.200      0 0 0 0 0 0
            115      0 -14.000  11.250   21.200      0 0 0 0 0 0
            116      0 -10.000 -10.000   21.200      0 0 0 0 0 0
            117      0 -10.000  10.000   21.200      0 0 0 0 0 0
            118      0   1.000 -10.000   21.200      0 0 0 0 0 0
            119      0   1.000   0.000   21.200      0 0 0 0 0 0
            120      0   1.000  10.000   21.200      0 0 0 0 0 0
            121      0 -11.300   0.550   21.200      0 0 0 0 0 0
            122      0 -11.300   2.750   21.200      0 0 0 0 0 0
            123      0 -11.300   4.950   21.200      0 0 0 0 0 0
(140)       124      0 -11.300   7.150   21.200      0 0 0 0 0 0
            125      0 -11.300   9.350   21.200      0 0 0 0 0 0
            126      0   1.000  -7.000   21.200      0 0 0 0 0 0
            127      0   1.000  -5.000   21.200      0 0 0 0 0 0
            128      0   1.000  -3.000   21.200      0 0 0 0 0 0
            129      0   1.000  -1.000   21.200      0 0 0 0 0 0
            130      0   1.000   1.000   21.200      0 0 0 0 0 0
            131      0   1.000   3.000   21.200      0 0 0 0 0 0
            132      0   1.000   5.000   21.200      0 0 0 0 0 0
            133      0   1.000   7.000   21.200      0 0 0 0 0 0
(150)       134      0 -14.000 -11.250   24.300      0 0 0 0 0 0
            135      0   1.000 -11.250   24.300      0 0 0 0 0 0
```

```
             136      0  16.000 -11.250   24.300      0 0 0 0 0 0
             137      0 -14.000  11.250   24.300      0 0 0 0 0 0
             138      0   1.000  11.250   24.300      0 0 0 0 0 0
             139      0  16.000  11.150   24.300      0 0 0 0 0 0
             140      0  -3.000   0.500   44.500      0 0 0 0 0 0
             141      0 -11.300   0.550  -60.000      0 0 0 0 0 0
             142      0 -11.300   2.750  -60.000      0 0 0 0 0 0
             143      0 -11.300   4.950  -60.000      0 0 0 0 0 0
(160)        144      0 -11.300   7.150  -60.000      0 0 0 0 0 0
             145      0 -11.300   9.350  -60.000      0 0 0 0 0 0
             146      0 -11.300   0.550  -45.000      0 0 0 0 0 0
             147      0 -11.300   2.750  -45.000      0 0 0 0 0 0
             148      0 -11.300   4.950  -45.000      0 0 0 0 0 0
             149      0 -11.300   7.150  -45.000      0 0 0 0 0 0
             150      0 -11.300   9.350  -45.000      0 0 0 0 0 0
             151      0   0.000  -7.000  -45.000      0 0 0 0 0 0
             152      0   0.000  -5.000  -45.000      0 0 0 0 0 0
             153      0   0.000  -3.000  -45.000      0 0 0 0 0 0
(170)        154      0   0.000  -1.000  -45.000      0 0 0 0 0 0
             155      0   0.000   1.000  -45.000      0 0 0 0 0 0
             156      0   0.000   3.000  -45.000      0 0 0 0 0 0
             157      0   0.000   5.000  -45.000      0 0 0 0 0 0
             158      0   0.000   7.000  -45.000      0 0 0 0 0 0
             159      0   4.300  -1.500  -45.000      0 0 0 0 0 0
             160      0 -11.300   0.550  -28.790      0 0 0 0 0 0
             161      0 -11.300   2.750  -28.790      0 0 0 0 0 0
             162      0 -11.300   4.950  -28.790      0 0 0 0 0 0
             163      0 -11.300   7.150  -28.790      0 0 0 0 0 0
(180)        164      0 -11.300   9.350  -28.790      0 0 0 0 0 0
             165      0   0.000  -7.000  -28.790      0 0 0 0 0 0
             166      0   0.000  -5.000  -28.790      0 0 0 0 0 0
             167      0   0.000  -3.000  -28.790      0 0 0 0 0 0
             168      0   0.000  -1.000  -28.790      0 0 0 0 0 0
             169      0   0.000   1.000  -28.790      0 0 0 0 0 0
             170      0   0.000   3.000  -28.790      0 0 0 0 0 0
             171      0   0.000   5.000  -28.790      0 0 0 0 0 0
             172      0   0.000   7.000  -28.790      0 0 0 0 0 0
             173      0   4.300  -1.500  -28.790      0 0 0 0 0 0
(190)        174      0 -11.300   0.550  -15.000      0 0 0 0 0 0
             175      0 -11.300   2.750  -15.000      0 0 0 0 0 0
             176      0 -11.300   4.950  -15.000      0 0 0 0 0 0
             177      0 -11.300   7.150  -15.000      0 0 0 0 0 0
             178      0 -11.300   9.350  -15.000      0 0 0 0 0 0
             179      0   0.000  -7.000  -15.000      0 0 0 0 0 0
             180      0   0.000  -5.000  -15.000      0 0 0 0 0 0
             181      0   0.000  -3.000  -15.000      0 0 0 0 0 0
             182      0   0.000  -1.000  -15.000      0 0 0 0 0 0
             183      0   0.000   1.000  -15.000      0 0 0 0 0 0
(200)        184      0   0.000   3.000  -15.000      0 0 0 0 0 0
             185      0   0.000   5.000  -15.000      0 0 0 0 0 0
             186      0   0.000   7.000  -15.000      0 0 0 0 0 0
             187      0   4.300  -1.500  -15.000      0 0 0 0 0 0
             188      0 -11.300   0.550   -2.670      0 0 0 0 0 0
             189      0 -11.300   2.750   -2.670      0 0 0 0 0 0
             190      0 -11.300   4.950   -2.670      0 0 0 0 0 0
             191      0 -11.300   7.150   -2.670      0 0 0 0 0 0
             192      0 -11.300   9.350   -2.670      0 0 0 0 0 0
             193      0   0.000  -7.000   -2.670      0 0 0 0 0 0
(210)        194      0   0.000  -5.000   -2.670      0 0 0 0 0 0
             195      0   0.000  -3.000   -2.670      0 0 0 0 0 0
             196      0   0.000  -1.000   -2.670      0 0 0 0 0 0
             197      0   0.000   1.000   -2.670      0 0 0 0 0 0
             198      0   0.000   3.000   -2.670      0 0 0 0 0 0
             199      0   0.000   5.000   -2.670      0 0 0 0 0 0
             200      0   0.000   7.000   -2.670      0 0 0 0 0 0
             201      0   4.300  -1.500   -2.670      0 0 0 0 0 0
             202      0 -11.300   0.550    8.000      0 0 0 0 0 0
             203      0 -11.300   2.750    8.000      0 0 0 0 0 0
(220)        204      0 -11.300   4.950    8.000      0 0 0 0 0 0
             205      0 -11.300   7.150    8.000      0 0 0 0 0 0
             206      0 -11.300   9.350    8.000      0 0 0 0 0 0
             207      0   0.000  -7.000    8.000      0 0 0 0 0 0
             208      0   0.000  -5.000    8.000      0 0 0 0 0 0
             209      0   0.000  -3.000    8.000      0 0 0 0 0 0
             210      0   0.000  -1.000    8.000      0 0 0 0 0 0
             211      0   0.000   1.000    8.000      0 0 0 0 0 0
             212      0   0.000   3.000    8.000      0 0 0 0 0 0
```

```
            213       0   0.000   5.000    8.000       0 0 0 0 0 0
(230)       214       0   0.000   7.000    8.000       0 0 0 0 0 0
            215       0   4.300   0.000    8.000       0 0 0 0 0 0
            216       0 -12.6341 12.6341   4.71        0 0 0 0 0 0
            217       0 -12.6341 -12.6341  4.71        0 0 0 0 0 0
            218       0  12.6341 -12.6341  4.71        0 0 0 0 0 0
        '
        '
        ELEM
        '    IELM   INOD1   INOD2   INOD3   NLOAD
               1       1       5       2       1
(240)          2       5      17       8       1
               3      17      32      19       1
               4      32      47      34       1
               5      47      56      48       1
               6      56      65      57       2
               7      65      78      66       3
               8      78      87      79       3
               9      87     217      88       4
              10      95     108      97       4
              11     108     134     111      -2
(250)         12       2       8       3       1
              13       8      19      11       1
              14      19      34      21       1
              15      34      48      36       1
              16      48      57      49       1
              17      57      66      58       2
              18      66      79      67       3
              19      79      88      80       3
              20      88     218      89       4
              21      97     111      99       4
(260)         22     111     136     112      -2
              23       3      11       4       1
              24      11      21      14       1
              25      21      36      23       1
              26      36      49      38       1
              27      49      58      50       1
              28      58      67      59       2
              29      67      80      68       3
              30      80      89      81       3
              31      89      99      90       4
(270)         32      99     112     101       4
              33     112     139     115      -2
              34       4      14       1       1
              35      14      23       5       1
              36      23      38      17       1
              37      38      50      32       1
              38      50      59      47       1
              39      59      68      56       2
              40      68      81      65       3
              41      81      90      78       3
(280)         42      90     216      87       4
              43     101     115      95       4
              44     115     137     108      -2
              45       5       6      14       1
              46       6       7      13       1
              47       7       8      12       1
              48       8       9       5       1
              49       9      10      16       1
              50      10      11      15       1
              51      11      12       8       1
(290)         52      12      13       7       1
              53      13      14       6       1
              54      14      15      11       1
              55      15      16      10       1
              56      16       5       9       1
              57      17      18      23       1
              58      18      19      22       1
              59      19      20      17       1
              60      20      21      24       1
              61      21      22      19       1
(300)         62      22      23      18       1
              63      23      24      21       1
              64      24      17      20       1
              65      18      20      26       1
              66      20      22      26       1
              67      22      24      26       1
```

```
            68     24     18     26      1
            69     18     25     17      1
            70     25     26     17      1
            71     26     27     24      1
(310)       72     27     22     24      1
            73     32     33     38      1
            74     33     34     37      1
            75     34     35     32      1
            76     35     36     39      1
            77     36     37     34      1
            78     37     38     33      1
            79     38     39     36      1
            80     39     32     35      1
            81     33     35     41      1
(320)       82     35     37     41      1
            83     37     39     41      1
            84     39     33     41      1
            85     33     40     32      1
            86     40     41     32      1
            87     41     42     39      1
            88     42     37     39      1
            89     47     51     50      1
            90     51     49     50      1
            91     48     51     47      1
(330)       92     51     50     47      1
            93     56     60     59      1
            94     60     58     59      1
            95     57     60     56      1
            96     60     59     56      1
            97     65     69     68      1
            98     69     73     68      1
            99     73     72     68      1
           100     72     67     68      1
           101     66     71     65      1
(340)      102     71     73     65      1
           103     73     70     65      1
           104     70     68     65      1
           105     69     70     65      1
           106     78     82     81      1
           107     82     86     81      1
           108     86     85     81      1
           109     85     80     81      1
           110     79     84     78      1
           111     84     86     78      1
(350)      112     86     83     78      1
           113     83     81     78      1
           114     82     83     78      1
           115     95    103    101      1
           116    103    107    101      1
           117    107    106    101      1
           118    106     99    101      1
           119     97    105     95      1
           120    105    107     95      1
           121    107    104     95      1
(360)      122    104    101     95      1
           123     95     96    101      1
           124     96     97    100      1
           125     97     98     95      1
           126     98     99    102      1
           127     99    100     97      1
           128    100    101     96      1
           129    101    102     99      1
           130    102     95     98      1
           131    108    109    115      1
(370)      132    109    110    114      1
           133    110    111    113      1
           134    111    112    108      1
           135    112    113    111      1
           136    113    114    110      1
           137    114    115    109      1
           138    115    108    112      1
           139    109    116    108      1
           140    116    121    108      1
           141    121    122    115      1
(380)      142    122    123    115      1
           143    123    124    115      1
           144    124    125    115      1
```

	145	125	117	115	1
	146	117	114	115	1
	147	110	118	108	1
	148	118	126	108	1
	149	126	127	108	1
	150	127	128	108	1
	151	128	129	108	1
(390)	152	129	119	108	1
	153	119	130	115	1
	154	130	131	115	1
	155	131	132	115	1
	156	132	133	115	1
	157	133	120	115	1
	158	120	113	115	1
	159	17	6	23	1
	160	6	18	13	1
	161	18	7	22	1
(400)	162	7	19	12	1
	163	19	9	17	1
	164	9	20	16	1
	165	20	10	24	1
	166	10	21	15	1
	167	21	12	19	1
	168	12	22	7	1
	169	22	13	18	1
	170	13	23	6	1
	171	23	15	21	1
(410)	172	15	24	10	1
	173	24	16	20	1
	174	16	17	9	1
	175	17	28	23	1
	176	28	34	30	1
	177	32	28	38	1
	178	28	19	30	1
	179	19	29	17	1
	180	29	36	31	1
	181	34	29	32	1
(420)	182	29	21	31	1
	183	21	30	19	1
	184	30	38	28	1
	185	36	30	34	1
	186	30	23	28	1
	187	23	31	21	1
	188	31	32	29	1
	189	38	31	36	1
	190	31	17	29	1
	191	32	43	38	1
(430)	192	43	48	45	1
	193	47	43	50	1
	194	43	34	45	1
	195	34	44	32	1
	196	44	49	46	1
	197	48	44	47	1
	198	44	36	46	1
	199	36	45	34	1
	200	45	50	43	1
	201	49	45	48	1
(440)	202	45	38	43	1
	203	38	46	36	1
	204	46	47	44	1
	205	50	46	49	1
	206	46	32	44	1
	207	47	52	50	1
	208	52	57	54	1
	209	56	52	59	1
	210	52	48	54	1
	211	48	53	47	1
(450)	212	53	58	55	1
	213	57	53	56	1
	214	53	49	55	1
	215	49	54	48	1
	216	54	59	52	1
	217	58	54	57	1
	218	54	50	52	1
	219	50	55	49	1
	220	55	56	53	1
	221	59	55	58	1

(460)	222	55	47	53	1
	223	56	61	59	1
	224	61	66	63	1
	225	65	61	68	1
	226	61	57	63	1
	227	57	62	56	1
	228	62	67	64	1
	229	66	62	65	1
	230	62	58	64	1
	231	58	63	57	1
(470)	232	63	68	61	1
	233	67	63	66	1
	234	63	59	61	1
	235	59	64	58	1
	236	64	65	62	1
	237	68	64	67	1
	238	64	56	62	1
	239	65	74	68	1
	240	74	79	76	1
	241	78	74	81	1
(480)	242	74	66	76	1
	243	66	75	65	1
	244	75	80	77	1
	245	79	75	78	1
	246	75	67	77	1
	247	67	76	66	1
	248	76	81	74	1
	249	80	76	79	1
	250	76	68	74	1
	251	68	77	67	1
(490)	252	77	78	75	1
	253	81	77	80	1
	254	77	65	75	1
	255	78	91	81	2
	256	91	97	93	2
	257	95	91	101	2
	258	91	79	93	2
	259	79	92	78	2
	260	92	99	94	2
	261	97	92	95	2
(500)	262	92	80	94	2
	263	80	93	79	2
	264	93	101	91	2
	265	99	93	97	2
	266	93	81	91	2
	267	81	94	80	2
	268	94	95	92	2
	269	101	94	99	2
	270	94	78	92	2
	271	95	110	101	3
(510)	272	110	97	113	3
	273	97	112	95	3
	274	99	113	97	3
	275	113	101	110	3
	276	115	95	112	3
	277	134	135	137	-2
	278	135	136	138	-2
	279	136	139	134	-2
	280	139	138	136	-2
	281	138	137	135	-2
(520)	282	137	134	139	-2
	283	134	140	139	-2
	284	136	140	137	-2
	285	139	140	134	-2
	286	137	140	136	-2
	287	151	152	65	-2
	288	152	153	65	-2
	289	153	154	65	-2
	290	154	155	65	-2
	291	155	156	68	-2
(530)	292	156	157	68	-2
	293	157	158	68	-2
	294	69	151	68	-2
	295	151	71	68	-2
	296	72	158	68	-2
	297	158	70	67	-2
	298	71	159	67	-2

```
          299    159     72     68     -2
          300    146    147     68     -2
          301    147    148     68     -2
(540)     302    148    149     68     -2
          303    149    150     68     -2
          304     69    146     65     -2
          305    150     70     68     -2
          306    179    180     78     -2
          307    180    181     78     -2
          308    181    182     78     -2
          309    182    183     78     -2
          310    183    184     81     -2
          311    184    185     81     -2
(550)     312    185    186     81     -2
          313     82    179     81     -2
          314    179     84     81     -2
          315     85    186     81     -2
          316    186     83     80     -2
          317     84    187     80     -2
          318    187     85     81     -2
          319    174    175     81     -2
          320    175    176     81     -2
          321    176    177     81     -2
(560)     322    177    178     81     -2
          323     82    174     78     -2
          324    178     83     81     -2
          325    207    208     95     -2
          326    208    209     95     -2
          327    209    210     95     -2
          328    210    211     95     -2
          329    211    212    101     -2
          330    212    213    101     -2
          331    213    214    101     -2
(570)     332    103    207    101     -2
          333    207    105    101     -2
          334    106    214    101     -2
          335    214    104     99     -2
          336    105    215     99     -2
          337    215    106    101     -2
          338    202    203    101     -2
          339    203    204    101     -2
          340    204    205    101     -2
          341    205    206    101     -2
(580)     342    103    202     95     -2
          343    206    104    101     -2
          344    141    146     68      1
          345    146    160     68      1
          346    160    174     81      1
          347    174    188     81      2
          348    188    202    101      2
          349    202    121    115      0
          350    142    147     68      1
          351    147    161     68      1
(590)     352    161    175     81      1
          353    175    189     81      2
          354    189    203    101      2
          355    203    122    115      0
          356    143    148     68      1
          357    148    162     68      1
          358    162    176     81      1
          359    176    190     81      2
          360    190    204    101      2
          361    204    123    115      0
(600)     362    144    149     68      1
          363    149    163     68      1
          364    163    177     81      1
          365    177    191     81      2
          366    191    205    101      2
          367    205    124    115      0
          368    145    150     68      1
          369    150    164     68      1
          370    164    178     81      1
          371    178    192     81      2
(610)     372    192    206    101      2
          373    206    125    115      0
          374    151    165     65      1
          375    165    179     78      1
```

```
            376    179    193     78      2
            377    193    207     95      2
            378    207    126    108      0
            379    152    166     65      1
            380    166    180     78      1
            381    180    194     78      2
(620)       382    194    208     95      2
            383    208    127    108      0
            384    153    167     65      1
            385    167    181     78      1
            386    181    195     78      2
            387    195    209     95      2
            388    209    128    108      0
            389    154    168     65      1
            390    168    182     78      1
            391    182    196     78      2
(630)       392    196    210     95      2
            393    210    129    108      0
            394    155    169     68      1
            395    169    183     81      1
            396    183    197     81      2
            397    197    211    101      2
            398    211    130    115      0
            399    156    170     68      1
            400    170    184     81      1
            401    184    198     81      2
(640)       402    198    212    101      2
            403    212    131    115      0
            404    157    171     68      1
            405    171    185     81      1
            406    185    199     81      2
            407    199    213    101      2
            408    213    132    115      0
            409    158    172     68      1
            410    172    186     81      1
            411    186    200     81      2
(650)       412    200    214    101      2
            413    214    133    115      0
            414    159    173     68      1
            415    173    187     81      1
            416    187    201     81      2
            417    201    215    101      2
            418    215    119    115      0
            419     26     41     17      1
            420     41     51     32      1
            421     51     60     47      2
(660)       422     60     73     56      0
            423     20     41     21      0
            424    216    101     87      4
            425    217     95     88      4
            426    218     97     89      4
        '
        '
        MATE
        '   IMAT         EMOD        POISS       ROSTRU        ALFA1        ALFA2       ROINSI
        ROOUT        CAM
(670)          1   2.100e+011   3.000e-001   7.800e+003   4.189e-002   8.488e-003   0.000e+000
        0.000e+000 0.000e+000
               2   2.100e+011   3.000e-001   7.800e+003   4.189e-002   8.488e-003   0.000e+000
        1.025e+003 1.000e+000
               3   2.100e+011   3.000e-001   7.800e+003   4.189e-002   8.488e-003   1.025e+003
        0.000e+000 1.000e+000
               4   2.100e+011   3.000e-001   7.800e+003   4.189e-002   8.488e-003   1.025e+003
        1.025e+003 1.000e+000
               5   2.100e+011   3.000e-001   9.051e+003   4.189e-002   8.488e-003   0.000e+000
        0.000e+000 0.000e+000
(680)          6   2.100e+011   3.000e-001   1.124e+004   4.189e-002   8.488e-003   0.000e+000
        0.000e+000 0.000e+000
               7   2.100e+011   3.000e-001   1.288e+004   4.189e-002   8.488e-003   0.000e+000
        1.025e+003 1.000e+000
               8   2.100e+011   3.000e-001   1.008e+004   4.189e-002   8.488e-003   0.000e+000
        1.025e+003 1.000e+000
               9   2.100e+011   3.000e-001   1.202e+004   4.189e-002   8.488e-003   0.000e+000
        1.025e+003 1.000e+000
              10   2.100e+011   3.000e-001   9.600e+003   4.189e-002   8.488e-003   0.000e+000
        1.025e+003 1.000e+000
(690)         11   3.600e+011   3.000e-001   7.800e+003   4.189e-002   8.488e-003   1.025e+003
```

```
        1.025e+003 1.000e+000
             12   5.000e+011   3.000e-001   0.000e+000   4.189e-002   8.488e-003   0.000e+000
        0.000e+000 0.000e+000
             13   2.100e+011   3.000e-001   1.560e+005   4.189e-002   8.488e-003   0.000e+000
        1.025e+003 1.000e+000
             14   2.100e+011   3.000e-001   7.800e+003   4.189e-002   8.488e-003   0.000e+000
        1.025e+003 1.000e+000
             15   2.100e+011   3.000e-001   7.800e+003   4.189e-002   8.488e-003   0.000e+000
        0.000e+000 0.000e+000
(700)   '
        '
        CROS
        '    CRTY  ITYP KN  IMAT      DIA       TH    CON
           TUBE      1   0    11   8.000 1.000e-001    0
           TUBE      2   0    11   8.000 1.000e-001    0
           TUBE      3   0     4   3.400 9.000e-002    0
           TUBE      4   0     4   2.900 9.000e-002    0
           TUBE      5   0     4   2.900 8.000e-002    0
           TUBE      6   0     4   2.900 7.000e-002    0
(710)      TUBE      7   0     4   2.000 9.500e-002    0
           TUBE      8   0     4   2.000 8.500e-002    0
           TUBE      9   0     1   2.000 8.500e-002    0
           TUBE     10   0     1   2.000 9.000e-002    0
           TUBE     11   0     1   1.900 9.500e-002    0
           TUBE     12   0    11   8.000 1.000e-001    0
           TUBE     13   0    11   8.000 1.000e-001    0
           TUBE     14   0     4   3.400 9.000e-002    0
           TUBE     15   0     4   2.900 9.000e-002    0
           TUBE     16   0     4   2.900 8.000e-002    0
(720)      TUBE     17   0     4   2.900 7.000e-002    0
           TUBE     18   0     4   2.000 9.500e-002    0
           TUBE     19   0     4   2.000 8.500e-002    0
           TUBE     20   0     1   2.000 8.500e-002    0
           TUBE     21   0     1   2.000 9.000e-002    0
           TUBE     22   0     1   1.900 9.500e-002    0
           TUBE     23   0    11   8.000 1.000e-001    0
           TUBE     24   0    11   8.000 1.000e-001    0
           TUBE     25   0     4   3.400 9.000e-002    0
           TUBE     26   0     4   2.900 9.000e-002    0
(730)      TUBE     27   0     4   2.900 8.000e-002    0
           TUBE     28   0     4   2.900 7.000e-002    0
           TUBE     29   0     4   2.000 9.500e-002    0
           TUBE     30   0     4   2.000 8.500e-002    0
           TUBE     31   0     1   2.000 8.500e-002    0
           TUBE     32   0     1   2.000 9.000e-002    0
           TUBE     33   0     1   1.900 9.500e-002    0
           TUBE     34   0    11   8.000 1.000e-001    0
           TUBE     35   0    11   8.000 1.000e-001    0
           TUBE     36   0     4   3.400 9.000e-002    0
(740)      TUBE     37   0     4   2.900 9.000e-002    0
           TUBE     38   0     4   2.900 8.000e-002    0
           TUBE     39   0     4   2.900 7.000e-002    0
           TUBE     40   0     4   2.000 9.500e-002    0
           TUBE     41   0     4   2.000 8.500e-002    0
           TUBE     42   0     1   2.000 8.500e-002    0
           TUBE     43   0     1   2.000 9.000e-002    0
           TUBE     44   0     1   1.900 9.500e-002    0
           TUBE     45   0     2   0.900 3.000e-002    0
           TUBE     46   0     2   0.900 3.000e-002    0
(750)      TUBE     47   0     2   0.900 3.000e-002    0
           TUBE     48   0     2   0.900 3.000e-002    0
           TUBE     49   0     2   0.900 3.000e-002    0
           TUBE     50   0     2   0.900 3.000e-002    0
           TUBE     51   0     2   0.900 3.000e-002    0
           TUBE     52   0     2   0.900 3.000e-002    0
           TUBE     53   0     2   0.900 3.000e-002    0
           TUBE     54   0     2   0.900 3.000e-002    0
           TUBE     55   0     2   0.900 3.000e-002    0
           TUBE     56   0     2   0.900 3.000e-002    0
(760)      TUBE     57   0     2   0.900 3.000e-002    0
           TUBE     58   0     2   0.900 3.000e-002    0
           TUBE     59   0     2   0.900 3.000e-002    0
           TUBE     60   0     2   0.900 3.000e-002    0
           TUBE     61   0     2   0.900 3.000e-002    0
           TUBE     62   0     2   0.900 3.000e-002    0
           TUBE     63   0     2   0.900 3.000e-002    0
           TUBE     64   0     2   0.900 3.000e-002    0
```

```
          TUBE    65   0    10   0.800 2.500e-002    0
          TUBE    66   0    10   0.800 2.500e-002    0
(770)     TUBE    67   0    10   0.800 2.500e-002    0
          TUBE    68   0    10   0.800 2.500e-002    0
          TUBE    69   0    10   0.800 2.500e-002    0
          TUBE    70   0    10   0.800 2.500e-002    0
          TUBE    71   0    10   0.800 2.500e-002    0
          TUBE    72   0    10   0.800 2.500e-002    0
          TUBE    73   0     2   1.000 3.000e-002    0
          TUBE    74   0     2   1.000 3.000e-002    0
          TUBE    75   0     2   1.000 3.000e-002    0
          TUBE    76   0     2   1.000 3.000e-002    0
(780)     TUBE    77   0     2   1.000 3.000e-002    0
          TUBE    78   0     2   1.000 3.000e-002    0
          TUBE    79   0     2   1.000 3.000e-002    0
          TUBE    80   0     2   1.000 3.000e-002    0
          TUBE    81   0     2   1.000 3.000e-002    0
          TUBE    82   0     2   1.000 3.000e-002    0
          TUBE    83   0     2   1.000 3.000e-002    0
          TUBE    84   0     2   1.000 3.000e-002    0
          TUBE    85   0    10   0.800 2.500e-002    0
          TUBE    86   0    10   0.800 2.500e-002    0
(790)     TUBE    87   0    10   0.800 2.500e-002    0
          TUBE    88   0    10   0.800 2.500e-002    0
          TUBE    89   0     9   0.900 4.000e-002    0
          TUBE    90   0     9   0.900 4.000e-002    0
          TUBE    91   0     9   0.900 4.000e-002    0
          TUBE    92   0     9   0.900 4.000e-002    0
          TUBE    93   0     9   0.900 3.000e-002    0
          TUBE    94   0     9   0.900 3.000e-002    0
          TUBE    95   0     9   0.900 3.000e-002    0
          TUBE    96   0     9   0.900 3.000e-002    0
(800)     TUBE    97   0     8   0.900 4.000e-002    0
          TUBE    98   0     8   0.900 4.000e-002    0
          TUBE    99   0     8   0.900 4.000e-002    0
          TUBE   100   0     8   0.900 4.000e-002    0
          TUBE   101   0     8   0.900 4.000e-002    0
          TUBE   102   0     8   0.900 4.000e-002    0
          TUBE   103   0     8   0.900 4.000e-002    0
          TUBE   104   0     8   0.900 4.000e-002    0
          TUBE   105   0     8   0.900 4.000e-002    0
          TUBE   106   0     7   0.900 5.000e-002    0
(810)     TUBE   107   0     7   0.900 5.000e-002    0
          TUBE   108   0     7   0.900 5.000e-002    0
          TUBE   109   0     7   0.900 5.000e-002    0
          TUBE   110   0     7   0.900 5.000e-002    0
          TUBE   111   0     7   0.900 5.000e-002    0
          TUBE   112   0     7   0.900 5.000e-002    0
          TUBE   113   0     7   0.900 5.000e-002    0
          TUBE   114   0     7   0.900 5.000e-002    0
          TUBE   115   0     6   0.800 2.500e-002    0
          TUBE   116   0     6   0.800 2.500e-002    0
(820)     TUBE   117   0     6   0.800 2.500e-002    0
          TUBE   118   0     6   0.800 2.500e-002    0
          TUBE   119   0     6   0.800 2.500e-002    0
          TUBE   120   0     6   0.800 2.500e-002    0
          TUBE   121   0     6   0.800 2.500e-002    0
          TUBE   122   0     6   0.800 2.500e-002    0
          TUBE   123   0     1   0.900 6.000e-002    0
          TUBE   124   0     1   0.900 6.000e-002    0
          TUBE   125   0     1   0.900 6.000e-002    0
          TUBE   126   0     1   0.900 6.000e-002    0
(830)     TUBE   127   0     1   0.900 6.000e-002    0
          TUBE   128   0     1   0.900 6.000e-002    0
          TUBE   129   0     1   0.900 6.000e-002    0
          TUBE   130   0     1   0.900 6.000e-002    0
          TUBE   131   0     5   1.200 3.500e-002    0
          TUBE   132   0     5   1.200 3.500e-002    0
          TUBE   133   0     5   1.200 3.500e-002    0
          TUBE   134   0     5   1.200 3.500e-002    0
          TUBE   135   0     5   1.200 3.500e-002    0
          TUBE   136   0     5   1.200 3.500e-002    0
(840)     TUBE   137   0     5   1.200 3.500e-002    0
          TUBE   138   0     5   1.200 3.500e-002    0
          TUBE   139   0     5   1.200 3.500e-002    0
          TUBE   140   0     5   1.200 3.500e-002    0
          TUBE   141   0     5   1.200 3.500e-002    0
```

```
          TUBE   142   0     5   1.200 3.500e-002    0
          TUBE   143   0     5   1.200 3.500e-002    0
          TUBE   144   0     5   1.200 3.500e-002    0
          TUBE   145   0     5   1.200 3.500e-002    0
          TUBE   146   0     5   1.200 3.500e-002    0
(850)     TUBE   147   0     5   1.200 3.500e-002    0
          TUBE   148   0     5   1.200 3.500e-002    0
          TUBE   149   0     5   1.200 3.500e-002    0
          TUBE   150   0     5   1.200 3.500e-002    0
          TUBE   151   0     5   1.200 3.500e-002    0
          TUBE   152   0     5   1.200 3.500e-002    0
          TUBE   153   0     5   1.200 3.500e-002    0
          TUBE   154   0     5   1.200 3.500e-002    0
          TUBE   155   0     5   1.200 3.500e-002    0
          TUBE   156   0     5   1.200 3.500e-002    0
(860)     TUBE   157   0     5   1.200 3.500e-002    0
          TUBE   158   0     5   1.200 3.500e-002    0
          TUBE   159   0     4   0.900 3.000e-002    0
          TUBE   160   0     4   0.900 3.000e-002    0
          TUBE   161   0     4   0.900 3.000e-002    0
          TUBE   162   0     4   0.900 3.000e-002    0
          TUBE   163   0     4   0.900 3.000e-002    0
          TUBE   164   0     4   0.900 3.000e-002    0
          TUBE   165   0     4   0.900 3.000e-002    0
          TUBE   166   0     4   0.900 3.000e-002    0
(870)     TUBE   167   0     4   0.900 3.000e-002    0
          TUBE   168   0     4   0.900 3.000e-002    0
          TUBE   169   0     4   0.900 3.000e-002    0
          TUBE   170   0     4   0.900 3.000e-002    0
          TUBE   171   0     4   0.900 3.000e-002    0
          TUBE   172   0     4   0.900 3.000e-002    0
          TUBE   173   0     4   0.900 3.000e-002    0
          TUBE   174   0     4   0.900 3.000e-002    0
          TUBE   175   0     4   1.600 2.500e-002    0
          TUBE   176   0     4   1.600 2.500e-002    0
(880)     TUBE   177   0     4   1.600 2.500e-002    0
          TUBE   178   0     4   1.600 2.500e-002    0
          TUBE   179   0     4   1.600 2.500e-002    0
          TUBE   180   0     4   1.600 2.500e-002    0
          TUBE   181   0     4   1.600 2.500e-002    0
          TUBE   182   0     4   1.600 2.500e-002    0
          TUBE   183   0     4   1.600 2.500e-002    0
          TUBE   184   0     4   1.600 2.500e-002    0
          TUBE   185   0     4   1.600 2.500e-002    0
          TUBE   186   0     4   1.600 2.500e-002    0
(890)     TUBE   187   0     4   1.600 2.500e-002    0
          TUBE   188   0     4   1.600 2.500e-002    0
          TUBE   189   0     4   1.600 2.500e-002    0
          TUBE   190   0     4   1.600 2.500e-002    0
          TUBE   191   0     2   1.200 3.000e-002    0
          TUBE   192   0     2   1.200 3.000e-002    0
          TUBE   193   0     2   1.200 3.000e-002    0
          TUBE   194   0     2   1.200 3.000e-002    0
          TUBE   195   0     2   1.200 3.000e-002    0
          TUBE   196   0     2   1.200 3.000e-002    0
(900)     TUBE   197   0     2   1.200 3.000e-002    0
          TUBE   198   0     2   1.200 3.000e-002    0
          TUBE   199   0     2   1.200 3.000e-002    0
          TUBE   200   0     2   1.200 3.000e-002    0
          TUBE   201   0     2   1.200 3.000e-002    0
          TUBE   202   0     2   1.200 3.000e-002    0
          TUBE   203   0     2   1.200 3.000e-002    0
          TUBE   204   0     2   1.200 3.000e-002    0
          TUBE   205   0     2   1.200 3.000e-002    0
          TUBE   206   0     2   1.200 3.000e-002    0
(910)     TUBE   207   0     2   1.300 3.000e-002    0
          TUBE   208   0     2   1.300 3.000e-002    0
          TUBE   209   0     2   1.300 3.000e-002    0
          TUBE   210   0     2   1.300 3.000e-002    0
          TUBE   211   0     2   1.300 3.000e-002    0
          TUBE   212   0     2   1.300 3.000e-002    0
          TUBE   213   0     2   1.300 3.000e-002    0
          TUBE   214   0     2   1.300 3.000e-002    0
          TUBE   215   0     2   1.300 3.000e-002    0
          TUBE   216   0     2   1.300 3.000e-002    0
(920)     TUBE   217   0     2   1.300 3.000e-002    0
          TUBE   218   0     2   1.300 3.000e-002    0
```

```
          TUBE   219   0     2   1.300 3.000e-002    0
          TUBE   220   0     2   1.300 3.000e-002    0
          TUBE   221   0     2   1.300 3.000e-002    0
          TUBE   222   0     2   1.300 3.000e-002    0
          TUBE   223   0     2   1.200 2.500e-002    0
          TUBE   224   0     2   1.200 2.500e-002    0
          TUBE   225   0     2   1.200 2.500e-002    0
          TUBE   226   0     2   1.200 2.500e-002    0
(930)     TUBE   227   0     2   1.200 2.500e-002    0
          TUBE   228   0     2   1.200 2.500e-002    0
          TUBE   229   0     2   1.200 2.500e-002    0
          TUBE   230   0     2   1.200 2.500e-002    0
          TUBE   231   0     2   1.200 2.500e-002    0
          TUBE   232   0     2   1.200 2.500e-002    0
          TUBE   233   0     2   1.200 2.500e-002    0
          TUBE   234   0     2   1.200 2.500e-002    0
          TUBE   235   0     2   1.200 2.500e-002    0
          TUBE   236   0     2   1.200 2.500e-002    0
(940)     TUBE   237   0     2   1.200 2.500e-002    0
          TUBE   238   0     2   1.200 2.500e-002    0
          TUBE   239   0     2   1.200 2.500e-002    0
          TUBE   240   0     2   1.200 2.500e-002    0
          TUBE   241   0     2   1.200 2.500e-002    0
          TUBE   242   0     2   1.200 2.500e-002    0
          TUBE   243   0     2   1.200 2.500e-002    0
          TUBE   244   0     2   1.200 2.500e-002    0
          TUBE   245   0     2   1.200 2.500e-002    0
          TUBE   246   0     2   1.200 2.500e-002    0
(950)     TUBE   247   0     2   1.200 2.500e-002    0
          TUBE   248   0     2   1.200 2.500e-002    0
          TUBE   249   0     2   1.200 2.500e-002    0
          TUBE   250   0     2   1.200 2.500e-002    0
          TUBE   251   0     2   1.200 2.500e-002    0
          TUBE   252   0     2   1.200 2.500e-002    0
          TUBE   253   0     2   1.200 2.500e-002    0
          TUBE   254   0     2   1.200 2.500e-002    0
          TUBE   255   0     2   0.900 6.500e-002    0
          TUBE   256   0     1   0.900 6.500e-002    0
(960)     TUBE   257   0     1   0.900 6.500e-002    0
          TUBE   258   0     2   0.900 6.500e-002    0
          TUBE   259   0     2   0.900 6.500e-002    0
          TUBE   260   0     1   0.900 6.500e-002    0
          TUBE   261   0     1   0.900 6.500e-002    0
          TUBE   262   0     2   0.900 6.500e-002    0
          TUBE   263   0     2   0.900 6.500e-002    0
          TUBE   264   0     1   0.900 6.500e-002    0
          TUBE   265   0     1   0.900 6.500e-002    0
          TUBE   266   0     2   0.900 6.500e-002    0
(970)     TUBE   267   0     2   0.900 6.500e-002    0
          TUBE   268   0     1   0.900 6.500e-002    0
          TUBE   269   0     1   0.900 6.500e-002    0
          TUBE   270   0     2   0.900 6.500e-002    0
          TUBE   271   0     1   1.000 5.500e-002    0
          TUBE   272   0     1   1.000 5.500e-002    0
          TUBE   273   0     1   1.000 5.000e-002    0
          TUBE   274   0     1   1.000 5.500e-002    0
          TUBE   275   0     1   1.000 5.500e-002    0
          TUBE   276   0     1   1.000 5.000e-002    0
(980)     TUBE   277   0    12   2.000 8.000e-002    0
          TUBE   278   0    12   2.000 8.000e-002    0
          TUBE   279   0    12   2.000 8.000e-002    0
          TUBE   280   0    12   2.000 8.000e-002    0
          TUBE   281   0    12   2.000 8.000e-002    0
          TUBE   282   0    12   2.000 8.000e-002    0
          TUBE   283   0    12   2.000 8.000e-002    0
          TUBE   284   0    12   2.000 8.000e-002    0
          TUBE   285   0    12   2.000 8.000e-002    0
          TUBE   286   0    12   2.000 8.000e-002    0
(990)     TUBE   287   0    12   2.000 8.000e-002    0
          TUBE   288   0    12   2.000 8.000e-002    0
          TUBE   289   0    12   2.000 8.000e-002    0
          TUBE   290   0    12   2.000 8.000e-002    0
          TUBE   291   0    12   2.000 8.000e-002    0
          TUBE   292   0    12   2.000 8.000e-002    0
          TUBE   293   0    12   2.000 8.000e-002    0
          TUBE   294   0    12   2.000 8.000e-002    0
          TUBE   295   0    12   2.000 8.000e-002    0
```

```
           TUBE   296   0    12   2.000 8.000e-002    0
(1000)     TUBE   297   0    12   2.000 8.000e-002    0
           TUBE   298   0    12   2.000 8.000e-002    0
           TUBE   299   0    12   2.000 8.000e-002    0
           TUBE   300   0    12   2.000 8.000e-002    0
           TUBE   301   0    12   2.000 8.000e-002    0
           TUBE   302   0    12   2.000 8.000e-002    0
           TUBE   303   0    12   2.000 8.000e-002    0
           TUBE   304   0    12   2.000 8.000e-002    0
           TUBE   305   0    12   2.000 8.000e-002    0
           TUBE   306   0    12   2.000 8.000e-002    0
(1010)     TUBE   307   0    12   2.000 8.000e-002    0
           TUBE   308   0    12   2.000 8.000e-002    0
           TUBE   309   0    12   2.000 8.000e-002    0
           TUBE   310   0    12   2.000 8.000e-002    0
           TUBE   311   0    12   2.000 8.000e-002    0
           TUBE   312   0    12   2.000 8.000e-002    0
           TUBE   313   0    12   2.000 8.000e-002    0
           TUBE   314   0    12   2.000 8.000e-002    0
           TUBE   315   0    12   2.000 8.000e-002    0
           TUBE   316   0    12   2.000 8.000e-002    0
(1020)     TUBE   317   0    12   2.000 8.000e-002    0
           TUBE   318   0    12   2.000 8.000e-002    0
           TUBE   319   0    12   2.000 8.000e-002    0
           TUBE   320   0    12   2.000 8.000e-002    0
           TUBE   321   0    12   2.000 8.000e-002    0
           TUBE   322   0    12   2.000 8.000e-002    0
           TUBE   323   0    12   2.000 8.000e-002    0
           TUBE   324   0    12   2.000 8.000e-002    0
           TUBE   325   0    12   2.000 8.000e-002    0
           TUBE   326   0    12   2.000 8.000e-002    0
(1030)     TUBE   327   0    12   2.000 8.000e-002    0
           TUBE   328   0    12   2.000 8.000e-002    0
           TUBE   329   0    12   2.000 8.000e-002    0
           TUBE   330   0    12   2.000 8.000e-002    0
           TUBE   331   0    12   2.000 8.000e-002    0
           TUBE   332   0    12   2.000 8.000e-002    0
           TUBE   333   0    12   2.000 8.000e-002    0
           TUBE   334   0    12   2.000 8.000e-002    0
           TUBE   335   0    12   2.000 8.000e-002    0
           TUBE   336   0    12   2.000 8.000e-002    0
(1040)     TUBE   337   0    12   2.000 8.000e-002    0
           TUBE   338   0    12   2.000 8.000e-002    0
           TUBE   339   0    12   2.000 8.000e-002    0
           TUBE   340   0    12   2.000 8.000e-002    0
           TUBE   341   0    12   2.000 8.000e-002    0
           TUBE   342   0    12   2.000 8.000e-002    0
           TUBE   343   0    12   2.000 8.000e-002    0
           TUBE   344   0    14   0.720 2.500e-002    0
           TUBE   345   0    14   0.720 2.500e-002    0
           TUBE   346   0    14   0.720 2.500e-002    0
(1050)     TUBE   347   0    14   0.720 2.500e-002    0
           TUBE   348   0    15   0.720 2.500e-002    0
           TUBE   349   0    15   0.720 2.500e-002    0
           TUBE   350   0    14   1.220 2.500e-002    0
           TUBE   351   0    14   1.220 2.500e-002    0
           TUBE   352   0    14   1.220 2.500e-002    0
           TUBE   353   0    14   1.220 2.500e-002    0
           TUBE   354   0    15   1.220 2.500e-002    0
           TUBE   355   0    15   1.220 2.500e-002    0
           TUBE   356   0    14   1.220 2.500e-002    0
(1060)     TUBE   357   0    14   1.220 2.500e-002    0
           TUBE   358   0    14   1.220 2.500e-002    0
           TUBE   359   0    14   1.220 2.500e-002    0
           TUBE   360   0    15   1.220 2.500e-002    0
           TUBE   361   0    15   1.220 2.500e-002    0
           TUBE   362   0    14   1.220 2.500e-002    0
           TUBE   363   0    14   1.220 2.500e-002    0
           TUBE   364   0    14   1.220 2.500e-002    0
           TUBE   365   0    14   1.220 2.500e-002    0
           TUBE   366   0    15   1.220 2.500e-002    0
(1070)     TUBE   367   0    15   1.220 2.500e-002    0
           TUBE   368   0    14   1.220 2.500e-002    0
           TUBE   369   0    14   1.220 2.500e-002    0
           TUBE   370   0    14   1.220 2.500e-002    0
           TUBE   371   0    14   1.220 2.500e-002    0
           TUBE   372   0    15   1.220 2.500e-002    0
```

```
           TUBE   373   0    15   1.220 2.500e-002    0
           TUBE   374   0    14   0.760 2.540e-002    0
           TUBE   375   0    14   0.760 2.540e-002    0
           TUBE   376   0    14   0.760 2.540e-002    0
(1080)     TUBE   377   0    15   0.760 2.540e-002    0
           TUBE   378   0    15   0.760 2.540e-002    0
           TUBE   379   0    14   0.760 2.540e-002    0
           TUBE   380   0    14   0.760 2.540e-002    0
           TUBE   381   0    14   0.760 2.540e-002    0
           TUBE   382   0    15   0.760 2.540e-002    0
           TUBE   383   0    15   0.760 2.540e-002    0
           TUBE   384   0    14   0.760 2.540e-002    0
           TUBE   385   0    14   0.760 2.540e-002    0
           TUBE   386   0    14   0.760 2.540e-002    0
(1090)     TUBE   387   0    15   0.760 2.540e-002    0
           TUBE   388   0    15   0.760 2.540e-002    0
           TUBE   389   0    14   0.760 2.540e-002    0
           TUBE   390   0    14   0.760 2.540e-002    0
           TUBE   391   0    14   0.760 2.540e-002    0
           TUBE   392   0    15   0.760 2.540e-002    0
           TUBE   393   0    15   0.760 2.540e-002    0
           TUBE   394   0    14   0.760 2.540e-002    0
           TUBE   395   0    14   0.760 2.540e-002    0
           TUBE   396   0    14   0.760 2.540e-002    0
(1100)     TUBE   397   0    15   0.760 2.540e-002    0
           TUBE   398   0    15   0.760 2.540e-002    0
           TUBE   399   0    14   0.760 2.540e-002    0
           TUBE   400   0    14   0.760 2.540e-002    0
           TUBE   401   0    14   0.760 2.540e-002    0
           TUBE   402   0    15   0.760 2.540e-002    0
           TUBE   403   0    15   0.760 2.540e-002    0
           TUBE   404   0    14   0.760 2.540e-002    0
           TUBE   405   0    14   0.760 2.540e-002    0
           TUBE   406   0    14   0.760 2.540e-002    0
(1110)     TUBE   407   0    15   0.760 2.540e-002    0
           TUBE   408   0    15   0.760 2.540e-002    0
           TUBE   409   0    14   0.760 2.540e-002    0
           TUBE   410   0    14   0.760 2.540e-002    0
           TUBE   411   0    14   0.760 2.540e-002    0
           TUBE   412   0    15   0.760 2.540e-002    0
           TUBE   413   0    15   0.760 2.540e-002    0
           TUBE   414   0    14   1.650 3.000e-002    0
           TUBE   415   0    14   1.650 3.000e-002    0
           TUBE   416   0    14   1.650 3.000e-002    0
(1120)     TUBE   417   0    15   1.650 3.000e-002    0
           TUBE   418   0    15   1.650 3.000e-002    0
           TUBE   419   0    13   0.760 3.000e-002    0
           TUBE   420   0    13   0.760 3.000e-002    0
           TUBE   421   0    13   0.760 3.000e-002    0
           TUBE   422   0    13   0.760 3.000e-002    0
           TUBE   423   0    13   0.760 3.000e-002    0
           TUBE   424   0     1   2.000 8.500e-002    0
           TUBE   425   0     1   2.000 8.500e-002    0
           TUBE   426   0     1   2.000 8.500e-002    0
(1130)   '
         '
         SPRI
         '   INOD    SP1      SP2      SP3      SP4      SP5      SP6
               1  6.65e+008  6.65e+008  8.68e+009  7.03e+010  7.03e+010  1.24e+010
               2  6.65e+008  6.65e+008  8.68e+009  7.03e+010  7.03e+010  1.24e+010
               3  6.65e+008  6.65e+008  8.68e+009  7.03e+010  7.03e+010  1.24e+010
               4  6.65e+008  6.65e+008  8.68e+009  7.03e+010  7.03e+010  1.24e+010
         '
         '
(1140)   'Nodal point masses for dry model
         '
         MASS
         ' NNOD
             218
         '   INOD     KN          MX          MY          MZ         MRX         MRY         MRZ
               1       0  0.00e+000  0.00e+000  0.00e+000  0.00e+000  0.00e+000  0.00e+000
               2       0  0.00e+000  0.00e+000  0.00e+000  0.00e+000  0.00e+000  0.00e+000
               3       0  0.00e+000  0.00e+000  0.00e+000  0.00e+000  0.00e+000  0.00e+000
               4       0  0.00e+000  0.00e+000  0.00e+000  0.00e+000  0.00e+000  0.00e+000
(1150)         5       0  2.86e+005  2.86e+005  2.86e+005  0.00e+000  0.00e+000  0.00e+000
               6       0  0.00e+000  0.00e+000  0.00e+000  0.00e+000  0.00e+000  0.00e+000
               7       0  0.00e+000  0.00e+000  0.00e+000  0.00e+000  0.00e+000  0.00e+000
```

	8	0	2.86e+005	2.86e+005	2.86e+005	0.00e+000	0.00e+000	0.00e+000
	9	0	0.00e+000	0.00e+000	0.00e+000	0.00e+000	0.00e+000	0.00e+000
	10	0	0.00e+000	0.00e+000	0.00e+000	0.00e+000	0.00e+000	0.00e+000
	11	0	2.86e+005	2.86e+005	2.86e+005	0.00e+000	0.00e+000	0.00e+000
	12	0	0.00e+000	0.00e+000	0.00e+000	0.00e+000	0.00e+000	0.00e+000
	13	0	0.00e+000	0.00e+000	0.00e+000	0.00e+000	0.00e+000	0.00e+000
	14	0	2.86e+005	2.86e+005	2.86e+005	0.00e+000	0.00e+000	0.00e+000
(1160)	15	0	0.00e+000	0.00e+000	0.00e+000	0.00e+000	0.00e+000	0.00e+000
	16	0	0.00e+000	0.00e+000	0.00e+000	0.00e+000	0.00e+000	0.00e+000
	17	0	5.00e+003	5.00e+003	5.00e+003	0.00e+000	0.00e+000	0.00e+000
	18	0	0.00e+000	0.00e+000	0.00e+000	0.00e+000	0.00e+000	0.00e+000
	19	0	5.00e+003	5.00e+003	5.00e+003	0.00e+000	0.00e+000	0.00e+000
	20	0	0.00e+000	0.00e+000	0.00e+000	0.00e+000	0.00e+000	0.00e+000
	21	0	5.00e+003	5.00e+003	5.00e+003	0.00e+000	0.00e+000	0.00e+000
	22	0	0.00e+000	0.00e+000	0.00e+000	0.00e+000	0.00e+000	0.00e+000
	23	0	5.00e+003	5.00e+003	5.00e+003	0.00e+000	0.00e+000	0.00e+000
	24	0	0.00e+000	0.00e+000	0.00e+000	0.00e+000	0.00e+000	0.00e+000
(1170)	25	0	0.00e+000	0.00e+000	0.00e+000	0.00e+000	0.00e+000	0.00e+000
	26	0	0.00e+000	0.00e+000	0.00e+000	0.00e+000	0.00e+000	0.00e+000
	27	0	0.00e+000	0.00e+000	0.00e+000	0.00e+000	0.00e+000	0.00e+000
	28	0	0.00e+000	0.00e+000	0.00e+000	0.00e+000	0.00e+000	0.00e+000
	29	0	0.00e+000	0.00e+000	0.00e+000	0.00e+000	0.00e+000	0.00e+000
	30	0	0.00e+000	0.00e+000	0.00e+000	0.00e+000	0.00e+000	0.00e+000
	31	0	0.00e+000	0.00e+000	0.00e+000	0.00e+000	0.00e+000	0.00e+000
	32	0	5.00e+003	5.00e+003	5.00e+003	0.00e+000	0.00e+000	0.00e+000
	33	0	0.00e+000	0.00e+000	0.00e+000	0.00e+000	0.00e+000	0.00e+000
	34	0	5.00e+003	5.00e+003	5.00e+003	0.00e+000	0.00e+000	0.00e+000
(1180)	35	0	0.00e+000	0.00e+000	0.00e+000	0.00e+000	0.00e+000	0.00e+000
	36	0	5.00e+003	5.00e+003	5.00e+003	0.00e+000	0.00e+000	0.00e+000
	37	0	0.00e+000	0.00e+000	0.00e+000	0.00e+000	0.00e+000	0.00e+000
	38	0	5.00e+003	5.00e+003	5.00e+003	0.00e+000	0.00e+000	0.00e+000
	39	0	0.00e+000	0.00e+000	0.00e+000	0.00e+000	0.00e+000	0.00e+000
	40	0	0.00e+000	0.00e+000	0.00e+000	0.00e+000	0.00e+000	0.00e+000
	41	0	0.00e+000	0.00e+000	0.00e+000	0.00e+000	0.00e+000	0.00e+000
	42	0	0.00e+000	0.00e+000	0.00e+000	0.00e+000	0.00e+000	0.00e+000
	43	0	0.00e+000	0.00e+000	0.00e+000	0.00e+000	0.00e+000	0.00e+000
	44	0	0.00e+000	0.00e+000	0.00e+000	0.00e+000	0.00e+000	0.00e+000
(1190)	45	0	0.00e+000	0.00e+000	0.00e+000	0.00e+000	0.00e+000	0.00e+000
	46	0	0.00e+000	0.00e+000	0.00e+000	0.00e+000	0.00e+000	0.00e+000
	47	0	5.00e+003	5.00e+003	5.00e+003	0.00e+000	0.00e+000	0.00e+000
	48	0	5.00e+003	5.00e+003	5.00e+003	0.00e+000	0.00e+000	0.00e+000
	49	0	5.00e+003	5.00e+003	5.00e+003	0.00e+000	0.00e+000	0.00e+000
	50	0	5.00e+003	5.00e+003	5.00e+003	0.00e+000	0.00e+000	0.00e+000
	51	0	0.00e+000	0.00e+000	0.00e+000	0.00e+000	0.00e+000	0.00e+000
	52	0	0.00e+000	0.00e+000	0.00e+000	0.00e+000	0.00e+000	0.00e+000
	53	0	0.00e+000	0.00e+000	0.00e+000	0.00e+000	0.00e+000	0.00e+000
	54	0	0.00e+000	0.00e+000	0.00e+000	0.00e+000	0.00e+000	0.00e+000
(1200)	55	0	0.00e+000	0.00e+000	0.00e+000	0.00e+000	0.00e+000	0.00e+000
	56	0	5.00e+003	5.00e+003	5.00e+003	0.00e+000	0.00e+000	0.00e+000
	57	0	5.00e+003	5.00e+003	5.00e+003	0.00e+000	0.00e+000	0.00e+000
	58	0	5.00e+003	5.00e+003	5.00e+003	0.00e+000	0.00e+000	0.00e+000
	59	0	5.00e+003	5.00e+003	5.00e+003	0.00e+000	0.00e+000	0.00e+000
	60	0	0.00e+000	0.00e+000	0.00e+000	0.00e+000	0.00e+000	0.00e+000
	61	0	0.00e+000	0.00e+000	0.00e+000	0.00e+000	0.00e+000	0.00e+000
	62	0	0.00e+000	0.00e+000	0.00e+000	0.00e+000	0.00e+000	0.00e+000
	63	0	0.00e+000	0.00e+000	0.00e+000	0.00e+000	0.00e+000	0.00e+000
	64	0	0.00e+000	0.00e+000	0.00e+000	0.00e+000	0.00e+000	0.00e+000
(1210)	65	0	5.00e+003	5.00e+003	5.00e+003	0.00e+000	0.00e+000	0.00e+000
	66	0	5.00e+003	5.00e+003	5.00e+003	0.00e+000	0.00e+000	0.00e+000
	67	0	5.00e+003	5.00e+003	5.00e+003	0.00e+000	0.00e+000	0.00e+000
	68	0	5.00e+003	5.00e+003	5.00e+003	0.00e+000	0.00e+000	0.00e+000
	69	0	0.00e+000	0.00e+000	0.00e+000	0.00e+000	0.00e+000	0.00e+000
	70	0	0.00e+000	0.00e+000	0.00e+000	0.00e+000	0.00e+000	0.00e+000
	71	0	0.00e+000	0.00e+000	0.00e+000	0.00e+000	0.00e+000	0.00e+000
	72	0	0.00e+000	0.00e+000	0.00e+000	0.00e+000	0.00e+000	0.00e+000
	73	0	0.00e+000	0.00e+000	0.00e+000	0.00e+000	0.00e+000	0.00e+000
	74	0	0.00e+000	0.00e+000	0.00e+000	0.00e+000	0.00e+000	0.00e+000
(1220)	75	0	0.00e+000	0.00e+000	0.00e+000	0.00e+000	0.00e+000	0.00e+000
	76	0	0.00e+000	0.00e+000	0.00e+000	0.00e+000	0.00e+000	0.00e+000
	77	0	0.00e+000	0.00e+000	0.00e+000	0.00e+000	0.00e+000	0.00e+000
	78	0	5.00e+003	5.00e+003	5.00e+003	0.00e+000	0.00e+000	0.00e+000
	79	0	5.00e+003	5.00e+003	5.00e+003	0.00e+000	0.00e+000	0.00e+000
	80	0	5.00e+003	5.00e+003	5.00e+003	0.00e+000	0.00e+000	0.00e+000
	81	0	5.00e+003	5.00e+003	5.00e+003	0.00e+000	0.00e+000	0.00e+000
	82	0	0.00e+000	0.00e+000	0.00e+000	0.00e+000	0.00e+000	0.00e+000
	83	0	0.00e+000	0.00e+000	0.00e+000	0.00e+000	0.00e+000	0.00e+000
	84	0	0.00e+000	0.00e+000	0.00e+000	0.00e+000	0.00e+000	0.00e+000

(1230)	85	0	0.00e+000	0.00e+000	0.00e+000	0.00e+000	0.00e+000	0.00e+000
	86	0	0.00e+000	0.00e+000	0.00e+000	0.00e+000	0.00e+000	0.00e+000
	87	0	0.00e+000	0.00e+000	0.00e+000	0.00e+000	0.00e+000	0.00e+000
	88	0	0.00e+000	0.00e+000	0.00e+000	0.00e+000	0.00e+000	0.00e+000
	89	0	0.00e+000	0.00e+000	0.00e+000	0.00e+000	0.00e+000	0.00e+000
	90	0	0.00e+000	0.00e+000	0.00e+000	0.00e+000	0.00e+000	0.00e+000
	91	0	0.00e+000	0.00e+000	0.00e+000	0.00e+000	0.00e+000	0.00e+000
	92	0	0.00e+000	0.00e+000	0.00e+000	0.00e+000	0.00e+000	0.00e+000
	93	0	0.00e+000	0.00e+000	0.00e+000	0.00e+000	0.00e+000	0.00e+000
	94	0	0.00e+000	0.00e+000	0.00e+000	0.00e+000	0.00e+000	0.00e+000
(1240)	95	0	5.00e+003	5.00e+003	5.00e+003	0.00e+000	0.00e+000	0.00e+000
	96	0	0.00e+000	0.00e+000	0.00e+000	0.00e+000	0.00e+000	0.00e+000
	97	0	5.00e+003	5.00e+003	5.00e+003	0.00e+000	0.00e+000	0.00e+000
	98	0	0.00e+000	0.00e+000	0.00e+000	0.00e+000	0.00e+000	0.00e+000
	99	0	5.00e+003	5.00e+003	5.00e+003	0.00e+000	0.00e+000	0.00e+000
	100	0	0.00e+000	0.00e+000	0.00e+000	0.00e+000	0.00e+000	0.00e+000
	101	0	5.00e+003	5.00e+003	5.00e+003	0.00e+000	0.00e+000	0.00e+000
	102	0	0.00e+000	0.00e+000	0.00e+000	0.00e+000	0.00e+000	0.00e+000
	103	0	0.00e+000	0.00e+000	0.00e+000	0.00e+000	0.00e+000	0.00e+000
	104	0	0.00e+000	0.00e+000	0.00e+000	0.00e+000	0.00e+000	0.00e+000
(1250)	105	0	0.00e+000	0.00e+000	0.00e+000	0.00e+000	0.00e+000	0.00e+000
	106	0	0.00e+000	0.00e+000	0.00e+000	0.00e+000	0.00e+000	0.00e+000
	107	0	0.00e+000	0.00e+000	0.00e+000	0.00e+000	0.00e+000	0.00e+000
	108	0	0.00e+000	0.00e+000	0.00e+000	0.00e+000	0.00e+000	0.00e+000
	109	0	0.00e+000	0.00e+000	0.00e+000	0.00e+000	0.00e+000	0.00e+000
	110	0	0.00e+000	0.00e+000	0.00e+000	0.00e+000	0.00e+000	0.00e+000
	111	0	0.00e+000	0.00e+000	0.00e+000	0.00e+000	0.00e+000	0.00e+000
	112	0	0.00e+000	0.00e+000	0.00e+000	0.00e+000	0.00e+000	0.00e+000
	113	0	0.00e+000	0.00e+000	0.00e+000	0.00e+000	0.00e+000	0.00e+000
	114	0	0.00e+000	0.00e+000	0.00e+000	0.00e+000	0.00e+000	0.00e+000
(1260)	115	0	0.00e+000	0.00e+000	0.00e+000	0.00e+000	0.00e+000	0.00e+000
	116	0	0.00e+000	0.00e+000	0.00e+000	0.00e+000	0.00e+000	0.00e+000
	117	0	0.00e+000	0.00e+000	0.00e+000	0.00e+000	0.00e+000	0.00e+000
	118	0	0.00e+000	0.00e+000	0.00e+000	0.00e+000	0.00e+000	0.00e+000
	119	0	0.00e+000	0.00e+000	0.00e+000	0.00e+000	0.00e+000	0.00e+000
	120	0	0.00e+000	0.00e+000	0.00e+000	0.00e+000	0.00e+000	0.00e+000
	121	0	0.00e+000	0.00e+000	0.00e+000	0.00e+000	0.00e+000	0.00e+000
	122	0	0.00e+000	0.00e+000	0.00e+000	0.00e+000	0.00e+000	0.00e+000
	123	0	0.00e+000	0.00e+000	0.00e+000	0.00e+000	0.00e+000	0.00e+000
	124	0	0.00e+000	0.00e+000	0.00e+000	0.00e+000	0.00e+000	0.00e+000
(1270)	125	0	0.00e+000	0.00e+000	0.00e+000	0.00e+000	0.00e+000	0.00e+000
	126	0	0.00e+000	0.00e+000	0.00e+000	0.00e+000	0.00e+000	0.00e+000
	127	0	0.00e+000	0.00e+000	0.00e+000	0.00e+000	0.00e+000	0.00e+000
	128	0	0.00e+000	0.00e+000	0.00e+000	0.00e+000	0.00e+000	0.00e+000
	129	0	0.00e+000	0.00e+000	0.00e+000	0.00e+000	0.00e+000	0.00e+000
	130	0	0.00e+000	0.00e+000	0.00e+000	0.00e+000	0.00e+000	0.00e+000
	131	0	0.00e+000	0.00e+000	0.00e+000	0.00e+000	0.00e+000	0.00e+000
	132	0	0.00e+000	0.00e+000	0.00e+000	0.00e+000	0.00e+000	0.00e+000
	133	0	0.00e+000	0.00e+000	0.00e+000	0.00e+000	0.00e+000	0.00e+000
	134	0	0.00e+000	0.00e+000	0.00e+000	0.00e+000	0.00e+000	0.00e+000
(1280)	135	0	0.00e+000	0.00e+000	0.00e+000	0.00e+000	0.00e+000	0.00e+000
	136	0	0.00e+000	0.00e+000	0.00e+000	0.00e+000	0.00e+000	0.00e+000
	137	0	0.00e+000	0.00e+000	0.00e+000	0.00e+000	0.00e+000	0.00e+000
	138	0	0.00e+000	0.00e+000	0.00e+000	0.00e+000	0.00e+000	0.00e+000
	139	0	0.00e+000	0.00e+000	0.00e+000	0.00e+000	0.00e+000	0.00e+000
	140	0	1.90e+007	1.90e+007	1.90e+007	2.91e+009	6.56e+009	6.07e+009
	141	0	0.00e+000	0.00e+000	0.00e+000	0.00e+000	0.00e+000	0.00e+000
	142	0	0.00e+000	0.00e+000	0.00e+000	0.00e+000	0.00e+000	0.00e+000
	143	0	0.00e+000	0.00e+000	0.00e+000	0.00e+000	0.00e+000	0.00e+000
	144	0	0.00e+000	0.00e+000	0.00e+000	0.00e+000	0.00e+000	0.00e+000
(1290)	145	0	0.00e+000	0.00e+000	0.00e+000	0.00e+000	0.00e+000	0.00e+000
	146	0	0.00e+000	0.00e+000	0.00e+000	0.00e+000	0.00e+000	0.00e+000
	147	0	0.00e+000	0.00e+000	0.00e+000	0.00e+000	0.00e+000	0.00e+000
	148	0	0.00e+000	0.00e+000	0.00e+000	0.00e+000	0.00e+000	0.00e+000
	149	0	0.00e+000	0.00e+000	0.00e+000	0.00e+000	0.00e+000	0.00e+000
	150	0	0.00e+000	0.00e+000	0.00e+000	0.00e+000	0.00e+000	0.00e+000
	151	0	0.00e+000	0.00e+000	0.00e+000	0.00e+000	0.00e+000	0.00e+000
	152	0	0.00e+000	0.00e+000	0.00e+000	0.00e+000	0.00e+000	0.00e+000
	153	0	0.00e+000	0.00e+000	0.00e+000	0.00e+000	0.00e+000	0.00e+000
	154	0	0.00e+000	0.00e+000	0.00e+000	0.00e+000	0.00e+000	0.00e+000
(1300)	155	0	0.00e+000	0.00e+000	0.00e+000	0.00e+000	0.00e+000	0.00e+000
	156	0	0.00e+000	0.00e+000	0.00e+000	0.00e+000	0.00e+000	0.00e+000
	157	0	0.00e+000	0.00e+000	0.00e+000	0.00e+000	0.00e+000	0.00e+000
	158	0	0.00e+000	0.00e+000	0.00e+000	0.00e+000	0.00e+000	0.00e+000
	159	0	0.00e+000	0.00e+000	0.00e+000	0.00e+000	0.00e+000	0.00e+000
	160	0	0.00e+000	0.00e+000	0.00e+000	0.00e+000	0.00e+000	0.00e+000
	161	0	0.00e+000	0.00e+000	0.00e+000	0.00e+000	0.00e+000	0.00e+000

```
            162       0  0.00e+000  0.00e+000  0.00e+000  0.00e+000  0.00e+000  0.00e+000
            163       0  0.00e+000  0.00e+000  0.00e+000  0.00e+000  0.00e+000  0.00e+000
            164       0  0.00e+000  0.00e+000  0.00e+000  0.00e+000  0.00e+000  0.00e+000
(1310)      165       0  0.00e+000  0.00e+000  0.00e+000  0.00e+000  0.00e+000  0.00e+000
            166       0  0.00e+000  0.00e+000  0.00e+000  0.00e+000  0.00e+000  0.00e+000
            167       0  0.00e+000  0.00e+000  0.00e+000  0.00e+000  0.00e+000  0.00e+000
            168       0  0.00e+000  0.00e+000  0.00e+000  0.00e+000  0.00e+000  0.00e+000
            169       0  0.00e+000  0.00e+000  0.00e+000  0.00e+000  0.00e+000  0.00e+000
            170       0  0.00e+000  0.00e+000  0.00e+000  0.00e+000  0.00e+000  0.00e+000
            171       0  0.00e+000  0.00e+000  0.00e+000  0.00e+000  0.00e+000  0.00e+000
            172       0  0.00e+000  0.00e+000  0.00e+000  0.00e+000  0.00e+000  0.00e+000
            173       0  0.00e+000  0.00e+000  0.00e+000  0.00e+000  0.00e+000  0.00e+000
            174       0  0.00e+000  0.00e+000  0.00e+000  0.00e+000  0.00e+000  0.00e+000
(1320)      175       0  0.00e+000  0.00e+000  0.00e+000  0.00e+000  0.00e+000  0.00e+000
            176       0  0.00e+000  0.00e+000  0.00e+000  0.00e+000  0.00e+000  0.00e+000
            177       0  0.00e+000  0.00e+000  0.00e+000  0.00e+000  0.00e+000  0.00e+000
            178       0  0.00e+000  0.00e+000  0.00e+000  0.00e+000  0.00e+000  0.00e+000
            179       0  0.00e+000  0.00e+000  0.00e+000  0.00e+000  0.00e+000  0.00e+000
            180       0  0.00e+000  0.00e+000  0.00e+000  0.00e+000  0.00e+000  0.00e+000
            181       0  0.00e+000  0.00e+000  0.00e+000  0.00e+000  0.00e+000  0.00e+000
            182       0  0.00e+000  0.00e+000  0.00e+000  0.00e+000  0.00e+000  0.00e+000
            183       0  0.00e+000  0.00e+000  0.00e+000  0.00e+000  0.00e+000  0.00e+000
            184       0  0.00e+000  0.00e+000  0.00e+000  0.00e+000  0.00e+000  0.00e+000
(1330)      185       0  0.00e+000  0.00e+000  0.00e+000  0.00e+000  0.00e+000  0.00e+000
            186       0  0.00e+000  0.00e+000  0.00e+000  0.00e+000  0.00e+000  0.00e+000
            187       0  0.00e+000  0.00e+000  0.00e+000  0.00e+000  0.00e+000  0.00e+000
            188       0  0.00e+000  0.00e+000  0.00e+000  0.00e+000  0.00e+000  0.00e+000
            189       0  0.00e+000  0.00e+000  0.00e+000  0.00e+000  0.00e+000  0.00e+000
            190       0  0.00e+000  0.00e+000  0.00e+000  0.00e+000  0.00e+000  0.00e+000
            191       0  0.00e+000  0.00e+000  0.00e+000  0.00e+000  0.00e+000  0.00e+000
            192       0  0.00e+000  0.00e+000  0.00e+000  0.00e+000  0.00e+000  0.00e+000
            193       0  0.00e+000  0.00e+000  0.00e+000  0.00e+000  0.00e+000  0.00e+000
            194       0  0.00e+000  0.00e+000  0.00e+000  0.00e+000  0.00e+000  0.00e+000
(1340)      195       0  0.00e+000  0.00e+000  0.00e+000  0.00e+000  0.00e+000  0.00e+000
            196       0  0.00e+000  0.00e+000  0.00e+000  0.00e+000  0.00e+000  0.00e+000
            197       0  0.00e+000  0.00e+000  0.00e+000  0.00e+000  0.00e+000  0.00e+000
            198       0  0.00e+000  0.00e+000  0.00e+000  0.00e+000  0.00e+000  0.00e+000
            199       0  0.00e+000  0.00e+000  0.00e+000  0.00e+000  0.00e+000  0.00e+000
            200       0  0.00e+000  0.00e+000  0.00e+000  0.00e+000  0.00e+000  0.00e+000
            201       0  0.00e+000  0.00e+000  0.00e+000  0.00e+000  0.00e+000  0.00e+000
            202       0  0.00e+000  0.00e+000  0.00e+000  0.00e+000  0.00e+000  0.00e+000
            203       0  0.00e+000  0.00e+000  0.00e+000  0.00e+000  0.00e+000  0.00e+000
            204       0  0.00e+000  0.00e+000  0.00e+000  0.00e+000  0.00e+000  0.00e+000
(1350)      205       0  0.00e+000  0.00e+000  0.00e+000  0.00e+000  0.00e+000  0.00e+000
            206       0  0.00e+000  0.00e+000  0.00e+000  0.00e+000  0.00e+000  0.00e+000
            207       0  0.00e+000  0.00e+000  0.00e+000  0.00e+000  0.00e+000  0.00e+000
            208       0  0.00e+000  0.00e+000  0.00e+000  0.00e+000  0.00e+000  0.00e+000
            209       0  0.00e+000  0.00e+000  0.00e+000  0.00e+000  0.00e+000  0.00e+000
            210       0  0.00e+000  0.00e+000  0.00e+000  0.00e+000  0.00e+000  0.00e+000
            211       0  0.00e+000  0.00e+000  0.00e+000  0.00e+000  0.00e+000  0.00e+000
            212       0  0.00e+000  0.00e+000  0.00e+000  0.00e+000  0.00e+000  0.00e+000
            213       0  0.00e+000  0.00e+000  0.00e+000  0.00e+000  0.00e+000  0.00e+000
            214       0  0.00e+000  0.00e+000  0.00e+000  0.00e+000  0.00e+000  0.00e+000
(1360)      215       0  0.00e+000  0.00e+000  0.00e+000  0.00e+000  0.00e+000  0.00e+000
            216       0  0.00e+000  0.00e+000  0.00e+000  0.00e+000  0.00e+000  0.00e+000
            217       0  0.00e+000  0.00e+000  0.00e+000  0.00e+000  0.00e+000  0.00e+000
            218       0  0.00e+000  0.00e+000  0.00e+000  0.00e+000  0.00e+000  0.00e+000
        '
        '
        '
        '
        SELF
        '        G   WDENSITY   SELFWEIGHT  BUOYANCY
(1370)  9.810e+000 1.025e+003       1       1
        '
        '
        STAT
        '  IDEAD   ILIVE  IENVI
             0       0      0
        '
        '
        OUTP
        '   NRNOD  NRELE   NDCAL
(1380)       16       8       0
        '
        NODR
        '   INOD   IDOF  ISCALE
```

```
               1       1       1
               2       1       1
               4       1       1
               3       1       1
               1       3       1
               2       3       1
(1390)         4       3       1
               3       3       1
              48       1       1
              48       2       1
              50       1       1
              50       2       1
             111       1       1
             111       2       1
             115       1       1
             115       2       1
(1400)   '
         ELER
         '   IELE   IDOF  ISCALE
               4       1       1
               5       1       1
              15       1       1
              16       1       1
              26       1       1
              27       1       1
              37       1       1
(1410)        38       1       1
         '
         BOTM
         '   NBASE   NOTM
               4       4
         '   IBASE   RBASE
               1  6.65e+008
               2  6.65e+008
               3  6.65e+008
               4  6.65e+008
(1420)   '   IOTM   ROTM
               5 -2.17e+011
               6  2.17e+011
               7 -2.17e+011
               8  2.17e+011
         '
         COMB
         '   NLCOMB
               1
         '   ICOMB  CENVI      CDEAD     CLIVE
(1430)         1  1.00e+000  1.00e+000  1.00e+000
         '
         '
         POST
         '   IEXMOD  STORM
               0  3.00e+000
         '
         '   ILOSTA  NFILT  NTRREF   FRQLO    FRQHI    PERIOD
               0       1      78  4.00e-002  5.00e-001  4.00e+000
         '
(1440)   '
         '-----------------------------------------------
         '     WAVE LOAD INPUT DATA
         '-----------------------------------------------
         '
         LOAD
         '   IFEF   ILOSS   ILOAD   NELIN   DCD       DCM         RO     FACLIN
               1       0       0     426  1.05e+000  1.20e+000  1.03e+003  1.00e+000
         '
         '   IELEM   DIADR   DIAIN   CCD   CCM   ACTDIA1   ACTDIA2
(1450)     1  8.00e+000  8.00e+000  1.05e+000  1.20e+000  8.00e+000  8.00e+000
           2  8.00e+000  8.00e+000  1.05e+000  1.20e+000  8.00e+000  8.00e+000
           3  3.46e+000  3.46e+000  1.05e+000  1.20e+000  3.46e+000  3.46e+000
           4  2.96e+000  2.96e+000  1.05e+000  1.20e+000  2.96e+000  2.96e+000
           5  2.96e+000  2.96e+000  1.05e+000  1.20e+000  2.96e+000  2.96e+000
           6  2.96e+000  2.96e+000  1.05e+000  1.20e+000  2.96e+000  2.96e+000
           7  2.12e+000  2.12e+000  1.05e+000  1.20e+000  2.12e+000  2.12e+000
           8  2.70e+000  2.20e+000  1.05e+000  1.20e+000  2.20e+000  2.20e+000
           9  2.70e+000  2.20e+000  8.50e-001  1.40e+000  2.20e+000  2.20e+000
          10  2.46e+000  2.05e+000  6.50e-001  1.60e+000  2.05e+000  2.05e+000
(1460)    11  0.00e+000  0.00e+000  6.50e-001  1.60e+000  0.00e+000  0.00e+000
```

	12	8.00e+000	8.00e+000	1.05e+000	1.20e+000	8.00e+000	8.00e+000
	13	8.00e+000	8.00e+000	1.05e+000	1.20e+000	8.00e+000	8.00e+000
	14	3.46e+000	3.46e+000	1.05e+000	1.20e+000	3.46e+000	3.46e+000
	15	2.96e+000	2.96e+000	1.05e+000	1.20e+000	2.96e+000	2.96e+000
	16	2.96e+000	2.96e+000	1.05e+000	1.20e+000	2.96e+000	2.96e+000
	17	2.96e+000	2.96e+000	1.05e+000	1.20e+000	2.96e+000	2.96e+000
	18	2.12e+000	2.12e+000	1.05e+000	1.20e+000	2.12e+000	2.12e+000
	19	2.12e+000	2.12e+000	1.05e+000	1.20e+000	2.12e+000	2.12e+000
	20	2.12e+000	2.12e+000	8.50e-001	1.40e+000	2.12e+000	2.12e+000
(1470)	21	2.00e+000	2.00e+000	6.50e-001	1.60e+000	2.00e+000	2.00e+000
	22	0.00e+000	0.00e+000	6.50e-001	1.60e+000	0.00e+000	0.00e+000
	23	8.00e+000	8.00e+000	1.05e+000	1.20e+000	8.00e+000	8.00e+000
	24	8.00e+000	8.00e+000	1.05e+000	1.20e+000	8.00e+000	8.00e+000
	25	3.46e+000	3.46e+000	1.05e+000	1.20e+000	3.46e+000	3.46e+000
	26	2.96e+000	2.96e+000	1.05e+000	1.20e+000	2.96e+000	2.96e+000
	27	2.96e+000	2.96e+000	1.05e+000	1.20e+000	2.96e+000	2.96e+000
	28	2.96e+000	2.96e+000	1.05e+000	1.20e+000	2.96e+000	2.96e+000
	29	3.46e+000	2.51e+000	1.05e+000	1.20e+000	2.51e+000	2.51e+000
	30	3.46e+000	2.51e+000	1.05e+000	1.20e+000	2.51e+000	2.51e+000
(1480)	31	3.46e+000	2.51e+000	8.50e-001	1.40e+000	2.51e+000	2.51e+000
	32	3.22e+000	2.34e+000	6.50e-001	1.60e+000	2.34e+000	2.34e+000
	33	0.00e+000	0.00e+000	6.50e-001	1.60e+000	0.00e+000	0.00e+000
	34	8.00e+000	8.00e+000	1.05e+000	1.20e+000	8.00e+000	8.00e+000
	35	8.00e+000	8.00e+000	1.05e+000	1.20e+000	8.00e+000	8.00e+000
	36	3.46e+000	3.46e+000	1.05e+000	1.20e+000	3.46e+000	3.46e+000
	37	2.96e+000	2.96e+000	1.05e+000	1.20e+000	2.96e+000	2.96e+000
	38	2.96e+000	2.96e+000	1.05e+000	1.20e+000	2.96e+000	2.96e+000
	39	2.96e+000	2.96e+000	1.05e+000	1.20e+000	2.96e+000	2.96e+000
	40	2.12e+000	2.12e+000	1.05e+000	1.20e+000	2.12e+000	2.12e+000
(1490)	41	2.12e+000	2.12e+000	1.05e+000	1.20e+000	2.12e+000	2.12e+000
	42	2.12e+000	2.12e+000	8.50e-001	1.40e+000	2.12e+000	2.12e+000
	43	2.00e+000	2.00e+000	6.50e-001	1.60e+000	2.00e+000	2.00e+000
	44	0.00e+000	0.00e+000	6.50e-001	1.60e+000	0.00e+000	0.00e+000
	45	9.00e-001	9.00e-001	1.05e+000	1.20e+000	9.00e-001	9.00e-001
	46	9.00e-001	9.00e-001	1.05e+000	1.20e+000	9.00e-001	9.00e-001
	47	9.00e-001	9.00e-001	1.05e+000	1.20e+000	9.00e-001	9.00e-001
	48	9.00e-001	9.00e-001	1.05e+000	1.20e+000	9.00e-001	9.00e-001
	49	9.00e-001	9.00e-001	1.05e+000	1.20e+000	9.00e-001	9.00e-001
	50	9.00e-001	9.00e-001	1.05e+000	1.20e+000	9.00e-001	9.00e-001
(1500)	51	9.00e-001	9.00e-001	1.05e+000	1.20e+000	9.00e-001	9.00e-001
	52	9.00e-001	9.00e-001	1.05e+000	1.20e+000	9.00e-001	9.00e-001
	53	9.00e-001	9.00e-001	1.05e+000	1.20e+000	9.00e-001	9.00e-001
	54	9.00e-001	9.00e-001	1.05e+000	1.20e+000	9.00e-001	9.00e-001
	55	9.00e-001	9.00e-001	1.05e+000	1.20e+000	9.00e-001	9.00e-001
	56	9.00e-001	9.00e-001	1.05e+000	1.20e+000	9.00e-001	9.00e-001
	57	9.00e-001	9.00e-001	1.05e+000	1.20e+000	9.00e-001	9.00e-001
	58	9.00e-001	9.00e-001	1.05e+000	1.20e+000	9.00e-001	9.00e-001
	59	9.00e-001	9.00e-001	1.05e+000	1.20e+000	9.00e-001	9.00e-001
	60	9.00e-001	9.00e-001	1.05e+000	1.20e+000	9.00e-001	9.00e-001
(1510)	61	9.00e-001	9.00e-001	1.05e+000	1.20e+000	9.00e-001	9.00e-001
	62	9.00e-001	9.00e-001	1.05e+000	1.20e+000	9.00e-001	9.00e-001
	63	9.00e-001	9.00e-001	1.05e+000	1.20e+000	9.00e-001	9.00e-001
	64	9.00e-001	9.00e-001	1.05e+000	1.20e+000	9.00e-001	9.00e-001
	65	8.00e-001	8.00e-001	1.05e+000	1.20e+000	8.00e-001	8.00e-001
	66	8.00e-001	8.00e-001	1.05e+000	1.20e+000	8.00e-001	8.00e-001
	67	8.00e-001	8.00e-001	1.05e+000	1.20e+000	8.00e-001	8.00e-001
	68	8.00e-001	8.00e-001	1.05e+000	1.20e+000	8.00e-001	8.00e-001
	69	8.00e-001	8.00e-001	1.05e+000	1.20e+000	8.00e-001	8.00e-001
	70	8.00e-001	8.00e-001	1.05e+000	1.20e+000	8.00e-001	8.00e-001
(1520)	71	8.00e-001	8.00e-001	1.05e+000	1.20e+000	8.00e-001	8.00e-001
	72	8.00e-001	8.00e-001	1.05e+000	1.20e+000	8.00e-001	8.00e-001
	73	1.00e+000	1.00e+000	1.05e+000	1.20e+000	1.00e+000	1.00e+000
	74	1.00e+000	1.00e+000	1.05e+000	1.20e+000	1.00e+000	1.00e+000
	75	1.00e+000	1.00e+000	1.05e+000	1.20e+000	1.00e+000	1.00e+000
	76	1.00e+000	1.00e+000	1.05e+000	1.20e+000	1.00e+000	1.00e+000
	77	1.00e+000	1.00e+000	1.05e+000	1.20e+000	1.00e+000	1.00e+000
	78	1.00e+000	1.00e+000	1.05e+000	1.20e+000	1.00e+000	1.00e+000
	79	1.00e+000	1.00e+000	1.05e+000	1.20e+000	1.00e+000	1.00e+000
	80	1.00e+000	1.00e+000	1.05e+000	1.20e+000	1.00e+000	1.00e+000
(1530)	81	1.00e+000	1.00e+000	1.05e+000	1.20e+000	1.00e+000	1.00e+000
	82	1.00e+000	1.00e+000	1.05e+000	1.20e+000	1.00e+000	1.00e+000
	83	1.00e+000	1.00e+000	1.05e+000	1.20e+000	1.00e+000	1.00e+000
	84	1.00e+000	1.00e+000	1.05e+000	1.20e+000	1.00e+000	1.00e+000
	85	8.00e-001	8.00e-001	1.05e+000	1.20e+000	8.00e-001	8.00e-001
	86	8.00e-001	8.00e-001	1.05e+000	1.20e+000	8.00e-001	8.00e-001
	87	8.00e-001	8.00e-001	1.05e+000	1.20e+000	8.00e-001	8.00e-001
	88	8.00e-001	8.00e-001	1.05e+000	1.20e+000	8.00e-001	8.00e-001

```
          89  9.00e-001  9.00e-001  1.05e+000  1.20e+000  9.00e-001  9.00e-001
          90  9.00e-001  9.00e-001  1.05e+000  1.20e+000  9.00e-001  9.00e-001
(1540)    91  9.00e-001  9.00e-001  1.05e+000  1.20e+000  9.00e-001  9.00e-001
          92  9.00e-001  9.00e-001  1.05e+000  1.20e+000  9.00e-001  9.00e-001
          93  9.00e-001  9.00e-001  1.05e+000  1.20e+000  9.00e-001  9.00e-001
          94  9.00e-001  9.00e-001  1.05e+000  1.20e+000  9.00e-001  9.00e-001
          95  9.00e-001  9.00e-001  1.05e+000  1.20e+000  9.00e-001  9.00e-001
          96  9.00e-001  9.00e-001  1.05e+000  1.20e+000  9.00e-001  9.00e-001
          97  1.52e+000  1.09e+000  1.05e+000  1.20e+000  1.09e+000  1.09e+000
          98  1.53e+000  1.09e+000  1.05e+000  1.20e+000  1.09e+000  1.09e+000
          99  1.53e+000  1.09e+000  1.05e+000  1.20e+000  1.09e+000  1.09e+000
         100  1.53e+000  1.09e+000  1.05e+000  1.20e+000  1.09e+000  1.09e+000
(1550)   101  1.53e+000  1.09e+000  1.05e+000  1.20e+000  1.09e+000  1.09e+000
         102  1.53e+000  1.09e+000  1.05e+000  1.20e+000  1.09e+000  1.09e+000
         103  1.53e+000  1.09e+000  1.05e+000  1.20e+000  1.09e+000  1.09e+000
         104  1.53e+000  1.09e+000  1.05e+000  1.20e+000  1.09e+000  1.09e+000
         105  9.00e-001  9.00e-001  1.05e+000  1.20e+000  9.00e-001  9.00e-001
         106  2.03e+000  1.23e+000  1.05e+000  1.20e+000  1.23e+000  1.23e+000
         107  2.03e+000  1.23e+000  1.05e+000  1.20e+000  1.23e+000  1.23e+000
         108  2.03e+000  1.23e+000  1.05e+000  1.20e+000  1.23e+000  1.23e+000
         109  2.03e+000  1.23e+000  1.05e+000  1.20e+000  1.23e+000  1.23e+000
         110  2.03e+000  1.23e+000  1.05e+000  1.20e+000  1.23e+000  1.23e+000
(1560)   111  2.03e+000  1.23e+000  1.05e+000  1.20e+000  1.23e+000  1.23e+000
         112  2.03e+000  1.23e+000  1.05e+000  1.20e+000  1.23e+000  1.23e+000
         113  2.03e+000  1.23e+000  1.05e+000  1.20e+000  1.23e+000  1.23e+000
         114  9.00e-001  9.00e-001  1.05e+000  1.20e+000  9.00e-001  9.00e-001
         115  1.35e+000  1.03e+000  6.50e-001  1.60e+000  1.03e+000  1.03e+000
         116  1.35e+000  1.03e+000  6.50e-001  1.60e+000  1.03e+000  1.03e+000
         117  1.35e+000  1.03e+000  6.50e-001  1.60e+000  1.03e+000  1.03e+000
         118  1.35e+000  1.03e+000  6.50e-001  1.60e+000  1.03e+000  1.03e+000
         119  1.35e+000  1.03e+000  6.50e-001  1.60e+000  1.03e+000  1.03e+000
         120  1.35e+000  1.03e+000  6.50e-001  1.60e+000  1.03e+000  1.03e+000
(1570)   121  1.35e+000  1.03e+000  6.50e-001  1.60e+000  1.03e+000  1.03e+000
         122  1.35e+000  1.03e+000  6.50e-001  1.60e+000  1.03e+000  1.03e+000
         123  9.00e-001  9.00e-001  6.50e-001  1.60e+000  9.00e-001  9.00e-001
         124  9.00e-001  9.00e-001  6.50e-001  1.60e+000  9.00e-001  9.00e-001
         125  9.00e-001  9.00e-001  6.50e-001  1.60e+000  9.00e-001  9.00e-001
         126  9.00e-001  9.00e-001  6.50e-001  1.60e+000  9.00e-001  9.00e-001
         127  9.00e-001  9.00e-001  6.50e-001  1.60e+000  9.00e-001  9.00e-001
         128  9.00e-001  9.00e-001  6.50e-001  1.60e+000  9.00e-001  9.00e-001
         129  9.00e-001  9.00e-001  6.50e-001  1.60e+000  9.00e-001  9.00e-001
         130  9.00e-001  9.00e-001  6.50e-001  1.60e+000  9.00e-001  9.00e-001
(1580)   131  1.20e+000  1.20e+000  6.50e-001  1.60e+000  1.20e+000  1.20e+000
         132  1.20e+000  1.20e+000  6.50e-001  1.60e+000  1.20e+000  1.20e+000
         133  1.20e+000  1.20e+000  6.50e-001  1.60e+000  1.20e+000  1.20e+000
         134  1.20e+000  1.20e+000  6.50e-001  1.60e+000  1.20e+000  1.20e+000
         135  1.20e+000  1.20e+000  6.50e-001  1.60e+000  1.20e+000  1.20e+000
         136  1.20e+000  1.20e+000  6.50e-001  1.60e+000  1.20e+000  1.20e+000
         137  1.20e+000  1.20e+000  6.50e-001  1.60e+000  1.20e+000  1.20e+000
         138  1.20e+000  1.20e+000  6.50e-001  1.60e+000  1.20e+000  1.20e+000
         139  1.20e+000  1.20e+000  6.50e-001  1.60e+000  1.20e+000  1.20e+000
         140  1.20e+000  1.20e+000  6.50e-001  1.60e+000  1.20e+000  1.20e+000
(1590)   141  1.20e+000  1.20e+000  6.50e-001  1.60e+000  1.20e+000  1.20e+000
         142  1.20e+000  1.20e+000  6.50e-001  1.60e+000  1.20e+000  1.20e+000
         143  1.20e+000  1.20e+000  6.50e-001  1.60e+000  1.20e+000  1.20e+000
         144  1.20e+000  1.20e+000  6.50e-001  1.60e+000  1.20e+000  1.20e+000
         145  1.20e+000  1.20e+000  6.50e-001  1.60e+000  1.20e+000  1.20e+000
         146  1.20e+000  1.20e+000  6.50e-001  1.60e+000  1.20e+000  1.20e+000
         147  1.20e+000  1.20e+000  6.50e-001  1.60e+000  1.20e+000  1.20e+000
         148  1.20e+000  1.20e+000  6.50e-001  1.60e+000  1.20e+000  1.20e+000
         149  1.20e+000  1.20e+000  6.50e-001  1.60e+000  1.20e+000  1.20e+000
         150  1.20e+000  1.20e+000  6.50e-001  1.60e+000  1.20e+000  1.20e+000
(1600)   151  1.20e+000  1.20e+000  6.50e-001  1.60e+000  1.20e+000  1.20e+000
         152  1.20e+000  1.20e+000  6.50e-001  1.60e+000  1.20e+000  1.20e+000
         153  1.20e+000  1.20e+000  6.50e-001  1.60e+000  1.20e+000  1.20e+000
         154  1.20e+000  1.20e+000  6.50e-001  1.60e+000  1.20e+000  1.20e+000
         155  1.20e+000  1.20e+000  6.50e-001  1.60e+000  1.20e+000  1.20e+000
         156  1.20e+000  1.20e+000  6.50e-001  1.60e+000  1.20e+000  1.20e+000
         157  1.20e+000  1.20e+000  6.50e-001  1.60e+000  1.20e+000  1.20e+000
         158  1.20e+000  1.20e+000  6.50e-001  1.60e+000  1.20e+000  1.20e+000
         159  9.60e-001  9.60e-001  1.05e+000  1.20e+000  9.60e-001  9.60e-001
         160  9.60e-001  9.60e-001  1.05e+000  1.20e+000  9.60e-001  9.60e-001
(1610)   161  9.60e-001  9.60e-001  1.05e+000  1.20e+000  9.60e-001  9.60e-001
         162  9.60e-001  9.60e-001  1.05e+000  1.20e+000  9.60e-001  9.60e-001
         163  9.60e-001  9.60e-001  1.05e+000  1.20e+000  9.60e-001  9.60e-001
         164  9.60e-001  9.60e-001  1.05e+000  1.20e+000  9.60e-001  9.60e-001
         165  9.60e-001  9.60e-001  1.05e+000  1.20e+000  9.60e-001  9.60e-001
```

	166	9.60e-001	9.60e-001	1.05e+000	1.20e+000	9.60e-001	9.60e-001
	167	9.60e-001	9.60e-001	1.05e+000	1.20e+000	9.60e-001	9.60e-001
	168	9.60e-001	9.60e-001	1.05e+000	1.20e+000	9.60e-001	9.60e-001
	169	9.60e-001	9.60e-001	1.05e+000	1.20e+000	9.60e-001	9.60e-001
	170	9.60e-001	9.60e-001	1.05e+000	1.20e+000	9.60e-001	9.60e-001
(1620)	171	9.60e-001	9.60e-001	1.05e+000	1.20e+000	9.60e-001	9.60e-001
	172	9.60e-001	9.60e-001	1.05e+000	1.20e+000	9.60e-001	9.60e-001
	173	9.60e-001	9.60e-001	1.05e+000	1.20e+000	9.60e-001	9.60e-001
	174	9.60e-001	9.60e-001	1.05e+000	1.20e+000	9.60e-001	9.60e-001
	175	1.66e+000	1.66e+000	1.05e+000	1.20e+000	1.66e+000	1.66e+000
	176	1.66e+000	1.66e+000	1.05e+000	1.20e+000	1.66e+000	1.66e+000
	177	1.66e+000	1.66e+000	1.05e+000	1.20e+000	1.66e+000	1.66e+000
	178	1.66e+000	1.66e+000	1.05e+000	1.20e+000	1.66e+000	1.66e+000
	179	1.66e+000	1.66e+000	1.05e+000	1.20e+000	1.66e+000	1.66e+000
	180	1.66e+000	1.66e+000	1.05e+000	1.20e+000	1.66e+000	1.66e+000
(1630)	181	1.66e+000	1.66e+000	1.05e+000	1.20e+000	1.66e+000	1.66e+000
	182	1.66e+000	1.66e+000	1.05e+000	1.20e+000	1.66e+000	1.66e+000
	183	1.66e+000	1.66e+000	1.05e+000	1.20e+000	1.66e+000	1.66e+000
	184	1.66e+000	1.66e+000	1.05e+000	1.20e+000	1.66e+000	1.66e+000
	185	1.66e+000	1.66e+000	1.05e+000	1.20e+000	1.66e+000	1.66e+000
	186	1.66e+000	1.66e+000	1.05e+000	1.20e+000	1.66e+000	1.66e+000
	187	1.66e+000	1.66e+000	1.05e+000	1.20e+000	1.66e+000	1.66e+000
	188	1.66e+000	1.66e+000	1.05e+000	1.20e+000	1.66e+000	1.66e+000
	189	1.66e+000	1.66e+000	1.05e+000	1.20e+000	1.66e+000	1.66e+000
	190	1.66e+000	1.66e+000	1.05e+000	1.20e+000	1.66e+000	1.66e+000
(1640)	191	1.26e+000	1.26e+000	1.05e+000	1.20e+000	1.26e+000	1.26e+000
	192	1.26e+000	1.26e+000	1.05e+000	1.20e+000	1.26e+000	1.26e+000
	193	1.26e+000	1.26e+000	1.05e+000	1.20e+000	1.26e+000	1.26e+000
	194	1.26e+000	1.26e+000	1.05e+000	1.20e+000	1.26e+000	1.26e+000
	195	1.26e+000	1.26e+000	1.05e+000	1.20e+000	1.26e+000	1.26e+000
	196	1.26e+000	1.26e+000	1.05e+000	1.20e+000	1.26e+000	1.26e+000
	197	1.26e+000	1.26e+000	1.05e+000	1.20e+000	1.26e+000	1.26e+000
	198	1.26e+000	1.26e+000	1.05e+000	1.20e+000	1.26e+000	1.26e+000
	199	1.26e+000	1.26e+000	1.05e+000	1.20e+000	1.26e+000	1.26e+000
	200	1.26e+000	1.26e+000	1.05e+000	1.20e+000	1.26e+000	1.26e+000
(1650)	201	1.26e+000	1.26e+000	1.05e+000	1.20e+000	1.26e+000	1.26e+000
	202	1.26e+000	1.26e+000	1.05e+000	1.20e+000	1.26e+000	1.26e+000
	203	1.26e+000	1.26e+000	1.05e+000	1.20e+000	1.26e+000	1.26e+000
	204	1.26e+000	1.26e+000	1.05e+000	1.20e+000	1.26e+000	1.26e+000
	205	1.26e+000	1.26e+000	1.05e+000	1.20e+000	1.26e+000	1.26e+000
	206	1.26e+000	1.26e+000	1.05e+000	1.20e+000	1.26e+000	1.26e+000
	207	1.36e+000	1.36e+000	1.05e+000	1.20e+000	1.36e+000	1.36e+000
	208	1.36e+000	1.36e+000	1.05e+000	1.20e+000	1.36e+000	1.36e+000
	209	1.36e+000	1.36e+000	1.05e+000	1.20e+000	1.36e+000	1.36e+000
	210	1.36e+000	1.36e+000	1.05e+000	1.20e+000	1.36e+000	1.36e+000
(1660)	211	1.36e+000	1.36e+000	1.05e+000	1.20e+000	1.36e+000	1.36e+000
	212	1.36e+000	1.36e+000	1.05e+000	1.20e+000	1.36e+000	1.36e+000
	213	1.36e+000	1.36e+000	1.05e+000	1.20e+000	1.36e+000	1.36e+000
	214	1.36e+000	1.36e+000	1.05e+000	1.20e+000	1.36e+000	1.36e+000
	215	1.36e+000	1.36e+000	1.05e+000	1.20e+000	1.36e+000	1.36e+000
	216	1.36e+000	1.36e+000	1.05e+000	1.20e+000	1.36e+000	1.36e+000
	217	1.36e+000	1.36e+000	1.05e+000	1.20e+000	1.36e+000	1.36e+000
	218	1.36e+000	1.36e+000	1.05e+000	1.20e+000	1.36e+000	1.36e+000
	219	1.36e+000	1.36e+000	1.05e+000	1.20e+000	1.36e+000	1.36e+000
	220	1.36e+000	1.36e+000	1.05e+000	1.20e+000	1.36e+000	1.36e+000
(1670)	221	1.36e+000	1.36e+000	1.05e+000	1.20e+000	1.36e+000	1.36e+000
	222	1.36e+000	1.36e+000	1.05e+000	1.20e+000	1.36e+000	1.36e+000
	223	1.26e+000	1.26e+000	1.05e+000	1.20e+000	1.26e+000	1.26e+000
	224	1.26e+000	1.26e+000	1.05e+000	1.20e+000	1.26e+000	1.26e+000
	225	1.26e+000	1.26e+000	1.05e+000	1.20e+000	1.26e+000	1.26e+000
	226	1.26e+000	1.26e+000	1.05e+000	1.20e+000	1.26e+000	1.26e+000
	227	1.26e+000	1.26e+000	1.05e+000	1.20e+000	1.26e+000	1.26e+000
	228	1.26e+000	1.26e+000	1.05e+000	1.20e+000	1.26e+000	1.26e+000
	229	1.26e+000	1.26e+000	1.05e+000	1.20e+000	1.26e+000	1.26e+000
	230	1.26e+000	1.26e+000	1.05e+000	1.20e+000	1.26e+000	1.26e+000
(1680)	231	1.26e+000	1.26e+000	1.05e+000	1.20e+000	1.26e+000	1.26e+000
	232	1.26e+000	1.26e+000	1.05e+000	1.20e+000	1.26e+000	1.26e+000
	233	1.26e+000	1.26e+000	1.05e+000	1.20e+000	1.26e+000	1.26e+000
	234	1.26e+000	1.26e+000	1.05e+000	1.20e+000	1.26e+000	1.26e+000
	235	1.26e+000	1.26e+000	1.05e+000	1.20e+000	1.26e+000	1.26e+000
	236	1.26e+000	1.26e+000	1.05e+000	1.20e+000	1.26e+000	1.26e+000
	237	1.26e+000	1.26e+000	1.05e+000	1.20e+000	1.26e+000	1.26e+000
	238	1.26e+000	1.26e+000	1.05e+000	1.20e+000	1.26e+000	1.26e+000
	239	1.32e+000	1.32e+000	1.05e+000	1.20e+000	1.32e+000	1.32e+000
	240	1.32e+000	1.32e+000	1.05e+000	1.20e+000	1.32e+000	1.32e+000
(1690)	241	1.32e+000	1.32e+000	1.05e+000	1.20e+000	1.32e+000	1.32e+000
	242	1.32e+000	1.32e+000	1.05e+000	1.20e+000	1.32e+000	1.32e+000

	243	1.32e+000	1.32e+000	1.05e+000	1.20e+000	1.32e+000	1.32e+000
	244	1.32e+000	1.32e+000	1.05e+000	1.20e+000	1.32e+000	1.32e+000
	245	1.32e+000	1.32e+000	1.05e+000	1.20e+000	1.32e+000	1.32e+000
	246	1.32e+000	1.32e+000	1.05e+000	1.20e+000	1.32e+000	1.32e+000
	247	1.32e+000	1.32e+000	1.05e+000	1.20e+000	1.32e+000	1.32e+000
	248	1.32e+000	1.32e+000	1.05e+000	1.20e+000	1.32e+000	1.32e+000
	249	1.32e+000	1.32e+000	1.05e+000	1.20e+000	1.32e+000	1.32e+000
	250	1.32e+000	1.32e+000	1.05e+000	1.20e+000	1.32e+000	1.32e+000
(1700)	251	1.32e+000	1.32e+000	1.05e+000	1.20e+000	1.32e+000	1.32e+000
	252	1.32e+000	1.32e+000	1.05e+000	1.20e+000	1.32e+000	1.32e+000
	253	1.32e+000	1.32e+000	1.05e+000	1.20e+000	1.32e+000	1.32e+000
	254	1.32e+000	1.32e+000	1.05e+000	1.20e+000	1.32e+000	1.32e+000
	255	1.02e+000	1.02e+000	1.05e+000	1.20e+000	1.02e+000	1.02e+000
	256	1.02e+000	1.02e+000	8.50e-001	1.40e+000	1.02e+000	1.02e+000
	257	1.02e+000	1.02e+000	8.50e-001	1.40e+000	1.02e+000	1.02e+000
	258	1.02e+000	1.02e+000	1.05e+000	1.20e+000	1.02e+000	1.02e+000
	259	1.02e+000	1.02e+000	1.05e+000	1.20e+000	1.02e+000	1.02e+000
	260	1.02e+000	1.02e+000	8.50e-001	1.40e+000	1.02e+000	1.02e+000
(1710)	261	1.02e+000	1.02e+000	8.50e-001	1.40e+000	1.02e+000	1.02e+000
	262	1.02e+000	1.02e+000	1.05e+000	1.20e+000	1.02e+000	1.02e+000
	263	1.02e+000	1.02e+000	1.05e+000	1.20e+000	1.02e+000	1.02e+000
	264	1.02e+000	1.02e+000	8.50e-001	1.40e+000	1.02e+000	1.02e+000
	265	1.02e+000	1.02e+000	8.50e-001	1.40e+000	1.02e+000	1.02e+000
	266	1.02e+000	1.02e+000	1.05e+000	1.20e+000	1.02e+000	1.02e+000
	267	1.02e+000	1.02e+000	1.05e+000	1.20e+000	1.02e+000	1.02e+000
	268	1.02e+000	1.02e+000	8.50e-001	1.40e+000	1.02e+000	1.02e+000
	269	1.02e+000	1.02e+000	8.50e-001	1.40e+000	1.02e+000	1.02e+000
	270	1.02e+000	1.02e+000	1.05e+000	1.20e+000	1.02e+000	1.02e+000
(1720)	271	1.00e+000	1.00e+000	6.50e-001	1.60e+000	1.00e+000	1.00e+000
	272	1.00e+000	1.00e+000	6.50e-001	1.60e+000	1.00e+000	1.00e+000
	273	1.00e+000	1.00e+000	6.50e-001	1.60e+000	1.00e+000	1.00e+000
	274	1.00e+000	1.00e+000	6.50e-001	1.60e+000	1.00e+000	1.00e+000
	275	1.00e+000	1.00e+000	6.50e-001	1.60e+000	1.00e+000	1.00e+000
	276	1.00e+000	1.00e+000	6.50e-001	1.60e+000	1.00e+000	1.00e+000
	277	2.00e+000	2.00e+000	0.00e+000	0.00e+000	2.00e+000	2.00e+000
	278	2.00e+000	2.00e+000	0.00e+000	0.00e+000	2.00e+000	2.00e+000
	279	2.00e+000	2.00e+000	0.00e+000	0.00e+000	2.00e+000	2.00e+000
	280	2.00e+000	2.00e+000	0.00e+000	0.00e+000	2.00e+000	2.00e+000
(1730)	281	2.00e+000	2.00e+000	0.00e+000	0.00e+000	2.00e+000	2.00e+000
	282	2.00e+000	2.00e+000	0.00e+000	0.00e+000	2.00e+000	2.00e+000
	283	2.00e+000	2.00e+000	0.00e+000	0.00e+000	2.00e+000	2.00e+000
	284	2.00e+000	2.00e+000	0.00e+000	0.00e+000	2.00e+000	2.00e+000
	285	2.00e+000	2.00e+000	0.00e+000	0.00e+000	2.00e+000	2.00e+000
	286	2.00e+000	2.00e+000	0.00e+000	0.00e+000	2.00e+000	2.00e+000
	287	0.00e+000	0.00e+000	1.05e+000	1.20e+000	0.00e+000	0.00e+000
	288	0.00e+000	0.00e+000	1.05e+000	1.20e+000	0.00e+000	0.00e+000
	289	0.00e+000	0.00e+000	1.05e+000	1.20e+000	0.00e+000	0.00e+000
	290	0.00e+000	0.00e+000	1.05e+000	1.20e+000	0.00e+000	0.00e+000
(1740)	291	0.00e+000	0.00e+000	1.05e+000	1.20e+000	0.00e+000	0.00e+000
	292	0.00e+000	0.00e+000	1.05e+000	1.20e+000	0.00e+000	0.00e+000
	293	0.00e+000	0.00e+000	1.05e+000	1.20e+000	0.00e+000	0.00e+000
	294	0.00e+000	0.00e+000	1.05e+000	1.20e+000	0.00e+000	0.00e+000
	295	0.00e+000	0.00e+000	1.05e+000	1.20e+000	0.00e+000	0.00e+000
	296	0.00e+000	0.00e+000	1.05e+000	1.20e+000	0.00e+000	0.00e+000
	297	0.00e+000	0.00e+000	1.05e+000	1.20e+000	0.00e+000	0.00e+000
	298	0.00e+000	0.00e+000	1.05e+000	1.20e+000	0.00e+000	0.00e+000
	299	0.00e+000	0.00e+000	1.05e+000	1.20e+000	0.00e+000	0.00e+000
	300	0.00e+000	0.00e+000	1.05e+000	1.20e+000	0.00e+000	0.00e+000
(1750)	301	0.00e+000	0.00e+000	1.05e+000	1.20e+000	0.00e+000	0.00e+000
	302	0.00e+000	0.00e+000	1.05e+000	1.20e+000	0.00e+000	0.00e+000
	303	0.00e+000	0.00e+000	1.05e+000	1.20e+000	0.00e+000	0.00e+000
	304	0.00e+000	0.00e+000	1.05e+000	1.20e+000	0.00e+000	0.00e+000
	305	0.00e+000	0.00e+000	1.05e+000	1.20e+000	0.00e+000	0.00e+000
	306	0.00e+000	0.00e+000	1.05e+000	1.20e+000	0.00e+000	0.00e+000
	307	0.00e+000	0.00e+000	1.05e+000	1.20e+000	0.00e+000	0.00e+000
	308	0.00e+000	0.00e+000	1.05e+000	1.20e+000	0.00e+000	0.00e+000
	309	0.00e+000	0.00e+000	1.05e+000	1.20e+000	0.00e+000	0.00e+000
	310	0.00e+000	0.00e+000	1.05e+000	1.20e+000	0.00e+000	0.00e+000
(1760)	311	0.00e+000	0.00e+000	1.05e+000	1.20e+000	0.00e+000	0.00e+000
	312	0.00e+000	0.00e+000	1.05e+000	1.20e+000	0.00e+000	0.00e+000
	313	0.00e+000	0.00e+000	1.05e+000	1.20e+000	0.00e+000	0.00e+000
	314	0.00e+000	0.00e+000	1.05e+000	1.20e+000	0.00e+000	0.00e+000
	315	0.00e+000	0.00e+000	1.05e+000	1.20e+000	0.00e+000	0.00e+000
	316	0.00e+000	0.00e+000	1.05e+000	1.20e+000	0.00e+000	0.00e+000
	317	0.00e+000	0.00e+000	1.05e+000	1.20e+000	0.00e+000	0.00e+000
	318	0.00e+000	0.00e+000	1.05e+000	1.20e+000	0.00e+000	0.00e+000
	319	0.00e+000	0.00e+000	1.05e+000	1.20e+000	0.00e+000	0.00e+000

	320	0.00e+000	0.00e+000	1.05e+000	1.20e+000	0.00e+000	0.00e+000
(1770)	321	0.00e+000	0.00e+000	1.05e+000	1.20e+000	0.00e+000	0.00e+000
	322	0.00e+000	0.00e+000	1.05e+000	1.20e+000	0.00e+000	0.00e+000
	323	0.00e+000	0.00e+000	1.05e+000	1.20e+000	0.00e+000	0.00e+000
	324	0.00e+000	0.00e+000	1.05e+000	1.20e+000	0.00e+000	0.00e+000
	325	0.00e+000	0.00e+000	1.05e+000	1.20e+000	0.00e+000	0.00e+000
	326	0.00e+000	0.00e+000	1.05e+000	1.20e+000	0.00e+000	0.00e+000
	327	0.00e+000	0.00e+000	1.05e+000	1.20e+000	0.00e+000	0.00e+000
	328	0.00e+000	0.00e+000	1.05e+000	1.20e+000	0.00e+000	0.00e+000
	329	0.00e+000	0.00e+000	1.05e+000	1.20e+000	0.00e+000	0.00e+000
	330	0.00e+000	0.00e+000	1.05e+000	1.20e+000	0.00e+000	0.00e+000
(1780)	331	0.00e+000	0.00e+000	1.05e+000	1.20e+000	0.00e+000	0.00e+000
	332	0.00e+000	0.00e+000	1.05e+000	1.20e+000	0.00e+000	0.00e+000
	333	0.00e+000	0.00e+000	1.05e+000	1.20e+000	0.00e+000	0.00e+000
	334	0.00e+000	0.00e+000	1.05e+000	1.20e+000	0.00e+000	0.00e+000
	335	0.00e+000	0.00e+000	1.05e+000	1.20e+000	0.00e+000	0.00e+000
	336	0.00e+000	0.00e+000	1.05e+000	1.20e+000	0.00e+000	0.00e+000
	337	0.00e+000	0.00e+000	1.05e+000	1.20e+000	0.00e+000	0.00e+000
	338	0.00e+000	0.00e+000	1.05e+000	1.20e+000	0.00e+000	0.00e+000
	339	0.00e+000	0.00e+000	1.05e+000	1.20e+000	0.00e+000	0.00e+000
	340	0.00e+000	0.00e+000	1.05e+000	1.20e+000	0.00e+000	0.00e+000
(1790)	341	0.00e+000	0.00e+000	1.05e+000	1.20e+000	0.00e+000	0.00e+000
	342	0.00e+000	0.00e+000	1.05e+000	1.20e+000	0.00e+000	0.00e+000
	343	0.00e+000	0.00e+000	1.05e+000	1.20e+000	0.00e+000	0.00e+000
	344	8.40e-001	8.40e-001	1.05e+000	1.20e+000	8.40e-001	8.40e-001
	345	8.40e-001	8.40e-001	1.05e+000	1.20e+000	8.40e-001	8.40e-001
	346	8.40e-001	8.40e-001	1.05e+000	1.20e+000	8.40e-001	8.40e-001
	347	8.40e-001	8.40e-001	1.05e+000	1.20e+000	8.40e-001	8.40e-001
	348	8.40e-001	8.40e-001	8.50e-001	1.40e+000	8.40e-001	8.40e-001
	349	7.20e-001	7.20e-001	6.50e-001	1.60e+000	7.20e-001	7.20e-001
	350	1.34e+000	1.34e+000	1.05e+000	1.20e+000	1.34e+000	1.34e+000
(1800)	351	1.34e+000	1.34e+000	1.05e+000	1.20e+000	1.34e+000	1.34e+000
	352	1.34e+000	1.34e+000	1.05e+000	1.20e+000	1.34e+000	1.34e+000
	353	1.34e+000	1.34e+000	1.05e+000	1.20e+000	1.34e+000	1.34e+000
	354	1.34e+000	1.34e+000	8.50e-001	1.40e+000	1.34e+000	1.34e+000
	355	1.22e+000	1.22e+000	6.50e-001	1.60e+000	1.22e+000	1.22e+000
	356	1.34e+000	1.34e+000	1.05e+000	1.20e+000	1.34e+000	1.34e+000
	357	1.34e+000	1.34e+000	1.05e+000	1.20e+000	1.34e+000	1.34e+000
	358	1.34e+000	1.34e+000	1.05e+000	1.20e+000	1.34e+000	1.34e+000
	359	1.34e+000	1.34e+000	1.05e+000	1.20e+000	1.34e+000	1.34e+000
	360	1.34e+000	1.34e+000	8.50e-001	1.40e+000	1.34e+000	1.34e+000
(1810)	361	1.22e+000	1.22e+000	6.50e-001	1.60e+000	1.22e+000	1.22e+000
	362	1.34e+000	1.34e+000	1.05e+000	1.20e+000	1.34e+000	1.34e+000
	363	1.34e+000	1.34e+000	1.05e+000	1.20e+000	1.34e+000	1.34e+000
	364	1.34e+000	1.34e+000	1.05e+000	1.20e+000	1.34e+000	1.34e+000
	365	1.34e+000	1.34e+000	1.05e+000	1.20e+000	1.34e+000	1.34e+000
	366	1.34e+000	1.34e+000	8.50e-001	1.40e+000	1.34e+000	1.34e+000
	367	1.22e+000	1.22e+000	6.50e-001	1.60e+000	1.22e+000	1.22e+000
	368	1.34e+000	1.34e+000	1.05e+000	1.20e+000	1.34e+000	1.34e+000
	369	1.34e+000	1.34e+000	1.05e+000	1.20e+000	1.34e+000	1.34e+000
	370	1.34e+000	1.34e+000	1.05e+000	1.20e+000	1.34e+000	1.34e+000
(1820)	371	1.34e+000	1.34e+000	1.05e+000	1.20e+000	1.34e+000	1.34e+000
	372	1.34e+000	1.34e+000	8.50e-001	1.40e+000	1.34e+000	1.34e+000
	373	1.22e+000	1.22e+000	6.50e-001	1.60e+000	1.22e+000	1.22e+000
	374	1.76e+000	1.24e+000	1.05e+000	1.20e+000	1.24e+000	1.24e+000
	375	1.76e+000	1.24e+000	1.05e+000	1.20e+000	1.24e+000	1.24e+000
	376	1.76e+000	1.24e+000	1.05e+000	1.20e+000	1.24e+000	1.24e+000
	377	1.76e+000	1.24e+000	8.50e-001	1.40e+000	1.24e+000	1.24e+000
	378	1.52e+000	1.07e+000	6.50e-001	1.60e+000	1.07e+000	1.07e+000
	379	1.76e+000	1.24e+000	1.05e+000	1.20e+000	1.24e+000	1.24e+000
	380	1.76e+000	1.24e+000	1.05e+000	1.20e+000	1.24e+000	1.24e+000
(1830)	381	1.76e+000	1.24e+000	1.05e+000	1.20e+000	1.24e+000	1.24e+000
	382	1.76e+000	1.24e+000	8.50e-001	1.40e+000	1.24e+000	1.24e+000
	383	1.52e+000	1.07e+000	6.50e-001	1.60e+000	1.07e+000	1.07e+000
	384	1.76e+000	1.24e+000	1.05e+000	1.20e+000	1.24e+000	1.24e+000
	385	1.76e+000	1.24e+000	1.05e+000	1.20e+000	1.24e+000	1.24e+000
	386	1.76e+000	1.24e+000	1.05e+000	1.20e+000	1.24e+000	1.24e+000
	387	1.76e+000	1.24e+000	8.50e-001	1.40e+000	1.24e+000	1.24e+000
	388	1.52e+000	1.07e+000	6.50e-001	1.60e+000	1.07e+000	1.07e+000
	389	1.76e+000	1.24e+000	1.05e+000	1.20e+000	1.24e+000	1.24e+000
	390	1.76e+000	1.24e+000	1.05e+000	1.20e+000	1.24e+000	1.24e+000
(1840)	391	1.76e+000	1.24e+000	1.05e+000	1.20e+000	1.24e+000	1.24e+000
	392	1.76e+000	1.24e+000	1.05e+000	1.20e+000	1.24e+000	1.24e+000
	393	1.52e+000	1.07e+000	1.05e+000	1.20e+000	1.07e+000	1.07e+000
	394	1.76e+000	1.24e+000	1.05e+000	1.20e+000	1.24e+000	1.24e+000
	395	1.76e+000	1.24e+000	1.05e+000	1.20e+000	1.24e+000	1.24e+000
	396	1.76e+000	1.24e+000	1.05e+000	1.20e+000	1.24e+000	1.24e+000

```
         397  1.76e+000  1.24e+000  1.05e+000  1.20e+000  1.24e+000  1.24e+000
         398  1.52e+000  1.07e+000  6.50e-001  1.60e+000  1.07e+000  1.07e+000
         399  1.76e+000  1.24e+000  1.05e+000  1.20e+000  1.24e+000  1.24e+000
         400  1.76e+000  1.24e+000  1.05e+000  1.20e+000  1.24e+000  1.24e+000
(1850)   401  1.76e+000  1.24e+000  1.05e+000  1.20e+000  1.24e+000  1.24e+000
         402  1.76e+000  1.24e+000  8.50e-001  1.40e+000  1.24e+000  1.24e+000
         403  1.52e+000  1.07e+000  6.50e-001  1.60e+000  1.07e+000  1.07e+000
         404  1.76e+000  1.24e+000  1.05e+000  1.20e+000  1.24e+000  1.24e+000
         405  1.76e+000  1.24e+000  1.05e+000  1.20e+000  1.24e+000  1.24e+000
         406  1.76e+000  1.24e+000  1.05e+000  1.20e+000  1.24e+000  1.24e+000
         407  1.76e+000  1.24e+000  8.50e-001  1.40e+000  1.24e+000  1.24e+000
         408  1.52e+000  1.07e+000  6.50e-001  1.60e+000  1.07e+000  1.07e+000
         409  1.76e+000  1.24e+000  1.05e+000  1.20e+000  1.24e+000  1.24e+000
         410  1.76e+000  1.24e+000  1.05e+000  1.20e+000  1.24e+000  1.24e+000
(1860)   411  1.76e+000  1.24e+000  1.05e+000  1.20e+000  1.24e+000  1.24e+000
         412  1.76e+000  1.24e+000  8.50e-001  1.40e+000  1.24e+000  1.24e+000
         413  1.52e+000  1.07e+000  6.50e-001  1.60e+000  1.07e+000  1.07e+000
         414  3.19e+000  2.04e+000  1.05e+000  1.20e+000  2.04e+000  2.04e+000
         415  3.19e+000  2.04e+000  1.05e+000  1.20e+000  2.04e+000  2.04e+000
         416  3.19e+000  2.04e+000  1.05e+000  1.20e+000  2.04e+000  2.04e+000
         417  3.19e+000  2.04e+000  1.05e+000  1.20e+000  2.04e+000  2.04e+000
         418  2.83e+000  1.86e+000  1.05e+000  1.20e+000  1.86e+000  1.86e+000
         419  1.61e+001  3.50e+000  1.05e+000  1.20e+000  3.50e+000  3.50e+000
         420  1.61e+001  3.50e+000  1.05e+000  1.20e+000  3.50e+000  3.50e+000
(1870)   421  1.61e+001  3.50e+000  1.05e+000  1.20e+000  3.50e+000  3.50e+000
         422  1.61e+001  3.50e+000  1.05e+000  1.20e+000  3.50e+000  3.50e+000
         423  1.61e+001  3.50e+000  1.05e+000  1.20e+000  3.50e+000  3.50e+000
         424  2.12e+000  2.12e+000  8.50e-001  1.40e+000  2.12e+000  2.12e+000
         425  2.70e+000  2.20e+000  8.50e-001  1.40e+000  2.20e+000  2.20e+000
         426  2.12e+000  2.12e+000  8.50e-001  1.40e+000  2.12e+000  2.12e+000
         '
         '
         '   NRAFT   ARAFT   HRAFT   ACCGRA
                   0  0.00e+000  0.00e+000  9.81e+000
(1880)   '
         '-----------------------------------------------
         '     WAVE CONTROL DATA
         '-----------------------------------------------
         '
         CSEA
         Kvitebjorn
         CWAV
         'IMODE   IDIM    ISEA    IVEL    IACC    ISOW
         1       3       1       1       1       0
(1890)   'DEPTH   SEACOR     VELCOR     ACCCOR
         190     1.0     1.0     1.0
         '
         WAVE
         'ITS    NW      FLOW      FHIGH     IEXCOD   THETA     ISURCH  X0     Y0
         0       4096    0.00    3.30e-001      6       75      3       -5.70e+001     -
         2.20e+001
         '
         'SEFILE  NRTS    NVER
         wav200401011200-hv-mwl.ts 1 1
(1900)   '
         'IDT    ND    EXPON
         2       50      4
         '
         WTIM
         'TLEN   DT      NSEED (1.3020e-001,0.1302047)
         1066.5984 1.3020e-001 1
         '
         RAND
         'IRAN   IAMP
(1910)   78246389 0
         '
         TIME
         'TSTOT  DT      ICO     BT      THETA   DELTA   ALFA    EKAPA   TSREP   TSDEL
         1035.4688 0.0079 0 4.00 1.00 0.00 0.00 0.00 0.00 0.00
         '1066.5984 1.3020e-001 0 4.00 1.00 0.00 0.00 0.00 0.00 0.00
         '505.2563456 0.0009637 0 4.00 1.00 0.00 0.00 0.00 0.00 0.00
         '262.144 0.001 0 4.00 1.00 0.00 0.00 0.00 0.00 0.00
         '235.9296 0.0009 0 4.00 1.00 0.00 0.00 0.00 0.00 0.00
         '471.8592 0.0009 0 4.00 1.00 0.00 0.00 0.00 0.00 0.00
(1920)   '1010.512691 0.0009637 0 4.00 1.00 0.00 0.00 0.00 0.00 0.00
         '266.0   1.3020e-001            0   4.00e+000   1.00e+000   0.00e+000   0.00e+000
         0.00e+000  0.00e+000  0.00e+000
```